The Viability of Modified Gravity Theories

Kotub Uddin

Thesis submitted for the degree of
Doctor of Philosophy (PhD)
of the University of London

Queen Mary, University of London

July 2009

Bismillahi al-Rahman al-Rahim

Al-hamdu Lillaahi nahmaduhu wa nasta'enahu wa nastaghfiruhu, wa na'odhu billaahi min shuroori anfusinaa wa min sayi'ati a'aalinaa. Man yahdih Illaahu falaa mudilla lahu wa man yudlil falaa haadiya lah. Wa ashhadu an laa ilaaha ill-llaah wahdahu la sharika lahu wa ashhadu anna Muhammadan 'abduhu wa rasooluhu sallalahu alayhi wa ala alihi wasallam.

Abstract

This thesis studies the viability of classes of modified gravity (MG) theories based on generalisations of the Einstein-Hilbert action. Particular emphasis is given to $f(R)$ theories in both the metric and Palatini formalisms, scalar-tensor theories and generalised Gauss-Bonnet theories. An urgent task at present is to devise stringent tests in order to reduce the range of candidate models based on these theories. In this thesis a detailed study is made of the viability of these models using constraints from requirement of stability, background cosmological dynamics, local gravity constraints (LGC) and matter density perturbations.

In each case the conditions required for stability and viability of the background dynamics are presented. In the case of generalised Gauss-Bonnet theories the circumstances leading to the existence and stability of cosmological scaling solutions are established.

In the scalar-tensor theories considered here, which includes metric-$f(R)$ theories as a special case, there is a strong coupling of the scalar field to matter in the Einstein frame which violates all LGC. It is shown that using a chameleon mechanism, models that are compatible with LGC may be constructed. It is found that such models, which are also consistent with background dynamics, are constrained to be close to the ΛCDM model during the radiation/matter epochs and can lead to the divergence of the equation of state of dark energy. In contrast, such constraints only impose mild restrictions on Palatini-$f(R)$ models.

Still more stringent constraints are provided by studying matter density perturbations. In particular, it is shown that the unconventional evolution of perturbations in the Palatini formalism leads to $f(R)$ models in this case to be practically identical to the ΛCDM model. For each case it is also shown that (for viable models) matter perturbation equations derived under a sub-horizon approximation are reliable even for super-Hubble scales provided the oscillating mode does not dominate over the matter-induced mode. Such approximate equations are especially reliable in the Palatini formalism, where the oscillating mode is absent. In summary, the analyses carried out in this thesis suggest that subjecting MG theories to observational constraints confines the viable range of models to be very close to (and in some cases indistinguishable from) the ΛCDM model.

Declaration

I hereby declare that the work presented in this thesis is my own, unless otherwise stated, and resulted from collaborations with James Lidsey, Shuntaro Mizuno, Reza Tavakol, Shinji Tsujikawa and Jun'ichi Yokoyama. Parts of the contents of *Chapters 3-7* have been published in the articles:

K. Uddin, J. E. Lidsey and R. Tavakol,
Cosmological scaling solutions in generalised Gauss-Bonnet gravity,
to appear in Gen. Relativ. Gravit.

S. Tsujikawa, **K. Uddin**, S. Mizuno, R. Tavakol and J. Yokoyama,
Constraints on scalar-tensor models of dark energy from observational and local gravity tests,
Phys. Rev. D **77**, 103009 (2008).

S. Tsujikawa, **K. Uddin** and R. Tavakol,
Density perturbations in f(R) gravity theories in metric and Palatini formalisms,
Phys. Rev. D **77**, 043007 (2008).

K. Uddin, J. E. Lidsey and R. Tavakol,
Cosmological perturbations in Palatini modified gravity,
Class. Quant. Grav. **24**, 3951 (2007).

Kotub Uddin

Acknowledgements

I would like to express my sincere gratitude to my supervisors Reza Tavakol and James Lidsey for their constant support, guidance and supervision. It is difficult for me to imagine getting this far without their help. Indeed, this thesis would not have been possible otherwise. I also thank them for showing a tremendous amount of patience during the whole time I have been at Queen Mary.

I am very grateful to Shinji Tsujikawa, a truly wonderful collaborator and a source of inspiration. I thank him for his invaluable help, exceptional kindness and gracious hospitality. It has been a privilege collaborating with him. I thank also my other collaborators (in addition to my supervisors) Shuntaro Mizuno and Jun'ichi Yokoyama.

I thank Carlos Hidalgo, Karim Malik and Douglas Shaw for the many useful discussions. I should also like to thank my fellow (past and present) students at Queen Mary.

I am very much indebted to my family, *ustadhs* and friends for their much needed support, guidance and encouragement. Most of all, I thank my parents, who have been the best of mentors.

Contents

Acknowledgements **5**

1 Background and Motivation **12**

2 The field equations and cosmological perturbations **21**
2.1 The field equations for modified theories of gravity 21
2.1.1 $f(R)$ theories in the metric variational approach 21
2.1.2 $f(R)$ theories in the Palatini variational approach 24
2.1.3 Scalar-tensor theories 27
2.1.4 General $f(R, P, Q)$ theories 29
2.2 The scalar-tensor equivalence 32
2.2.1 Conformal transformations 32
2.2.2 $f(R)$ theories in the metric variational approach 33
2.2.3 $f(R)$ theories in the Palatini variational approach 35
2.2.4 General gravity theories based on curvature invariants 35
2.3 Cosmological equations 38
2.3.1 Friedmann-Lemaitre-Robertson-Walker cosmology 38
2.3.2 Cosmological equations for MG theories 40
2.4 Cosmological Perturbations 43
2.4.1 Metric and matter perturbations 43
2.4.2 Coordinate transformations 46
2.4.3 Field equations for scalar perturbations 47

3 Cosmological perturbations in Palatini-modified gravity **51**
3.1 The evolution of density perturbations 51
3.2 Analytical comparison 54
3.3 Numerical comparison 57
3.4 Summary 59

4 Density perturbations in $f(R)$ gravity theories in metric and Palatini formalisms **61**
4.1 LGC and cosmological viability in the metric formalism 62
4.1.1 Background cosmological dynamics 63
4.1.2 LGC and the chameleon mechanism 65
4.2 LGC and cosmological viability in the Palatini formalism 72
4.2.1 Background cosmological dynamics 72
4.2.2 Local gravity constraints 73
4.3 Density perturbations in the metric formalism 77

4.3.1 Comoving gauge ($v = 0$) . . . 77
4.3.2 Longitudinal gauge ($\chi = 0$) . . . 79
4.3.3 The appearance of scalarons . . . 81
4.3.4 Numerical study of the validity of approximations . . . 82
4.3.5 Constraints on the models $m(r) = C(-r-1)^p$ . . . 87
4.4 Density perturbations in the Palatini formalism . . . 90
4.4.1 Comoving gauge . . . 90
4.4.2 Longitudinal gauge . . . 92
4.4.3 Analytic estimate for the growth of perturbations . . . 93
4.4.4 Constraints on model parameters . . . 97
4.5 Summary . . . 105

5 Observational constraints on scalar-tensor models of dark energy 108
5.1 Scalar-tensor theories . . . 109
5.2 Background cosmological dynamics . . . 111
5.2.1 Constant λ . . . 112
5.2.2 Varying λ . . . 116
5.3 Local gravity constraints . . . 121
5.3.1 Solar system constraints . . . 121
5.3.2 Equivalence principle constraints . . . 123
5.3.3 General properties for models consistent with LGC . . . 123
5.4 The equation of state of dark energy . . . 126
5.5 Matter density perturbations . . . 129
5.5.1 The case $M^2/F \gg k^2/a^2$ . . . 132
5.5.2 The case $M^2/F \ll k^2/a^2$ . . . 133
5.5.3 The matter power spectra . . . 133
5.6 Summary . . . 137

6 Cosmological scaling solutions in generalised Gauss-Bonnet gravity 139
6.1 Cosmological Field Equations . . . 139
6.2 Cosmological scaling solutions . . . 141
6.3 Vacuum solutions . . . 143
6.4 Non-vacuum solutions . . . 144
6.5 Summary . . . 147

7 Summary 151

A Appendix 153
A.1 The $f(R)$ field equations for scalar perturbations in the Palatini formalism . 153
A.2 The thin-shell boundary conditions . . . 156
A.3 Equations convenient for numerical simulations in the Palatini formalism . 158

List of Figures

3.1 Illustrating how the fractional difference parameter, Δ, varies with the normalised scale factor a as b is increased. Here $c = 4.38$ and values of b are assigned to each curve. The case $b = 0$ corresponds to the ΛCDM model. The left hand panel corresponds to $k = 5$ whereas the right hand panel corresponds to $k = 20$. 58

3.2 Illustrating the evolution of the parameter ζ defined by Eq. (3.13) in the text for the parameter values $k = 5$ (left panel) and $k = 20$ (right panel). The LuSS procedure for the evolution of the perturbations becomes progressively less accurate as the deviation of this quantity from unity becomes more pronounced. 60

4.1 The evolution of the matter perturbation $\delta_m^{(v)}$ in the comoving gauge for the model $m(r) = (-r-1)^3$ with the mode $k/a_0H_0 = 10$. Initial conditions were chosen to be $x_1 = 0$, $x_2 = -0.5000$, $x_3 = 0.5001$, $\delta_m^{(v)} = 10^{-3}$, $\delta_m^{(v)\prime} = 10^{-3}$, $\delta\tilde{F} = 8.0 \times 10^{-15}$, $\delta\tilde{F}' = 0$ and $k/a_iH_i = 4.1$ at the redshift $z = 28.9$. The solid curve is obtained by solving the exact equations (4.92) and (4.93) numerically, whereas the dotted one is obtained by solving the approximate equation (4.94). 84

4.2 The evolution of $\delta_m^{(\chi)}$ and Φ_{eff} in the longitudinal gauge for the model $m(r) = (-r-1)^3$ with a mode $k = a_0H_0$. The results were obtained by numerically integrating Eqs. (4.96), (4.97) and (4.98) with initial conditions $\Phi_{\text{eff}} = 10^{-5}$, $\Phi'_{\text{eff}} = 0$ and $k/a_iH_i = 0.36$ and with $\delta_m^{(\chi)}$ and $\delta_m^{(\chi)\prime}$ satisfying Eqs. (4.102) and (4.103). Initial conditions for the background quantities were chosen to be the same as in Fig. 4.1. We also plot $\delta_m^{(\chi)}$ and Φ_{eff} obtained by solving the approximate equations (4.104) and (4.80). The approximation is valid even when the mode is initially outside the Hubble radius. 87

4.3 The evolution of the growth rate $s = \delta'_m/\delta_m$ with respect to the redshift z in the model $m(r) = (-r-1)^3$ with four different values of k. Initial conditions were chosen as in Fig. 4.2. The transition redshift z_k, defined as the redshift where $k/a = M$, becomes larger for smaller scales. After the matter perturbation enters the region $z < z_k$ the growth rate begins to increase toward the value $s = 1.186$, but it starts to decrease once the Universe enters the stage of accelerated expansion. 88

4.4 The evolution of perturbations for the model: $f(R) = \alpha R^{1+m} - \Lambda$ with positive values of m. In the left panel we show the growth rate, $s = \delta'_m/\delta_m$, versus the redshift, z, for the mode $k/a_0H_0 = 600$ with three different values of m. The black dots represent the points at which ξ crosses 1. The right panel depicts the evolution of s for $m = 1.5 \times 10^{-5}$ with three different values of k. 98
4.5 The evolution of perturbations for the model: $f(R) = \alpha R^{1+m} - \Lambda$ for negative m. In the left panel we show the growth rate $s = \delta'_m/\delta_m$ versus the redshift z for the mode $k/a_0H_0 = 600$ with three different values of m. The black dots represent the points at which the quantity $|\xi|$ crosses 1. The right panel depicts the evolution of s for $m = -2.0 \times 10^{-5}$ with three different values of k. 99
4.6 The evolution of perturbations for the model $f(R) = R - \lambda R_c(R/R_c)^\beta$ with positive β and $\lambda = 1$. The left-hand panel depicts $s = \delta'_m/\delta_m$ versus the redshift, z, for the mode $k/a_0H_0 = 600$ with three different values of β. The right-hand panel shows the evolution of m with respect to z for $k/a_0H_0 = 600$. From the requirement (1.2) we obtain the constraint $\beta < 8.2 \times 10^{-5}$. . 101
4.7 The evolution of perturbations for the model $f(R) = R - \lambda R_c(R/R_c)^\beta$ with negative β and $\lambda = 1$. The left-hand panel depicts $s = \delta'_m/\delta_m$ versus the redshift, z, for the mode $k/a_0H_0 = 600$ with three different values of β. The right-hand panel shows the evolution of the quantity m with respect to z for $k/a_0H_0 = 600$. If we use the criterion $s(z = 0) > -1$, we obtain the constraint $\beta > -1.2 \times 10^{-4}$. 102
4.8 The evolution of perturbations for the model $f(R) = R - \lambda R_c[1-(1 + R^2/R_c^2)^{-n}]$ with $\lambda = 2.5$. The left-hand panel depicts $s = \delta'_m/\delta_m$ versus the redshift, z, for the mode $k/a_0H_0 = 600$ with three different values of n. The right-hand panel shows the evolution of the quantity m with respect to z for $k/a_0H_0 = 600$. 103

5.1 The evolution of $\Omega_{\rm DE}$, Ω_m, Ω_r and $w_{\rm eff}$ for the model (5.47) with parameters $Q = 0.01$, $p = 0.2$ and $C = 0.7$ and initial conditions $x_1 = 0$, $x_2 = 2.27 \times 10^{-7}$, $x_3 = 0.7$ and $x_4 - 1 = -5.0 \times 10^{-13}$. 119
5.2 This illustration describes a field potential $V(\varphi)$ that is consistent with LGC. For a coupling Q that is positive (negative) the potential evolves in the region $\varphi \geq 0$ ($\varphi \leq 0$). In the figure φ_m represents the field value during the radiation/matter eras, which instantaneously changes in time. The field value $\varphi_{\rm dS}$ corresponds to the one at the de-Sitter point. Note that both φ_m and $\varphi_{\rm dS}$ are sustained by the presence of the coupling Q having potential minima characterised by the condition (5.64). In the early stages of the cosmological evolution, the mass M of the field φ is heavy for consistency with LGC. This mass gradually gets smaller as the system approaches the de-Sitter point. . . 124
5.3 Figure depicting the evolution of $w_{\rm DE}$ for $Q = 0.1$ and $C = 0.95$ with three different values of p $(0.3, 0.55, 0.7)$. The redshift z_c at which the divergence of $w_{\rm DE}$ occurs decreases for smaller p. 127

5.4 The evolution of the growth rate, s, of matter perturbations in terms of the redshift, z, for $Q = 1.08$ and $k = 600a_0H_0$ with three different values of p. For smaller p the critical redshift, z_k, gets larger. The growth rate, s, reaches a maximum value and begins to decrease after the system enters the accelerated epoch. For smaller p the maximum value of s tends to approach the analytic value given in Eq. (5.97). 135
5.5 The allowed region of the parameter space in the (p, Q) plane. We show the bounds coming from the conditions $\Delta n(t_\Lambda) < 0.05$ and $s < 2$ as well as the solar-system constraint (5.59) and the EP constraint (5.63). 136

6.1 Illustrating the effective equation of state w_{eff} for the vacuum solutions $\mathcal{V}^+$ and $\mathcal{V}^-$. Requiring that the fixed points are real yields the condition $\alpha \geq -9/192$. The left-hand panel corresponds to $\mathcal{V}^+$, which shows that $\mathcal{V}^+$ is an accelerating solution for $\alpha > 0$ and corresponds to the de Sitter solution if $\alpha = 3/8$. The middle panel corresponds to $\mathcal{V}^-$ when $\alpha < 0$ and in this regime $w_{eff} \geq 1$. The right-hand panel corresponds to $\mathcal{V}^-$ when $\alpha > 0$ and in this regime $w_{eff} < -1$. 144
6.2 Illustrating the nature of the equilibrium points $\mathcal{V}^+$ (left-hand panel) and $\mathcal{V}^-$ (right-hand panel) in the parameter space spanned by (w_m, α). Both fixed points are real if $\alpha \geq -9/192$. On the boundary (denoted by the solid line) that distinguishes the stability of the fixed point $\mathcal{V}^+$, one of the eigenvalues $\mu^+_{1,2}$ vanishes. This is indicated in the figure by a change in colour. The dotted line in the left-hand panel represents the invariant sub-manifold $y_1 = 0$. In the case of the point $\mathcal{V}^-$, neither of the eigenvalues vanishes in any region of the (w_m, α) plane. 145
6.3 Illustrating the stability of the scaling equilibrium points $\mathcal{S}^\pm$ in the parameter space spanned by (w_m, α). The region of parameter space is restricted by the requirement that the equilibrium points are real, $\alpha(1 + 3w_m) \leq 0$, and also correspond to physically realistic solutions where $\Omega_m \geq 0$. The shaded areas depict the regions of parameter space where the solutions are unphysical. These restrictions imply that the analysis can be separated into regions where $\alpha > 0$ (left-hand panels) and $\alpha < 0$ (right-hand panels). The regions of parameter space where the fixed points correspond to either a saddle point or a stable/spiral node are identified. On the line $\Omega_m = 0$, the eigenvalue $\mu^+_1 = 0$ (for the scaling point $\mathcal{S}^+$) when $\alpha > 0$. Conversely, $\mu^-_2 = 0$ (for the scaling point $\mathcal{S}^-$) when $\Omega_m = 0$ and $\alpha < 0$. 149
6.4 Illustrating the dynamics of the model (6.18) for the particular case where $(\alpha, w_m) = (0.05, -0.6)$. The left-hand panel depicts the phase space, where the straight line $y_1 = 1 - y_2$ corresponds to the vacuum solution $\Omega_m = 0$. The red dot represents the scaling fixed point $\mathcal{S}^+$. For the range of initial conditions chosen, all non-vacuum, physically acceptable solutions are attracted to $\mathcal{S}^+$. The right-hand panel depicts the evolution of the fractional energy densities of the perfect fluid, Ω_m, and the GB contribution, $\Omega_\mathcal{G}$, for the initial conditions $\Omega_m = \Omega_\mathcal{G} = 0.5$. It is seen that the fractional densities asymptote to constant values at late times, thus indicating that the solution is scaling. 150

6.5 Illustrating the dynamics of the model (6.18) for the particular case where $(\alpha, w_m) = (-0.005, -0.05)$. The left-hand panel depicts the phase space for this scenario, whereas the right-hand panel depicts the evolution of the fractional energy densities Ω_m and $\Omega_{\mathcal{G}}$. The initial conditions were chosen such that $\Omega_m = \Omega_{\mathcal{G}} = 0.5$. At late times, the fractional energy densities of the fluid and GB contribution tend to constant values. 150

Chapter 1

Background and Motivation

The recent high-precision measurements of the cosmic microwave background (CMB) provided by the Wilkinson Microwave Anisotropy Probe (WMAP), together with other high redshift surveys, have produced a wealth of information regarding the early Universe. The analysis of the resulting data has provided strong evidence for the predictions of inflationary cosmology, including the almost spatial flatness of the Universe [1]. Furthermore, these observations coupled with the low redshift Supernovae surveys [2; 3; 4; 5] and observations of large scale structure [6; 7] and baryon acoustic oscillations [8] suggest that the Universe is at present undergoing a phase of accelerated expansion [9]. Consequently a 'standard' model of cosmology has emerged which is characterised by four distinct dynamical phases: accelerated expansions at both early and late times, mediated by radiation-dominated and matter-dominated eras [10]. The two phases of accelerated expansion pose a serious challenge for cosmology since they are difficult to explain within the original general relativistic framework.

Concerning the phase of late time accelerated expansion, the simplest phenomenological way to generate such a phase is through the addition of a cosmological constant (Λ) to the Einstein field equations. In the classical setting this is equivalent to a constant energy density with a negative pressure that permeates the entire Universe homogeneously. Quantum mechanically, however, Λ is associated with the energy density of the vacuum which is equal to the sum of zero-point energies of quantum fields. Although this sum is formally infinite, we expect that quantum mechanics will only be valid up to the Planck scale indicating an ultraviolet momentum cut-off. In this case the integral is finite [9]. In spite of this, the predicted quantum mechanical value of Λ still differs from the observed value by more than a hundred orders of magnitude [11].

In order to resolve the problem an almost, but not exact, cancellation is required by an equally large term of the opposite sign. Super-symmetric field theories, for example, assert that for every bosonic degree of freedom there exists a fermionic counterpart contributing negatively to the zero-point energy, thereby cancelling the vacuum energy [11]. Unfortu-

nately, the predicted value of Λ is still substantially different from the observed value. This problem, i.e., the problem of how to consistently account for Λ within a theory of quantum gravity, is usually referred to as *'the cosmological constant problem'*, (which, in many respects, is also a *'fine-tuning problem'*) [9].

In the Λ-Cold Dark Matter (ΛCDM) model, Λ accounts for approximately 73% of the present energy-density of the Universe, cold dark matter 23% and baryonic matter 4%. In this case, an additional *fine-tuning problem* arises: given that the matter energy density scales as $(\mathrm{time})^{-2}$, the problem is to understand why Λ is comparable to the present cosmological matter density. This is known as the *'cosmic coincidence problem'* and is shared with other dark energy[1] (DE) models in general. Thus far, there is no conclusive solution to this problem, nor is there a successful mechanism whereby *the cosmological constant problem* can be explained. This has motivated a large number of alternative models.

Within the framework of general relativity (GR), a number of attempts have been made to account for the apparent DE as an effect of spatial averaging in an inhomogeneous Universe [12; 13; 14]. Consider, for example, the scenario proposed by Kolb *et al.* [14], where it is argued that the backreaction of cosmological perturbations exhibits an effect that may be interpreted as cosmic acceleration. The authors demonstrate through the effective Friedmann equations describing an inhomogeneous Universe after smoothing, that acceleration in our local Hubble patch may be possible even if the fluid elements do not individually drive accelerated expansion. This would then violate the *"no-go theorem"* that there can be no acceleration in our local Hubble patch if the Universe only contains irrotational dust. On the other hand, other authors have pointed out that the effect of averaging nonlinear inhomogeneities has an insignificant impact on the average cosmological dynamics [15; 16]. As a result, it is uncertain whether the backreaction of perturbations would be able to account for the present epoch of accelerated expansion.

Alternatively, a number of articles have recently considered the *"Swiss-cheese"* model of the inhomogeneous Universe, where each spherical void is described by the inhomogeneous, spherically symmetric, Lemaitre-Tolman-Bondi (LTB) solution. At the boundary of these regions the LTB metric is matched with the Friedmann-Lemaitre-Robertson-Walker (FLRW) metric that describes the evolution between the inhomogeneities [17; 18]. The idea is that the less dense regions (voids) act as a concave lens, bending the light from a distant object away from the observer. Therefore, light from Supernovae that travelled through a series of voids would appear dimmer than expected without the need to invoke DE. However, it has been argued that the above set up is too idealised [19] . In a more realistic Universe, light from the Supernovae would pass through both under dense and over dense regions. Therefore, contrary to observations, some Supernovae (the light from which passes predominantly through

[1]Dark energy refers to a hypothetical form of energy responsible for the present phase of accelerated expansion.

voids) would appear dimmer, whereas others would appear brighter (because the light was passing mainly through denser regions and bending towards the observer).

In summary, it is fair to say that the models proposed within the context of general relativity, so far, are not completely satisfactory in explaining the current phase of accelerated expansion. Consequently a large number of studies have recently focused on the possibility of modifying Einstein's (original) theory of GR. Such theories can be classified into two broad groups: those that invoke an exotic matter source for the dark energy and those that modify the gravitational sector of the theory.

An important subset of the former classes of theories are the so-called 'Quintessence' models based on a scalar field that minimally couples to gravity [20]. In these models, the potential energy of the dynamical field can give rise to the present epoch of accelerated expansion. In addition, if the field's self-interaction potential is of an exponential form [21], these models possess cosmological *'scaling solutions'* [22; 23; 24; 25; 26] in which the field energy density is proportional to the fluid energy density. It is well known that such solutions can be useful in developing a viable background cosmological evolution.

In addition to the quintessence models, there have been a number of scalar field models proposed in the literature[2], of which a partially complete list includes: Quintessential inflation, which attempts to unify both the early and late phases of accelerated expansion via a single scalar field [27]; scalar field models of Chaplygin gas, which attempt to unify DE with dark matter by allowing for a fluid with an equation of state that interpolates between the two [28]; models with a non-canonical kinetic term, known as K-essence [29]; phantom or dilatonic dark energy, where the kinetic term in the lagrangian density has the opposite sign to quintessence [30]; and string inspired tachyonic models [31]. Details and references for all these models, including additional ones, can be found in Refs. [9; 26; 32; 33; 34].

On the other hand, a great deal of effort has gone into the study of modified gravity (MG) theories where the gravitational sector of the theory is different from the one in GR. Among these classes of theories are $f(R)$ theories, which involve non-linear generalisations to the (linear) Einstein-Hilbert action. Such modifications are expected to arise in the effective action of the gravitational field when string/M-theory corrections are considered [35]. An important motivation for the recent interest in $f(R)$ theories has been the demonstration that generalised lagrangians of this type – which include negative and positive powers of the curvature scalar – can lead to accelerating phases both at early [36] and late [37] times in the history of the Universe.

In deriving the Einstein field equations from the Einstein-Hilbert action there are two approaches that may be taken. These depend on the choice of independent fields with respect to which the action is varied. In the *'metric'* approach only variations with respect to the metric are considered, whereas in the *'Palatini'* approach the action is varied with respect to

[2]We note that scalar field models also involve *fine-tuning* when confronted with observations.

both the metric and the connection. In the latter formulation, the Riemann tensor, R^{abcd}, and the Ricci tensor, R^{ab}, are defined with respect to the independent connection, $\hat{\Gamma}^{a}_{\ bc}$, and do not necessarily coincide with the Ricci and Riemann tensors of the metric g_{ab}. Consequently, the Ricci scalar is constructed from the connection $\hat{\Gamma}^{a}_{\ bc}$ and metric. If the lagrangian is linear in R, variation with respect to the independent connection forces it to reduce to the Levi-Civita connection of the metric, while variation with respect to the metric gives the standard Einstein equations. Therefore, in the case of the Einstein-Hilbert action both approaches result in identical field equations. However, in the more general cases with nonlinear $f(R)$ lagrangians the metric approach results in fourth-order field equations, whereas the Palatini variation generates a second-order system.

For some of the simplest choices of $f(R)$ in the metric formalism (e.g., $f(R) = R - \mu^{2(n+1)}/R^n$ with $n > 0$ [37]), Dolgov and Kawasaki [38] have shown that the solutions of the fourth-order field equations in the interior of some matter distributions, such as a star, are unstable and grow with time. Such models are therefore ruled out in the metric approach. The instabilities are found to occur if the condition $\partial^2 f/\partial R^2 > 0$ is violated [39; 40]. In the Palatini formalism, on the other hand, these instabilities are absent due to the second-order nature of the field equations. Therefore, the simple models that are excluded in the metric formalism may be allowed in the Palatini formalism [41]. (This discussion is made more transparent in Sections 2.1.1 and 2.1.2 where the field equations for the $f(R)$ theories have been derived.)

The viability of the background cosmological dynamics of $f(R)$ gravity models in the metric formulation has been the focus of a number of studies in recent years. The issue was first studied in Ref. [42], where the authors demonstrated that for all models possessing a lagrangian density that behaves as a power of R at large or small scales, the scale factor during the matter era grows as $t^{1/2}$ as opposed to the standard $t^{2/3}$. In a detailed extension of this work [43], the conditions [imposed on $f(R)$] required to produce the conventional background dynamics, i.e., an era of late time accelerated expansion preceded by a standard matter era, were derived without specifying the form of $f(R)$. Under these conditions, many functional forms of $f(R)$ are ruled out, although there still exist some special cases of $f(R)$ that can be viable.

In contrast, a wide range of $f(R)$ models in the Palatini formalism (including $f(R) = R - \mu^{2(n+1)}/R^n$) are capable of producing the correct sequence of radiation-dominated, matter-dominated and de-Sitter periods [10]. Moreover, models featuring both positive and negative powers of R in addition to the Einstein-Hilbert term have been shown to consistently produce both early as well as late accelerating phases.

Local gravity experiments can impose strong restrictions on the viability of $f(R)$ gravity models. In Ref. [44], Teyssandier and Tourrenc pointed out that $f(R)$ theories in the metric approach are dynamically equivalent to Brans-Dicke theories with a potential and a Brans-

Dicke parameter $\omega_{BD} = 0$. Since interferometry observations of the deflection by the sun of radiation from radio quasars constrain the Brans-Dicke parameter to satisfy $\omega_{BD} > 40000$ [45; 46], it was originally argued that such theories are incompatible with solar system tests[3]. It was quickly realised, however, that the bounds given in Refs. [45; 46] apply only to the usual Brans-Dicke theories (without a potential), in which case the mass of the scalar field vanishes. In the presence of a potential (which leads to a non-zero effective scalar field mass) these theories can be made compatible with local gravity experiments using a chameleon mechanism.

Briefly, a chameleon mechanism is realised by certain scalar fields that have a potential and a coupling to matter. These combine to create an effective potential for the field [47]. The values of the scalar field at the minima of the effective potential generally depend on the local density of matter, and since the mass squared of the effective scalar field is given by the second derivative of the effective potential evaluated at the minima, the scalar field mass will depend on the ambient matter density [48]. In particular, the field is nearly massless in the underdense regions of the universe, where the matter density is extremely small. On the other hand, the effective scalar field mass in sufficiently dense regions of the Universe, such as the solar system, is large. In Sec. 4.1.2 a more detailed discussion on the implications of chameleon fields on the viability of cosmological models is provided.

The possibility of finding consistent solutions for static, spherically-symmetric matter configurations in the Palatini formulation has been an issue of interest recently. This debate originated from Ref. [49], in which the authors claimed that choosing a polytropic equation of state, with index $\frac{3}{2} < \gamma < 2$, to describe the fluid in the vicinity of the surface of a sphere results in curvature singularities, independently of the form of $f(R)$. This implies that stellar configurations can not be described within the Palatini framework. Immediately one notices two major drawbacks of this conclusion, however. Firstly, a polytropic equation of state is too idealised to give a detailed description of a matter configuration that resembles an astrophysical star. Secondly, even if we were to accept a polytrope, the range in which the singularities have been shown to occur is restricted to $\frac{3}{2} < \gamma < 2$. It should be noted that there are at least two physical matter configurations which are exactly described by a $\gamma = \frac{5}{3}$ polytrope: a monatomic isentropic gas and a degenerate non-relativistic electron gas. The conclusions of Ref. [49] are further disputed in Ref. [50], where the authors calculate the tidal forces arising due to the presence of the surface singularities. They find that the length scale on which the tidal forces diverge due to the curvature singularity is shorter than the mean free path of the fluid and conclude that the system is therefore not well-described by the fluid approximation. In summary, it is fair to say that this issue is not completely

[3] As will be illustrated later on, the Palatini formalism corresponding to $\omega_{BD} = -3/2$ is a special case in which the weak-field description of Brans-Dicke theories breaks down. Hence, such observations can not be applied in the same way.

resolved.

Another issue, that has recently been discussed in the literature, concerns the *well-posedness* of the Cauchy problem of $f(R)$ gravity in the Palatini approach. By considering the dynamical equivalence between these theories and Brans-Dicke theories with $w_{BD} = -\frac{3}{2}$, the authors of Ref. [51] argue that the Cauchy problem is *ill-posed*. They argue that the non-dynamical nature of the scalar field makes it impossible to eliminate second-order derivatives of the field in the $3+1$ ADM framework. This leads to an *ill-formulated* and therefore *ill-posed* initial value problem[4]. On the other hand, the authors of Ref. [53] have rigorously demonstrated that an appropriate choice of coordinates can lead to a *well-formulated* and *well-posed* Cauchy problem in the vacuum[5]. Moreover, by introducing matter fields, one can define a suitable scalar field that allows the theory to be written in scalar-tensor form and also allows the form of $f(R)$ to be related to the trace of the energy-momentum tensor. It is then argued that this results in a *well-formulated* Cauchy problem that is free from singularities [54].

The $f(R)$ gravity theories can be further generalised by including terms in $R^{ab}R_{ab}$, $R^{abcd}R_{abcd}$, or other invariants of the Riemann tensor. (It is informative to note that these higher-order gravity theories are conformally related to Einstein gravity minimally coupled to one or more scalar fields. Additionally, as will be illustrated in Sec. 2.2, such higher-order theories can always be expressed as scalar-tensor theories). However, unless these extra terms appear in the Gauss-Bonnet combination, one will generally be faced with ghost instabilities (instabilities associated with a positive scalar field kinetic term in the equivalent scalar-tensor gravitational action) in the theory [55; 56].

In this thesis a detailed study of the viability of modified gravity theories is performed, focusing on a number of specific classes of theories that include: $f(R)$ theories in the metric formalism; $f(R)$ theories in the Palatini formalism; scalar-tensor theories; and generalised Gauss-Bonnet theories. Given the large number of models that have been (or can potentially be) considered within the context of these theories, the aim here will be to reduce the range of viable candidates by employing constraints provided by the following set of observational tests:

1. the requirement of stability,

2. the background cosmological dynamics[6],

[4]Note that in the $3+1$ ADM formulation, if the system of equations are *well-formulated* and satisfy hyperbolicity, then the initial value problem is said to be *well-posed* [52].

[5]Because $f(R)$ theories (like GR) are gauge theories, the Cauchy problem depends on suitable constraints and choice of coordinates [54].

[6]As is often done in studies of dark energy, we shall ignore the early epoch of inflation and concentrate on the three later phases of cosmic evolution. That is, we consider the observed temperature fluctuations in the CMB as initial conditions without discussing the mechanism that produced them.

3. the local gravity constraints (LGC),

4. the evolution of matter density perturbations.

In the solar system, GR is in excellent agreement with experiments. Classically these experiments include: the perihelion precession of Mercury; the deflection by the sun of light from distant sources; and the gravitational redshift of light. More recent experiments include: (i) testing the Shapiro effect (the time delay in photon signals caused by the time dilation in the gravitational potential of the sun [57; 58]); (ii) gravitational lensing [59]; and (iii) tests of the equivalence principle. Thus, any candidate theory of gravity should reproduce GR on solar system scales.

In order to provide a framework in which the weak-field tests of gravity may be interpreted, the parametrised post-Newtonian (PPN) approach has been developed [60]. In this formalism, a set of post-Newtonian parameters completely characterise the weak-field behaviour of GR. These parameters are then severely constrained by solar system tests. For example, gravitational lensing effects and the time delay of the Cassini tracking constrain the Eddington parameter, γ. (This is a parametrisation of the amount of deflection of light caused by a gravitational source). It is found that [61]

$$|\gamma - 1| < 2.3 \times 10^{-5} \tag{1.1}$$

and further experimental bounds on the PPN parameters can be found in Ref. [61].

In addition to background dynamics and local gravity constraints, the study of perturbations can be used to place bounds on the parameters of models. For this purpose, the observed large scale structure [7; 62] provides a useful probe. It is well known that the large scale structure that is seen in the Universe today grew via gravitational instability from small initial density perturbations. These initial perturbations are believed to have originated from quantum fluctuations generated during an early epoch of inflationary expansion. The evolution of these density perturbations is determined by the theory of gravity. Therefore, the viability of a given theory may be tested by confronting it with observables such as the matter power spectrum [63].

Another useful observable is the linear growth rate, s, which measures how rapidly structure grows as a function of time. Recently a number of surveys have aimed to constrain this quantity by observing the clustering of galaxies. At a redshift $z \sim 3$, McDonald *et al.* [64] obtained the constraint $s = 1.46 \pm 0.49$ from observations of the matter power spectrum of the Lyman-α forests. Taking into account the more recent data reported by Viel and Haehnelt [65] in the redshift range $2 < z < 4$, the maximum value for the growth rate allowed by current observations is given by [66]

$$s \equiv \frac{\mathrm{d}\ln\delta_m}{\mathrm{d}\ln a} \lesssim 1.5\,. \tag{1.2}$$

The current data still has large error bars and some data even allows for values in the range $-1 < s < 2$ [65]. However, it is expected that future observations will further constrain the growth rate.

This thesis is organised as follows. We begin in Chapter 2 by formally introducing the classes of MG theories that are to be considered in this thesis. The corresponding field equations are derived and the basic characteristics of the theories are discussed. We proceed by introducing conformal transformations, which are then utilised to show the equivalence between some MG theories and scalar-tensor theories. The conformal equivalence between certain MG theories and GR is also demonstrated. Thereafter, the field equations for a spatially isotropic FLRW Universe sourced by a perfect barotropic fluid are presented.

The framework for studying cosmological perturbations is also outlined in Chapter 2. Describing an inhomogeneous space-time in terms of a homogeneous background with perturbations is equivalent to specifying a mapping between space-time points in the background and points in the inhomogeneous universe [67]. This mapping is not unique and leads to a *gauge problem*. Moreover, the separation of quantities into background and perturbed parts is not a covariant procedure. This can lead to gauge dependencies in perturbed quantities, which means that physical quantities can have different descriptions depending on the choice of coordinates [67]. After a short discussion aimed at clarifying the *gauge problem*, we proceed by deriving the perturbed field equations for those MG theories that we consider in later chapters.

In contrast to this 'standard approach' of studying cosmological perturbations in the context of generalised gravity, an alternative method has been developed that is essentially based on utilising a generalisation of Birkhoff's theorem. In Chapter 3, we begin by comparing and contrasting both approaches in the context of Palatini $f(R)$ gravity [68]. The general form of the gravitational lagrangian for which the two frameworks yield identical results in the long-wavelength limit is derived. This class of models includes the case where the lagrangian is a power-law of the Ricci curvature scalar. The evolution of density perturbations in theories of the type $f(R) = R - \mu^{2(n+1)}/R^n$ is investigated numerically [68].

Pursuing this further, in Chapter 4 a detailed study of matter density perturbations in $f(R)$ gravity for both the metric and Palatini formalisms is made within the context of the standard approach [69]. In each case, a brief review of the constraints provided by background cosmological dynamics, as well as LGC, is presented. In the case of the metric formalism, this requires a discussion of the Chameleon mechanism. We proceed by deriving the evolution equations for matter density perturbations in each case in a number of gauges, including the comoving, longitudinal and uniform density gauges. In addition, the perturbation equations are also derived under a sub-horizon approximation and are shown to be accurate for the models that satisfy the background and local gravity constraints. Using these equations, a comparative study of the behaviour of matter density perturbations, as well

as gravitational potentials for a number of classes of $f(R)$ theories, is carried out both analytically and numerically. Employing the constraints provided by the above set of tests, the parameter $m = Rf_{,RR}/f_{,R}$ (which characterises the deviation from the ΛCDM concordance model) is constrained.

Given that a number of classes of theories – including $f(R)$ metric and Palatini theories, and low energy effective superstring theories [70] – can be expressed in terms of scalar-tensor theories, the analysis of Chapter 4 is extended to include a general class of scalar-tensor theories in Chapter 5. In this way a unified framework is achieved, allowing for the simultaneous study of a range of theories. A class of scalar-tensor theories where the scalar field couples to matter with a constant coupling, Q, is considered. We begin by studying the background cosmological dynamics and consider the cases of constant as well as varying λ (the slope of the potential in the physical frame). The stability analysis which is crucial in determining the background evolution is also presented. A family of potentials which are natural generalisations of a viable family of models in $f(R)$ gravity is introduced. By employing the chameleon mechanism (as in the case of $f(R)$ gravity), experimental bounds on the parameters of viable scalar-tensor models are then derived using solar-system and equivalence principle constraints. For the models that are compatible with LGC, a study of the evolution of the equation of state of DE reveals that the divergence of $w_{\rm DE}$ previously found in $f(R)$ theories is also present in these cases. Finally, the evolution of density perturbations is discussed and used to place constraints on the coupling and model parameters by considering differences in the slopes of the power spectra over large scale structure and CMB scales.

In Chapter 6, a general class of theories where the Einstein-Hilbert action is modified by the inclusion of a function of the Gauss-Bonnet curvature invariant, $f(\mathcal{G})$, is considered [71]. In this case, the most general form for the function $f(\mathcal{G})$ that results in power-law (scaling) solutions is identified. By employing an equivalence between the Gauss-Bonnet action and a scalar-tensor theory of gravity, the field equations are expressed as a plane autonomous system. A dynamical systems analysis is then employed to study the stability of the vacuum and non-vacuum solutions.

Finally, we conclude in Chapter 7 with a summary.

Chapter 2

The field equations and cosmological perturbations

The field equations for the classes of modified gravity theories which we study in subsequent chapters are presented here. In each case, we introduce the theories, outline the derivations of the field equations, show their equivalence to scalar-tensor theories, derive the corresponding background equations, and state the perturbed field equations. We also introduce notations and motivate the assumptions that will subsequently be made in this thesis.

2.1 The field equations for modified theories of gravity

2.1.1 $f(R)$ theories in the metric variational approach

Let us first consider the action

$$S_{f(R)} = \frac{1}{16\pi G_N}\int d^4x\sqrt{-g}f(R) + S_m[g_{ab},\psi_m], \tag{2.1}$$

where G_N is the gravitational constant, f is a general differentiable function of the Ricci scalar, R, the idicies a, b (later) c, d and e are summed from 0 to 3, and the matter action is a functional only of the metric tensor g_{ab} and matter fields ψ_m. We adopt the metric signature $(-,+,+,+)$. When varying the action to derive the field equations, the usual (*metric*) approach is to use the metric compatible connection, Γ^c_{ab}. This means that the covariant derivative formed from the connection satisfies $\nabla_c\, g_{ab} = 0$ and the connection is the usual Levi-Civita connection written in terms of the metric as:

$$\Gamma^c_{ab} = \frac{1}{2}g^{cd}(\partial_a g_{bd} + \partial_b g_{da} - \partial_d g_{ab}). \tag{2.2}$$

In this case the metric g_{ab} is the only field that mediates the gravitational interaction and any other fields that exist are included in the matter action S_m. In this subsection we adopt the metric variational approach to derive the field equations of the theory whose action is given by (2.1).

Varying the gravitational lagrangian with respect to g^{ab} gives [72]:

$$\begin{aligned}\delta(\sqrt{-g}f) &= \sqrt{-g}\left[F\delta R - \frac{1}{2}g_{ab}f\delta g^{ab}\right] \\ &= \sqrt{-g}\left[Fg^{cd}\delta R_{cd} + \left(\frac{1}{2}g^{ab}f - FR^{ab}\right)\delta g_{ab}\right], \end{aligned} \tag{2.3}$$

where, $F \equiv \partial f/\partial R$ and we have used the relation

$$\delta g^{ab} = -g^{ac}g^{bd}\delta g_{cd}. \tag{2.4}$$

Given that the Ricci tensor satisfies the following relation:

$$R_{cd} = \Gamma^n_{cd,n} - \Gamma^n_{nc,d} + \Gamma^n_{nm}\Gamma^m_{cd} - \Gamma^n_{dm}\Gamma^m_{nc}\,, \tag{2.5}$$

where a comma denotes partial differentiation, it follows that

$$\delta R_{cd} = \delta\Gamma^n_{cd;n} - \delta\Gamma^n_{nc;d}\,, \tag{2.6}$$

where a semi-colon denotes a covariant derivative defined in terms of the Levi-Civita connection. Bearing in mind that

$$\delta\Gamma^a_{bc} = \frac{1}{2}[\delta g^k_{\ b;c} + \delta g^k_{\ c;b} - \delta g_{bc;}^{\ \ k}]\,, \tag{2.7}$$

Eq. (2.6) becomes

$$\begin{aligned}\delta R_{cd} &= -\frac{1}{2}g^{kn}[\delta g_{cd;kn} + \delta g_{kn;cd} - \delta g_{ck;dn} - \delta g_{dn;ck}] \\ \delta R_{cd} &= g^{kn}[\delta g_{ck;dn} - \delta g_{cd;kn}]. \end{aligned} \tag{2.8}$$

Contracting δR_{cd} with the metric g^{cd} then yields

$$g^{cd}\delta R_{cd} = \delta g^{cd}_{\ \ ;cd} - \Box\delta g_c^{\ c}\,, \tag{2.9}$$

where $\Box \equiv g^{ab}\nabla_a\nabla_b$, and since

$$\begin{aligned}\Box(F\delta g_c^{\ c}) &= \delta g_c^{\ c}\Box F + F\Box\delta g_c^{\ c} + F_{;c}\delta g^{cd}_{\ \ ;d} + F_{;d}\delta g^{cd}_{\ \ ;c}\,, \\ (F\delta g^{cd})_{;cd} &= F_{;cd}\delta g^{cd} + F\delta g^{cd}_{\ \ ;cd} + F_{;c}\delta g^{cd}_{\ \ ;d} + F_{;d}\delta g^{cd}_{\ \ ;c}\,, \end{aligned}$$

it follows that Eq. (2.9) can be expressed in the form

$$Fg^{cd}\delta R_{cd} = \delta g_c{}^c\Box F - \delta g^{cd}F_{;cd} + (F\delta g^{cd})_{;cd} - \Box(F\delta g_c{}^c). \tag{2.10}$$

The last two terms of Eq. (2.10) are total derivatives. These can be eliminated here as they can be transformed via Gauss's theorem to terms on the boundary, which are assumed to vanish. There is however a slight subtlety related to the presence of F in the total derivative terms (see Ref. [73] for a detailed discussion). In contrast to the case of the Einstein-Hilbert action, the total derivative terms in (2.10) are not expressible as the total variation of a functional when $F \neq \text{constant}$. This implies that it is not possible to eliminate these terms by imposing suitable boundary conditions on the metric. However, because up to fourth-order derivatives of the metric arise in the field equations [cf. Eqs. (2.9) and (2.10)], it is possible to fix more degrees of freedom on the boundary other than the metric itself in order to eliminate the total derivative terms [74]. In general, choosing and fixing degrees of freedom on the boundary has physical implications. Nonetheless, we proceed by adopting the standard approach of assuming that a suitable fixing has been chosen in such a way that we can ignore the surface terms [36; 72; 73; 75; 76]. It then follows that

$$\begin{aligned} Fg^{cd}\delta R_{cd} &= \delta g_c{}^c\Box F - \delta g^{cd}F_{;cd} \\ &= \delta g^{cd}(g_{cd}\Box F - F_{;cd}) \\ &= \delta g_{cd}(F^{;cd} - g^{cd}\Box F), \end{aligned} \tag{2.11}$$

and substituting Eq. (2.11) into Eq. (2.3), we find that

$$\delta(\sqrt{-g}f) = \sqrt{-g}[-FR^{ab} + \frac{1}{2}g^{ab}f + \nabla^a\nabla^b F - g^{ab}\Box F]\delta g_{ab}. \tag{2.12}$$

Finally, the variation of the matter lagrangian yields

$$\begin{aligned} \delta(\sqrt{-g}\mathcal{L}_m) &= \frac{1}{2}\sqrt{-g}T^{ab}\delta g_{ab}, \\ &= -\frac{1}{2}\sqrt{-g}T_{ab}\delta g^{ab}, \end{aligned} \tag{2.13}$$

where T^{ab} is the *energy-momentum* tensor, and the field equations are then given by [72]

$$F(R)R_{ab} - \frac{1}{2}f(R)g_{ab} - \nabla_a\nabla_b F(R) + g_{ab}\Box F(R) = 8\pi G_N T_{ab}. \tag{2.14}$$

This is clearly different from the case of the second-order field equations of GR, corresponding to $f(R) \propto R$. The trace of Eq. (2.14),

$$FR - 2f + 3\Box F = 8\pi G_N T, \tag{2.15}$$

further highlights the discrepancy with GR, chiefly because R and T are related differentially rather than algebraically (note that in GR, $R = -8\pi G_N T$). In fact, this property leads to the Dolgov and Kawasaki instability [38] mentioned in Sec. 1. That is, the first-order perturbative solution of Eq. (2.15) around a general relativistic background (i.e., $R = -8\pi G_N T + R^{(1)}$) inside some spatially finite matter distribution is highly unstable.

2.1.2 $f(R)$ theories in the Palatini variational approach

The $f(R)$ action (2.1) in this case is re-written as

$$S_{f(\hat{R})} = \frac{1}{16\pi G_N}\int d^4x\sqrt{-g}f(\hat{R}) + S_m[g_{ab},\psi_m], \tag{2.16}$$

where $\hat{R} = g^{ab}R_{ab}(\hat{\Gamma})$ and the Ricci tensor, which depends on the affine connection $\hat{\Gamma}$, is given by

$$R_{ab}(\hat{\Gamma}) = \hat{\Gamma}^n_{ab,n} - \hat{\Gamma}^n_{na,b} + \hat{\Gamma}^n_{nm}\hat{\Gamma}^m_{ab} - \hat{\Gamma}^n_{bm}\hat{\Gamma}^m_{na}. \tag{2.17}$$

The matter action is assumed to be independent of the affine connection $\hat{\Gamma}$. In this case, because there are two independent fields which mediate gravity: g_{ab} and $\hat{\Gamma}^c_{ab}$, the gravitational action is varied with respect to each of these fields independently[1]. Henceforth, for simplicity, the use of over-hats to denote a quantity defined by the connection $\hat{\Gamma}^n_{ab}$ is omitted , except where its use may make the discussion more transparent.

Varying the gravitational lagrangian (2.16) with respect to g^{ab} leads to

$$\delta(\sqrt{-g}f) = \left[FR_{ab} - \frac{1}{2}fg_{ab}\right]\delta g^{ab}, \tag{2.18}$$

where $F \equiv \partial f(\hat{R})/\partial\hat{R}$. The last equality follows from the fact that in the Palatini formalism $R = R(\Gamma)$. Consequently, the variation, δR_{ab}, with respect to the metric is zero. Using Eq. (2.13), the generalised Einstein field equations in the Palatini approach are then given by

$$F(R)R_{ab} - \frac{1}{2}f(R)g_{ab} = 8\pi G_N T_{ab}. \tag{2.19}$$

Interestingly, allowing the connection to be a dynamical variable has reduced rather than increased the number of degrees of freedom in the theory [78]. As in GR, the field equations here are second-order equations. Furthermore, the algebraic relation between R and T is

[1] Although this method is generally attributed to Palatini, it should be noted that it was first used by Einstein [77].

manifest in the trace of (2.19):

$$RF - 2f = 8\pi G_N T. \tag{2.20}$$

Therefore, in contrast to the metric formulation where the field equations are generally fourth-order and in practice difficult to analyse, the Palatini formalism is more tractable. In addition, unlike the metric formalism, the Dolgov and Kawasaki instability is absent in the Palatini formalism because Eq. (2.20) is algebraic. This illustrates the better stability properties of the second-order differential system compared with its fourth-order counterpart. Obviously, this mathematical convenience does not single out the Palatini approach as the fundamentally correct variational procedure. Nevertheless, its second-order nature is conceptually more compatible with other known laws of physics. More specifically, in the metric alternative one has to specify initial values up to third derivatives in order to determine the evolution of the system [79].

To proceed, the variation of action (2.16) with respect to the affine connection, $\hat{\Gamma}^a_{bc}$, yields

$$\delta(\sqrt{-g}f) = \sqrt{-g}g^{ab}F\delta R_{ab}. \tag{2.21}$$

The variation of the Ricci tensor, R_{ab}, in this case is identical to that of the metric approach, except that the connection is the affine connection $\hat{\Gamma}$. Thus

$$\delta R_{ab} = \hat{\nabla}_n \delta\hat{\Gamma}^n_{ab} - \hat{\nabla}_b \delta\hat{\Gamma}^n_{na}\,, \tag{2.22}$$

where $\hat{\nabla}$ is the covariant derivative defined by $\hat{\Gamma}^a_{bc}$. Substituting (2.22) into (2.21) gives

$$\delta(\sqrt{-g}f) = [\sqrt{-g}g^{ab}F(\hat{\nabla}_n \delta\hat{\Gamma}^n_{ab} - \hat{\nabla}_b \delta\hat{\Gamma}^n_{na})]\,, \tag{2.23}$$

and after integrating by parts and ignoring the surface terms as before by setting $\delta\hat{\Gamma}^a_{bx} = 0$ on the boundary, Eq. (2.23) reduces to [80]

$$\begin{aligned}\delta(\sqrt{-g}f) &= -[\hat{\nabla}_n(\sqrt{-g}g^{ab}F)\delta\hat{\Gamma}^n_{ab}) - (\hat{\nabla}_b(\sqrt{-g}g^{ab}F)\delta\hat{\Gamma}^n_{na}] \\ &= -\delta\hat{\Gamma}^m_{ka}[\delta^k_{\ b}\hat{\nabla}_m(\sqrt{-g}g^{ab}F) - \delta^k_{\ m}\hat{\nabla}_b(\sqrt{-g}g^{ab}F)]\,.\end{aligned} \tag{2.24}$$

Requiring that the variation of the action (2.16) vanishes leads to the condition

$$\delta^k_{\ b}\hat{\nabla}_m(\sqrt{-g}g^{ab}F) - \delta^k_{\ m}\hat{\nabla}_b(\sqrt{-g}g^{ab}F) = 0, \tag{2.25}$$

and contracting over the indices m and k leads to the field equation for $\hat{\Gamma}^a_{bc}$ [80]

$$\hat{\nabla}_b[F\sqrt{-g}g^{ab}] = 0\,. \tag{2.26}$$

If we now define a conformal metric

$$h_{ab} \equiv F g_{ab}\,, \tag{2.27}$$

it is easy to show that in terms of the new metric, Eq. (2.26) can be written as

$$\hat{\nabla}_b[\sqrt{-h}h^{ab}] = 0\,. \tag{2.28}$$

The solution to Eq. (2.26) can therefore be expressed by writing $\hat{\Gamma}^n_{ab}$ as the Levi-Civita connection for a new metric h_{ab} which is conformally equivalent to the spacetime metric g_{ab}. The expression for the affine connection, $\hat{\Gamma}^n_{ab}$, in this case is given by

$$\begin{aligned}
\hat{\Gamma}^n_{ab} &= \frac{1}{2}h^{nm}(h_{bm,a} + h_{ma,b} - h_{ab,m}) \\
&= \frac{1}{2F}g^{nm}[F g_{bm,a} + F g_{ma,b} - F g_{ab,m} + g_{bm}F_{,a} + g_{ma}F_{,b} - g_{ab}F_{,m}] \\
&= \Gamma^n_{ab} + \frac{1}{2F}(\delta^n_b\partial_a F + \delta^n_a\partial_b F - g_{ab}g^{nm}\partial_m F).
\end{aligned} \tag{2.29}$$

We recall that the Ricci tensor defined in Eq. (2.17) is written in terms of the affine connection only. It is desirable, however, to express the Ricci tensor in terms of quantities that can be computed for a given metric [80]. Re-writing Eq. (2.29) in the form

$$\hat{\Gamma}^n_{ab} = \Gamma^n_{ab} + C^n_{ab}, \tag{2.30}$$

implies that the Ricci tensor becomes

$$\begin{aligned}
R_{ab} &= R_{ab}(g) + C^n_{ab,n} - C^n_{na,b} + \Gamma^n_{nm}C^m_{ab} + \Gamma^m_{ab}C^n_{nm} \\
&\quad + C^n_{nm}C^m_{ab} - \Gamma^n_{bm}C^m_{na} - \Gamma^m_{na}C^n_{bm} - C^n_{bm}C^m_{na},
\end{aligned}$$

or equivalently,

$$R_{ab} = R_{ab}(g) + C^n_{ab;n} - C^n_{na;b} + C^n_{nm}C^m_{ab} - C^n_{bm}C^m_{na}, \tag{2.31}$$

where $R_{ab}(g)$ is the Ricci tensor of the Levi-Civita connection. We now compute each term after $R_{ab}(g)$ on the right hand side (r.h.s) of Eq. (2.31). The second term becomes

$$\begin{aligned}
C^n_{ab;n} &= -\frac{F_{;n}}{2F^2}(\delta^n_a F_{;b} + \delta^n_b F_{;a} - g^{nm}g_{ab}F_{;m}) + \frac{1}{2F}(2F_{;ab} - g_{ab}\Box F) \\
&= -\frac{1}{F^2}(F_{;a}F_{;b} - \frac{1}{2}g_{ab}F^{;n}F_{;n}) + \frac{1}{2F}(2F_{;ab} - g_{ab}\Box F),
\end{aligned} \tag{2.32}$$

where $F = F(\hat{R}(R))$. The third term is

$$C^n_{na;b} = \frac{2}{F}F_{;ab} - \frac{2}{F^2}F_{;a}F_{;b}\,, \tag{2.33}$$

where we have used $C^n_{na} = 2F_{;a}/F$, which follows from contracting over the indices n and b in Eq. (2.29). The fourth term on the right hand side of (2.31) is

$$\begin{aligned} C^n_{nm}C^m_{ab} &= \frac{2}{F}F_{;m}C^m_{ab} \\ &= \frac{1}{F^2}(2F_{;a}F_{;b} - g_{ab}F^{;n}F_{;n})\,, \end{aligned} \tag{2.34}$$

and the last term is

$$\begin{aligned} C^n_{bm}C^m_{na} &= \frac{1}{4F^2}(\delta^n_b F_{;m} + \delta^n_m F_{;b} - g^{nk}g_{mb}F_{;k})(\delta^m_a F_{;n} + \delta^m_n F_{;a} - g^{mt}g_{na}F_{;t}) \\ &= \frac{1}{2F^2}(3F_{;a}F_{;b} - g_{ab}F^{;n}F_{;n}). \end{aligned} \tag{2.35}$$

Finally, by replacing the terms in Eq. (2.31) with Eqs. (2.32)-(2.35), the expression for the Ricci tensor of the affine connection, $R_{ab}(\hat{\Gamma})$, becomes

$$R_{ab}(\hat{\Gamma}) = R_{ab}(g) + \frac{3}{2F^2}\nabla_a F\nabla_b F - \frac{1}{F}\nabla_a\nabla_b F - \frac{1}{2F}g_{ab}\Box F\,. \tag{2.36}$$

Moreover, by taking the trace of Eq. (2.36), we can relate the curvature scalar of the affine connection, $\hat{R}$, to the curvature scalar of the Levi-Civita connection, R, thus:

$$R(\hat{\Gamma}) = R(g) + \frac{3}{2F^2}\nabla_a F\nabla^a F - \frac{3}{F}\Box F\,. \tag{2.37}$$

2.1.3 Scalar-tensor theories

We next consider the following class of scalar-tensor theories [81]

$$S_{ST} = \frac{1}{16\pi G_N}\int d^4x\sqrt{-g}\left[F(\phi)R - Z(\phi)g^{ab}\partial_a\phi\partial_b\phi - V(\phi)\right] + S_m[g_{ab},\psi_m], \tag{2.38}$$

where $F(\phi)$ needs to be a positive-definite function of ϕ for gravitons to carry positive energy, $Z(\phi)$ is an arbitrary function of ϕ and $V(\phi)$ is the field potential. Such theories satisfy hyperbolicity (i.e., possess a well posed Cauchy problem even when formulated in the Jordan frame) [82]. Setting the variation of the action (2.38) with respect to g^{ab} to zero, we obtain

the following field equations

$$F(\phi)[R_{ab}-\frac{1}{2}g_{ab}R] = 8\pi G_N T_{ab}+Z(\phi)[\partial_a\phi\partial_b\phi-\frac{1}{2}g_{ab}\partial^c\phi\partial_c\phi] -\frac{1}{2}g_{ab}V(\phi)+g^{ab}F(\phi)\frac{\delta R_{ab}}{\delta g^{ab}}. \quad (2.39)$$

Using the relation (2.11), the gravitational field equations (2.39) are [81]

$$F(\phi)[R_{ab}-\frac{1}{2}g_{ab}R] = 8\pi G_N T_{ab}+Z(\phi)[\partial_a\phi\partial_b\phi-\frac{1}{2}g_{ab}\partial^c\phi\partial_c\phi] -\frac{1}{2}g_{ab}V(\phi)-g_{ab}\Box F(\phi)+\partial_a\partial_b F(\phi). \quad (2.40)$$

On the other hand, varying action (2.38) with respect to ϕ gives the scalar field evolution equation:

$$2Z\Box\phi = -F_{,\phi}R - Z_{,\phi}\partial^c\phi\partial_c\phi + V_{,\phi}. \quad (2.41)$$

The trace of Eq. (2.40),

$$-FR = 8\pi G_N T - Z\partial^c\phi\partial_c\phi - 2V - 3\Box F, \quad (2.42)$$

can then be used to replace the Ricci scalar, R, in Eq. (2.41), thus leading to the relation

$$(2ZF+3F_{,\phi}{}^2)\Box\phi = 8\pi G_N F_{,\phi}T-\frac{1}{2}\partial^c\phi\partial_c\phi(2ZF+3F_{,\phi}{}^2)_{,\phi} +FV_{,\phi}-2VF_{,\phi}\,. \quad (2.43)$$

A special class of scalar-tensor theories that have been well studied in the literature are the Brans-Dicke theories [83]. These are defined by the action

$$S_{BD}=\frac{1}{16\pi G_N}\int d^4x\sqrt{-g}\left[\phi R-\frac{\omega_{BD}}{\phi}\partial_a\phi\partial^a\phi-V(\phi)\right]+S_m[g_{ab},\psi_m], \quad (2.44)$$

where ω_{BD} is the Brans-Dicke (BD) parameter. To be precise, in the original work of Brans and Dicke [83] the action did not include a potential. Despite this, the more general form of the action (2.44) is considered here because this is the form that is relevant to our subsequent discussions. For simplicity, we shall refer to the action (2.44) as the Brans-Dicke action.

Assuming that the Brans-Dicke parameter, ω_{BD}, is a constant, the field equations obtained from action (2.44) are given by substituting $F(\phi)=\phi$ and $Z(\phi)=\omega_{BD}/\phi$ in the field

equations (2.40) and (2.43). In this case, the field equations become

$$\begin{aligned} R_{ab} - \frac{1}{2}g_{ab}R &= \frac{8\pi G_N}{\phi}T_{ab} + \frac{\omega_{BD}}{\phi^2}\left(\partial_a\phi\partial_b\phi - \frac{1}{2}g_{ab}\partial^c\phi\partial_c\phi\right) \\ &\quad + \frac{1}{\phi}(\partial_a\partial_b\phi - g_{ab}\Box\phi) - \frac{V}{2\phi}g_{ab} \end{aligned} \tag{2.45}$$

and

$$(2\omega_{BD}+3)\Box\phi = 8\pi G_N T + \phi V_{,\phi} - 2V\,, \tag{2.46}$$

respectively.

2.1.4 General $f(R,P,Q)$ theories

Finally, we consider gravitational theories that include both linear and quadratic contractions of the Riemann curvature tensor: R, $P \equiv R_{ab}R^{ab}$ and $Q \equiv R_{abcd}R^{abcd}$. The general action we consider is [84]

$$S_{RPQ} = \frac{1}{16\pi G_N}\int d^4x\sqrt{-g}f(R,P,Q) + S_m[g_{ab},\psi_m], \tag{2.47}$$

where f is a general differentiable function of R, P and Q. Varying the gravitational lagrangian with respect to the metric gives

$$\delta\sqrt{-g}f(R,P,Q) = \sqrt{-g}\left[\frac{1}{2}fg^{ab}\delta g_{ab} + f_{,R}\delta R + f_{,P}\delta P + f_{,Q}\delta Q\right], \tag{2.48}$$

where

$$\begin{aligned} \delta R &= R_{ab}\delta g^{ab} + g^{ab}\delta R_{ab}\,, \\ \delta P &= (R^c{}_bR_{ac} + R^c{}_aR_{bc})\delta g^{ab} + 2R^{ab}\delta R_{ab}\,, \\ \delta Q &= (R_{cdeb}R_a{}^{edc} + R_{cdea}R_b{}^{edc})\delta g^{ab} + 2R_a{}^{bcd}\delta R^a{}_{bcd}\,. \end{aligned} \tag{2.49}$$

Substituting the relations (2.49) into Eq. (2.48) then implies that

$$\begin{aligned} \delta(\sqrt{-g}f) &= \sqrt{-g}\left[\frac{1}{2}fg^{ab}\delta g_{ab} + f_{,R}(R_{ab}\delta g^{ab} + g^{ab}\delta R_{ab})\right] \\ &\quad + \sqrt{-g}\left[2f_{,P}(R^c_{(a}R_{b)c}\delta g^{ab} + R^{ab}\delta R_{ab})\right] \\ &\quad + \sqrt{-g}\left[2f_{,Q}(R_{cde(b}R_{a)}{}^{edc}\delta g^{ab} + R_a{}^{bcd}\delta R^a{}_{bcd})\right], \end{aligned} \tag{2.50}$$

where we use the subscripts () to indicate a totally symmetric quantity [i.e., $U_{(ab)} = \frac{1}{2}(U_{ab} + U_{ba})$]. It then follows that by using the relations [84]

$$f_{,P}R^{ab}\delta R_{ab} \stackrel{=}{\mathrm{d}} \frac{1}{2}\left[\Box(f_{,P}R^{ab}) + (f_{,P}R^{cd})_{;cd}g^{ab} - 2(f_{,P}R^{c(a}{}_{;}{}^{b)}{}_{c}\right]\delta g_{ab},$$
$$f_{,Q}R_{a}{}^{bcd}\delta R^{a}{}_{bcd} \stackrel{=}{\mathrm{d}} -2(f_{,Q}R^{c(ab)d})_{;cd}\delta g_{ab}, \tag{2.51}$$

where $\stackrel{=}{\mathrm{d}}$ means equal up to terms which are pure divergences, together with Eqs. (2.11) and (2.13), that the field equations can be expressed in the form [84; 85]

$$\begin{aligned} 8\pi G_N T^{ab} = & -\frac{1}{2}fg^{ab} + f_R R^{ab} + 2f_{,P}R^{c(a}R^{b)}{}_{c} + 2f_{,Q}R^{edc(a}R^{b)}{}_{cde} \\ & + g^{ab}\Box f_{,R} - f_{,R}{}^{;ab} + \Box(f_{,P}R^{ab}) + g^{ab}(f_{,P}R^{cd})_{;cd} \\ & - 2(f_{,P}R^{c(a}{}_{;}{}^{b)}{}_{c} - 4(f_{,Q}R^{c(ab)d})_{;cd}\,. \end{aligned} \tag{2.52}$$

A well-motivated action of the type (2.47) follows from the low-energy action of string theory, where the Gauss-Bonnet (GB) combination of curvature invariants, defined by

$$\mathcal{G} \equiv R^2 - 4R^{ab}R_{ab} + R^{abcd}R_{abcd}, \tag{2.53}$$

arises as a leading-order correction [31]. In four dimensions, the GB term is a topological invariant and introducing a term proportional to $\mathcal{G}$ into the Einstein-Hilbert action does not modify the dynamics. Recently, however, the cosmology of models based on a class of generalised theories with an action of the form

$$S_{GB} = \frac{1}{16\pi G_N}\int d^4x\sqrt{-g}[R + f(\mathcal{G})] + S_m[g_{ab}, \psi_m], \tag{2.54}$$

have been considered. Varying the Einstein-Hilbert term in this action yields the usual Einstein tensor, whereas varying the $f(\mathcal{G})$ term implies that

$$\delta(\sqrt{-g}f) = \sqrt{-g}\left[\frac{1}{2}fg^{ab}\delta g_{ab} + f_G(2R\delta R - 4\delta P + \delta Q)\right]. \tag{2.55}$$

By employing the same procedure as for the previous example, the field equations for the theory (2.54) are then found to be given by [86]

$$\begin{aligned} R_{ab} - \frac{1}{2}g_{ab}R = & \; 8\pi G_N T_{ab} + \frac{1}{2}g_{ab}f - 2FRR_{ab} + 4FR^{c}{}_{a}R_{bc} \\ & -2FR_{acde}R_{b}{}^{cde} - 4FR_{acdb}R^{cd} + 2R\nabla_a\nabla_b F \\ & -2g_{ab}R\Box F - 4R^{c}{}_{a}\nabla_b\nabla_c F - 4R^{c}{}_{b}\nabla_a\nabla_c F \\ & +4R_{ab}\Box F + 4g_{ab}R^{cd}\nabla_c\nabla_d F - 4R_{acbd}\nabla^c\nabla^d F, \end{aligned} \tag{2.56}$$

where $F \equiv \partial f/\partial\mathcal{G}$. As in the case of the metric $f(R)$ theories, introducing non-linear

curvature invariants into the Einstein-Hilbert action also leads to field equations which contain fourth-order derivatives of the metric. This is expected since the curvature invariants themselves contain second-order derivatives of the metric. In the Palatini formalism, the field equations are second-order equations precisely because the curvature invariants are independent of the metric. This discussion is made more transparent in the next section by considering the dynamical equivalence of these theories to scalar-tensor theories.

2.2 The scalar-tensor equivalence

The MG theories presented in the previous section can be recast into a scalar-tensor form by employing suitable field redefinitions. In fact, as will be shown below, any *metric* gravity theory based on curvature corrections to the Einstein-Hilbert action can always be expressed in terms of a scalar-tensor theory where the scalar-field has a vanishing kinetic term. This dynamical equivalence[2] proves useful when studying more complicated theories of gravity, such as $f(\mathcal{G})$ gravity, as we shall see later in Sec. 6.

2.2.1 Conformal transformations

There is no unique prescription to redefine the fields of a theory. One can employ auxiliary scalar fields, for example, to re-write the action or the field equations of a theory [87], or use conformal transformations. Here, we briefly review conformal transformations.

A conformal transformation is a position-dependent transformation, mapping the original metric, g_{ab}, into a new 'conformal' metric, $\tilde{g}_{ab}$, such that

$$\tilde{g}_{ab} = \Omega^2 g_{ab}\,, \tag{2.57}$$

where $\Omega = \Omega(x)$ is a function of spacetime coordinates and is referred to as the conformal factor. The transformation is known as conformal, since it leaves the angle between two vectors in the space-time invariant [88]. The line element is transformed to

$$d\tilde{s}^2 = \Omega^2 ds^2 \tag{2.58}$$

and the volume elements in four dimensions are related by

$$\sqrt{-\tilde{g}} = \Omega^4 \sqrt{-g}. \tag{2.59}$$

The transformation yields a new Ricci scalar given by [88]

$$\tilde{R} = \frac{1}{\Omega^2}\left[R - \frac{12\Box\sqrt{\Omega}}{\sqrt{\Omega}} - \frac{3g^{ab}\nabla_a\Omega\nabla_b\Omega}{\Omega^2}\right] \tag{2.60}$$

in four dimensions.

The conformal factor Ω in general can depend implicitly on the scalar curvature and on the matter fields. By carefully choosing the conformal factor, one can map a non-standard theory of gravity formulated in the Jordan frame to one that is standard in the Einstein

[2] As a clarifying remark: two theories are considered 'dynamically equivalent' if, under a suitable redefinition of the gravitational and matter fields, one can make their field equations and/or their actions coincide.

frame, where gravity takes the usual Einstein form. The Jordan frame is the frame in which the energy-momentum tensor is covariantly conserved and in which test particles follow geodesics of the space-time metric. Under a conformal transformation, which is a field redefinition as opposed to a coordinate redefinition, the gravitational and matter degrees of freedom become mixed [89]. Thus, in the Einstein frame, the energy-momentum tensor of the matter fields are not always covariantly conserved and test particles do not necessarily follow geodesics of the space-time metric.

There is a long standing debate in the literature regarding the physical status of the different frames. Essentially, this dispute concerns the physical equivalence of two conformally related theories. Some authors argue that conformal equivalence does not necessarily indicate physical equivalence [90], while others assert that provided standard clocks and rulers are adjusted appropriately, a mathematically equivalent theory is always physically equivalent [91]. The latter viewpoint implies that one can choose to work in any conformal frame so long as the transformations are consistent.

Given that there is, so far, no conclusive way to single out a "physical" frame, the usual practice is to proceed by choosing the frame that is most convenient. For example, in the Einstein frame the field equations are always second-order and this frame is therefore particularly useful for finding vacuum solutions. In the presence of matter fields, however, the Einstein frame may be less useful [89]. In this study we consider the Jordan frame to be the physical frame, since this is the frame in which the conservation laws hold and which usually corresponds to the frame in which the theory is formulated.

In the following, we illustrate the dynamical equivalence between various MG theories and scalar-tensor theories.

2.2.2 $f(R)$ theories in the metric variational approach

By introducing an auxiliary field, ϕ, the action (2.1) can be shown to be equivalent to [44; 87]

$$S = \frac{1}{16\pi G_N}\int d^4x\sqrt{-g}\,[f(\phi) + (R-\phi)F(\phi)] + S_m[g_{ab},\psi_m], \tag{2.61}$$

where $F(\phi) = \partial f(\phi)/\partial\phi$. Indeed, if $\partial^2 f/\partial\phi^2 \neq 0$ one can easily verify that the ϕ-field equation is $\phi = R$, which reproduces the original action (2.1). The theories (2.1) and (2.61) are formulated in the Jordan frame. Redefining the field ϕ by $\chi = F(\phi)$ without loss of generality, the action (2.61) takes the form

$$S = \frac{1}{16\pi G_N}\int d^4x\sqrt{-g}\,[\chi R - V(\chi)] + S_m[g_{ab},\psi_m], \tag{2.62}$$

where the potential $V(\chi)$ is defined as

$$V(\chi) \equiv \chi\phi(\chi) - f(\phi(\chi)) = RF(R) - f(R). \tag{2.63}$$

A comparison with (2.44) reveals that the action (2.62) is the action of a Brans-Dicke theory with the BD parameter $\omega_{BD} = 0$. Thus, the $f(R)$ gravity theories in the metric variational approach are dynamically equivalent to a class of Brans-Dicke theories with a potential and vanishing kinetic term [87]. This equivalence holds only for theories where the matter action depends only on g_{ab} and the matter fields ψ_m.

Anticipating the later sections, it is useful to derive the corresponding Einstein frame action here. Consider again the action (2.61). Making a conformal transformation

$$\tilde{g}_{ab} = F g_{ab}, \tag{2.64}$$

where $\phi = R$, the action (2.61) is transformed into the Einstein frame action [92; 93]

$$\begin{aligned} S_E &= \frac{1}{16\pi G_N}\int d^4x\sqrt{-\tilde{g}}\Bigg[\tilde{R} - \frac{3}{2F(\phi)^2}\tilde{g}^{ab}\tilde{\nabla}_a F(\phi)\tilde{\nabla}_b F(\phi) \\ &\quad - \frac{\phi F(\phi) - f(\phi)}{F(\phi)^2}\Bigg] + S_m[F(\phi)^{-1}\tilde{g}_{ab}, \psi_m], \end{aligned} \tag{2.65}$$

where gravity is minimally coupled to the scalar field. Here we have used the relation (2.60). The metric $\tilde{g}_{ab}$ is the Einstein frame metric and quantities with a tilde denote those that are defined using the metric $\tilde{g}_{ab}$. Introducing a canonical scalar field, φ_k, such that

$$\varphi_k = \frac{\sqrt{6}}{16\pi G_N}\ln F(\phi), \tag{2.66}$$

the action (2.65) can be re-written in the more conventional form [87; 93]:

$$S_E = \int d^4x\sqrt{-\tilde{g}}\left(\frac{\tilde{R}}{16\pi G_N} - \frac{1}{2}(\tilde{\nabla}\varphi_k)^2 - V(\varphi_k)\right) + S_m(F(\varphi_k)^{-1}\tilde{g}_{ab}, \psi_m), \tag{2.67}$$

where the potential, $V(\varphi_k)$, is defined using Eq. (2.66) to be

$$V(\varphi_k) \equiv \frac{\phi F(\phi) - f(\phi)}{16\pi G_N F(\phi)^2}. \tag{2.68}$$

In the class of theories (2.67), the scalar field couples to matter with the same strength as gravity.

2.2.3 $f(R)$ theories in the Palatini variational approach

Proceeding in the same way as for the metric case, i.e., by introducing a field, ϕ, into the action (2.16) and then redefining it in terms of χ, leads to the action

$$S = \frac{1}{16\pi G_N}\int d^4x\sqrt{-g}\,[\chi\hat{R} - V(\chi)] + S_m[g_{ab},\psi_m], \tag{2.69}$$

where the potential, $V(\chi)$, is defined in Eq. (2.63). Using the redefinition $\chi = F(\phi)$, the conformal metric (2.27) is expressed as $h_{ab} = \chi g_{ab}$. By using the Eq. (2.37), we may then relate the Ricci scalar of the affine connection, $\hat{R}$, to the Ricci scalar of the metric compatible connection, R, thus:

$$\hat{R} = R + \frac{3}{2\chi^2}(\nabla\chi)^2 - \frac{3}{\chi}\Box\chi. \tag{2.70}$$

Replacing $\hat{R}$ in (2.69) with (2.70) and ignoring the total divergence terms, we have

$$S = \frac{1}{16\pi G_N}\int d^4x\sqrt{-g}\,[\chi R + \frac{3}{2\chi}(\nabla\chi)^2 - V(\chi)] + S_m[g_{ab},\psi_m]. \tag{2.71}$$

Comparison with Eq. (2.44) indicates that the action (2.71) is equivalent to the BD action with $\omega_{BD} = -\frac{3}{2}$. This is a special case of the Brans-Dicke theories where the kinetic term of the BD field vanishes, i.e., the Klein-Gordon equation (2.45) becomes a constraint. This reduction in the number of degrees of freedom is an intrinsic property of Palatini $f(R)$ gravity, which reflects its second-order nature.

2.2.4 General gravity theories based on curvature invariants

Finally, we consider a general class of theories based on the action

$$S = \int d^4x\sqrt{-g}\left(\frac{R}{16\pi G_N} + f(\mathcal{Y})\right), \tag{2.72}$$

where $f(\mathcal{Y})$ is some arbitrary differentiable function of curvature invariants $\mathcal{Y}$. In particular, $\mathcal{Y}$ could take the form

$$\mathcal{Y} = \alpha_1 R^2 + \alpha_2 R^{ab}R_{ab} + \alpha_3 R^{abcd}R_{abcd}, \tag{2.73}$$

where $\alpha_1, \alpha_2, \alpha_3$ are constants. In the case of $\alpha_1 = 1, \alpha_2 = -4, \alpha_3 = 1$, the combination reduces to the GB invariant defined in Eq. (2.53).

Action (2.72) may be expressed in an alternative form by introducing two auxiliary scalar

fields χ and ζ such that

$$S = \int d^4x\sqrt{-g}\left(\frac{R}{16\pi G_N} + \zeta(\mathcal{Y} - \chi) + f(\chi)\right). \tag{2.74}$$

Varying Eq. (2.74) with respect to ζ yields the constraint $\chi = \mathcal{Y}$, thereby reproducing action (2.72). On the other hand, varying the action (2.74) with respect to χ implies that $\zeta = F(\chi)$, where $F(\chi) \equiv \partial f(\chi)/\partial\chi$. Substituting this condition back into Eq. (2.74) then leads to the action

$$S = \int d^4x\sqrt{-g}\left(\frac{R}{16\pi G_N} + F(\chi)(\mathcal{Y} - \chi) + f(\chi)\right). \tag{2.75}$$

It follows, therefore, that the action (2.72) is equivalent to the action

$$S = \int d^4x\sqrt{-g}\left(\frac{R}{16\pi G_N} - V(\phi) - h(\phi)\mathcal{Y}\right), \tag{2.76}$$

where the scalar field, ϕ, is defined implicitly by

$$h(\phi) \equiv -F(\mathcal{Y}) \tag{2.77}$$

for some function $h(\phi)$ and has an effective self-interaction potential

$$V(\phi) \equiv \mathcal{Y}F(\mathcal{Y}) - f(\mathcal{Y}), \tag{2.78}$$

where $F \equiv \partial f/\partial\mathcal{Y}$.

In summary, any generalised gravity theory of the form (2.72) featuring a general function of higher-order curvature invariants can be expressed as a scalar-tensor theory of the form (2.76).

Let us focus on $f(\mathcal{G})$ gravity, defined by (2.54), in which case the action (2.76) becomes

$$S = \int d^4x\sqrt{-g}\left(\frac{R}{16\pi G_N} - V(\phi) - h(\phi)\mathcal{G}\right) + S_m[g_{ab}, \psi_m]. \tag{2.79}$$

Before we proceed to vary the action, it is worth noting that while a term proportional to $\mathcal{G}$ in the gravitational action does not modify the field equations, terms such as $\phi\sqrt{-g}\mathcal{G}$ do so. The reason is that $\phi\delta\sqrt{-g}\mathcal{G}$ is not a total derivative, and therefore can not be eliminated by evaluating it on the boundary [94]. Taking this into account, the variation of (2.79) with

respect to g_{ab} leads to the following field equations [95]

$$\begin{aligned} R^{ab} - g^{ab}R = & - g^{ab}(V(\phi) + h(\phi)\mathcal{G}) + 2h(\phi)RR^{ab} - 2(h(\phi)R)^{;ab} \\ & + 2g^{ab}\Box(h(\phi)R) - 8h(\phi)R^{a}{}_{c}R^{bc} + 4(h(\phi)R^{bc})_{;c}{}^{a} \\ & + 4(h(\phi)R^{ac})_{;c}{}^{b} - 4\Box(h(\phi)R^{ab}) - 4g^{ab}(h(\phi)R^{cd})_{;cd} \\ & + 2h(\phi)R^{acde}R^{b}{}_{cde} - 4(h(\phi)R^{acdb})_{;cd} + T^{ab}_{m}. \end{aligned} \tag{2.80}$$

The equation of motion for the scalar field is given by

$$V_{,\phi}(\phi) + h_{,\phi}(\phi)\mathcal{G} = 0 \tag{2.81}$$

and is an algebraic relation between ϕ and $\mathcal{G}$. Therefore, the scalar field dynamics is inferred from the derivatives of the Gauss-Bonnet coupling $h(\phi)$ in the field equations (2.80). Furthermore, the fourth-order nature of the theory can be straightforwardly deduced by recalling that $h(\phi) = -F(\mathcal{G})$.

Following Ref. [95] we use the relations:

$$\begin{aligned} R_{ceab}{}^{;c} &= R_{be;a} - R_{ae;b} \\ R_{ca}{}^{;c} &= \frac{1}{2}R_{;a} \\ R^{acbd}{}_{;cd} &= \Box R^{ab} - R^{ac}{}_{;c}{}^{b} \\ R^{ac}{}_{;c}{}^{b} &= \frac{1}{2}R^{;ab} - R^{acbd}R_{cd} + R^{a}{}_{c}R^{bc} \\ R^{ab}{}_{;ab} &= \frac{1}{2}\Box R, \end{aligned} \tag{2.82}$$

obtained through the Bianchi identities, to re-write the field equations (2.80) in the form

$$\begin{aligned} R^{ab} - g^{ab}R = & - g^{ab}(V(\phi) + h(\phi)\mathcal{G}) + 2h(\phi)RR^{ab} + 4h(\phi)R^{a}{}_{c}R^{bc} \\ & - 2h(\phi)R^{acde}R^{b}{}_{cde} - 4h(\phi)R^{acdb}R_{cd} - 2Rh(\phi)^{;ab} \\ & + 2g^{ab}R\Box h(\phi) + 4R^{bc}h(\phi)_{;c}{}^{a} + 4R^{ac}h(\phi)_{;c}{}^{b} \\ & - 4R^{ab}\Box h(\phi) - 4g^{ab}R^{cd}h(\phi)_{;cd} + 4R^{acbd}h(\phi)_{;cd} + T^{ab}_{m}. \end{aligned} \tag{2.83}$$

It follows that since the standard field equations of GR must be recovered when $h(\phi) = \text{constant}$, only those terms involving derivatives of $h(\phi)$ arise in the r.h.s of Eq. (2.83). This implies that [94]

$$\begin{aligned} R^{ab} - \frac{1}{2}g^{ab}R = & - g^{ab}V(\phi) - 2Rh(\phi)^{;ab} + 2g^{ab}R\Box h(\phi) \\ & + 4R^{bc}h(\phi)_{;c}{}^{a} + 4R^{ac}h(\phi)_{;c}{}^{b} - 4R^{ab}\Box h(\phi) \\ & - 4g^{ab}R^{cd}h(\phi)_{;cd} + 4R^{acbd}h(\phi)_{;cd} + T^{ab}_{m}. \end{aligned} \tag{2.84}$$

2.3 Cosmological equations

In this section, following a brief review of FLRW cosmology, the field equations for the MG theories corresponding to a flat FLRW universe sourced by a perfect barotropic fluid are presented.

2.3.1 Friedmann-Lemaitre-Robertson-Walker cosmology

In spherical polar coordinates the FLRW metric is given by the line element

$$ds^2 = -dt^2 + a^2(t)\left[\frac{dr^2}{1-\mathcal{K}r^2} + r^2(d\theta^2 + sin^2(\theta)d\phi^2)\right], \tag{2.85}$$

where t is cosmic time, $a(t)$ is the normalised scale factor and $\mathcal{K}$ describes the geometry of the universe, i.e., $\mathcal{K} = \{+1, 0, -1\}$ corresponds to a closed, flat or open geometry, respectively. The source of the energy-momentum tensor is modelled as a perfect barotropic fluid, specified by an energy density ρ and an isotropic pressure p, i.e.,

$$T_{ab} = (\rho + p)u_a u_b + p g_{ab}, \tag{2.86}$$

where u^a denotes the comoving fluid four-velocity. The Einstein equations,

$$R_{ab} - \frac{1}{2}g_{ab}R = 8\pi G_N T_{ab}, \tag{2.87}$$

in this case reduce to the Friedmann equation:

$$H^2 \equiv \left(\frac{\dot{a}}{a}\right)^2 = \frac{8\pi G_N}{3}\rho - \frac{\mathcal{K}}{a^2}, \tag{2.88}$$

where H is the Hubble parameter and a dot denotes differentiation with respect to cosmic time, and the Raychaudhuri equation

$$\frac{\ddot{a}}{a} = -\frac{4\pi G_N}{3}(\rho + 3p). \tag{2.89}$$

The conservation of energy-momentum, following from the Bianchi identities, leads to the continuity equation

$$\dot{\rho} + 3H(\rho + p) = 0. \tag{2.90}$$

We note that only two of the equations (2.88)-(2.90) are independent. Using the continuity equation with either the Friedmann or Raychaudhuri equation, the remaining equation can always be derived.

The Friedmann equation (2.88) can be written in the dimensionless form:

$$\Omega(t) = 1 + \frac{\mathcal{K}}{a^2 H^2}, \tag{2.91}$$

where $\Omega(t) \equiv \rho(t)/\rho_c(t)$ is the dimensionless energy density parameter and the critical energy density is defined as $\rho_c(t) \equiv 3H^2(t)/8\pi G_N$. Clearly the spatial geometry of the universe depends on the amount of matter present, i.e., $\Omega > 1$, $\Omega = 1$ and $\Omega < 1$ correspond to a closed, flat and open geometry of the universe, respectively. The recent WMAP observations [1] indicate that our universe is very close to being spatially flat. Therefore, we shall assume $\mathcal{K} = 0$ in what follows.

The energy density and pressure of a barotropic perfect fluid are related by the equation of state (e.o.s) parameter defined by

$$w = p/\rho. \tag{2.92}$$

We will assume w to be constant. In this case, integrating the Friedmann equation (2.88) along with the equation

$$\dot{H} = -4\pi G_N(\rho + p), \tag{2.93}$$

we obtain

$$a(t) \propto t^{\frac{2}{3(1+w)}} \qquad \text{and} \qquad \rho(t) \propto a^{-3(1+w)}. \tag{2.94}$$

The special cases $w = 1/3$ and $w = 0$ correspond to radiation and dust, respectively. In this context, a more useful form of equation (2.89) is

$$\frac{\ddot{a}}{a} = -\frac{4\pi G_N}{3}\rho(1 + 3w). \tag{2.95}$$

This implies that both a radiation and a dust filled universe lead to a decelerated cosmic expansion. To accommodate for the current phase of accelerated expansion, the dominant fluid in the universe (at present) must violate the strong energy condition: $\rho + 3p \geq 0$. Consider, for example, the simplest modification to Einstein's theory given by the addition of a cosmological constant to the field equations. Assuming that such a term behaves like a perfect fluid, it can readily be seen from Eq. (2.90) that the e.o.s. should be $w_\Lambda = -1$. With this correction the Friedmann equation becomes

$$H^2 = \frac{8\pi G_N}{3}(\rho + \rho_\Lambda), \tag{2.96}$$

and

$$\frac{\ddot{a}}{a} = -\frac{4\pi G_N}{3}(\rho + 3p - 2\rho_\Lambda), \tag{2.97}$$

where $\rho_\Lambda \equiv \Lambda/8\pi G_N$. This clearly demonstrates that the cosmological constant contributes negatively to the pressure term and therefore exhibits a repulsive effect.

2.3.2 Cosmological equations for MG theories

In order to compute the Friedmann equations for the MG theories discussed above, it is worth recalling that the non-zero components of the Levi-Civita connection are

$$\Gamma^0_{ij} = a\dot{a}\delta_{ij}\ , \qquad \Gamma^i_{0j} = \frac{\dot{a}}{a}\delta^i{}_j, \tag{2.98}$$

where the indices i, j and (later) k are summed from 1 to 3 (the so-called spatial components). The non-zero components of the Ricci tensor that depend on the metric are

$$R_{00}(g) = -3\frac{\ddot{a}}{a}\ , \qquad R_{ij}(g) = (\ddot{a} + 2\dot{a}^2)\delta_{ij}. \tag{2.99}$$

Since $F(R)$ is a scalar quantity, the covariant derivative of F is just the partial derivative: $F_{,a}$. This means, for example, that $F_{;ab} = F_{,ab} - \Gamma^c_{ab}F_{,c}$. Moreover, due to spatial homogeneity the Ricci scalar, R, is a function of time only, so $F_{,i} = 0$. Below we summarise the cosmological equations for each modified gravity theory in turn. For simplicity, we set $8\pi G_N = 1$ and restore it when it makes the discussions more transparent.

- $f(R)$ **gravity in the metric formulation**

  The time-time component of the field equations (2.14) leads to [37]

$$3FH^2 = \rho + \frac{1}{2}(FR - f) - 3H\dot{F}\,, \tag{2.100}$$

which replaces the usual Friedmann equation (2.88), recovered by setting $f = R$. The space-space components of (2.14) lead to the other independent field equation,

$$-2F\dot{H} = (\rho + p) + \ddot{F} - H\dot{F}\,. \tag{2.101}$$

The curvature scalar satisfies the following relation:

$$R = 6(2H^2 + \dot{H}). \tag{2.102}$$

- $f(R)$ **gravity in the Palatini formulation**

Consider the following combination of components [80]: $\hat{R}_{00} + \frac{3}{a^2}\hat{R}^k_k$. Using Eq. (2.36) this combination equals

$$6H^2 + \frac{3}{2}\left(\frac{\dot{F}}{F}\right)^2 + 6H\frac{\dot{F}}{F}\,. \tag{2.103}$$

On the other hand, by using the field equations (2.19), it can be shown that this combination is equivalent to

$$\frac{f}{F} + \frac{\rho + 3p}{F}\,. \tag{2.104}$$

Equating expressions (2.103) and (2.104) therefore leads to the Friedmann equation:

$$6F\left(H + \frac{\dot{F}}{2F}\right)^2 - f = \rho + 3p\,. \tag{2.105}$$

The curvature scalar is given by

$$R = 6(2H^2 + \dot{H}) + \frac{3}{F}\left(\ddot{F} + 3H\dot{F} - \frac{\dot{F}^2}{2F}\right). \tag{2.106}$$

In the Palatini formalism it is possible, for $w = 0$, to express the Hubble parameter as a function of R only. For this purpose we require an expression for $\dot{R}$ in order to eliminate the time derivatives of F on the left hand side of Eq. (2.105). Taking the time derivative of the trace equation,

$$FR - 2f = -\rho + 3p\,, \tag{2.107}$$

and substituting for the resulting $\dot{\rho}$ term using the continuity equation (2.90), we obtain

$$\dot{R} = -\frac{3H}{F - RF_{,R}}(\rho + p)\,(1 - 3w)\ . \tag{2.108}$$

To derive this equation we used the relation $\dot{p}/\dot{\rho} = w = \mathrm{const}$ for a barotropic fluid. In the matter dominated era (where $p_m = w = 0$) an expression for $H(R)$ follows from Eqs. (2.105) and (2.108):

$$H^2 = \frac{3f - RF}{6F}\left(1 - \frac{3}{2}\frac{F_{,R}(2f - RF)}{F(F - RF_{,R})}\right)^{-2}\ . \tag{2.109}$$

- **Scalar-tensor gravity**

The generalised field equations (2.40) reduce to the Friedmann and Raychaudhuri equations

$$3FH^2 = \rho + \frac{1}{2}(Z\dot{\phi}^2 - 6H\dot{F} + V) \tag{2.110}$$

and

$$-2F\dot{H} = (\rho + p) + Z\dot{\phi}^2 + \ddot{F} - H\dot{F}\,, \tag{2.111}$$

respectively. The equation of motion for the scalar field ϕ follows from (2.43) and is given by

$$Z(\ddot{\phi} + 3H\dot{\phi}) \;\; = \;\; 3F_{,\phi}(\dot{H} + 2H^2) - \frac{1}{2}Z_{,\phi}\dot{\phi}^2 - \frac{1}{2}V_{,\phi}. \tag{2.112}$$

- $f(\mathcal{G})$ **gravity**

The time-time component of the field equations (2.56) leads to the Friedmann equation

$$3H^2 = \mathcal{G}F - f - 24H^3\dot{F} + \rho\,. \tag{2.113}$$

The scalar curvature and Gauss-Bonnet invariant $\mathcal{G}$ satisfy the following relations

$$R = 6(2H^2 + \dot{H}) \tag{2.114}$$

and

$$\mathcal{G} = 24H^2(H^2 + \dot{H}), \tag{2.115}$$

respectively. It is worth mentioning that all of the modified gravity theories presented here satisfy the continuity equation (2.90).

2.4 Cosmological Perturbations

Here, we briefly review the basic features of relativistic perturbation theory in the context of the FLRW space-time. We briefly discuss the *gauge problem* in first-order perturbation theory and then proceed to state the governing evolution equations for the cosmological perturbations that will be required in subsequent chapters.

2.4.1 Metric and matter perturbations

Although the flat FLRW spacetime is a good approximation of the Universe, a more precise description requires anisotropies and inhomogeneities. In order to describe such features we employ a perturbative approach, where the departure from homogeneity and isotropy is characterised by small perturbations about the FLRW background. This leads to observable quantities being decomposed into homogeneous background and inhomogeneous perturbation contributions. As an essential feature of this analysis, we assume that the deviations from homogeneity and isotropy have been small during most of the history of the universe, so that they can be treated as first-order effects [96].

The metric tensor, which has ten independent components, is decomposed into background ($\bar{g}_{ab}$) and perturbation (δg_{ab}) parts such that

$$g_{ab} = \bar{g}_{ab} + \delta g_{ab}. \tag{2.116}$$

In this case, the line-element can be expressed as

$$\begin{aligned} ds^2 &= -(1+2\alpha)dt^2 - 2a(t)(b_{,i} + \beta_i)dtdx^i \\ &\quad + a^2(t)[(1+2\varphi)\delta_{ij} + 2E_{|ij} + c_{(i|j)} + h_{ij}]dx^i dx^j, \end{aligned} \tag{2.117}$$

where a vertical-bar subscript denotes a covariant derivative with respect to the spatial three-metric $g^{(3)}_{ij}$. It proves useful to classify the metric perturbations according to their transformational properties under spatial transformations. Following the terminology of Bardeen [97], the perturbations can be labelled as scalar, vector or tensor. In linear perturbation theory this is particularly useful because the governing equations decouple, which implies that each can be solved separately [67]. The metric perturbations are decomposed as follows: the four linear scalar perturbations are α, b, φ and E; the divergenceless 3-vector fields β_i and c_i contribute four vector degrees of freedom; and the symmetric, transverse and traceless 3-tensor, h_{ij}, which describes gravitational waves, contributes two tensor degrees of freedom.

The main purpose of considering perturbations in the present context is to study the formation of large-scale structure. For this purpose, only the scalar perturbations contribute

significantly. The vectors are exponentially suppressed in the early universe[3], and the tensor modes make only a small, but important, contribution to the B-mode of the CMB polarisation. Consequently, we restrict our attention to the four scalar metric perturbations, in which case the perturbed line-element (2.117) reduces to

$$ds^2 = -(1+2\alpha)dt^2 - 2a(t)b_{,i}dtdx^i + a^2(t)[(1+2\varphi)\delta_{ij} + 2E_{|ij}]dx^i dx^j. \qquad (2.118)$$

In general, linearly perturbing the energy-momentum tensor sourced by a fluid with energy density ρ, isotropic pressure p, and 4-velocity u^a, gives

$$\begin{aligned} T^0_{\ 0} &= -(\rho+\delta\rho), \quad T^0_{\ i} = (\rho+p)(V_i - b_{,i}), \qquad (2.119)\\ T^i_{\ j} &= (p+\delta p)\delta^i_{\ j} + \Pi^i_j, \end{aligned}$$

where the 3-velocity V_i comes from the spatial part of the perturbed 4-velocity. The vector quantity V_i can always be split into a scalar part (velocity potential V) and and a vector part (V_i^{vec}) such that $V_i = V_{,i} + V_i^{vec}$. Similarly, the anisotropic stress, Π^i_j, has terms originating from scalar, vector and tensor contributions. As before, we only consider the irrotational scalar perturbations because these are the components relevant for structure formation. Furthermore, because we consider a pressureless fluid (with a barotropic equation of state) as the matter source, by definition $p = \delta p = \Pi^i_j = 0$. Hence, the components of the energy-momentum tensor reduce to

$$T^0_{\ 0} = -(\rho_m + \delta\rho_m), \quad T^0_{\ i} = \rho_m(V-b)_{,i} \equiv -\rho_m v_{m,i}\,, \quad T^i_{\ j} = 0, \qquad (2.120)$$

where we have introduced the scalar velocity perturbation, v_m, which is related to the velocity potential through [98]:

$$v_m = -(V-b). \qquad (2.121)$$

If we consider the perturbed variables in Fourier space where, for example, a perturbed variable σ is written as a Fourier series

$$\sigma = \sum \sigma_{\mathbf{k}}(t)e^{i\mathbf{k}\cdot\mathbf{x}},$$

we find that each $\mathbf{k}$-mode evolves independently. Ignoring the $\mathbf{k}$ subscripts for notational simplicity, the matter perturbation can be shown to satisfy the following equations of motion

[3]It is well known that in an expanding FLRW universe (sourced by a perfect fluid with $\Pi^i_j = 0$), first-order metric vector perturbations decay and hence rapidly become insignificant.

[81; 99; 100; 69]

$$\dot{v}_m + Hv_m = \frac{1}{a}\alpha\,, \tag{2.122}$$

$$\delta\dot{\rho}_m + 3H\delta\rho_m = \rho_m\left(\kappa - 3H\alpha - \frac{k^2}{a}v_m\right)\,, \tag{2.123}$$

where k is a comoving wavenumber,

$$\kappa \equiv 3(H\alpha - \dot{\varphi}) + \frac{k^2}{a^2}\chi\,, \tag{2.124}$$

and

$$\chi \equiv a(b + a\dot{E}). \tag{2.125}$$

If we now define the following variables

$$v \equiv av_m = -a(V - b)\,, \quad \delta \equiv \frac{\delta\rho_m}{\rho_m}\,, \tag{2.126}$$

where v is a covariant velocity perturbation [101], Eqs. (2.123) and (2.122) can be written as

$$\dot{\delta} = \kappa - 3H\alpha - \frac{k^2}{a^2}v\,, \tag{2.127}$$

$$\alpha = \dot{v}\,. \tag{2.128}$$

As will be explained in the next subsection, in order to avoid the *gauge problem* associated with perturbation theory, it is necessary to consider gauge-invariant quantities only. Choosing a comoving orthogonal hypersurface, the density perturbation can be expressed in a gauge-invariant way as [98]:

$$\delta\tilde{\rho}_m = \delta\rho_m + a\dot{\rho}_m(V - b)\,. \tag{2.129}$$

We shall define the density contrast on comoving orthogonal hypersurfaces as

$$\delta_m = \frac{\delta\rho_m}{\rho_m} + 3Hv\,. \tag{2.130}$$

It then follows that since the right hand side of Eq. (2.130) is gauge-invariant, δ_m can be evaluated in any gauge and the evolution equation for δ_m is then given by

$$\ddot{\delta}_m + 2H\dot{\delta}_m + \frac{k^2}{a^2}(\alpha - \dot{\chi}) = 3\ddot{B} + 6H\dot{B}\,, \tag{2.131}$$

where $B = Hv - \varphi$.

2.4.2 Coordinate transformations

A central feature of general relativity is that it is covariant under diffeomorphisms. This covariance is broken under the *non-covariant* procedure of splitting quantities into background and perturbation parts, which can lead to the latter becoming coordinate dependant [67]. Quantities such as the line-element, ds^2, and the energy density, ρ, however, remain invariant regardless of the choice of coordinates. This provides a relation between two coordinate systems, which allows us to deduce how the perturbed quantities will transform once a gauge transformation has been specified[4] [67].

To elucidate this, let us consider the first-order gauge transformation

$$\tilde{x}^a = x^a + \theta^a, \tag{2.132}$$

where quantities with a tilde represent those in the new coordinate system, and θ^0 determines the choice of temporal gauge. We require the line-element to satisfy

$$ds^2 = g_{ab}dx^a dx^b = \tilde{g}_{ab}d\tilde{x}^a d\tilde{x}^b, \tag{2.133}$$

which relates the two metric tensors g_{ab} and $\tilde{g}_{ab}$. Perturbing the right hand side of Eq. (2.133) using the expansions of (2.132), the line element in the new coordinate system can be expressed as [98]

$$\begin{aligned} ds^2 = &- (1+2\tilde{\alpha})d\tilde{t}^2 - 2a(\tilde{t})(\tilde{b}_{,i} + \tilde{\beta}_i)d\tilde{t}d\tilde{x}^i \\ &+ a^2(\tilde{t})[(1+2\tilde{\varphi})\delta_{ij} + 2\tilde{E}_{|ij} + \tilde{c}_{(i|j)} + \tilde{h}_{ij}]d\tilde{x}^i d\tilde{x}^j, \end{aligned} \tag{2.134}$$

where the tilded perturbation variables are expressible in terms of combinations of the original (untilded) metric perturbations and components of θ^a and $\dot{\theta}^a$. A similar analysis reveals that the perturbation $\delta\rho_m$ transforms as [67]

$$\delta\tilde{\rho}_m = \delta\rho_m + \theta^0\dot{\rho}_m\,. \tag{2.135}$$

In summary, gauge transformations can induce gauge dependencies in perturbed quantities.

Consequently, Bardeen [97] proposed that only variables that are explicitly gauge-invariant should be considered. By construction, such variables would eliminate the effects of gauge modes induced by gauge transformations. Considering the scalar metric perturbations, the idea essentially is to use the temporal and spatial gauge transformations (θ^0 and θ^i, respectively) to substitute for two of the scalar metric perturbations, thus allowing for the construction of two gauge-invariant combinations [67]. Hence, we replace the gauge-dependant metric perturbations b and E, with the spatially gauge-invariant combinations χ and κ, de-

[4] This is referred to as the *'passive approach to gauge transformations'* in Ref. [67].

fined in Eqs. (2.125) and (2.124), respectively [102]. We thus have a set of quantities: α, χ, φ and κ, that are spatially gauge-invariant, of which only three are independent. The advantage of using these variables is that by writing equations in terms of them, we can conveniently fix the gauge degrees of freedom by setting specific metric perturbations to zero [79]. For example, the longitudinal gauge would correspond to $\chi = 0$.

Here we are interested in the quantity δ_m, which is defined in a gauge-invariant way in the comoving orthogonal gauge in Eq. (2.130). In what follows, we evaluate the gauge invariant combination on the right hand side of Eq. (2.130), for three different gauge choices that are relevant for this study.

- **Comoving gauge:** in which the spatial hypersurfaces correspond to those where the 3-velocity and the scalar shift function vanish (i.e., $v = 0$). This implies that along with the 3-velocity the momentum vanishes as well [97]. Thus the gauge-invariant δ_m in this gauge becomes

$$\delta_m^{(v)} = \left.\frac{\delta\rho_m}{\rho_m}\right|_{v=0} . \tag{2.136}$$

- **Longitudinal gauge:** in which one chooses to work on spatial hypersurfaces with vanishing shear, i.e., the shift vector, b, and the anisotropic potential, E, both vanish, resulting in $\chi = 0$ [103; 104]. The gauge-invariant δ_m in this gauge is

$$\delta_m^{(\chi)} = \left.\frac{\delta\rho_m}{\rho_m} + 3Hv\right|_{\chi=0} . \tag{2.137}$$

- **Uniform density gauge:** in which one defines perturbed quantities on constant density hypersurfaces, i.e. $\delta\rho_m = 0$ [105]. The gauge-invariant δ_m in this gauge is

$$\delta_m^{(\delta)} = \left.3Hv\right|_{\delta\rho_m=0} . \tag{2.138}$$

The latter gauge choice does not imply that the matter perturbation vanishes, it is just carried by other perturbation quantities; in this case by the covariant velocity perturbation v. Detailed and comprehensive reviews of first-order perturbation theory can be found in a number of publications, including Refs. [67; 102; 103; 104; 106; 107].

2.4.3 Field equations for scalar perturbations

In this subsection we present the equations in Fourier space that govern the evolution of scalar perturbations set out in Sec. 2.4.1. Essentially, these equations correspond to components of the linearised field equations for the particular theories at hand. The equations

are presented in a gauge-invariant (also known as gauge-ready [102]) formalism where the temporal gauge condition is unspecified.

- **General scalar-tensor theories**

We begin with a slightly revised form of the general scalar-tensor action (2.38):

$$S = \int \mathrm{d}^4x\sqrt{-g}\left[\frac{1}{2}f(\phi,R) - \frac{1}{2}\omega(\phi)(\nabla\phi)^2 - V(\phi)\right] + S_m(g_{\mu\nu},\psi_m)\,, \tag{2.139}$$

where we have set $8\pi G_N = 1$. The perturbed field equations in this case have been derived in Ref. [99]. The energy constraint (the G^0_0 component of the field equations) for this generalised gravity theory is

$$-\frac{k^2}{a^2}\varphi + H\kappa = -\frac{1}{2F}\left[\omega\dot\phi\delta\dot\phi + \frac{1}{2}[\omega_{,\phi}\dot\phi^2 - (f-2V)_{,\phi}]\delta\phi + \right. \tag{2.140}$$
$$\left.\left(3\dot H + 3H^2 - \frac{k^2}{a^2}\right)\delta F - 3H\delta\dot F + (3H\dot F - \omega\dot\phi^2)\alpha + \dot F\kappa + \delta\rho_m\right].$$

The momentum constraint (the G^0_i component of the field equations) is

$$\kappa - \frac{k^2}{a^2}\chi = \frac{3}{2F}\left(\omega\dot\phi\delta\phi + \delta\dot F - H\delta F - \dot F\alpha + \rho_m v\right)\,. \tag{2.141}$$

The shear propagation equation (the $G^i_j - \frac{1}{3}\delta^i_j G^0_0$ component) is given by

$$\dot\chi + \left(H + \frac{\dot F}{F}\right)\chi - \alpha - \varphi = \frac{\delta F}{F}. \tag{2.142}$$

The Raychaudhuri equation (the $G^i_i - G^0_0$ component) is

$$\begin{aligned}\dot\kappa \;+\; & \left(2H + \frac{\dot F}{2F}\right)\kappa + \frac{3\dot F}{2F}\dot\alpha + \left(3\dot H + \frac{1}{2F}(6\ddot F + 3H\dot F + 4\omega\dot\phi^2) - \frac{k^2}{a^2}\right)\alpha \qquad (2.143)\\ = \;& \frac{1}{2F}\left[4\omega\dot\phi\delta\dot\phi + [2\omega_{,\phi}\dot\phi^2 + (f-2V)_{,\phi}]\delta\phi + \left(\frac{k^2}{a^2} - 6H^2\right)\delta F\right.\\ & \left. +3H\delta\dot F + 3\delta\ddot F + \delta\rho_m\right].\end{aligned}$$

The trace equation (the G^i_i component) is

$$\begin{aligned}\delta\ddot F \;+\; & 3H\delta\dot F + \left(\frac{k^2}{a^2} - \frac{R}{3}\right)\delta F + \frac{2}{3}\omega\dot\phi\delta\dot\phi + \frac{1}{3}[\omega_{,\phi}\dot\phi^2 + 2(f-2V)_{,\phi}]\delta\phi \qquad (2.144)\\ = \;& \frac{1}{3}\delta\rho_m + \dot F(\kappa+\dot\alpha) + \left(\frac{2}{3}\omega\dot\phi^2 + 2\ddot F + 3H\dot F\right)\alpha - \frac{1}{3}F\delta R\,,\end{aligned}$$

where the perturbed scalar curvature is given by

$$\delta R = 2\left[-\dot{\kappa} - 4H\kappa + \left(\frac{k^2}{a^2} - 3\dot{H}\right)\alpha + 2\frac{k^2}{a^2}\varphi\right] . \tag{2.145}$$

Finally, the scalar field equation of motion is

$$\begin{aligned} & \delta\ddot{\phi} + \left(3H + \frac{\omega_{,\phi}}{\omega}\dot{\phi}\right)\delta\dot{\phi} + \left[\frac{k^2}{a^2} + \left(\frac{\omega_{,\phi}}{\omega}\right)_{,\phi}\frac{\dot{\phi}^2}{2} + \left(\frac{(2V-f)_{,\phi}}{2\omega}\right)_{,\phi}\right]\delta\phi \\ = \; & \dot{\phi}(\kappa + \dot{\alpha}) + \left(2\ddot{\phi} + 3H\dot{\phi} + \frac{\omega_{,\phi}}{\omega}\dot{\phi}^2\right)\alpha + \frac{1}{2\omega}F_{,\phi}\delta R\,. \end{aligned} \tag{2.146}$$

- $f(R)$ **theories in the metric formalism**

By eliminating the contributions from the scalar field, ϕ, in the equations of section 2.4.3, one can readily derive the perturbed field equations for $f(R)$ gravity theories. The energy constraint reduces to [99]

$$\begin{aligned} - \; & \frac{k^2}{a^2}\varphi + 3H(H\alpha - \dot{\varphi}) + \frac{k^2}{a^2}H\chi \\ = \; & \frac{1}{2F}\left[3H\delta\dot{F} - \left(3\dot{H} + 3H^2 - \frac{k^2}{a^2}\right)\delta F - 3H\dot{F}\alpha - \dot{F}\kappa - \delta\rho_m\right] , \end{aligned} \tag{2.147}$$

and the momentum constraint becomes

$$H\alpha - \dot{\varphi} = \frac{1}{2F}\left[\delta\dot{F} - H\delta F - \dot{F}\alpha + \rho_m v\right] . \tag{2.148}$$

The shear propagation equation is given by

$$\dot{\chi} + H\chi - \alpha - \varphi = \frac{1}{F}(\delta F - \dot{F}\chi)\,, \tag{2.149}$$

and the Raychaudhuri equation takes the form

$$\begin{aligned} & \dot{\kappa} + 2H\kappa + \left(3\dot{H} - \frac{k^2}{a^2}\right)\alpha = \frac{1}{2F}\left[\left(-6H^2 + \frac{k^2}{a^2}\right)\delta F\right. \\ & \left. +3H\delta\dot{F} + 3\delta\ddot{F} - \dot{F}\kappa - 3(2\ddot{F} + H\dot{F})\alpha - 3\dot{F}\dot{\alpha} + \delta\rho_m\right]. \end{aligned} \tag{2.150}$$

Finally, the trace equation is

$$\begin{aligned} & \delta\ddot{F} + 3H\delta\dot{F} + \left(\frac{k^2}{a^2} - \frac{R}{3}\right)\delta F = \\ & \frac{1}{3}\delta\rho_m + \dot{F}(\kappa + \dot{\alpha}) + (2\ddot{F} + 3H\dot{F})\alpha - \frac{1}{3}F\delta R\,. \end{aligned} \tag{2.151}$$

- $f(R)$ **theories in the Palatini formalism**

Here we present the $f(R)$ field equations for scalar perturbations in the Palatini formalism [69; 79]. More details are given in Appendix A.1. The energy constraint is

$$-\frac{k^2}{a^2}\varphi + \left(H + \frac{\dot{F}}{2F}\right)\kappa + \frac{1}{2F}\left(\frac{3\dot{F}^2}{2F} + 3H\dot{F}\right)\alpha$$
$$= \frac{1}{2F}\left[\left(3H^2 - \frac{3\dot{F}^2}{4F^2} - \frac{R}{2} + \frac{k^2}{a^2}\right)\delta F + \left(\frac{3\dot{F}}{2F} + 3H\right)\delta\dot{F} - \delta\rho_m\right], \qquad (2.152)$$

and the momentum constraint is

$$H\alpha - \dot{\varphi} = \frac{1}{2F}\left[\delta\dot{F} - \left(H + \frac{3\dot{F}}{2F}\right)\delta F - \dot{F}\alpha + \rho_m v\right]. \qquad (2.153)$$

The shear propagation equation corresponds to

$$\dot{\chi} + H\chi - \alpha - \varphi = \frac{1}{F}(\delta F - \dot{F}\chi), \qquad (2.154)$$

and the Raychaudhuri equation is

$$\dot{\kappa} + \left(2H + \frac{\dot{F}}{2F}\right)\kappa + \left(3\dot{H} + \frac{3\ddot{F}}{F} + \frac{3H\dot{F}}{2F} - \frac{3\dot{F}^2}{F^2} - \frac{k^2}{a^2}\right)\alpha + \frac{3}{2}\frac{\dot{F}}{F}\dot{\alpha} \qquad (2.155)$$
$$= \frac{1}{2F}\left[\delta\rho_m + \left(6H^2 + 6\dot{H} + \frac{3\dot{F}^2}{F^2} - R + \frac{k^2}{a^2}\right)\delta F + \left(3H - \frac{6\dot{F}}{F}\right)\delta\dot{F} + 3\delta\ddot{F}\right].$$

Finally, the trace equation is

$$R\delta F - F\delta R = -\delta\rho_m. \qquad (2.156)$$

Chapter 3

Cosmological perturbations in Palatini-modified gravity

In addition to the standard procedure employed in relativistic perturbation theory for studying cosmological perturbations, outlined in Sections 2.4, an alternative procedure has recently been developed. This alternative, put forward by Lue, Scoccimarro and Starkman (LuSS) [108], employs a generalised version of Birkhoff's theorem (see also Ref. [109]). This procedure has the benefit of greatly simplifying the analysis, but suffers from the drawback that the degree of its applicability in more general settings is presently not known in detail.

Here, the aim is to perform a detailed comparative study of the evolution of perturbations obtained by employing the LuSS procedure and the direct linearisation of the field equations [68]. Such a comparison can serve as a crucial step in clarifying the status of the LuSS approach in non-linear gravity theories. In the following, we consider $f(R)$ theories based on the Palatini variational method.

3.1 The evolution of density perturbations

In conventional cosmology, there exists an interesting equivalence between the Newtonian and general relativistic frameworks. Both approaches result in identical background evolution equations (i.e. Friedmann equations) as well as evolution equations for the scalar perturbations. The former coincidence results from the fact that there is an analogue of Newton's sphere theorem in general relativistic settings, i.e., Birkhoff's theorem holds. The correspondence for the evolution of perturbations arises in the absence of vector and tensor fluctuations.

Recently, a procedure has been put forward by Lue, Scoccimarro and Starkman [108] which relies on the assumption that this Newtonian analogy, including Birkhoff's theorem, holds in the more general setting of modified gravity theories. According to this procedure,

it is assumed that the growth of large-scale structure can be modelled in terms of a uniform sphere of dust of constant mass, such that the evolution inside the sphere is determined by the FLRW metric. Using Birkhoff's theorem, the spacetime metric in the empty exterior is then taken to be Schwarzschild-like. The components of the exterior metric are then uniquely determined by smoothly matching the interior and exterior regions.

The overdensity $\delta_m(t)$ of the spherical distribution of pressureless matter with mass M and radius r is defined by[1]

$$1 + \delta_m(t) \equiv \frac{3M}{4\pi\rho r^3}\,. \tag{3.1}$$

The matching conditions (relating the Schwarzschild radius, r, to the interior cosmic evolution) imply that $\ddot{r} = r(H^2 + \dot{H})$ and the evolution of the density perturbation is then given by [108; 110]

$$\ddot{\delta}_m + 2H\dot{\delta}_m - \left(2\dot{H} + \frac{\ddot{H}}{H}\right)\delta_m = 0, \tag{3.2}$$

or, equivalently, by

$$\delta_{m,\tau\tau} + \mathcal{H}\delta_{m,\tau} - \left(\frac{\mathcal{H}_{,\tau\tau}}{\mathcal{H}} - 2\mathcal{H}_{,\tau}\right)\delta_m = 0, \tag{3.3}$$

where $\tau \equiv \int \frac{dt}{a(t)}$ defines the conformal time and $\mathcal{H} \equiv aH = \dot{a}$. Eq. (3.3) can also be derived by assuming that the continuity and Friedmann equations apply directly to the fluctuations [109].

Recently, the evolution of perturbations in $f(R)$ gravity was investigated using the LuSS procedure [108; 111]. The advantage of this approach is that the growth of the density contrast can be expressed in terms of a single quadrature involving the Hubble parameter and the scale factor [108]:

$$\delta_m \propto H \int \frac{dt}{a^2 H^2}. \tag{3.4}$$

In principle, therefore, the evolution of the perturbations can be determined once the background dynamics has been specified. However, the validity of the LuSS procedure has yet to be established in generalised gravity. It is important, therefore, to compare this approach with the method that directly linearises the gravitational field equations.

To this aim, let us consider the perturbations defined on constant density hypersurfaces

[1] While this definition is not related to the gauge invariant combination, Eq. (2.130), it clearly coincides with the density contrats defined in Eq. (2.136). We therefore choose to keep this notation and note that this will be of use later when we compare the two approaches for studying density perturbations.

($\delta\rho_m = 0$) where

$$\delta F = \delta R = 0,$$

from Eq. (2.156) and Eq. (4.107), and

$$\dot{v} = \alpha, \qquad \kappa = 3H\dot{v} + \frac{k^2}{a^2}v,$$

from Eqs. (2.127) and (2.128). Substituting these relations for the subsequent terms in Eq. (2.155), and using Eq. (2.106) to rewrite R, we obtain

$$\begin{aligned} 3\left(H + \frac{\dot{F}}{2F}\right)\ddot{v} \quad &+ \quad \left(6H^2 + 6\dot{H} + \frac{3\ddot{F}}{F} + \frac{3H\dot{F}}{F} - \frac{3\dot{F}^2}{F^2}\right)\dot{v} \\ &+ \quad \frac{\dot{F}}{2F}\frac{k^2}{a^2}v = 0\,. \end{aligned} \tag{3.5}$$

It then follows that the evolution equation for comoving matter density perturbations, $\delta_m = 3Hv$, in a pressureless universe satisfies

$$\ddot{\delta}_m + c_1\dot{\delta}_m + c_2\delta_m = 0\,, \tag{3.6}$$

where

$$c_1 = \frac{2H}{1 + \dot{F}/2HF}\left[1 + \left(1 - \frac{\dot{H}}{H^2}\right)\frac{\dot{F}}{2HF} - \frac{\dot{F}^2}{2H^2F^2} + \frac{\ddot{F}}{2H^2F}\right], \tag{3.7}$$

$$\begin{aligned} c_2 = \frac{H^2}{1 + \dot{F}/2HF}\Bigg[&-\frac{\ddot{H}}{H^3} - \frac{2\dot{H}}{H^2} + \frac{\dot{H}}{H^2}\left(\frac{\dot{F}}{HF}\right)^2 \\ &+\frac{\dot{F}}{HF}\left(\frac{\dot{H}^2}{H^4} - \frac{\ddot{H}}{2H^3} - \frac{\dot{H}}{H^2} + \frac{k^2}{6a^2H^2}\right) - \frac{\dot{H}}{H^2}\frac{\ddot{F}}{H^2F}\Bigg]. \end{aligned} \tag{3.8}$$

(3.9)

Eq. (3.6) can be expressed in terms of conformal time such that

$$\begin{aligned} \delta_{m,\tau\tau} \quad &+ \quad 3\mathcal{H}\frac{2F\mathcal{H}(F\mathcal{H}^2 + F_{,\tau\tau}) - 2F_{,\tau}^2\mathcal{H} + F_{,\tau}F(-2\mathcal{H}_{,\tau} + \mathcal{H}^2)}{3F\mathcal{H}^2(2F\mathcal{H} + F_{,\tau})}\delta_{m,\tau} \\ &- \Big[6F^2\mathcal{H}^2(\mathcal{H}_{,\tau\tau} - 2\mathcal{H}_{,\tau}\mathcal{H}) + 6F_{,\tau}^2\mathcal{H}(\mathcal{H}^2 - \mathcal{H}_{,\tau}) \\ &\qquad +F_{,\tau}F(3\mathcal{H}_{,\tau\tau}\mathcal{H} - 6\mathcal{H}_{,\tau}^2 - \mathcal{H}^2k^2) + 6F_{,\tau\tau}F\mathcal{H}(\mathcal{H}_{,\tau} - \mathcal{H}^2)\Big] \\ &\qquad\qquad 3F\mathcal{H}^2(2F\mathcal{H} + F_{,\tau})\delta_m = 0. \end{aligned} \tag{3.10}$$

We will refer to Eqs. (3.3) and (3.10) as the LuSS and KKS (Koivisto and Kurki-Suonio

[79]) perturbation equations, respectively. We will be interested in identifying the domain where the equation based on the LuSS procedure provides an accurate description for the evolution of the perturbations. In the following section, we adopt an analytical approach with the aim of identifying the general form of the gravitational lagrangian, $f(R)$, for this to be the case.

3.2 Analytical comparison

A direct comparison between the LuSS equation (3.3) and the KKS equation (3.10) suggests that the latter should be rewritten in the form

$$\delta_{m,\tau\tau} + \xi\mathcal{H}\delta_{m,\tau} - \zeta\left(\frac{\mathcal{H}_{,\tau\tau}}{\mathcal{H}} - 2\mathcal{H}_{,\tau}\right)\delta_m = 0, \tag{3.11}$$

where the parameters ξ and ζ are defined by

$$\xi \equiv 1 + \frac{2FF_{,\tau\tau}\mathcal{H} - 2F_{,\tau}^2\mathcal{H} - 2FF_{,\tau}\mathcal{H}_{,\tau}}{F\mathcal{H}^2(2F\mathcal{H} + F_{,\tau})}, \tag{3.12}$$

and

$$\zeta \equiv 1 + \frac{\mathcal{H}^2 - \mathcal{H}_{,\tau}}{\mathcal{H}_{,\tau\tau} - 2\mathcal{H}_{,\tau}\mathcal{H}}(1-\xi) - \frac{F_{,\tau}\mathcal{H}}{3(2F\mathcal{H} + F_{,\tau})(\mathcal{H}_{,\tau\tau} - 2\mathcal{H}_{,\tau}\mathcal{H})}k^2, \tag{3.13}$$

respectively. The form of Eq. (3.11) implies that the LuSS and KKS equations are equivalent when $\xi = \zeta = 1$, but it is clear that this occurs only for Einstein gravity where $F_{,\tau} = 0$. Indeed, the most striking difference is the presence of the gradient term in the KKS equation. Such a term also arises in the corresponding density perturbation equation derived in the metric variational approach, as we shall see later in Sec. 4.3. The origin of this term can be understood from the dynamical equivalence between $f(R)$ Palatini gravity and Brans-Dicke theory, as expressed in Eq. (2.71). Fluctuations in the pressureless matter induce perturbations in the scalar field χ (i.e., the Ricci curvature, see Eq. (2.70)), which in turn generate a pressure gradient in the fluid. In general, the phase speed (see Ref. [112]) of the fluctuations in the cold dark matter is given by

$$c_s^2 = \frac{F_{,\tau}}{3(2F\mathcal{H} + F_{,\tau})}. \tag{3.14}$$

The magnitude of ξ is independent of k and is therefore unaffected by the specific choice of scale. However, ζ contains a gradient term which is proportional to k^2 and this may be significant on small scales. Consequently, the evolution of the perturbations will indeed be different in the two approaches. However, the gradient term becomes negligible in the long-

wavelength limit (which corresponds formally to $k^2 \to 0$). In this limit, a necessary and sufficient condition for equivalence between the LuSS and KKS equations is that $\xi = 1$ and this constraint is satisfied when

$$FF_{,\tau\tau}\mathcal{H} - F_{,\tau}^2\mathcal{H} - FF_{,\tau}\mathcal{H}_{,\tau} = 0. \tag{3.15}$$

Eq. (3.15) may be viewed as a second-order, non-linear differential equation for $F(\tau)$. One solution to this equation is that of general relativity with a cosmological constant, $f(R) = R - \Lambda$. More generally, if $F_{,\tau} \neq 0$ and $F_{,\tau\tau} \neq 0$, we may define a parameter $Y \equiv F_{,\tau}/F$. This reduces Eq. (3.15) to the remarkably simple form

$$\frac{Y_{,\tau}}{Y} = \frac{\mathcal{H}_{,\tau}}{\mathcal{H}}, \tag{3.16}$$

which admits the integral $Y = Y_0\mathcal{H}$, where Y_0 is an arbitrary integration constant. This in turn implies that

$$F = F_0 a^{Y_0}, \tag{3.17}$$

where F_0 is a second integration constant.

On the other hand, the trace equation (2.20) for a universe sourced by pressureless matter reduces to the condition [111]

$$a \propto \left(2f - R\frac{df}{dR}\right)^{-1/3}. \tag{3.18}$$

Hence, substitution of Eq. (3.18) into Eq. (3.17) yields a first-order, non-linear differential equation in the gravitational lagrangian $f(R)$:

$$\left(\frac{df}{dR}\right)^n \left(2f - R\frac{df}{dR}\right) = \text{constant}, \tag{3.19}$$

where $n \equiv 3/Y_0$.

Eq. (3.19) is a particular example of d'Alembert's equation and may be solved in full generality [113]. Since we are interested in the functional dependence of the lagrangian on the Ricci scalar, we may rescale f without loss of generality such that the constant on the right-hand side of Eq. (3.19) is unity. If we now define the functions

$$M \equiv \frac{1}{2}\frac{df}{dR}, \qquad N \equiv \frac{1}{2}\left(\frac{df}{dR}\right)^{-n} \tag{3.20}$$

and denote $\bar{p} \equiv df/dR$, Eq. (3.19) can be expressed in the form $f(R) = RM(\bar{p}) + N(\bar{p})$.

Differentiating this expression with respect to R then yields

$$\bar{p} = M(\bar{p}) + \frac{d\bar{p}}{dR}\left[R\frac{dM(\bar{p})}{d\bar{p}} + \frac{dN(\bar{p})}{d\bar{p}}\right]. \tag{3.21}$$

However, Eq. (3.21) can be expressed as a linear differential equation in the dependent variable R and independent variable $\bar{p}$:

$$\frac{dR}{d\bar{p}} - \frac{R}{\bar{p}} = -\frac{n}{\bar{p}^{2+n}}. \tag{3.22}$$

Hence, solving Eq. (3.22) by the method of integrating factors yields the general solution to Eq. (3.19) in a parametric form:

$$R = C_0 P + \frac{n}{n+2}\frac{1}{P^{1+n}} \tag{3.23}$$

$$f = \frac{1}{2}RP + \frac{1}{2P^n}, \tag{3.24}$$

where C_0 is an arbitrary integration constant and P is a free parameter.

Eqs. (3.23)-(3.24) represent the general form of the gravitational lagrangian $f(R)$ for the LuSS and KKS equations to be compatible in the long wavelength limit. It is interesting that for this class of theories the sound speed of the fluctuations is constant with a numerical value given by

$$c_s^2 = \frac{1}{3+2n}. \tag{3.25}$$

When $C_0 = 0$, which is equivalent to the asymptotic limit where R is sufficiently small, the gravitational action depends on a simple power of the Ricci scalar:

$$f(R) \propto R^{n/(1+n)}. \tag{3.26}$$

For this class of theories the Friedmann equation (2.109) reduces to

$$H^2 = \frac{3+2n}{6n}\left(1+\frac{3}{2n}\right)^{-2} R, \tag{3.27}$$

which in turn implies that the background dynamics is given by a power-law solution for the scale factor, $a \propto \mathcal{H}^{-2n/(3+n)} \propto \tau^{2n/(3+n)}$. Consequently, the cosmic dynamics is equivalent to that of a conventional relativistic universe dominated by a perfect fluid with a constant equation of state. Finally, the parameter ζ simplifies in this case to

$$\zeta = 1 - \frac{2n^2}{3(1+n)(3+n)(3+2n)}\frac{k^2}{\mathcal{H}^2}. \tag{3.28}$$

In conclusion, therefore, the above analysis indicates that the LuSS equation should provide a good approximation to the full evolution equation for the linear density perturbation on sufficiently large scales in any modified gravity theory that asymptotes in the low-energy limit to a power-law in the Ricci curvature scalar. On the other hand, for fixed values of n and $\mathcal{H}$, the LuSS equation becomes progressively less accurate as we move to smaller scales (i.e. as k increases). In the following section, we will quantify these conclusions further by performing numerical calculations for a specific class of modified gravity theories.

3.3 Numerical comparison

Motivated by the results of the previous section, we consider the class of gravity theories defined by

$$f(R) = R - \frac{c}{R^b}\,, \tag{3.29}$$

where b and c are free parameters whose values are constrained by observations. Such theories have been considered as possible candidates for explaining the late-time acceleration of the universe [37; 10; 114]. In particular, a recent study found that data obtained from CMB, baryon oscillation and large-scale structure observations constrains the parameters (b, c) to lie in the ranges $b \in [-0.2, 1.2]$ and $c \in [-3.5, 6.6]$ at the 68% confidence level [10]. The best-fit model corresponds to the values $(b, c) = (0.027, 4.63)$ and the ΛCDM concordance model is represented by $(b, c) = (0, 4.38)$. These values are consistent with the results of other studies that employ CMB and supernovae data [111].

For the above choice of parameters, we have made a detailed comparative study of the evolution of the density perturbations for both the LuSS equation (3.3) and the KKS equation (3.10). The results of such a comparison can be quantified by defining a 'fractional difference' parameter

$$\Delta \equiv \frac{\delta_m^{LuSS} - \delta_m^{KKS}}{\delta_m^{KKS}}, \tag{3.30}$$

where subscripts 'LuSS' and 'KKS' refer to the results obtained using the LuSS and KKS equations, respectively. Thus, the two approaches are completely identical when $\Delta = 0$. This parameter is defined in such a way that the difference between the two approaches is of the same order as the KKS approach when $\Delta \simeq \mathcal{O}(1)$. To a first approximation, therefore, it is reasonable to suppose that the LuSS equation becomes unreliable when $\Delta \approx 1$.

There are three physical parameters in the field equations whose values need to be specified in the numerical integrations. These are Ω_{m0}, R_0 and H_0, where a subscript zero indi-

cates present-day values and Ω_m is the normalised matter energy density[2]. However, only two constraint equations are available, corresponding to the Friedmann equation (2.109) and the trace equation (2.107). In order to be consistent, therefore, we specify the value of H_0 to be unity, as is the usual practice (see, e.g., [111]). We then use the constraint equations (2.107) and (2.109) to determine Ω_{m0} and R_0. The choice of Eq. (3.30) implies that the initial value of the perturbation δ_m is unimportant. Finally, we need to specify the scale of the perturbations. By fixing the wavenumber at a particular value, one focuses on perturbations that entered the horizon at a particular epoch. For illustrative purposes we consider the values $k = 5$ and $k = 20$, corresponding to scales which remain within the horizon throughout our numerical evolution.

The left hand panel of Fig. 3.1 illustrates the evolution of Δ when $c = 4.38$ and $k = 5$, with b taking values in the range $b \in [0, 1]$. As expected, $\Delta = 0$ for the ΛCDM concordance model (given by $b = 0$), since it is known that the LuSS equation is exact in this case. On the other hand, increasing the value of b causes the behaviour of the two approaches to deviate and the quantitative difference becomes more pronounced as b is increased.

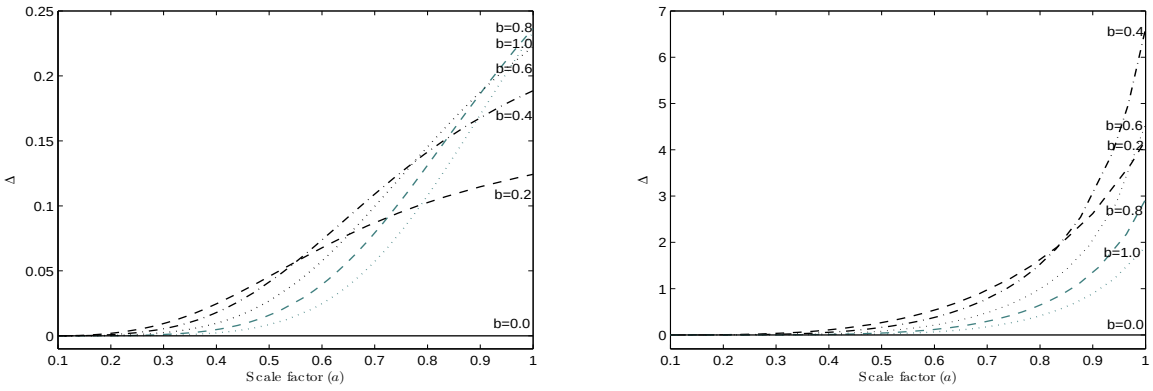

Figure 3.1: Illustrating how the fractional difference parameter, Δ, varies with the normalised scale factor a as b is increased. Here $c = 4.38$ and values of b are assigned to each curve. The case $b = 0$ corresponds to the ΛCDM model. The left hand panel corresponds to $k = 5$ whereas the right hand panel corresponds to $k = 20$.

We have verified that these results remain qualitatively similar when the parameter values lie in the ranges $b \in [-0.2, 1.2]$ and $c \in [-3.5, 6.6]$, respectively. An important outcome of these results is that for values of the parameters consistent with recent observations, the agreement between the LuSS and KKS approaches is good in the sense that $\Delta < 0.1$ for $b < 0.2$. This implies that the LuSS equation provides a good approximation to the full (linear) perturbation theory (for this value of k). This can be understood by noting that observations constrain theoretical models to lie close to the ΛCDM point, where it is known

[2]Note that in modified gravity theories of the type considered here, this parameter need not necessarily be unity in a spatially flat universe.

that the LuSS equation is exact.

Further inspection of the left hand panel of Fig. 3.1 indicates that as the value of b is increased, the models take longer to move away from the ΛCDM point $\Delta = 0$, but those with smaller values of b subsequently find it easier to approach $\Delta = 0$ at later times. We may gain further insight into the origin of this behaviour by investigating the evolution of the quantity $Q \equiv 1 - F$. This vanishes at all times for Einstein gravity but is given by $Q = -bcR^{-(1+b)}$ for the class of models (3.29). This parameter therefore provides a measure of the deviation away from general relativity. Our numerical calculations indicate that initially $R \approx \mathcal{O}(10^3)$ and, consequently for larger values of b, the scale factor must grow to a larger value before the Ricci scalar has fallen sufficiently for the correction term Q to become dynamically significant. In other words, the onset of acceleration occurs at later times for larger b. On the other hand, the correction term in $f(R)$ that is proportional to R^{-b} will become more important as the universe expands. The analysis of Sec. 3.2 then indicates that the accuracy of the LuSS equation will improve as $f(R)$ asymptotes to a power-law form. Consequently, Δ will begin to decrease back to zero at later times.

We find qualitatively similar behaviour at larger values of k. The right hand panel of Fig. 3.1 illustrates the corresponding evolution of Δ when $k = 20$. As expected, models with lower values of b move away from the $\Delta = 0$ point at smaller values of the scale factor. The model with the lowest non-zero value of $b = 0.2$ crosses the solutions for $b = 0.4$ and $b = 0.6$. This can be understood from Eq. (3.28), which implies that the magnitude of ζ depends on the ratio $k^2/\mathcal{H}^2 = k^2/\dot{a}^2$. At a formal level, therefore, increasing the value of k is equivalent to ending the numerical calculation at a fixed k but with a smaller value for the scale factor.

However, the quantitative agreement between the solutions of the LuSS and KKS equations is poor when $k = 20$ and Δ rapidly exceeds unity in this case. This discrepancy arises primarily because the deviation of the parameter ζ away from unity is more pronounced at larger k. Fig. 3.2 illustrates the evolution of ζ for the different values of k.

3.4 Summary

In this chapter, we have studied the evolution of density perturbations in generalised theories of gravity where the field equations are derived via the Palatini variational approach [68]. We focused on models where the energy-momentum tensor is sourced by a pressureless perfect fluid. Two approaches to the study of density perturbations have recently been developed in the literature [79; 108; 109]. These involve, respectively, an application of Birkoff's theorem to modified gravity (the LuSS method) and the linearisation of the full field equations (the KKS approach). In the former case, the evolution of the perturbations is determined entirely by the background dynamics and no pressure gradients are present in the perturbation evo-

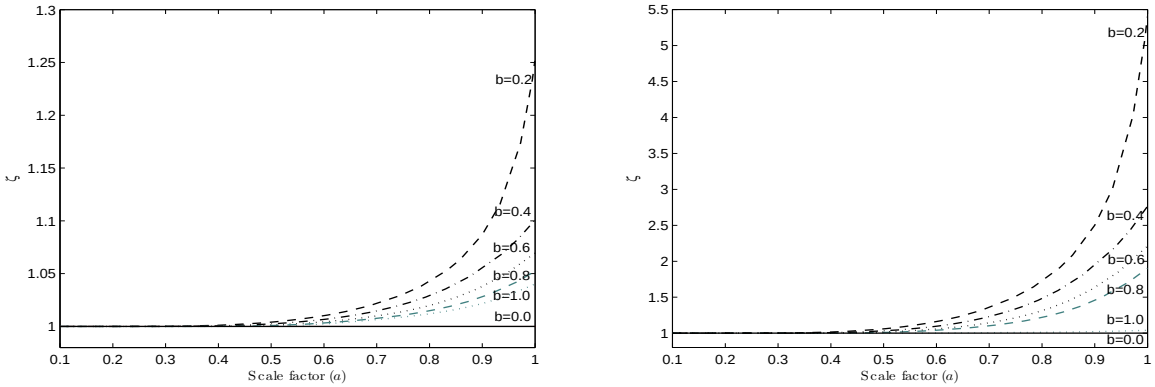

Figure 3.2: Illustrating the evolution of the parameter ζ defined by Eq. (3.13) in the text for the parameter values $k = 5$ (left panel) and $k = 20$ (right panel). The LuSS procedure for the evolution of the perturbations becomes progressively less accurate as the deviation of this quantity from unity becomes more pronounced.

lution equation. However, such terms do arise in the linearisation approach, which takes into account the fact that perturbations in the fluid induce fluctuations in the Ricci curvature, which in turn modify the sound speed of the fluctuations in the matter.

In the long-wavelength limit, these gradient terms are negligible. We have identified the most general $f(R)$ theory of gravity, as summarised in Eqs. (3.23) and (3.24), for the LuSS and KKS approaches to be equivalent in this limit. A particular case of this class of theories arises when $f(R)$ is a simple power law of the Ricci curvature scalar. This is interesting because such terms are expected to arise as corrections to the Einstein-Hilbert action at low energies. Furthermore, theories of this type result in a background scaling solution, in the sense that the homogeneous dynamics is equivalent to that of a conventional relativistic cosmology where the pressure and energy density of the perfect fluid redshift at the same rate [68]. It would be interesting to explore whether this scaling behaviour is a necessary condition for compatibility between the LuSS and linearisation methods in more general theories of modified gravity. For example, a power-law cosmology arises in the Palatini variation of Ricci squared gravity, where $f \propto (R^{\mu\nu}R_{\mu\nu})^{n/2}$ [115].

We numerically investigated a specific class of power-law theories of the type (3.29) and compared the LuSS and KKS approaches on smaller scales where gradient terms become significant. We found that when the parameters of the underlying theory take values that are consistent with cosmological observations, the LuSS procedure provides a reasonably good approximation to the complete linearised theory if k is not too large (i.e. of the order of a few or less). However, the agreement between the two approaches soon breaks down on smaller scales [68].

Chapter 4

Density perturbations in $f(R)$ gravity theories in metric and Palatini formalisms

In this chapter we make a detailed study of the viability of $f(R)$ gravity theories in the context of both metric and Palatini variational formalisms. In each case, we first summarise the constraints provided by the requirements of stability and viable background dynamics, and then proceed to discuss the constraints provided by local gravity constraints (LGC). Compatibility of $f(R)$ theories with LGC in the metric formalism requires the use of a chameleon mechanism, which we briefly review in the following section before deriving the resulting bounds on the $f(R)$ models.

Despite the importance of these constraints in limiting the range of viable $f(R)$ models, the study of density perturbations allows for more stringent constraints to be placed on the parameters of the models. We thus study the evolution of density perturbations and the resulting observational consequences for $f(R)$ theories in both metric and Palatini formalisms.

In exploring the evolution of scalar perturbations we utilise a sub-horizon type approximation, under which approximate perturbation equations are derived. In the metric approach, where the oscillating (so-called scalaron) mode [116] is present, this approximation can be invalid if the scalaron is overproduced in the early Universe. However, as long as the scalaron is sub-dominant relative to a matter induced mode, we shall show that approximate perturbation equations can be valid even for the super-Hubble modes in the models that satisfy LGC. The approximation is especially reliable in the Palatini case because of the absence of scalarons [69]. The simplicity of the equations derived facilitates the estimation of the growth rate of perturbations both analytically and numerically.

Using these equations we make a comparative study of the behaviour of matter density perturbations in both formalisms, for a number of classes of $f(R)$ models satisfying the

LGC as well as the background constraints [69]. These include viable $f(R)$ models recently proposed in the literature [116; 117].

4.1 LGC and cosmological viability in the metric formalism

The effective Newtonian gravitational coupling, $G_{\rm N}^{\rm eff}$, in the Brans-Dicke theory (2.44) can be derived under a weak-field approximation, by considering a spherically symmetric body with a mass $M_\star$ of constant density ρ and a radius $\ell_\star$ in the vacuum ($\rho = 0$). Decomposing the field, ϕ, into background and perturbation parts ($\phi = \phi_0 + \delta\phi$) and using a linear perturbation theory in the Minkowski background with a perturbation $h_{\mu\nu}$, the effective gravitational coupling is given by [118]:

$$G_{\rm N}^{\rm eff} = \frac{G_N}{\bar{\phi}}\left(1 + \frac{e^{-M\ell}}{3 + 2\omega_{\rm BD}}\right) , \tag{4.1}$$

where ℓ is a distance from the centre of the body and the effective scalar field mass squared is defined to be [118; 119; 120]

$$M^2 \equiv \frac{1}{3 + 2\omega_{\rm BD}}\left(\bar{\phi}\frac{{\rm d}^2 V}{{\rm d}\bar{\phi}^2} - \frac{{\rm d}V}{{\rm d}\bar{\phi}}\right) , \tag{4.2}$$

where $\bar{\phi}$ is a local field in Minkowski spacetime. We should emphasise here that the expression (4.1) is only valid subject to the condition $M\ell_\star \ll 1$ [119; 120]. The definition of the effective scalar field mass, M, comes from writing the linear expansion of the scalar field equation of motion (2.46) in the form of the Klein-Gordon equation

$$[\nabla^2 - M^2]\bar{\phi} = -\frac{8\pi G_N}{3}\rho.$$

In the usual Brans-Dicke theory where $V(\phi) = 0$ and $\omega_{\rm BD} \neq -\frac{3}{2}$, the mass ($M$) vanishes because ϕ propagates freely. Consequently, the Yukawa-correction term, $e^{-M\ell}$, in Eq. (4.1) becomes 1, in which case the Brans-Dicke parameter, $\omega_{\rm BD}$, is constrained by local gravity experiments to be larger than 40000 [45; 46]. An alternative way to understand this bound is to consider the Eddington parameter, γ, which in the usual Brans-Dicke case is given by [118]

$$\gamma = \frac{1 + \omega_{\rm BD}}{2 + \omega_{\rm BD}}. \tag{4.3}$$

To satisfy the local gravity constraint (1.1), the parameter ω_{BD} is required to be larger than 40000. As was mentioned in Sec. 1, this constraint does not necessarily apply to $f(R)$ gravity

theories where the presence of a field potential can make such theories compatible with local gravity constraints under certain conditions.

In the presence of a potential, $V(\phi)$, the scalar field is massive. If the scalar field mass is large, it can happen that the condition for the applicability of linear perturbation theory ($\delta\phi \ll \phi_0$) becomes invalid. Moreover, this validity depends on the distribution of scalar-field mass inside and outside the body. When the mass in the region $\ell < \ell_\star$ is much larger than the corresponding mass in the region $\ell > \ell_\star$, a *"thin-shell"* can be formed inside the body so as to satisfy local gravity constraints through a Chameleon mechanism[1] [47]. The formation of the thin-shell occurs in a non-linear region in which the above linear result (4.1) ceases to be valid [119].

An important point to note here is that the Palatini formalism, corresponding to $\omega_{\rm BD} = -\frac{3}{2}$, is rather special in a number of fundamental ways. For example, we recall that the ϕ-field's kinetic term in Eq. (2.46) vanishes in this case, whereas it is non-zero in the metric case with $\omega_{\rm BD} = 0$. As we shall see below this has the important consequence that the oscillatory scalaron mode is absent in $f(R)$ theories based on the Palatini formalism, whereas it is present in all other models with $\omega_{\rm BD} \neq -\frac{3}{2}$, including $f(R)$ theories based on the metric formalism.

Furthermore, as $\omega_{\rm BD}$ approaches $-\frac{3}{2}$, the scalar field mass, M, diverges for finite potential-dependent terms in the parenthesis of Eq. (4.2). For theories with $\omega_{\rm BD} \neq -\frac{3}{2}$, the scalar field mediates a *"fifth-force"* with an interaction range M^{-1}. Because the mass, M, defined in Eq. (4.2) becomes singular as $\omega_{\rm BD}$ approaches $-\frac{3}{2}$, the usual notion of an interaction range determined by the mass, M, does not hold in the Palatini formalism. Therefore, the Palatini case should be treated separately compared to the other theories with $\omega_{\rm BD} \neq -\frac{3}{2}$.

Before we proceed to discuss the constraints provided by LGC, we review the background cosmological dynamics in $f(R)$ gravity.

4.1.1 Background cosmological dynamics

The study of the background cosmological evolution for $f(R)$ theories in the metric formalism has been carried out in Ref. [43]. In order to study the background dynamics, it is useful

[1] A Chameleon mechanism is one by which a scalar field can obtain a mass that is greater in high-density regions than in sparse ones. In a spherically symmetric body of constant energy density this leads to the scalar field, ϕ, being nearly constant everywhere inside the body apart from in a small surface region (as will be demonstrated in Sec. 4.1.2). This means that $\nabla\phi$ vanishes everywhere apart from in this thin surface layer. Since the force mediated by ϕ is proportional to $\nabla\phi$, it is only this "thin-shell" that both feels and contributes to the fifth-force mediated by ϕ (note that there exists strong solar system bounds on the fifth-force). Furthermore, since the chameleon field couples to a small fraction of matter of the large body, the Chameleon force is weak. Thus, through a Chameleon mechanism it is possible to evade stringent solar system tests [48].

to define the following dimensionless variables

$$x_1 = -\frac{\dot{F}}{HF}\,, \quad x_2 = -\frac{f}{6FH^2}\,, \quad x_3 = \frac{R}{6H^2} = \frac{\dot{H}}{H^2} + 2\,. \tag{4.4}$$

In terms of these variables, the energy fraction Ω_m of the pressureless matter and the effective equation of state, $w_{\rm eff}$, are given by

$$\Omega_m \equiv \frac{\rho_m}{3FH^2} = 1 - x_1 - x_2 - x_3\,, \quad w_{\rm eff} \equiv -1 - \frac{2}{3}\frac{\dot{H}}{H^2} = -\frac{1}{3}(2x_3 - 1)\,. \tag{4.5}$$

To study the background dynamics, it is also useful to define the parameters m and r [43]. The parameter m, defined as

$$m \equiv \frac{Rf_{,RR}}{f_{,R}}\,, \tag{4.6}$$

characterises the deviation from the ΛCDM model. In the ΛCDM case, $m = 0$. The parameter r is defined as

$$r \equiv -\frac{Rf_{,R}}{f} = \frac{x_3}{x_2}. \tag{4.7}$$

The cosmological behaviour of $f(R)$ models can be understood by studying $m(r)$ curves in the $(r,\, m)$ plane.

The background evolution equations (2.90), (2.100) and (2.101) can now be expressed as

$$\frac{dx_1}{dN} = -1 - x_3 - 3x_2 + x_1^2 - x_1x_3\,, \tag{4.8}$$

$$\frac{dx_2}{dN} = \frac{x_1x_3}{m} - x_2(2x_3 - 4 - x_1)\,, \tag{4.9}$$

$$\frac{dx_3}{dN} = -\frac{x_1x_3}{m} - 2x_3(x_3 - 2)\,, \tag{4.10}$$

where $N \equiv \ln(a)$ is the number of e-foldings. For later use we also introduce the variable $x_4 \equiv aH$, which satisfies

$$\frac{dx_4}{dN} = (x_3 - 1)x_4\,. \tag{4.11}$$

The critical points of the autonomous system (4.8)-(4.10) include [43]

$$P_m:\ (x_1, x_2, x_3) = \left(\frac{3m}{1+m}, -\frac{1+4m}{2(1+m)^2}, \frac{1+4m}{2(1+m)}\right), \tag{4.12}$$

$$w_{\rm eff} = -\frac{m}{1+m}\,, \quad \Omega_m = 1 - \frac{m(7+10m)}{2(1+m)^2}\,,$$

which corresponds to a matter epoch. Since m (which characterises the deviation from

ΛCDM) needs to be much smaller than unity during the matter era, the critical point, P_m, becomes $P_m : (x_1, x_2, x_3) \simeq (0, -\frac{1}{2}, \frac{1}{2})$ for viable $f(R)$ models. The fixed point corresponding to a de-Sitter phase is given by

$$P_{ds} : \ (x_1, x_2, x_3) = (0, -1, 2) \,, \quad w_{\rm eff} = -1 \,, \quad \Omega_m = 0 \,. \tag{4.13}$$

In the (r, m) plane the matter fixed point corresponds to $P_m : (r, m) \approx (-1, 0)$. In order to have a saddle matter era followed by a phase of late-time acceleration, the following conditions must hold [43]

$$m > 0 \,, \quad -1 < \frac{{\rm d}m}{{\rm d}r} < 0 \,, \quad {\rm at} \quad (r, m) \approx (-1, 0) \,. \tag{4.14}$$

The de-Sitter fixed point, P_{ds}, lies on the line $r = -2$. It is stable provided that

$$0 < m \leq 1 \,, \quad {\rm at} \quad r = -2 \,. \tag{4.15}$$

If the conditions (4.14) and (4.15) are satisfied, an $m(r)$ curve exists which connects the matter fixed point to the de-Sitter fixed point, leading to viable cosmological dynamics.

There are a number of models in the literature that satisfy the above cosmological constraints. Examples include
(i) $f(R) = \alpha(R^b - \Lambda)^c$ with $c \geq 1$, $bc \approx 1$ [121], and
(ii) $f(R) = R - \alpha R^\beta$ with $\alpha > 0$ and $0 < \beta < 1$.
For these models, the parameters m and r satisfy the relation $m = C(-r - 1)$, where C is a positive constant. Using observational constraints on the background dynamics from SN Ia and the sound horizon of the CMB, the parameter m has been constrained to be $m < \mathcal{O}(0.1)$ [122].

4.1.2 LGC and the chameleon mechanism

If information from local gravity constraints is also included, the bounds on the model parameters become very strong. The usual procedure to determine the LGC for $f(R)$ theories is to consider their Brans-Dicke representations (2.62), and expand the equations of motion around a background Minkowski metric [118]. As was shown in Sec. (2.2.2), $f(R)$ theories in the metric approach correspond to Brans-Dicke theories with $\omega_{\rm BD} = 0$,

$$\phi = F(R) \quad \ \ {\rm and} \quad \ \ V(\phi) = R(\phi)F - f(R(\phi)) \,. \tag{4.16}$$

To define the potential, $V(\phi)$, in this way, we require F to be invertible. This invertibility is generally associated with the condition $f_{,RR} \neq 0$ [119]. Using the correspondence given in

Eq. (4.16), the scalar field mass defined in Eq. (4.2) becomes

$$M^2 = \frac{1}{3}\left(\frac{f_{,R}}{f_{,RR}} - R\right) . \tag{4.17}$$

If $M^2 < 0$, the Yukawa correction, $e^{-M\ell}$, is replaced by an oscillating function $\cos(|M|\ell)$. For very light fields, which represent long-range interactions, this case is excluded by the experimental requirement that the Eddington parameter [118]

$$\gamma = \frac{3 - e^{-M\ell}}{3 + e^{-M\ell}} \approx 1. \tag{4.18}$$

Hence, the mass squared (M^2) is required to be positive.

For consistency with local gravity experiments (which require $\omega_{BD} > 40000$) a large mass, M, is needed. In that case, however, the effective gravitational coupling (4.1) obtained under the linear approximation ceases to be valid. As was already mentioned above, a thin-shell begins to form through a chameleon effect in this non-linear regime. To consider this chameleon effect in $f(R)$ gravity, it is convenient to write the theories as Einstein gravity minimally coupled to a scalar field. For this purpose it is useful to define a new metric (as we did in section 2.2.2) thus:

$$\tilde{g}_{ab} = \phi g_{ab} , \quad \phi = e^{-2Q\varphi} . \tag{4.19}$$

(We recall that a quantity or operator in the Einstein frame is denoted with a tilde). The Einstein frame action then takes the form (2.67):

$$S_E = \int \mathrm{d}^4x\sqrt{-\tilde{g}}\left[\frac{1}{2}\tilde{R} - \frac{1}{2}(\tilde{\nabla}\varphi)^2 - U(\varphi)\right] + S_m(\tilde{g}_{ab}e^{2Q\varphi}, \psi_m) , \tag{4.20}$$

where the coupling, Q, in $f(R)$ models and the potential, U, are given by

$$Q = -\frac{1}{\sqrt{6}} , \quad U = \frac{R(\phi)\phi - f}{2\phi^2} . \tag{4.21}$$

We recall that in the Einstein conformal frame the energy-momentum tensor is not covariantly conserved, but instead satisfies

$$\tilde{\nabla}_a \tilde{T}^a{}_b = Q\tilde{T}\tilde{\nabla}_b\,\varphi , \tag{4.22}$$

where $\tilde{T} = e^{4Q\varphi}T$ and $T = g^{\mu\nu}T_{\mu\nu}$, with $T_{\mu\nu}$ being the energy-momentum tensor of matter in the Jordan frame. This implies that matter will generally feel a so-called *"fifth-force"* due to gradients in the field φ.

A Chameleon mechanism can be realised in scalar-field theories of the type (4.20), pro-

vided the potential holds certain properties (see Ref. [48] for more details). In these circumstances, the $f(R)$ theories would admit a chameleon mechanism. In general, Q, which parametrises the strength of the coupling of the matter-fields ψ_m to the field φ, could take any value. However, in the case of $f(R)$ theories Q is fixed to be $-\frac{1}{\sqrt{6}}$.

1. The thin-shell condition

Theories which possess a Chameleon mechanism do not behave like usual linear theories of massive scalar fields. In circumstances where massive bodies are involved, the chameleon field is trapped inside these bodies and its influence (on other bodies) is only apparent due to a thin-shell on the outer edge of the massive body [47; 117; 119; 123; 124]. As a result, the field outside the massive body for distances less than the range of the chameleon force in the outer vacuum is effectively damped. This leads to a shielded fifth-force, which becomes undetectable [125]. In this section, we derive the conditions required for a thin-shell to form. Under these conditions the $f(R)$ theories become compatible with LGC.

Let us consider the Einstein frame action (4.20). The variation of this action with respect to φ leads to the following equation of motion

$$\tilde{\Box}\varphi - U_{,\varphi} = -Q\tilde{T}\,. \tag{4.23}$$

In a spherically symmetric setting with an energy density $\rho \equiv -T$, the field, φ, satisfies the following equation [123]:

$$\frac{\mathrm{d}^2\varphi}{\mathrm{d}\tilde{\ell}^2} + \frac{2}{\tilde{\ell}}\frac{\mathrm{d}\varphi}{\mathrm{d}\tilde{\ell}} = \frac{\mathrm{d}U_{\text{eff}}}{\mathrm{d}\varphi}\,, \tag{4.24}$$

where $\tilde{\ell}$ is the distance from the centre of symmetry in the Einstein frame and

$$U_{\text{eff}}(\varphi) = U(\varphi) + e^{Q\varphi}\rho^*\,. \tag{4.25}$$

Here we have introduced an energy density ρ^* which is conserved in the Einstein frame (i.e., $\rho^*\tilde{\ell}^3$ =constant) and is related to the energy density ρ in the Jordan frame via the relation $\rho^* = e^{3Q\varphi}\rho$ [47].

We consider a configuration in which the spherically symmetric body has a constant energy density $\rho^* = \rho^*_A$ inside the body ($\tilde{\ell} < \tilde{\ell}_\star \equiv e^{-Q\varphi}\ell_\star$). The energy density outside the body ($\tilde{\ell} > \tilde{\ell}_\star$) is given by $\rho^* = \rho^*_B$, which is much smaller than ρ^*_A. The mass of this body is then given by

$$M_\star = \frac{4\pi\ell_\star^3\rho_A}{3} = \frac{4\pi\tilde{\ell}_\star^3\rho^*_A}{3}. \tag{4.26}$$

Let us denote the field value at the minimum of the effective potential $U_{\text{eff}}(\varphi)$, corresponding

to the density ρ_A^* (ρ_B^*), by $\varphi = \varphi_A$ ($\varphi = \varphi_B$). That is, they are defined by

$$U_{,\varphi}(\varphi_A) + Qe^{Q\varphi_A}\rho_A^* = 0\,, \qquad U_{,\varphi}(\varphi_B) + Qe^{Q\varphi_B}\rho_B^* = 0\,. \tag{4.27}$$

Under the condition $\rho_A^* \gg \rho_B^*$ the mass squared $m_A^2 \equiv U''_{\rm eff}(\varphi_A)$ is much larger than $m_B^2 \equiv U''_{\rm eff}(\varphi_B)$.

Imposing appropriate boundary conditions at $\tilde{\ell} = 0$ and $\tilde{\ell} = \tilde{\ell}_\star$ (see Appendix A.2 for more details), the solution to Eq. (4.24) in the region $\tilde{\ell} > \tilde{\ell}_\star$ can be approximated by [47; 119]

$$\varphi(\tilde{\ell}) \simeq -\frac{Q_{\rm eff}}{4\pi}\frac{M_\star e^{-m_B(\tilde{\ell}-\tilde{\ell}_\star)}}{\tilde{\ell}} + \varphi_B\,, \tag{4.28}$$

where

$$Q_{\rm eff} \equiv 3Q\frac{\Delta\tilde{\ell}_\star}{\tilde{\ell}_\star}\,, \qquad \frac{\Delta\tilde{\ell}_\star}{\tilde{\ell}_\star} \simeq \frac{\varphi_B - \varphi_A}{6Q\Phi_\star} \quad \text{and} \quad \Phi_\star = \frac{G_N M_\star}{\tilde{\ell}_\star}. \tag{4.29}$$

A thin-shell is developed under the condition $\Delta\tilde{\ell}_\star/\tilde{\ell}_\star \ll 1$. In this case the effective coupling $|Q_{\rm eff}|$ becomes much smaller than unity so that the models can be consistent with LGC, even if $|Q|$ itself is of the order unity.

2. Constraints from solar system tests

The presence of the fifth-force interaction, mediated by the field φ, leads to a modification to the spherically symmetric metric. Under the weak-field approximation, the spherically symmetric metric in the Jordan frame is given by [123; 124]

$${\rm d}s^2 = -\left(1 - \frac{2G_N^{\rm eff}M_\star}{\ell}\right){\rm d}t^2 + \left(1 + \frac{2\gamma G_N^{\rm eff}M_\star}{\ell}\right){\rm d}\ell^2 + \ell^2({\rm d}\theta^2 + \sin^2\theta{\rm d}\varphi^2)\,, \tag{4.30}$$

where the effective gravitational coupling, $G_N^{\rm eff}$, and the Eddington parameter, γ, are given by

$$G_N^{\rm eff} \simeq G_N\left[1 - \frac{\sqrt{6}}{3}Q_{\rm eff}e^{-m_B(\ell-\ell_\star)}\right] \tag{4.31}$$

and

$$\gamma \simeq \frac{1 + (\sqrt{6}Q_{\rm eff}/3)(1+m_B\ell)e^{-m_B(\ell-\ell_\star)}}{1 - (\sqrt{6}Q_{\rm eff}/3)e^{-m_B(\ell-\ell_\star)}}\,. \tag{4.32}$$

Note that in writing these expressions we have used the approximation $\tilde{\ell} \simeq \ell$ that is valid in the region $|Q\varphi| \ll 1$.

Provided that the condition $m_B\ell \ll 1$ holds in the environment where local gravity

experiments are carried out, we have

$$\gamma \simeq \frac{1+\sqrt{6}Q_{\rm eff}/3}{1-\sqrt{6}Q_{\rm eff}/3}. \tag{4.33}$$

Hence, if $|Q_{\rm eff}|$ is much smaller than unity through the chameleon mechanism, it is possible to satisfy the severest solar system constraint presented in Eq. (1.1). Using the thin-shell parameter, this bound translates into

$$\frac{\Delta\ell_\star}{\ell_\star} < \frac{4.7\times 10^{-6}}{|Q|}\,. \tag{4.34}$$

If the body does not have a thin-shell for $|Q|$ of the order of unity, the condition (1.1) is not satisfied.

3. Models that satisfy LGC

Models that satisfy the thin-shell condition have recently been proposed by (i) Hu & Sawicki [117], and (ii) Starobinsky [116]:

$$\text{(i)}\;\; f(R) = R - \lambda R_c \frac{(R/R_c)^{2n}}{(R/R_c)^{2n}+1}\,, \tag{4.35}$$

$$\text{(ii)}\;\; f(R) = R - \lambda R_c \left[1-\left(1+\frac{R^2}{R_c^2}\right)^{-n}\right]\,, \tag{4.36}$$

where n, λ and R_c are positive constants. In both models the cosmological constant disappears in a flat spacetime, i.e., $f(R=0)=0$. Note that R_c is roughly of the order of the present cosmological Ricci scalar, R_0, for $n=\mathcal{O}(1)$ and $\lambda=\mathcal{O}(1)$. In high curvature regimes, $R \gg R_c$, these models behave as

$$f(R) \simeq R - \lambda R_c \left[1-\left(\frac{R_c}{R}\right)^{2n}\right]\,, \tag{4.37}$$

with

$$m \simeq C(-r-1)^{2n+1}\,, \tag{4.38}$$

where C is a positive constant, and m and r are defined in Eqs. (4.6) and (4.7), respectively. Thus, they are very close to the ΛCDM model with suppressed values of m during matter and radiation eras ($r \simeq -1$).

In the regimes $R \gg R_c$ one can show that the term $|\varphi_B - \varphi_A|$ in Eq. (4.29) is of the order of $m(R_B)$ for $n=\mathcal{O}(1)$, where R_B is the Ricci scalar in the neighbourhood of φ_B (which is generally much larger than R_c in an environment where local tests of gravity are carried

out). Hence the thin-shell is developed under the condition

$$m(R_B) \ll \Phi_\star \,. \tag{4.39}$$

This can be regarded as a criterion for the compatibility with local gravity constraints. In the case of the Earth, the condition (4.39) corresponds to $m(R_B) \ll \Phi_\star \sim 10^{-9}$. Since $\Phi_\star \ll 1$ in most local gravity experiments, the parameter m is constrained to be much smaller than unity in the region where the Ricci scalar R_B is much larger than its present cosmological value ($R_0 \sim R_c$).

Cosmologically the condition (4.39) implies that viable models need to be very close to the ΛCDM model during the radiation and matter dominated epochs ($R \gg R_0$). However, deviations from the ΛCDM model are allowed at around the present, accelerated epoch ($R \sim R_0$). Thus, for viable models, the parameter m is negligibly small during the radiation and matter eras, but continues to grow up to the present epoch.

For theories of the type (4.37) the corresponding Brans-Dicke field $\phi \equiv F(R)$, the potential $V(\phi)$ [defined in Eq. (2.63)] and the mass squared are given by

$$\phi \simeq 1 - 2n\lambda (R_c/R)^{2n+1} \,, \tag{4.40}$$

$$V(\phi) \simeq \lambda R_c \left[1 - (2n+1) \left(\frac{1-\phi}{2n\lambda} \right)^{\frac{2n}{2n+1}} \right] \,, \tag{4.41}$$

$$M^2 \simeq \frac{R_c}{3(2n+1)} (2n\lambda)^{\frac{1}{2n+1}} (1-\phi)^{-\frac{2n+2}{2n+1}} \,, \tag{4.42}$$

which in the limit $\frac{R}{R_c} \to \infty$ become: $\phi \to 1$, $V(\phi) \to \lambda R_c$ and $M^2 \to \infty$, respectively. In these regimes the field is fixed around $\phi = 1$ due to the presence of a ρ-dependent term. When R decreases to the order of R_c, the field begins to evolve along the potential $V(\phi)$ with a lighter mass M which is not very much different from R_c. Therefore, in the Brans-Dicke description, the departure from the point $\phi = 1$ amounts to a deviation from the ΛCDM model.

The models (4.35) and (4.36) are constructed to satisfy the stability conditions

$$f_{,R} > 0 \,, \quad f_{,RR} > 0 \,, \quad \text{for } \; R > R_1 \, (> 0) \,, \tag{4.43}$$

where R_1 is the value of the curvature scalar at the late-time de-Sitter point. The first condition is required to avoid repulsive gravity, whereas the second ensures the absence of tachyons or ghosts. The second condition is also required for consistency with LGC (as discussed above) as well as to ensure the stability of density perturbations [39] (as we shall see below). We also note that the requirements (4.39) and (4.43) are entirely consistent with the condition $0 < m(R) \ll 1$ derived in Ref. [43] which is necessary for the existence of a standard matter era.

To summarise, the conditions (4.39) and (4.43), together with the existence of the de-Sitter point (4.15), are required for the viability of $f(R)$ models in the metric formalism. The condition for the existence of the saddle matter era given in Eq. (4.14) is automatically satisfied under the requirements (4.39) and (4.43).

4.2 LGC and cosmological viability in the Palatini formalism

Before we consider the local gravity constraints, we review the background dynamics of Palatini $f(R)$ gravity.

4.2.1 Background cosmological dynamics

The background cosmological evolution of $f(R)$ theories in the Palatini formalism has been studied in Ref. [10]. By introducing dimensionless variables, the cosmological equations (2.90), (2.105) and (2.108) were written as a plane autonomous system. It was shown that equilibrium points corresponding to radiation (P_r), matter (P_m) and de-Sitter (P_{ds}) epochs exist irrespective of the form of $f(R)$, provided that the function

$$C(R) = -3\frac{(FR-2f)F_{,R}R}{(FR-f)(F_{,R}R-F)} \tag{4.44}$$

is well-behaved (i.e., it does not show discontinuous or divergent behaviour). Note that effective equations of state corresponding to points P_r, P_m and P_{ds} are given by $w_{\rm eff} = \frac{1}{3}, 0, -1$, respectively. It can be seen from Eq. (2.107) that the de-Sitter point, P_{ds}, corresponds to $FR-2f=0$, in which case $C(R)=0$. Furthermore, this implies that the de-Sitter solution exists on the line $r=-2$, which is the same as in the case of the metric approach.

The stability of the equilibrium points P_r, P_m and P_{ds} was also studied in Ref. [10] by obtaining the eigenvalues of the Jacobian matrix for perturbations around each point. The eigenvalues of the point P_{ds} are $(\lambda_1, \lambda_2) = (-3-C(R), -4-C(R))$, which implies that the de-Sitter point on the line $r=-2$ is always a stable attractor. This situation is different from the metric case in which the stability of the de-Sitter point requires the additional condition $0 < m(r=-2) \leq 1$. The stability of the radiation and matter points, on the other hand, depends upon the particular $f(R)$ models chosen. The eigenvalues corresponding to the point P_r are: $(\lambda_1, \lambda_2) = (4+C(R), 1)$ and those corresponding to the point P_m are: $(\lambda_1, \lambda_2) = (3+C(R), -1)$. Consequently, the models with $C(R) > -3$ give rise to an unstable node for P_r and a saddle point for P_m. Hence, models satisfying the condition $C(R) > -3$ lead to a sequence of radiation, matter and de-Sitter epochs.

As an example, let us consider the following model [37; 126]

$$f(R) = R - \frac{\mu^{2(n+1)}}{R^n}\,, \tag{4.45}$$

where μ and n are constants. In this case one has $C(R) = 3n$ in the regime $R^{n+1} \gg \mu^{2(n+1)}$, which means that a successful background trajectory is realised for $n > -1$. Note that a stable de-Sitter solution exists with $R_1^{1+n} = (2+n)\mu^{2(n+1)}$ and $C(R) = 0$. Obviously

the constraints for a successful trajectory, at least at the background level, are not so severe compared to the metric formalism. Indeed, one does not even require the condition $m > 0$ for the existence of a viable matter era.

4.2.2 Local gravity constraints

The usual determination of the interaction range in terms of the inverse mass, M^{-1}, can not be applied to the case $\omega_{\rm BD} = -\frac{3}{2}$. In order to study the LGC, therefore, one needs to proceed in a different way [118]. From the trace equation (2.20) we note that the field $\phi = F(R)$ depends on the value of the trace T, i.e., $\phi = \phi(T)$. We will therefore expand the field around the vacuum: $\phi(T) = \phi_0 + (\partial_T \phi_0)T + \cdots$, where $\phi_0 = \phi(T = 0)$ and $T \approx -\rho[1 - \mathcal{O}\left(v^2/c^2\right)]$. (Note that we use the non-relativistic approximation here under which the velocity, v, of matter is much smaller than the speed of light c). Carrying out a post-Newtonian expansion around the Minkowski vacuum ($g_{\mu\nu} = \eta_{\mu\nu} + h_{\mu\nu}$) in the solar system then implies that the solutions for the second-order perturbation equations are given by [118]

$$h_{00}^{(2)} \simeq \frac{2G_{\rm N}^{\rm eff} M_\odot}{\ell} - \frac{V_0}{6\phi_0}\ell^2 + \log\left(\frac{\phi}{\phi_0}\right), \tag{4.46}$$

$$h_{ij}^{(2)} \simeq \left[\frac{2\gamma G_{\rm N}^{\rm eff} M_\odot}{\ell} + \frac{V_0}{6\phi_0}\ell^2 - \log\left(\frac{\phi}{\phi_0}\right)\right]\delta_{ij}\,, \tag{4.47}$$

where $V_0 = V(\phi_0)$. The effective gravitational coupling and the post-Newtonian (Eddington) parameter are

$$G_{\rm N}^{\rm eff} = \frac{G}{\phi_0}\left(1 + \frac{M_V}{M_\odot}\right), \quad \gamma = \frac{M_\odot - M_V}{M_\odot + M_V}\,, \tag{4.48}$$

where $M_\odot$ and M_V are given by

$$M_\odot = \int {\rm d}^3x\, \rho(t, {\rm x})\frac{\phi_0}{\phi}\,, \quad M_V = \phi_0 \int {\rm d}^3x \left(\frac{V_0}{\phi_0} - \frac{V}{\phi}\right), \tag{4.49}$$

and ρ is the energy density of the Sun.

To ensure compatibility with LGC, three conditions must be satisfied [118]:

(i) $|M_V| \ll |M_\odot|\,,$

(ii) $|V_0\,\ell^2/\phi_0| \ll 1\,,$

(iii) the contribution of the term $\log\left(\phi/\phi_0\right)$ must be negligible.

The first condition arises from the experimental requirement $\gamma \approx 1$. Since it is not easy to interpret this requirement directly, we shall elucidate this by considering a specific $f(R)$

model later. Concerning condition (ii), setting $T = 0$ in Eq. (2.20) and using (4.16) to obtain $V_0 = f(R_0)$ translates this condition into

$$\left| \frac{f(R_0)}{f_{,R_0}(R_0)} \right| \ell^2 \ll 1 \,. \tag{4.50}$$

When the deviation from the ΛCDM model is small, the term $\frac{f(R_0)}{f_{,R_0}(R_0)}$ is of the order of the present cosmological Ricci scalar $R_0 \sim H_0^2$. Hence, on scales of the solar system this condition is well satisfied.

Regarding condition (iii), the presence of the term $\log(\phi/\phi_0)$ in Eqs. (4.46) and (4.47) leads to an additional acceleration of particles that should be small in order to be consistent with experiments. From the validity of the classical Euler equation, the condition (iii) translates to [118]

$$\left| \frac{\rho_s \partial\phi/\partial T}{\phi} \right| \ll 1 \,, \tag{4.51}$$

where ρ_s is the energy density of the local structure. This implies that the field, $\phi(T)$, should not have a strong dependence on T. Using the relations $T = 2V - \phi V_{,\phi}$ and $\phi V_{,\phi\phi} - V_{,\phi} = f_{,R}/f_{,RR} - R$, this condition translates to

$$\left| \frac{\rho_s / f_{,R_s}}{f_{,R_s}/f_{,R_sR_s} - R_s} \right| \ll 1 \,, \tag{4.52}$$

where R_s is the Ricci scalar corresponding to the local structure. It is sometimes useful to rewrite this condition in terms of the variable m defined in (4.6) thus:

$$\left| \frac{1}{m(R_s)} - 1 \right| \gg \frac{1}{f_{,R_s}} \frac{\rho_s}{R_s} \,. \tag{4.53}$$

When $|m(R_s)| \ll 1$, this is well satisfied since both $f_{,R_s}$ and ρ_s/R_s are of the order of unity. Note that this constraint is not so restrictive compared to the metric formalism. This can be understood by recalling that in the Palatini case the field is non-dynamical without an interaction range. In the metric formalism one needs a large scalaron mass, M, to satisfy the thin-shell condition, which leads to a very small value of $m(R_s)$ satisfying Eq. (4.39). We also note that in the Palatini case the condition $f_{,RR} > 0$ is not required in order to satisfy LGC.

As a concrete example, let us apply the above constraints to the theories given by Eq. (4.45) with $n > -1$. In order to give rise to a late-time acceleration, μ needs to be of the order of the present Hubble radius H_0. The field, ϕ, and the potential, $V(\phi)$, defined in

Eq. (4.16) are in this case given by

$$\phi = 1 + n\left(\frac{\mu^2}{R}\right)^{n+1}\,, \tag{4.54}$$

$$V(\phi) = (n+1)\mu^2\left(\frac{\mu^2}{R}\right)^{n} = (n+1)\mu^2\left(\frac{\phi-1}{n}\right)^{\frac{n}{(n+1)}}\,. \tag{4.55}$$

Now in the de-Sitter case [vacuum ($T=0$)], the solution R_0 satisfies

$$F(R_0)R_0 - 2f(R_0) = 0\,, \tag{4.56}$$

which for the model (4.45) gives

$$R_0 = (n+2)^{\frac{1}{(n+1)}}\mu^2\,, \tag{4.57}$$

and

$$\phi_0 = \frac{2(n+1)}{n+2}\,, \quad V_0 = \frac{n+1}{(n+2)^{\frac{n}{(n+1)}}}\mu^2\,. \tag{4.58}$$

In settings where local gravity experiments are carried out, the parameter $\epsilon \equiv \frac{\mu^2}{R_s} \sim \frac{\rho_0}{\rho_s}$ is much smaller than unity. For example, if we take the mean density $\rho_s = 10^{-11}\,\mathrm{g/cm^3}$ and use the typical values $\mu^2 \sim H_0^2 \sim \rho_0 = 10^{-29}\,\mathrm{g/cm^3}$ and $R_s \sim \rho_s$, then ϵ is of the order of 10^{-18}.

When $n > 0$, then in the limit $\epsilon \to 0$, we have $\phi \to 1$ and $V(\phi) \to 0$. Thus, in the expression for M_V given in Eq. (4.49) the term $\frac{V_0}{\phi_0}$ dominates over the term $\frac{V}{\phi}$. This implies that

$$M_V \approx \int \mathrm{d}^3x\, V_0 \approx \int \mathrm{d}^3x\, \mu^2 \quad \text{and} \quad M_\odot \approx \int \mathrm{d}^3x\, \rho_s\,. \tag{4.59}$$

Moreover, since $\mu^2 \sim \rho_0 \ll \rho_s$, the condition (i) is easily satisfied.

When $-1 < n < 0$, one has $\phi \to 1$ in the limit $\epsilon \to 0$ and the potential, V, becomes of the order $V \sim \mu^2(\mu^2/R)^n \gg V_0 \sim \mu^2$. This gives

$$|M_V| \approx \int \mathrm{d}^3x\, \mu^2(\mu^2/R)^n \approx \int \mathrm{d}^3x\, \rho_0(\rho_0/\rho_s)^n\,, \tag{4.60}$$

where $M_\odot$ is the same as that in Eq. (4.59). The ratio of the integrands in the expressions for M_V and $M_\odot$ can be estimated to be $(\rho_0/\rho_s)^{n+1} \ll 1$, which means that the condition $|M_V| \ll M_\odot$ is again satisfied.

The parameter m in this case is given by

$$m = -\frac{(n+1)n\epsilon^{n+1}}{1+n\epsilon^{n+1}}\,. \tag{4.61}$$

Now, since ϵ is much smaller than 1, we find that $|m(R_s)| \ll 1$. Hence, theories of the type (4.45) with $n > -1$ can satisfy local gravity constraints.

The above discussion shows that it is easier to satisfy the local gravity constraints in the Palatini formalism than in the metric approach. In the latter case, we also require the condition $f_{,RR} > 0$ to ensure that the scalaron mass squared is positive. Moreover, the requirement of a heavy field-mass, M, leads to very small values for $m(R_s)$, which imposes the condition that viable $f(R)$ models need to be very close to the ΛCDM model during the matter and radiation epochs. We also note that even though the condition $|m(R_s)| \ll 1$ is also required in the Palatini case, the absolute values of $|m(R_s)|$ do not need to be vanishingly small. Indeed, even models (4.45) with $n > 0$ can satisfy the correct Newtonian limit, whereas they are excluded in the metric formalism because $f_{,RR}$ is negative in these cases. Thus, in the Palatini formalism models of the type $f(R) = R - g(R)$ can be consistent with local gravity tests provided that the contribution of the term $g(R)$ is not significant relative to the linear term.

4.3 Density perturbations in the metric formalism

In this section, we discuss the evolution of matter perturbations and gravitational potentials for $f(R)$ theories in the metric formalism. When studying matter perturbations it is useful to work in the comoving gauge. In this gauge, the perturbation equations can be written in a closed form using the dimensionless variables (4.4). This allows the exact evolution of matter perturbations to be determined by solving the perturbation equations simultaneously with the background equations. When studying the gravitational potential, however, it is more convenient to work in the longitudinal gauge. We therefore consider the perturbation equations in these two gauges. We carry out a detailed analysis for a number of $f(R)$ models that can satisfy both the cosmological and local gravity constraints and use the evolution of density perturbations to place further constraints on the model parameters as well as their deviations from the ΛCDM model.

4.3.1 Comoving gauge ($v = 0$)

Here we derive the evolution equations for matter perturbations in the comoving gauge ($v = 0$). When $v = 0$ we have $\alpha = 0$ and $\dot{\delta}_m^{(v)} = \kappa$ from Eqs. (2.122) and (2.123). Hence, from Eq. (2.150) we find that

$$\ddot{\delta}_m^{(v)} + \left(2H + \frac{\dot{F}}{2F}\right)\dot{\delta}_m^{(v)} = \frac{1}{2F}\left[\left(-6H^2 + \frac{k^2}{a^2}\right)\delta F + 3H\delta\dot{F} + 3\delta\ddot{F} + \delta\rho_m\right] , \quad (4.62)$$

whereas from Eq. (2.151), the perturbation δF satisfies

$$\delta\ddot{F} + 3H\delta\dot{F} + \left(\frac{k^2}{a^2} + \frac{f_{,R}}{3f_{,RR}} - 4H^2 - 2\dot{H}\right)\delta F = \frac{1}{3}\delta\rho_m + \dot{F}\dot{\delta}_m^{(v)} . \quad (4.63)$$

The evolution of the matter perturbations $\delta_m^{(v)}$ can then be obtained by solving Eqs. (4.62) and (4.63) numerically.

1. Sub-horizon approximation

For models that satisfy local gravity constraints the mass squared term defined in Eq. (4.17) is well approximated by $M^2 \simeq \frac{f_{,R}}{3f_{,RR}}$. Such a term appears on the left-hand side of Eq. (4.63). Now, we are mainly interested in the evolution of perturbations on sub-horizon scales, i.e.,

$$\frac{k^2}{a^2} \gg \{H^2, |\dot{H}|\} . \quad (4.64)$$

We also recall that for the models satisfying LGC, the mass squared of the scalar field is much larger than $R \sim H^2 \sim |\dot{H}|$. Hence, either the terms $\frac{k^2}{a^2}$ or M^2 (or both) are dominant

in the parenthesis on the left-hand side of Eq. (4.63). Let us first consider the case in which the time-derivative terms in δF are neglected, i.e.,

$$\left\{\frac{k^2}{a^2}|\delta F|, M^2|\delta F|\right\} \gg \{|H\delta\dot{F}|, |\delta\ddot{F}|\}\,. \tag{4.65}$$

The condition (4.65) amounts to neglecting the term $\delta\ddot{F}$ that leads to the oscillations of δF. This is the approximation used to study scalar-tensor models in Refs. [9; 81; 127]. Later we explore the validity of such an approximation, paying particular attention to the conditions that should be satisfied.

Under the conditions (4.64) and (4.65), Eq. (4.63) gives

$$\delta R \simeq \frac{1}{F}\frac{\delta\rho_m + 3\dot{F}\dot{\delta}_m^{(v)}}{1+3\xi}\,, \tag{4.66}$$

where

$$\xi \equiv \frac{k^2}{a^2}\frac{f_{,RR}}{f_{,R}} = \frac{k^2}{a^2R}m\,. \tag{4.67}$$

Using the approximation (4.65) in Eq. (4.62), we obtain

$$\ddot{\delta}_m^{(v)} + \left(2H + \frac{1}{1+3\xi}\frac{\dot{F}}{2F}\right)\dot{\delta}_m^{(v)} - 4\pi G_{\rm eff}^{\rm cosmo}\rho_m\delta_m^{(v)} \simeq 0\,, \tag{4.68}$$

where the "cosmological" effective gravitational coupling is given by

$$G_{\rm eff}^{\rm cosmo} = \frac{G_N}{F}\left(\frac{1+4\xi}{1+3\xi}\right)\,, \tag{4.69}$$

and we have restored the bare gravitational constant G_N.

Introducing a physical wavelength $l = \frac{a}{k}$, the parameter ξ defined in Eq. (4.67) can be written as

$$\xi = \frac{1}{l^2}\frac{f_{,RR}}{f_{,R}} \simeq \frac{1}{3}\frac{1}{(Ml)^2}\,, \tag{4.70}$$

where in the last approximate equality we have used the approximate relation $M^2 \simeq \frac{f_{,R}}{3f_{,RR}}$.

In the regimes $\xi \ll 1$, i.e., $(Ml)^2 \gg 1$, Eq. (4.69) gives $G_{\rm eff}^{\rm cosmo} \simeq G_N/F$. In this case $m \ll 1$ for sub-horizon modes ($k \gg aH$). Thus, the deviation from the ΛCDM model is small, i.e., $|\dot{F}/HF| \ll 1$ in Eq. (4.68). Consequently, the evolution of matter perturbations is similar to that of the standard GR case. We reiterate that this General Relativistic behaviour can be realised even for $\omega_{\rm BD} = 0$ because of the presence of a potential with a heavy scalar-field mass ($M^2 \gg k^2/a^2$).

In the regimes $\xi \gg 1$, i.e., $(Ml)^2 \ll 1$, Eq. (4.69) gives $G_{\rm eff}^{\rm cosmo} \simeq 4G_N/3F$. Thus,

the evolution of matter perturbations is different from that of GR because of the appearance of the $\frac{4}{3}$ factor. If the mass of the Brans-Dicke scalar field is light ($M^2 \ll k^2/a^2$), the cosmological effective gravitational constant in Brans-Dicke theory is given by [127]

$$G_{\rm eff}^{\rm cosmo} \simeq \frac{G_N}{\phi}\left(\frac{4+2\omega_{\rm BD}}{3+2\omega_{\rm BD}}\right). \tag{4.71}$$

Thus, in the regime $\xi \gg 1$, the $f(R)$ theories in the metric formalism behave like Brans-Dicke theories (with $\omega_{\rm BD}=0$), with a light scalar-field mass ($M^2 \ll k^2/a^2$).

4.3.2 Longitudinal gauge ($\chi = 0$)

We shall also derive the approximate equations in the longitudinal gauge ($\chi = 0$) for sub-horizon modes satisfying Eq. (4.64). We use the notation $\alpha = \Phi$ and $\varphi = -\Psi$, which then gives the relation $\Psi = \Phi + \delta F/F$ from Eq. (2.149). In addition to Eq. (4.65), we impose the following conditions

$$|\dot{X}| \lesssim |HX|\,, \quad \text{where} \quad X = F, \dot{F}, \Phi, \Psi\,, \tag{4.72}$$

and

$$\left\{\frac{k^2}{a^2}|\Phi|, \frac{k^2}{a^2}|\Psi|, \frac{k^2}{a^2}|\delta F|\right\} \gg \left\{H^2|B|, H^2|\Phi|, H^2|\Psi|\right\}\,. \tag{4.73}$$

If the deviation from the ΛCDM model is not significant, the conditions (4.72) are well satisfied. The conditions (4.73) are also satisfied for sub-horizon modes given in Eq. (4.64) provided that Φ, Ψ and B are of the same order.

Under these approximations we obtain, from Eqs. (2.131), (2.147), (2.150) and (2.151), the following relations

$$\ddot{\delta}_m^{(\chi)} + 2H\dot{\delta}_m^{(\chi)} + \frac{k^2}{a^2}\Phi \simeq 0\,, \tag{4.74}$$

$$\frac{k^2}{a^2}\Phi \simeq -\frac{1}{2F}\left(\frac{1+4\xi}{1+3\xi}\right)\delta\rho_m\,, \tag{4.75}$$

$$\frac{k^2}{a^2}\Psi \simeq -\frac{1}{2F}\left(\frac{1+2\xi}{1+3\xi}\right)\delta\rho_m\,, \tag{4.76}$$

$$\delta F \simeq \frac{f_{,RR}}{f_{,R}}\left(\frac{1}{1+3\xi}\right)\delta\rho_m\,. \tag{4.77}$$

Eq. (2.148) suggests that the term v is of the order of $H\Phi/\rho_m$ provided that the devia-

tion from the ΛCDM model is not significant. Using Eq. (4.75) we find that the ratio $3Hv/(\delta\rho_m/\rho_m)$ is of the order of $\frac{(aH)^2}{k^2}$, which is much smaller than unity for sub-horizon modes. This gives $\delta_m^{(\chi)} \simeq \delta\rho_m/\rho_m$ in Eq. (2.138). Now using Eqs. (4.74) and (4.75), the matter perturbation in the longitudinal gauge satisfies the following approximate equation:

$$\ddot{\delta}_m^{(\chi)} + 2H\dot{\delta}_m^{(\chi)} - \frac{\rho_m}{2F}\left(\frac{1+4\xi}{1+3\xi}\right)\delta_m^{(\chi)} \simeq 0\,. \tag{4.78}$$

Compared to the comoving gauge the difference appears only in the friction term. Since viable $f(R)$ models satisfy the condition $|\dot{F}/HF| \ll 1$, Eq. (4.68) reduces to Eq. (4.78). It is trivial to check that in the uniform density gauge ($\delta\rho_m = 0$) the perturbation $\delta_m^{(\delta)}$ satisfies the same approximate equation as Eq. (4.78).

Before ending this subsection, we shall introduce a number of useful parameters. One such parameter is the effective gravitational potential

$$\Phi_{\rm eff} \equiv (\Phi + \Psi)/2\,, \tag{4.79}$$

which characterises the deviation of light rays. This is directly linked to the Integrated Sachs-Wolfe (ISW) effect in the CMB [39; 40] and weak lensing of distant galaxies [128; 127]. From Eqs. (4.75) and (4.76) we can approximate this parameter by

$$\Phi_{\rm eff} \simeq -\frac{a^2}{2k^2}\frac{\rho_m}{F}\delta_m^{(\chi)}\,. \tag{4.80}$$

A further parameter is the so-called anisotropic parameter

$$\eta \equiv \frac{\Phi - \Psi}{\Psi} \simeq \frac{2\xi}{1+2\xi}\,, \tag{4.81}$$

which behaves as $\eta \to 1$ for $\xi \gg 1$ and $\eta \to 2\xi$ for $\xi \ll 1$. We also define the quantity

$$\Sigma \equiv q(1+\eta/2)\,, \tag{4.82}$$

where q is defined via $(k^2/a^2)\Psi = -(1/2)q\rho_m\delta_m^{(\chi)}$. Using the above expressions, Σ can be approximated by

$$\Sigma \simeq 1/F\,. \tag{4.83}$$

Note that Σ is directly linked with $\Phi_{\rm eff}$. The parameters (Σ, η) will be especially important in future surveys of weak lensing [128; 127].

4.3.3 The appearance of scalarons

Among the approximations we have used in the previous two subsections, the conditions (4.43) and (4.65) can be violated if an oscillating mode (scalaron) dominates over the matter induced mode discussed above. Let us clarify when the oscillating mode becomes important for viable $f(R)$ models satisfying the conditions $m \ll 1$ and $|\dot{F}/HF| \ll 1$. For the sub-horizon modes, Eq. (4.63) is approximately given by

$$\delta\ddot{F} + 3H\delta\dot{F} + \left(\frac{k^2}{a^2} + M^2\right)\delta F \simeq \frac{1}{3}\delta\rho_m\,. \tag{4.84}$$

The solution of this equation is the sum of the matter induced mode $\delta F_{\rm ind}$ and the oscillatory scalaron mode $\delta F_{\rm osc}$ satisfying

$$\delta\ddot{F}_{\rm osc} + 3H\delta\dot{F}_{\rm osc} + \left(\frac{k^2}{a^2} + M^2\right)\delta F_{\rm osc} = 0\,. \tag{4.85}$$

Under the condition $\{M^2, k^2/a^2\} \gg H^2$ this equation reduces to the form

$$(a^{3/2}\delta F_{\rm osc})^{\cdot\cdot} + \omega^2(a^{3/2}\delta F_{\rm osc}) \simeq 0, \tag{4.86}$$

where $\omega = \sqrt{k^2/a^2 + M^2}$. In the adiabatic regime characterised by $|\dot{\omega}/\omega^2| \ll 1$ we obtain the following WKB solution

$$\delta F_{\rm osc} \simeq \frac{c}{a^{\frac{3}{2}}}\frac{1}{\sqrt{2\omega}}\cos\left(\int \omega {\rm d}t\right)\,, \tag{4.87}$$

where c is a constant. Hence, the solution of the perturbation δR is expressed by

$$\delta R \simeq \frac{1}{f_{,R}}\frac{1}{1+3\xi}\delta\rho_m + \frac{c}{a^{\frac{3}{2}}}\frac{1}{f_{,RR}\sqrt{2\omega}}\cos\left(\int \omega {\rm d}t\right)\,. \tag{4.88}$$

For viable $f(R)$ models, the scale factor, a, and the background Ricci scalar, $R^{(0)}$, evolve as $a \propto t^{2/3}$ and $R^{(0)} \simeq 4/(3t^2)$ during the matter era. In this case the amplitude of $\delta R_{\rm osc}$ relative to $R^{(0)}$ has a time-dependence

$$\frac{|\delta R_{\rm osc}|}{R^{(0)}} \propto \frac{M^2 t}{(k^2/a^2 + M^2)^{1/4}}\,. \tag{4.89}$$

Let us consider the models $m(r) = C(-r-1)^p$ ($p > 0$) for which the mass, M, evolves as $M \propto t^{-(p+1)}$ during the matter-dominated epoch. When $\xi \ll 1$ and $\xi \gg 1$ we have $|\delta R_{\rm osc}|/R^{(0)} \propto t^{-(3p+1)/2}$ and $|\delta R_{\rm osc}|/R^{(0)} \propto t^{-2(p+1/3)}$, respectively. Hence the amplitude of the oscillating mode decreases faster than the background Ricci scalar. This implies that if the scalaron is over-produced in the early Universe such that $|\delta R| > R^{(0)}$, the stability condition (4.43) can be violated. This property persists in the radiation-dominated epoch as

well [116]. Thus, in order to ensure the viability of $f(R)$ theories of gravity in the metric formalism, we need to ensure that $|\delta R|$ is smaller than $R^{(0)}$ at the beginning of the radiation era. This can be achieved by choosing the constant c in Eq. (4.87) to be sufficiently small which amounts to a fine tuning for these theories. We note that this fine tuning concerns the stability of these theories and is an additional constraint to those usually imposed on the parameters of these theories by observations.

Under the condition that the scalaron mode $\delta R_{\rm osc}$ is negligible relative to the matter-induced mode $\delta R_{\rm ind}$, one can derive the evolution for the matter perturbation δ_m as well as the effective gravitational potential $\Phi_{\rm eff}$. When $\xi \ll 1$ the evolutions of δ_m and $\Phi_{\rm eff}$ during the matter era are given by

$$\delta_m \propto t^{2/3}\,, \quad \Phi_{\rm eff} = {\rm constant}\,. \tag{4.90}$$

Note that the ratio of the matter induced mode relative to the background Ricci scalar evolves as $|\delta R_{\rm ind}|/R^{(0)} \propto t^{2/3} \propto \delta_m$. For the models that satisfy cosmological and local gravity constraints, the Universe typically starts from the regime $\xi \ll 1$ and evolves into the regime $\xi \gg 1$ during the matter-dominated epoch [116; 129]. When $\xi \gg 1$, δ_m and $\Phi_{\rm eff}$ evolve as

$$\delta_m \propto t^{(\sqrt{33}-1)/6}\,, \quad \Phi_{\rm eff} \propto t^{(\sqrt{33}-5)/6}\,. \tag{4.91}$$

For the models $m(r) = C(-r-1)^p$, we have the time-dependence $|\delta R_{\rm ind}|/R^{(0)} \propto t^{-2p+(\sqrt{33}-5)/6}$ in the regime $\xi \gg 1$. This decreases more slowly relative to the ratio $|\delta R_{\rm osc}|/R^{(0)} \propto t^{-2(p+1/3)}$, so the scalaron mode tends to become unimportant with time.

4.3.4 Numerical study of the validity of approximations

In this subsection we numerically solve the exact perturbation equations in order to check the validity of the approximations used to reach Eqs. (4.68), (4.78) and (4.80). We choose initial conditions such that the scalaron mode is suppressed relative to the matter induced mode, i.e. $|\delta R^i_{\rm osc}| < |\delta R^i_{\rm ind}|$. (See Ref. [129] for a comprehensive and detailed study of the scalaron mode. This study also gives the conditions under which the scalaron mode dominates over the matter induced mode at the initial stages.)

1. Comoving gauge

To study the dynamics of matter perturbations in the metric formalism, we use the dimensionless variables defined in Eq. (4.4). In terms of theses variables, the perturbation Eqs. (4.62)

and (4.63), in the comoving gauge, become

$$\delta_m^{(v)\prime\prime} + \left(x_3 - \frac{1}{2}x_1\right)\delta_m^{(v)\prime} - \frac{3}{2}(1 - x_1 - x_2 - x_3)\delta_m^{(v)} = \frac{1}{2}\Bigg[3\delta\tilde{F}'' + 3(-2x_1 + x_3 - 1)\delta\tilde{F}' + \left(\frac{k^2}{x_4^2} - 3 + 3x_1 + 9x_2 + 3x_3\right)\delta\tilde{F}\Bigg], \tag{4.92}$$

$$\delta\tilde{F}'' \;+\; (1 - 2x_1 + x_3)\,\delta\tilde{F}' + \left[\frac{k^2}{x_4^2} - x_3 + \frac{2x_3}{m} + 1 - x_1 + 3x_2\right]\delta\tilde{F} = (1 - x_1 - x_2 - x_3)\delta_m^{(v)} - x_1\delta_m^{(v)\prime}\,, \tag{4.93}$$

where $\delta\tilde{F} \equiv \delta F/F$ and a prime denotes a derivative with respect to the number of e-foldings $N = \ln(a)$. The exact evolution of the matter perturbations can be obtained by solving these equations together with the background equations (4.8)-(4.11) for x_1, x_2, x_3 and x_4. Meanwhile, the approximate equation (4.68) can be expressed in terms of these variables as

$$\delta_m^{(v)\prime\prime} + \left[x_3 - \frac{x_1}{2(1+3\xi)}\right]\delta_m^{(v)\prime} - \frac{3}{2}(1 - x_1 - x_2 - x_3)\left(\frac{1+4\xi}{1+3\xi}\right)\delta_m^{(v)} \simeq 0\,, \tag{4.94}$$

where

$$\xi = \frac{k^2}{(aH)^2}\frac{m}{6x_3}\,. \tag{4.95}$$

Let us consider the case in which the condition $M^2 \gg k^2/a^2$ (i.e., $\xi \ll 1$) is satisfied. Since M needs to be large during the matter-dominated epoch to satisfy LGC, this condition holds in viable $f(R)$ models at the beginning of the matter era for the modes relevant to large scale structure [116; 129]. Consequently the term $2x_3/m$ dominates over the term k^2/x_4^2 in Eq. (4.93), which gives $\delta\tilde{F} \sim m\delta_m^{(v)}$ under the neglect of scalarons. Hence, the right-hand side of Eq. (4.92) can be neglected relative to the left-hand side, which means that Eq. (4.92) reduces to Eq. (4.94). The above argument shows that, in the regime $\xi \ll 1$, Eq. (4.94) can be valid even for super-Hubble modes as long as the contribution of the scalaron is unimportant. In this regime the matter perturbations evolve as in the case of standard GR, i.e. $\delta_m^{(v)} \propto t^{2/3}$.

The perturbations can enter the regime $M^2 \ll k^2/a^2$ (i.e., $\xi \gg 1$) before reaching the present epoch, depending on the mode k and on the evolution of M [116; 129]. For example, for the model $m(r) = (-r-1)^3$ this occurs for the modes $k/a_0H_0 > 3.5$, where a subscript 0 represents present values. In the case $k/a_0H_0 = 300$, the redshift ($z \equiv \frac{a_0}{a} - 1$) at $k/a = M$ corresponds to $z_k = 4.83$. Since M^2 is always larger than H^2 in the past because of the requirement $m \ll 1$, the modes are inside the Hubble radius ($k^2/a^2H^2 > 1$) after the perturbations enter the regime $M^2 < k^2/a^2$. Hence the approximation we used to reach Eq. (4.94) is valid in this regime. In the regime $M^2 < k^2/a^2$ the term $(k^2/x_4^2)\delta\tilde{F}$ in Eq. (4.93)

balances the term $(1 - x_1 - x_2 - x_3)\delta_m^{(v)}$, which gives rise to an additional contribution on the right-hand side of Eq. (4.92). This then leads to the approximate equation (4.94) with $\xi \gg 1$, which has a growing-mode solution $\delta_m \propto t^{(\sqrt{33}-1)/6}$.

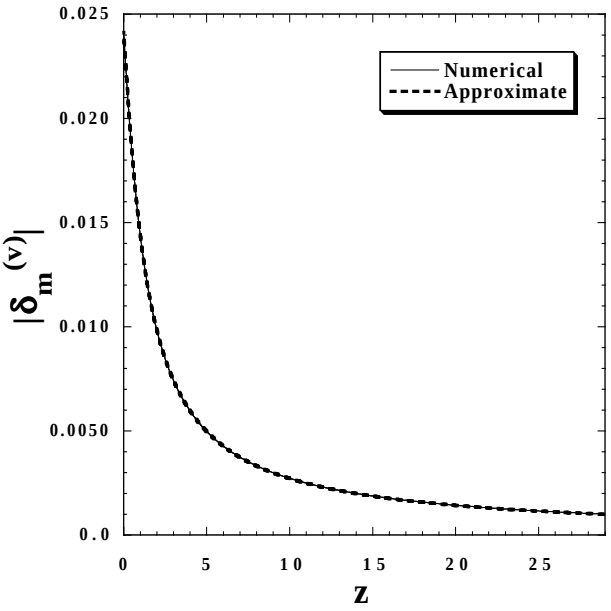

Figure 4.1: The evolution of the matter perturbation $\delta_m^{(v)}$ in the comoving gauge for the model $m(r) = (-r-1)^3$ with the mode $k/a_0H_0 = 10$. Initial conditions were chosen to be $x_1 = 0$, $x_2 = -0.5000$, $x_3 = 0.5001$, $\delta_m^{(v)} = 10^{-3}$, $\delta_m^{(v)\prime} = 10^{-3}$, $\delta\tilde{F} = 8.0 \times 10^{-15}$, $\delta\tilde{F}' = 0$ and $k/a_iH_i = 4.1$ at the redshift $z = 28.9$. The solid curve is obtained by solving the exact equations (4.92) and (4.93) numerically, whereas the dotted one is obtained by solving the approximate equation (4.94).

In Fig. 4.1 we plot the evolution of $\delta_m^{(v)}$ for the model $m(r) = (-r-1)^3$ with the mode $k/a_0H_0 = 10$. Initial conditions are chosen so that the scalaron mode does not dominate over the matter-induced mode. In this case the transition from the regime $M^2 > k^2/a^2$ to the region $M^2 < k^2/a^2$ occurs at the redshift $z_k = 1.62$. We find that the approximate equation (4.94) shows an excellent agreement with the results obtained by numerically solving the exact equations (4.92) and (4.93). The argument also holds for modes that are initially outside the Hubble radius. Thus the approximate equation (4.68) is reliable in estimating the growth of matter perturbations and the resulting matter power spectrum, provided that the scalaron does not dominate in the early Universe.

2. Longitudinal gauge

In the longitudinal gauge the combination of Eqs. (2.147)-(2.151) leads to the following perturbation equations

$$\Phi'' + \left(2-\frac{3}{2}x_1+x_3\right)\Phi' + (3x_2+3x_3)\Phi = \frac{3}{2}x_2\delta\tilde{F} - \left(\frac{1}{2}x_3+1\right)\delta\tilde{F}' - \frac{1}{2}\delta\tilde{F}'\,, \tag{4.96}$$

$$\delta\tilde{F}'' + (x_3+2)\delta\tilde{F}' + \left(\frac{4}{3}\frac{k^2}{x_4^2}+3x_2+\frac{2x_3}{m}\right)\delta\tilde{F} = \left(6x_2+2x_3-\frac{2}{3}\frac{k^2}{x_4^2}\right)\Phi - (3x_1+2)\Phi', \tag{4.97}$$

$$\delta_m^{(\chi)} = \frac{1}{1-x_1-x_2-x_3}\left[\left(2+3x_2-x_3+\frac{2x_3}{m}+\frac{k^2}{x_4^2}\right)\delta\tilde{F} + (2+x_1+x_3)\delta\tilde{F}' + \delta\tilde{F}'' + (x_1-6x_2-2x_3)\Phi + (4x_1+2)\Phi'\right], \tag{4.98}$$

$$\frac{\rho_m v}{FH} = 2\Phi' + (2-x_1)\Phi + \delta\tilde{F}' + (1+x_1)\delta\tilde{F}\,, \tag{4.99}$$

where we have used $\Psi = \Phi + \delta\tilde{F}$. The effective potential defined in Eq. (4.79) is given by

$$\Phi_{\rm eff} = \Phi + \frac{1}{2}\delta\tilde{F}\,. \tag{4.100}$$

In order to understand the evolution of perturbations at the initial stages of the matter era, let us consider the regime $\xi \ll 1$ without assuming the sub-horizon condition $k/(aH) \gg 1$. We have in mind viable $f(R)$ models with vanishingly small values of m deep inside the matter epoch. Equation (4.97) then becomes

$$\delta\tilde{F} \simeq -2m\left[1+\frac{k^2}{3(aH)^2}\right]\Phi - 2m\Phi'\,. \tag{4.101}$$

Note that under the sub-horizon approximation we have $\delta\tilde{F} \simeq -2mk^2\Phi/3(aH)^2$, which agrees with Eq. (4.75). Using Eq. (4.101) we find that the right-hand side of Eq. (4.96) can be neglected relative to the left-hand side, thus giving the solution $\Phi = {\rm constant}$ (together with a decaying mode proportional to $t^{-5/3}$). From Eqs. (4.79) and (4.98) we obtain $\Phi_{\rm eff} \simeq \Phi$ and

$$\delta_m^{(\chi)} \simeq -\frac{2k^2}{3(aH)^2\Omega_m}\Phi_{\rm eff}\,, \tag{4.102}$$

$$\delta_m^{(\chi)\prime} \simeq \delta_m^{(\chi)}\,. \tag{4.103}$$

Equation (4.102) agrees with the expression (4.80) obtained under the sub-horizon approx-

imation ($k/a \gg H$). Since $\Phi_{\rm eff}$ is a constant, the matter perturbation can be seen from Eq. (4.102) to evolve as $\delta_m^{(\chi)} \propto a$. This is consistent with the approximate equation (4.78), i.e.,

$$\delta_m^{(\chi)\prime\prime} + x_3 \delta_m^{(\chi)\prime} - \frac{3}{2}(1 - x_1 - x_2 - x_3)\frac{1+4\xi}{1+3\xi}\delta_m^{(\chi)} \simeq 0\,, \tag{4.104}$$

which has the growing mode solution $\delta_m^{(\chi)} = \delta_m^{(\chi)\prime} \propto a$ in the regime $\xi \ll 1$.

One may ask why the above method reproduces the result derived under the sub-horizon approximation, without employing the approximation $k/a \gg H$. In the regime $\xi \ll 1$ the perturbation $\delta\tilde{F}$ is suppressed relative to Φ as given in Eq. (4.101). This allows us to neglect the right-hand side of Eq. (4.96), giving a constant Φ. This mimics the situation in General Relativity where $\delta\tilde{F} = 0$ and $\Phi = {\rm constant}$ together with Eq. (4.102), resulting in $\delta_m^{(\chi)} \propto a$. Moreover, from Eq. (4.99), the quantity $B = Hv + \Psi$ is well approximated by $B \simeq 5\Phi/3 = {\rm constant}$. Hence the right-hand side of Eq. (2.131) can be neglected even without assuming the sub-horizon approximation. Thus, using the relation (4.102) we can obtain Eq. (4.78) in the regime $\xi \ll 1$ without assuming $k/a \gg H$. The above approximation corresponds to the limit of large M ($M^2 \gg k^2/a^2$), which gives rise to the evolution of perturbations that is similar to the case of General Relativity. In General Relativity ($\delta F = 0$ and $\dot{F} = 0$), one has the exact equation (4.102) from Eqs. (2.147) and (2.148). Thus the perturbations in the large M case ($\xi \ll 1$) mimic those in General Relativity, apart from the fact that the scalaron is present in the former but not in the latter.

When $\xi \gg 1$ one has $k^2/a^2 \gg M^2 \gg H^2$, which means that the sub-horizon type approximation we used in Sec. 4.3.2 holds in this regime. This situation is similar to the case of the comoving gauge. For the modes that start from the regime $M^2 \gg k^2/a^2$ and enter the regime $M^2 \ll k^2/a^2$ before the end of the matter era, the evolution of perturbations changes from the standard general relativistic form (4.90) to the non-standard form (4.91).

In Fig. 4.2 we plot the evolution of $\delta_m^{(\chi)}$ and $\Phi_{\rm eff}$ in the model $m(r) = (-r-1)^3$ for the mode $k = a_0 H_0$ that lies outside the Hubble radius at the start of integration ($z = 28.9$). Together with numerically integrating Eqs. (4.96)-(4.98), we also solve the approximate equation (4.104) with $\Phi_{\rm eff}$ derived from (4.80). From Fig. 4.2 we find that the approximate equations agree well with the exact numerical results, even if the mode is initially slightly outside the Hubble radius. We note, however, that for large-scale modes far outside the Hubble radius the scalaron can be important. In fact, we have numerically verified that the oscillating mode appears for such super-Hubble modes unless the coefficient of the scalaron in Eq. (4.88) is fine-tuned to be small. In Fig. 4.2 the growth of the gravitational potential is not seen in the region $z < z_k$, since the transition redshift is small ($z_k = 0.36$). It can, however, be observed if we consider modes on smaller scales.

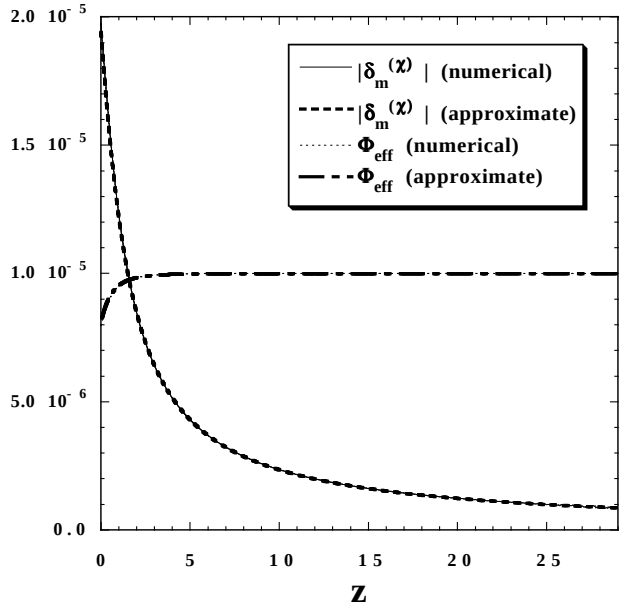

Figure 4.2: The evolution of $\delta_m^{(\chi)}$ and $\Phi_{\rm eff}$ in the longitudinal gauge for the model $m(r) = (-r-1)^3$ with a mode $k = a_0 H_0$. The results were obtained by numerically integrating Eqs. (4.96), (4.97) and (4.98) with initial conditions $\Phi_{\rm eff} = 10^{-5}$, $\Phi'_{\rm eff} = 0$ and $k/a_i H_i = 0.36$ and with $\delta_m^{(\chi)}$ and $\delta_m^{(\chi)\prime}$ satisfying Eqs. (4.102) and (4.103). Initial conditions for the background quantities were chosen to be the same as in Fig. 4.1. We also plot $\delta_m^{(\chi)}$ and $\Phi_{\rm eff}$ obtained by solving the approximate equations (4.104) and (4.80). The approximation is valid even when the mode is initially outside the Hubble radius.

In summary, for viable $f(R)$ models that satisfy the cosmological and local gravity constraints, the approximate Eqs. (4.104) and (4.80) are valid even for those modes outside the Hubble radius, as long as the scalaron is suppressed relative to the matter-induced mode.

4.3.5 Constraints on the models $m(r) = C(-r-1)^p$

We consider the current and future constraints on models of the type $m(r) = C(-r-1)^p$ with $0 < C \leq 1$. At the background level, compatibility with the SNIa observations could result in the divergence of the equation of state of dark energy [122; 129]. Interestingly the redshift at which such a divergence may occur could be of order unity. However, the current SNIa observations are not yet sufficiently accurate to rule out such cases. Some constraints on the model parameters can be obtained from the present equation of state of dark energy, but even models with $p = 1.5$ and $C = 1$ are allowed [129]. Thus, the background does not provide strong constraints. However, this situation may change in the future when higher redshift data become available from SNIa and Gamma Ray burst observations.

On the other hand, we recall from Sec. 1 that there are a number of constraints on the

growth rate of matter perturbations, s, defined as

$$s \equiv \frac{\mathrm{d} \ln \delta_m}{\mathrm{d}N}. \tag{4.105}$$

(Note that in the standard general relativistic case, where $\delta_m \propto a$, the growth rate $s = 1$). From Eqs. (4.90) and (4.91) we have $s = 1$ for $M^2 \gg k^2/a^2$ and $s = (\sqrt{33} - 1)/4 = 1.186$ for $M^2 \ll k^2/a^2$. In Fig. 4.3 we plot the evolution of the growth rate for models $m(r) = (-r-1)^3$ for a number of different values of k. The increase of s from unity implies that the perturbations enter the regime $M^2 \ll k^2/a^2$. For smaller scale modes this transition occurs earlier, which leads to a larger maximum value of s. The growth rate begins to decrease once the Universe enters the late-time accelerated epoch. As estimated analytically, the growth rate is bounded by $s < 1.186$. Hence the current observational constraint (1.2) is still too weak to place constraints on $m(r) = C(-r-1)^p$ models.

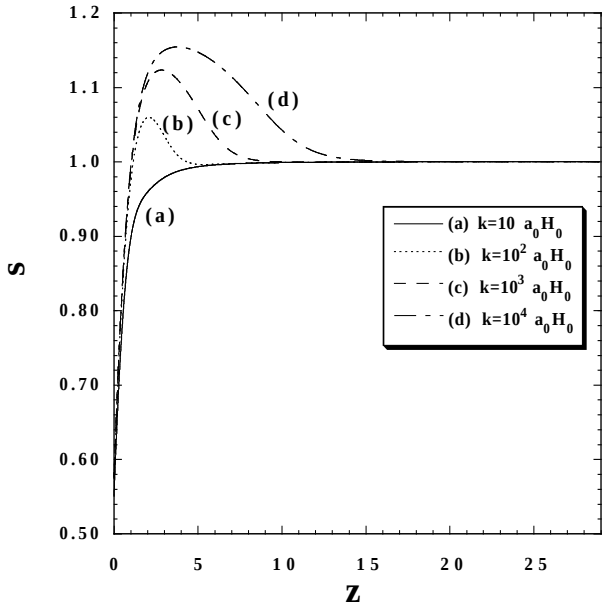

Figure 4.3: The evolution of the growth rate $s = \delta_m'/\delta_m$ with respect to the redshift z in the model $m(r) = (-r-1)^3$ with four different values of k. Initial conditions were chosen as in Fig. 4.2. The transition redshift z_k, defined as the redshift where $k/a = M$, becomes larger for smaller scales. After the matter perturbation enters the region $z < z_k$ the growth rate begins to increase toward the value $s = 1.186$, but it starts to decrease once the Universe enters the stage of accelerated expansion.

However, these models exhibit peculiar features in the matter power spectrum. This is a consequence of the fact that there is a transition redshift z_k at which the growth rate begins to change from $s = 1$ to $s = 1.186$. For the modes relevant to galaxy clusters

[$k/a_0H_0 = \mathcal{O}(10^2)$], this transition typically occurs during the matter-dominated epoch (see Fig. 4.3). Since the time t_k at $z = z_k$ depends upon the modes k ($t_k \propto k^{-3/(3p+1)}$), this leads to a change in the slope of the matter power spectrum. The difference between the slopes of the matter power spectrum determined from galaxy surveys and the CMB spectrum, on the scales $k/a_0H_0 = \mathcal{O}(10^2)$, is given by [116; 129]

$$\Delta n \simeq \frac{\sqrt{33}-5}{3p+1}\,. \tag{4.106}$$

This analytic result agrees well with numerical results except for models with $p \gg 1$ [129]. Observationally no significant differences have so far been found between the two power spectra. If we take the bound $\Delta n < 0.05$, we obtain the constraint $p \geq 5$. To place further constraints on models, a likelihood analysis is required which employs the data from both the galaxy power spectrum and the CMB.

Numerically, we find that the models $m(r) = (-r-1)^5$ are constrained by a limit on the present value of the deviation parameter given by $m(z=0) \lesssim 10^{-1}$. Thus, even though m is constrained to be very small during the matter era, a notable deviation from the ΛCDM model can occur around the present epoch.

Finally, the ISW effect in the CMB power spectrum is important for large scale modes with $k/a_0H_0 = \mathcal{O}(1)$. As can be seen from Fig. 4.2, even models with $p = 3$ and $C = 1$ do not give rise to a significant amplification of the gravitational potential. The models with $p \geq 2$ are consistent with the low multipoles in the CMB data [129]. Thus, this effect does not generally provide stronger additional constraints.

4.4 Density perturbations in the Palatini formalism

Given the non-dynamical nature of Eq. (2.156), it is clear that the scalaron mode does not exist in the Palatini case. This is associated with the fact that the Palatini formalism corresponds to a generalised Brans-Dicke theory with $\omega_{\rm BD} = -\frac{3}{2}$. The perturbation δF is directly determined by the matter perturbation $\delta\rho_m$ as

$$\delta F = \frac{F_{,R}}{F}\frac{\delta\rho_m}{1-m}\,, \tag{4.107}$$

where m is defined in Eq. (4.6).

As in the metric case, we choose to work in different gauges depending on convenience. For the study of matter density perturbations it is convenient to consider the comoving gauge, where the perturbation equations close. On the other hand, the longitudinal gauge can be more useful when discussing gravitational potentials.

4.4.1 Comoving gauge

In the comoving gauge ($v = 0$) one has $\alpha = 0$ and $\kappa = \dot{\delta}_m^{(v)}$. Then, from Eq. (2.155), we find

$$\ddot{\delta}_m^{(v)} + \left(2H + \frac{\dot{F}}{2F}\right)\dot{\delta}_m^{(v)} = \frac{1}{2F}\Bigg[\delta\rho_m + 3\delta\ddot{F} + \left(3H - \frac{6\dot{F}}{F}\right)\delta\dot{F} + \left(6H^2 + 6\dot{H} + \frac{3\dot{F}^2}{F^2} - R + \frac{k^2}{a^2}\right)\delta F\Bigg]. \tag{4.108}$$

As in the metric case this equation needs to be solved simultaneously with the background equations (2.105)-(2.107). Unlike the metric case, however, it is not easy to find dimensionless variables in terms of which both sets of equations close. As a result we proceed to integrate the equations directly. Using the background equations and ignoring the radiation, the perturbation equation (4.108) can be written as

$$P_1\delta_m^{(v)\prime\prime} + P_2\delta_m^{(v)\prime} + P_3\delta_m^{(v)} = 0\,, \tag{4.109}$$

where the coefficients P_1, P_2, P_3 are given by

$$P_1 = \left(1 - \frac{3J}{2F}\right)H^2\,, \tag{4.110}$$

$$P_2 = \left(2 + \frac{15J}{2F}\right)H^2 + \left(1 - \frac{3J}{2F}\right)\dot{H} + \left(\frac{1}{2} + \frac{6J}{F}\right)\frac{\dot{F}H}{F} - \frac{3J}{F}\frac{H\dot{F}_{,R}}{F_{,R}} - \frac{3J}{F}\frac{H\dot{m}}{1-m}\,, \tag{4.111}$$

$$
\begin{aligned}
P_3 \;=\; & \frac{-\rho_m}{2F} - \frac{J}{2F}\left(6H^2 + 6\dot{H} + \frac{3\dot{F}^2}{F^2} - R + \frac{k^2}{a^2}\right) \\
& -\frac{J}{2F}\left(3H - \frac{6\dot{F}}{F}\right)\left(\frac{\dot{F}_{,R}}{F_{,R}} - 3H - \frac{\dot{F}}{F} + \frac{\dot{m}}{1-m}\right) \\
& -\frac{3J}{2F}\left[\left(\frac{\dot{F}_{,R}}{F_{,R}} - 3H - \frac{\dot{F}}{F} + \frac{\dot{m}}{1-m}\right)^2 + \frac{\ddot{F}_{,R}}{F_{,R}} - \left(\frac{\dot{F}_{,R}}{F_{,R}}\right)^2\right. \\
& \left. - 3\dot{H} - \frac{\ddot{F}}{F} + \left(\frac{\dot{F}}{F}\right)^2 + \frac{\ddot{m}}{1-m} + \left(\frac{\dot{m}}{1-m}\right)^2\right],
\end{aligned}
\tag{4.112}
$$

and J is defined as

$$
J \equiv \frac{F_{,R}}{F}\frac{\rho_m}{1-m}. \tag{4.113}
$$

All the terms in the coefficients P_1, P_2, P_3 can be expressed in terms of the scale factor a (or equivalently N), which thus allows Eq. (4.109) to close and be readily integrated numerically.

On the other hand, since we are mostly interested in the evolution of modes on sub-horizon scales, it makes sense to consider the approximate equations similar to those considered in the metric case.

Using a sub-horizon type approximation, such that only those terms containing k^2/a^2 and $\delta\rho_m$ are considered on the right-hand side of Eq. (4.108), together with Eq. (4.107), we obtain the following approximate perturbation equation

$$
\ddot{\delta}_m^{(v)} + \left(2H + \frac{\dot{F}}{2F}\right)\dot{\delta}_m^{(v)} - \frac{\rho_m}{2F}\left(1 + \frac{\xi}{1-m}\right)\delta_m^{(v)} \simeq 0\,, \tag{4.114}
$$

where ξ is defined in Eq. (4.67).

Alternatively we may study the case in which the deviation from the ΛCDM model is small, i.e.,

$$
|m| \ll 1\,, \tag{4.115}
$$

as required from the local gravity constraint (4.53). The derivative terms such as $|m'|$ and $|m''|$ are also assumed to be much smaller than unity. Using the fact that from Eqs. (2.107) and (4.107) the perturbation δF in this case is of the order of $m\delta_m^{(v)}$, Eq. (4.114) can be obtained under condition (4.115) without using the sub-horizon approximation. Thus, if the deviation from the ΛCDM model is small, the approximate equation (4.114) is valid even for modes outside the Hubble radius. This situation is similar to the metric case. In fact, we have confirmed this property by numerically solving the exact equation (4.108) and comparing it

with the solutions of the approximate equation (4.114).

One can estimate the order of the term $R\delta F$ on the right-hand side of Eq. (2.155) by using Eq. (4.107), i.e., $R\delta F = m\delta\rho_m/(1-m)$. This gives rise to the contribution of the order of $(\rho_m/2F)m\delta_m^{(v)}$ in the third term of Eq. (4.114), which is negligible under the condition (4.115). As long as we neglect this contribution, we can approximate $\xi/(1-m) \simeq \xi$ in the third term of Eq. (4.114). In the following, we implicitly assume this when we write the term $(1-m)$ in the denominator.

In the limit $\xi = \frac{k^2}{a^2R}m \ll 1$, Eq. (4.114) agrees with Eq. (4.68) of the metric formalism. However, a significant difference appears in the regime $\xi \gg 1$. In that case there is a strong amplification of the matter perturbation in the Palatini case due of the growth of the term ξ in Eq. (4.114).(We recall from Sec. 3 that this property leads to the discrepancy between the evolution of matter perturbations that we derived using the LuSS and KKS approaches). We shall estimate this growth rate for a number of concrete models in Sec. 4.4.3 below.

4.4.2 Longitudinal gauge

We next consider the Longitudinal gauge ($\chi = 0$), and as in the metric case we use the notation $\alpha = \Phi$ and $\varphi = -\Psi$. Under the sub-horizon type approximation used in the comoving case above, the evolution equation reduces to Eq. (4.74) obtained in the metric formalism. Using Eqs. (2.152) and (2.154), together with Eq. (4.107), these approximations also give

$$\frac{k^2}{a^2}\Phi \simeq -\frac{1}{2F}\left(1+\frac{\xi}{1-m}\right)\delta\rho_m\,, \quad \frac{k^2}{a^2}\Psi \simeq -\frac{1}{2F}\left(1-\frac{\xi}{1-m}\right)\delta\rho_m\,. \tag{4.116}$$

Hence, the matter perturbations satisfy the following approximate equation

$$\ddot{\delta}_m^{(\chi)} + 2H\dot{\delta}_m^{(\chi)} - \frac{\rho_m}{2F}\left(1+\frac{\xi}{1-m}\right)\delta_m^{(\chi)} \simeq 0\,. \tag{4.117}$$

The effective gravitational potential $\Phi_{\rm eff}$ defined in Eq. (4.79) satisfies

$$\Phi_{\rm eff} \simeq -\frac{a^2}{2k^2}\frac{\rho_m}{F}\delta_m^{(\chi)}\,, \tag{4.118}$$

which is the same as in the metric case. Finally, the parameters η and Σ defined in Eqs. (4.81) and (4.82) become

$$\eta \simeq \frac{2\xi}{1-m-\xi}\,, \quad \Sigma \simeq \frac{1}{F}\,. \tag{4.119}$$

We note that while the expression for η is different from that in the metric case, Σ remains the same.

The above approximate equations (4.117) and (4.118) are valid under the conditions

(4.115) and $\xi \ll 1$ even without the sub-horizon approximation. Indeed, the argument is similar to the metric case in which Eqs. (4.78) and (4.80) reduce to the corresponding GR equations for $\xi \ll 1$.

We also note that in the regime $\xi \gg 1$ the perturbation modes are inside the Hubble radius, which shows that the sub-horizon approximation is still valid. Thus, as long as the condition (4.115) is satisfied, we can safely use Eqs. (4.117) and (4.118) even for super-Hubble modes. Furthermore, since in the Palatini formalism the perturbation δR is sourced only by the matter induced mode, we do not need to worry about the dominance of the scalaron oscillations for super-Hubble modes.

In Sec. 3.1 the evolution equation for matter perturbations, Eq. (3.6), was derived in the uniform density gauge [68]. This is an exact equation as is the corresponding equation in the comoving gauge. Given that under the approximation (4.115), the term $|\dot{F}/HF|$ is of the order of $|m|$, the coefficients c_1 and c_2 given by Eqs. (3.7) and (3.8) become:

$$c_1 = 2H\,, \quad c_2 = H^2 \left[-\frac{\ddot{H}}{H^3} - \frac{2\dot{H}}{H^2} + \frac{\dot{F}}{6HF}\frac{k^2}{(aH)^2} \right]. \tag{4.120}$$

We can estimate the first two terms in the square bracket of c_2 by employing the following approximate relations

$$2F\dot{H} \simeq -\rho_m\,, \quad 2F\ddot{H} \simeq 3H\rho_m\,, \tag{4.121}$$

which follows from Eqs. (2.105) and (2.107). Moreover, Eq. (2.108) implies that

$$\dot{F} = -\frac{3\rho_m F_{,R} H}{F - RF_{,R}}\,. \tag{4.122}$$

Using these relations, we find that the matter perturbation satisfies the following approximate equation of motion:

$$\ddot{\delta}_m^{(\delta)} + 2H\dot{\delta}_m^{(\delta)} - \frac{\rho_m}{2F}\left(1 + \frac{\xi}{1-m}\right)\delta_m^{(\delta)} \simeq 0\,. \tag{4.123}$$

This is the same as the evolution equation arising in the longitudinal gauge, Eq. (4.117).

Since the evolution of matter perturbations do not physically depend on the gauge chosen, we shall denote the matter perturbation simply by δ_m in what follows.

4.4.3 Analytic estimate for the growth of perturbations

As was discussed above, the evolution of perturbations in the regime $\xi \ll 1$ is similar to the standard GR case where $\delta_m \propto t^{2/3}$, $s = \delta_m'/\delta_m = 1$ and $\Phi = \text{constant}$. In this subsection, we shall estimate the growth rate of perturbations after the system enters the regime $\xi > 1$.

We shall consider models with $|m| \ll 1$ to be consistent with the local gravity constraint (4.53).

During the matter era, in which the Ricci scalar evolves as $R \propto t^{-2}$, the parameter ξ is given by $\xi = \pm ma/m_k a_k$, where the subscript "k" denotes values when the system crosses $\xi = 1$. Here we note that the plus sign corresponds to a positive m and the negative sign to a negative m. As we have shown in Sec. 4.2.2, the latter case is allowed, which is not so for the metric formalism. It follows that under the condition $|m| \ll 1$, the matter perturbation (4.117) satisfies the following equation

$$\delta_m'' + \frac{1}{2}\delta_m' - \frac{3}{2}\left(1 \pm \frac{m}{m_k}e^{N-N_k}\right)\delta_m \simeq 0\,. \tag{4.124}$$

We now consider the case in which the evolution of the parameter m is given by

$$m \propto t^{2p}\,, \tag{4.125}$$

where p is a constant. Several different $f(R)$ models are parametrised by specific values of p in the following way:

(i) $f(R) = \alpha R^{1+m} - \Lambda$: $p = 0$ (here Λ is a constant),

(ii) $f(R) = R - \lambda R_c \left(\frac{R}{R_c}\right)^{\beta}$: $p = 1 - \beta$ for $R \gg R_c$,

(iii) $f(R) = R - \lambda R_c \frac{(R/R_c)^{2n}}{(R/R_c)^{2n}+1}$: $p = 2n + 1$ for $R \gg R_c$,

(iv) $f(R) = R - \lambda R_c \left[1 - \left(1 + \frac{R^2}{R_c^2}\right)^{-n}\right]$: $p = 2n + 1$ for $R \gg R_c$,

where n and λ are positive constants. With the above choice of m, Eq. (4.124) reduces to

$$\delta_m'' + \frac{1}{2}\delta_m' - \frac{3}{2}\left[1 \pm e^{(3p+1)(N-N_k)}\right]\delta_m \simeq 0\,. \tag{4.126}$$

Taking the positive sign in Eq. (4.126), i.e., $m > 0$, the solution of Eq. (4.126) can be written in terms of a linear combination of Bessel functions J_ν and Y_ν:

$$\delta_m = e^{-(N-N_k)/4}\left[\alpha_1 J_\nu(ix) + \alpha_2 Y_\nu(ix)\right]\,, \tag{4.127}$$

where α_1, α_2 are constants and

$$x = \frac{\sqrt{6}e^{(3p+1)(N-N_k)/2}}{3p+1}\,, \quad \nu = \frac{5}{6p+2}\,. \tag{4.128}$$

For the negative sign in Eq. (4.126), i.e., $m < 0$, the solution of Eq. (4.126) is given by

$$\delta_m = e^{-(N-N_k)/4}\left[\alpha_1 J_\nu(x) + \alpha_2 Y_\nu(x)\right]\,, \tag{4.129}$$

where x and ν are defined in (4.128).

In the following, we shall discuss both positive and negative cases in turn.

1. $m > 0$

As an example, we consider the constant m models ($p = 0$). In this case, the Bessel function $J_\nu(ix)$ has a growing mode solution $J_{5/2}(ix) \propto I_{5/2}(x) \propto e^x/\sqrt{x}$ for $x \gg 1$, where $I_{5/2}(x)$ is a modified Bessel function with $x = \sqrt{6}e^{(N-N_k)/2}$. Consequently, in the regime $\xi \gg 1$, the evolution of the matter perturbation and its growth rate are given by

$$\delta_m \propto \exp(\sqrt{6}e^{(N-N_k)/2})\,, \quad s = \frac{\delta_m'}{\delta_m} = \frac{\sqrt{6}}{2}e^{(N-N_k)/2}\,, \tag{4.130}$$

where we have used $\sqrt{6}e^{(N-N_k)/2} \gg (N-N_k)/2$. Thus, the growth rate of matter perturbations increases very rapidly. Moreover, it follows from Eq. (4.118) that in the regime $\xi \gg 1$ the effective gravitational potential grows exponentially as

$$\Phi_{\rm eff} \propto \exp(e^{\sqrt{6}(N-N_k)/2})\,, \tag{4.131}$$

which leads to a strong and observable ISW effect.

Similarly, in models with $p \neq 0$, one can estimate the evolution of perturbations in the regime $\xi \gg 1$:

$$\delta_m \propto \Phi_{\rm eff} \propto \exp\left(\frac{\sqrt{6}e^{(3p+1)(N-N_k)/2}}{3p+1}\right)\,, \quad s = \frac{\sqrt{6}}{2}e^{(3p+1)(N-N_k)/2}\,. \tag{4.132}$$

This shows that for models with $p > 0$ the growth rate increases faster than in the constant m models. When $p < -1/3$ the above instability can be avoided, but in that case m increases towards the past. Thus, unless the present value of m is negligibly small, the condition $|m| \ll 1$ required by LGC can be violated during the matter era. We conclude, therefore, that these models are indistinguishable from ΛCDM in the present Universe.

2. $m < 0$

When m is negative, the Bessel functions in the regime $|\xi| \gg 1$ behave as

$$J_\nu(x) \sim \sqrt{\frac{2}{\pi x}}\cos\left(x - \frac{(2\nu+1)\pi}{4}\right)$$

and

$$Y_\nu(x) \sim \sqrt{\frac{2}{\pi x}}\sin\left(x - \frac{(2\nu+1)\pi}{4}\right)$$

respectively. Thus, the solution (4.129) in this asymptotic region becomes

$$\delta_m \simeq Ce^{-(3p+2)(N-N_k)/4}\,\cos(x+\theta)\,, \tag{4.133}$$

where C and θ are constants. Using this solution, we obtain

$$\delta_m' \simeq -\frac{1}{4}(3p+2)\delta_m - \frac{\sqrt{6}}{2}Ce^{3p(N-N_k)/4}\sin(x+\theta)\,, \tag{4.134}$$

$$s \simeq -\frac{1}{4}(3p+2) - \frac{3p+1}{2}x\tan(x+\theta)\,. \tag{4.135}$$

When $p > 0$, δ_m exhibits damped oscillations whereas $|\delta_m'|$ increases in time with the oscillations. The averaged value of the growth rate s is given by $\bar{s} = -\frac{3p+2}{4}$, but it shows a divergence every time x changes by π.

If the Universe crosses the critical point $|\xi| = 1$ around the end of the matter era, it does not necessarily reach the regime $|\xi| \gg 1$. In such cases one can not fully use the above approximate solutions. We shall confirm later that, in some cases, the Universe can enter the accelerated stage without oscillations in δ_m occurring up to the present epoch[2]. The frequency of oscillations tends to grow for larger values of p. The models that enter the regimes $|\xi| \gg 1$ are generally inconsistent with observations, since they typically lead to large negative values of s as given by Eq. (4.135).

3. Constraints on $|m|$ from the requirement $|\xi| < 1$

The $f(R)$ models can be consistent with observations if the Universe does not enter the regime $|\xi| > 1$ until the end of the matter-dominated epoch. One can estimate the ratio of the comoving Hubble radius $(aH)^{-1}$ during the matter era to its present value thus:

$$\frac{a_0H_0}{aH} \simeq c\left(\frac{a}{a_0}\right)^{\frac{1}{2}} = c(1+z)^{-\frac{1}{2}}\,, \tag{4.136}$$

where $c = 1$ in the absence of the dark energy dominated epoch. The presence of a dark energy era leads to a change in the value of c. Numerically this factor is around $c = 1.7$-1.9. Using the relation $R \simeq 3H^2$ that holds during the matter era for $|m| \ll 1$, we find that $|\xi|$ crosses 1 at a critical redshift

$$z_c \approx |m|\left(\frac{k}{a_0H_0}\right)^2 - 1\,. \tag{4.137}$$

If z_c is smaller than order unity, the Universe does not enter the regime $|\xi| > 1$ during the matter dominated epoch. This gives the following constraint to be consistent with observa-

[2]Oscillations in δ_m typically arise when we we choose larger values of $|m|$ and k.

tions;

$$|m(z)| \lesssim \left(\frac{a_0 H_0}{k}\right)^2 , \quad \text{for} \quad z > \mathcal{O}(1) . \tag{4.138}$$

The matter power spectrum has been observed over scales in the regime $0.02h\,\mathrm{Mpc}^{-1} \lesssim k \lesssim 0.2h\,\mathrm{Mpc}^{-1}$. Non-linear effects can be important for smaller scales with $k > 0.2h\,\mathrm{Mpc}^{-1}$ [130]. Taking the value $k = 0.2h\,\mathrm{Mpc}^{-1} \simeq 600 a_0 H_0$, below which linear perturbation theory is valid, we obtain the constraint $|m(z)| \lesssim 3 \times 10^{-6}$ during the matter era.

Of course this is a rough estimate and the actual constraints on $m(z)$ depend upon the particular models considered. For example, even if $|\xi|$ crosses 1 during the matter era, the models can be consistent with observations provided that $|\xi|$ does not grow rapidly after it exceeds unity. Whether or not ξ reaches the regime $|\xi| \gg 1$ depends on the particular models chosen. In order to place constraints on m, therefore, we need a detailed analysis for each particular model. In the next subsection, we shall provide a numerical investigation of a number of $f(R)$ models presented above and place constraints on the present values of m as well as the model parameters.

4.4.4 Constraints on model parameters

In this subsection we shall employ the information provided by the growth of matter density perturbations to place constraints on the parameters of the $f(R)$ models presented in Sec. 4.4.3 above. This is done by numerically solving the exact evolution equation for the perturbations, Eq. (4.109), together with the background equations (2.105) and (2.107). We refer the reader to Appendix A.3 for equations written in a form more convenient for numerical integration.

1. Constant m models: $f(R) = \alpha R^{1+m} - \Lambda$

Compared to other models considered here, the growth of $|\xi|$ is rather mild in the constant m models, being of the form $|\xi| \propto a = e^N$. Thus, in order for $|\xi|$ to grow from 0.1 to 10, one would require an increase in the number of e-foldings by 4.6.

We shall first consider the positive m case. In the left panel of Fig. 4.4 we plot the evolution of the growth rate, s, for the mode $k = 600 a_0 H_0$ for several values of m. For $m = 3 \times 10^{-5}$ we numerically obtain $z_c \sim 11$, denoted by a black dot in Fig. 4.4. This almost agrees with the analytical estimate (4.137) which gives $z_c \approx 10$. In the regime $\xi \ll 1$ the evolution of matter perturbations is given by $\delta_m = \delta_m' \propto a$, which results in $s \simeq 1$. The growth rate begins to move away from unity as ξ becomes of order 0.1, and then continues to grow before the Universe enters the stage of accelerated expansion. For this model we find $s_{\max} \sim 2.06$ and $\xi_{\max} \sim 3.13$, which shows that the model does not enter the regime $\xi \gg 1$

where the evolution of perturbations is described by Eqs. (4.130) and (4.131).

For a model with $m = 1.5 \times 10^{-5}$, the critical redshift occurs at around $z_c \sim 5$ with $s \sim 1.4$. The maximum value of the growth rate is $s_{\max} \sim 1.57$, which corresponds to the marginal case satisfying the observational criterion (1.2). For a model with $m = 2.0 \times 10^{-6}$, the evolution of perturbations is not much different from the general relativistic case.

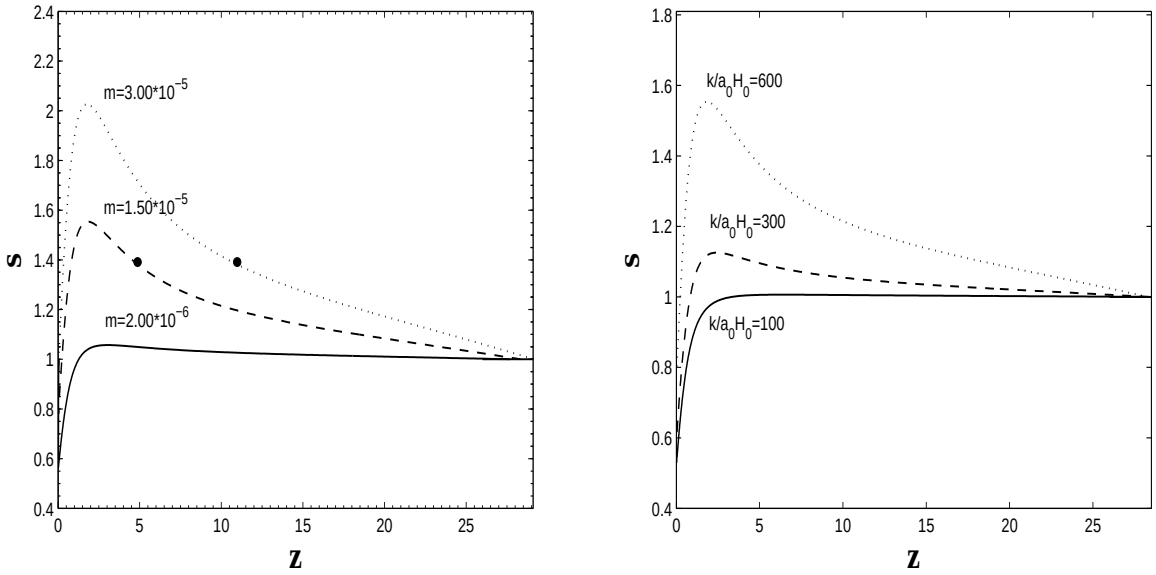

Figure 4.4: The evolution of perturbations for the model: $f(R) = \alpha R^{1+m} - \Lambda$ with positive values of m. In the left panel we show the growth rate, $s = \delta'_m/\delta_m$, versus the redshift, z, for the mode $k/a_0H_0 = 600$ with three different values of m. The black dots represent the points at which ξ crosses 1. The right panel depicts the evolution of s for $m = 1.5 \times 10^{-5}$ with three different values of k.

To show the variation of the growth rate as a function of scale, we depict in the right panel of Fig. 4.4 the evolution of s for the model $m = 1.5 \times 10^{-5}$ for three different values of k. As can be seen, the maximum value of the growth rate s decreases as k is decreased (i.e. the scales become larger). In particular, for the mode $k = 100a_0H_0$ (corresponding to $k = 0.033h$ Mpc^{-1}), the evolution of perturbations exhibits no difference compared to the corresponding evolution in the general relativistic case. Hence the matter power spectrum is enhanced on small scales ($k = 0.1h$-$0.2h$ Mpc^{-1}), while the spectrum remains similar to the standard general relativistic case on larger scales ($k = 0.02h$-$0.04h$ Mpc^{-1}). This results in different spectral indices on different scales. Placing more precise constraints on m would require performing a likelihood analysis using the data from the matter power spectrum. However, in order to obtain an order of magnitude estimate for the maximum value of m, it is sufficient to use the criterion (1.2) for the mode $k = 600a_0H_0$. For the constant m models we find the constraint to be $m \lesssim 10^{-5}$.

When m is negative, the growth rate s decreases unlike the positive m case. In the left panel of Fig. 4.5 we plot the evolution of s for three different negative values of m for the mode $k/a_0H_0 = 600$. As can be seen s tends to decrease more rapidly with increasing $|m|$. If $m = -2.0 \times 10^{-5}$, the present value of s becomes very small ($s < -1$). As we see in the right panel of Fig. 4.5, when $m = -2.0 \times 10^{-5}$, there is a significant fall in the values of s between $k/a_0H_0 = 300$ and $k/a_0H_0 = 600$. This can lead to large differences in the spectral indices of the matter power spectrum for small and large scale modes. From the above argument $|m|$ should be smaller than the order of 10^{-5}, which has an upper bound similar to the positive m case.

When $m = -2.0 \times 10^{-5}$ the Universe crosses the point $|\xi| = 1$ at the redshift $z_c \sim 7.4$, but the increase of $|\xi|$ for $z < z_c$ is mild. Moreover, the quantity $|\xi|$ begins to decrease after the Universe enters the accelerated stage. Numerically we obtain the value $\xi \sim -0.77$ at present ($z = 0$). Thus the system does not reach the regime $|\xi| \gg 1$, and hence not a single period of oscillation occurs by the present epoch. However, for larger values of $|m|$, we have numerically checked that the oscillations of δ_m indeed occur.

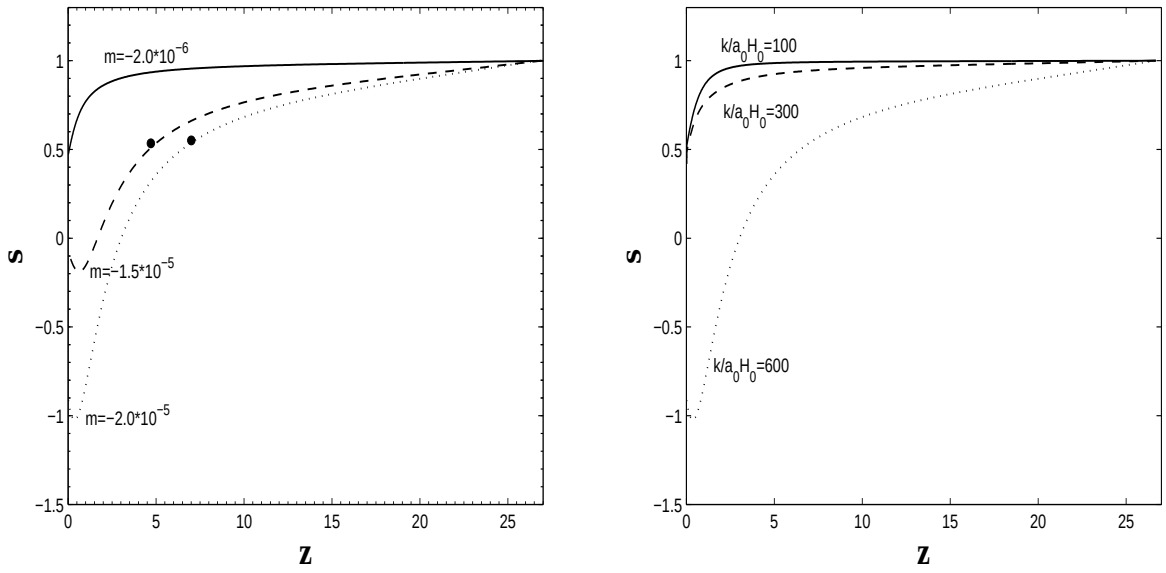

Figure 4.5: The evolution of perturbations for the model: $f(R) = \alpha R^{1+m} - \Lambda$ for negative m. In the left panel we show the growth rate $s = \delta'_m/\delta_m$ versus the redshift z for the mode $k/a_0H_0 = 600$ with three different values of m. The black dots represent the points at which the quantity $|\xi|$ crosses 1. The right panel depicts the evolution of s for $m = -2.0 \times 10^{-5}$ with three different values of k.

We also recall that growth of the effective gravitational potential $\Phi_{\rm eff}$ leads to an ISW effect in the CMB spectrum on large scales ($k/a_0H_0 \sim$a few). However, when $|m| \sim 10^{-5}$, $\Phi_{\rm eff}$ does not grow for these modes. As a result the ISW effect does not provide stronger

constraints on m than those provided by the matter power spectrum.

2. $f(R) = R - \lambda R_c (R/R_c)^{\beta}$

The observational constraints on the parameters of this model were studied in Ref. [79]. (Note that R_c is not very much different from the present value of the cosmological Ricci scalar R_0.) Here, we shall obtain constraints on the parameter m, which for this model is given by

$$m = \frac{\lambda\beta(1-\beta)(R/R_c)^{\beta-1}}{1-\lambda\beta(R/R_c)^{\beta-1}}\,, \tag{4.139}$$

and make a comparison between our results. The late-time de-Sitter point ($R = R_1$) is obtained from the constraint equation $FR - 2f = 0$, to give $(R_1/R_c)^{1-\beta} = \lambda(2-\beta)$. Thus at this de-Sitter point the variable m satisfies

$$m(R_1) = \beta/2\,. \tag{4.140}$$

For $\beta < 1$, the parameter m in the regime $R \gg R_c$ is given by

$$m \simeq \lambda\beta(1-\beta)(R/R_c)^{\beta-1} \propto t^{2(1-\beta)}\,, \tag{4.141}$$

which decreases towards the past.

If $\beta\,(<1)$ is of order unity, the quantity m is too large to satisfy the requirement (4.138) for the mode $k = 600 a_0 H_0$ during the matter era. (Recall that from Eq. (4.140) the present value of m is of the order of β). This is basically associated with the fact that, in the regime $R \gg R_c$, the model gives a linear relation between m and r [$m = C(-r-1)$]. Consequently we need the condition $|\beta| \ll 1$ in order to be compatible with the criterion (4.138).

To determine the changes in the behaviour of this model as a function of β, we considered three distinct values of β and calculated the corresponding growth rate, s, and the parameter m in each case. Our results are summarised in Fig. 4.6. The left-hand panel shows the evolution of the growth rate for $\lambda = 1$ and $k = 600 a_0 H_0$ with the three different values of β. For $\beta = 1.5 \times 10^{-4}$ the present value of the parameter m is around $m(z_0) \sim 6.7 \times 10^{-5}$, which is close to the value of m at the de-Sitter point ($m(R_1) = 7.5 \times 10^{-5}$). We also find that the parameter ξ crosses 1 at a redshift $z_c \sim 3$ with $m(z_c) \sim 1.2 \times 10^{-5}$.

Furthermore, we find that the growth rate is larger for these models than in the case of constant m models. This is due to the fact that ξ in this case evolves faster, as $\xi \propto t^{2(4/3-\beta)}$. The maximum growth rate reached for $\beta = 1.5 \times 10^{-4}$ corresponds to $s_{\rm max} \sim 1.88$ with $\xi \sim 4$. As expected, models with smaller values of β possess growth rates which are more compatible with observational constraints. Employing the criterion (1.2) for the mode $k = 600 a_0 H_0$, we find the constraint $\beta < 8.2 \times 10^{-5}$. This is slightly larger than the constraint

$\beta < 3.0 \times 10^{-5}$ obtained in [131] from the likelihood analysis of the SDSS data[3]. In the left panel of Fig. 4.6 we also consider this case in order to find the corresponding evolution of s. The maximum value of the growth rate in this case is found to be $s_{\rm max} \sim 1.095$, which indicates that the constraint (1.2) is rather weak. Nevertheless, the criterion (1.2) is certainly sufficient in order to extract an order of magnitude bound on β.

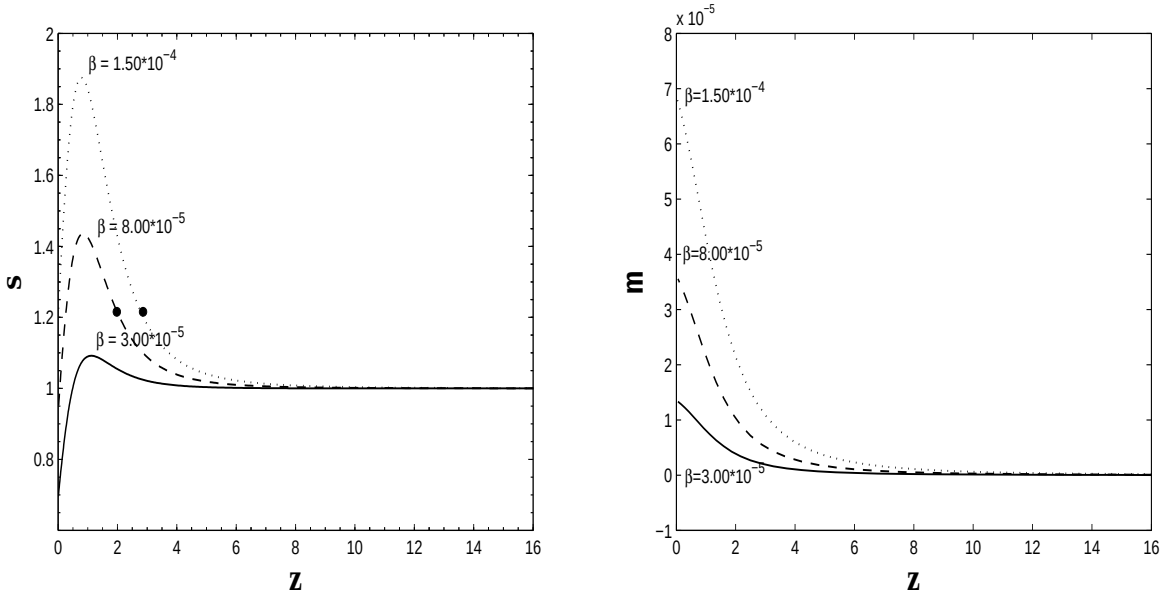

Figure 4.6: The evolution of perturbations for the model $f(R) = R - \lambda R_c (R/R_c)^{\beta}$ with positive β and $\lambda = 1$. The left-hand panel depicts $s = \delta_m'/\delta_m$ versus the redshift, z, for the mode $k/a_0 H_0 = 600$ with three different values of β. The right-hand panel shows the evolution of m with respect to z for $k/a_0 H_0 = 600$. From the requirement (1.2) we obtain the constraint $\beta < 8.2 \times 10^{-5}$.

The right panel of Fig. 4.6 depicts the evolution of the parameter m for the case with $\lambda = 1$ and $k = 600 a_0 H_0$ for the three different values of β. As can be seen m increases from the past to the present. Using the criterion (1.2) we obtain the bound $m(z = 0) < 3.5 \times 10^{-5}$. If we adopt the stronger criterion $s < 1.1$, the constraint becomes $m(z = 0) < 1.3 \times 10^{-5}$. Thus the deviation from the ΛCDM model is constrained to be small ($m(z = 0) \lesssim 10^{-5}$).

We also examine the effects of changing the parameter λ on the bounds on β. We consider two cases: $\lambda = 10$ and $\lambda = 100$. We find that these changes in λ have negligible effects on the constraints imposed on β and $m(z = 0)$, in comparison to that obtained from the case with $\lambda = 1$. The reason for this lack of sensitivity is that a change in λ is compensated for by corresponding changes to the values of R_i, a_0 and H_0.

When $\beta < 0$ the parameter m is negative from Eq. (4.141). In the left panel of Fig. 4.7

[3]In Ref. [132] it was shown that the combined analysis using the SDSS, CMB and Supernovae Ia data gives more stringent constraints: $\beta \lesssim 10^{-6}$.

we plot the evolution of s for three different values of β with $k/a_0H_0 = 600$. We find that the present values of s become smaller than -1 for $|\beta| \gtrsim 1.2 \times 10^{-4}$, in which case $|m(z=0)|$ is smaller than the order of 5.3×10^{-5} (see the right panel of Fig. 4.7). Thus, if we use the criterion $s(z=0) \gtrsim -1$ for the models to be viable, the upper bounds on $|\beta|$ and $|m(z=0)|$ are similar to those in the positive β case.

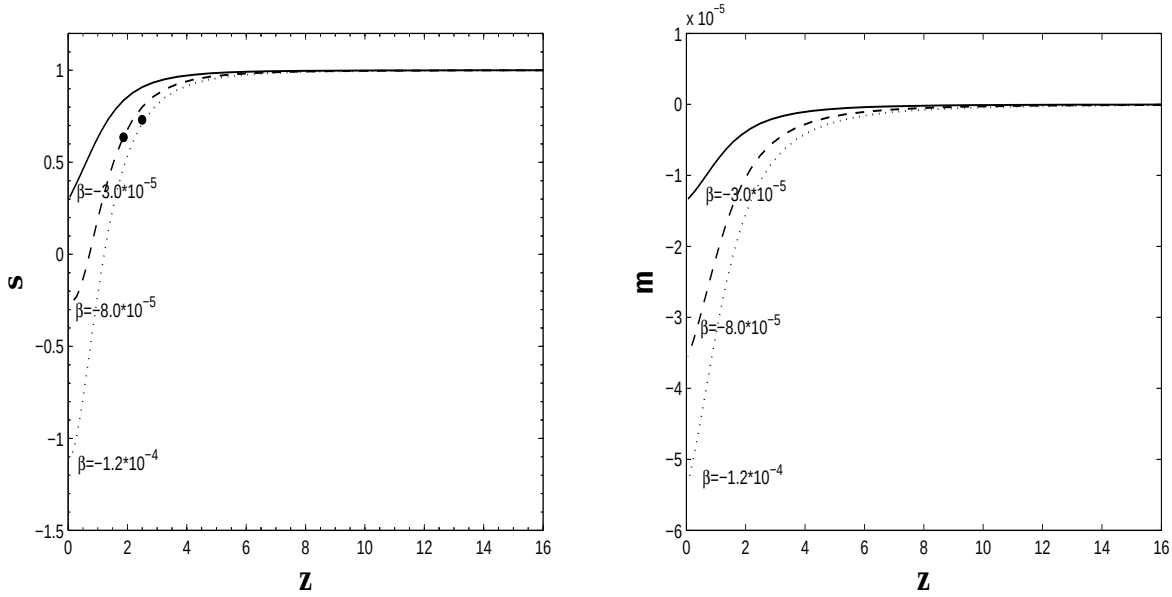

Figure 4.7: The evolution of perturbations for the model $f(R) = R - \lambda R_c(R/R_c)^\beta$ with negative β and $\lambda = 1$. The left-hand panel depicts $s = \delta'_m/\delta_m$ versus the redshift, z, for the mode $k/a_0H_0 = 600$ with three different values of β. The right-hand panel shows the evolution of the quantity m with respect to z for $k/a_0H_0 = 600$. If we use the criterion $s(z=0) > -1$, we obtain the constraint $\beta > -1.2 \times 10^{-4}$.

3. $f(R) = R - \lambda R_c[1 - (1 + R^2/R_c^2)^{-n}]$

Finally we consider the above model (where $n > 0$) recently discussed by Starobinsky [116]. The parameter m for this model is given by

$$m = \frac{2n\lambda x(1+x^2)^{-n-2}[(2n+1)x^2 - 1]}{1 - 2n\lambda x(1+x^2)^{-n-1}}, \quad \text{where} \quad x \equiv R/R_c, \tag{4.142}$$

and the de-Sitter point at $R = R_1$ corresponds to

$$\lambda = \frac{x_1(1+x_1^2)^{n+1}}{2[(1+x_1^2)^{n+1} - 1 - (n+1)x_1^2}, \quad \text{where} \quad x_1 \equiv R_1/R_c\,. \tag{4.143}$$

Once we fix the value of λ, x_1 is known accordingly. In the regime $R \gg R_c$ the parameter m behaves as

$$m \simeq 2n(2n+1)\lambda(R_c/R)^{2n+1} \propto t^{2(2n+1)} . \tag{4.144}$$

Due to the presence of a larger power of (R_c/R) in the expression for m in this case, m decreases more rapidly towards the past compared to the model $f(R) = R - \lambda R_c(R/R_c)^\beta$ discussed above. For the mode $k = 600 a_0 H_0$, the bound (4.138) implies that m has to be smaller than the order of 10^{-6}-10^{-5} by the end of the matter-dominated epoch if the model is not enter the regime $\xi > 1$.

In Fig. 4.8 we plot, for the mode $k = 600 a_0 H_0$, the evolution of s and m for $\lambda = 2.5$ with three different values of n. When $n = 3.07$ the critical redshift is given by $z_c \sim 1.05$ with $m \sim 1 \times 10^{-5}$. The rapid increase of s occurs in the regime $\xi > 1$, after which the growth rate reaches a maximum value $s_{\max} \sim 2$. The present value of m is found to be $m = 4.5 \times 10^{-4}$, which is an order of magnitude larger than its corresponding value at $\xi = 1$. Using the criterion (1.2), we obtain the constraints $n > 3.23$ and $m(z=0) < 2.9 \times 10^{-4}$ for $\lambda = 2.5$. The present value of m in this model is an order of magnitude larger than the corresponding values arising in the constant m models, as well as the $f(R) = R - \lambda R_c(R/R_c)^\beta$ model.

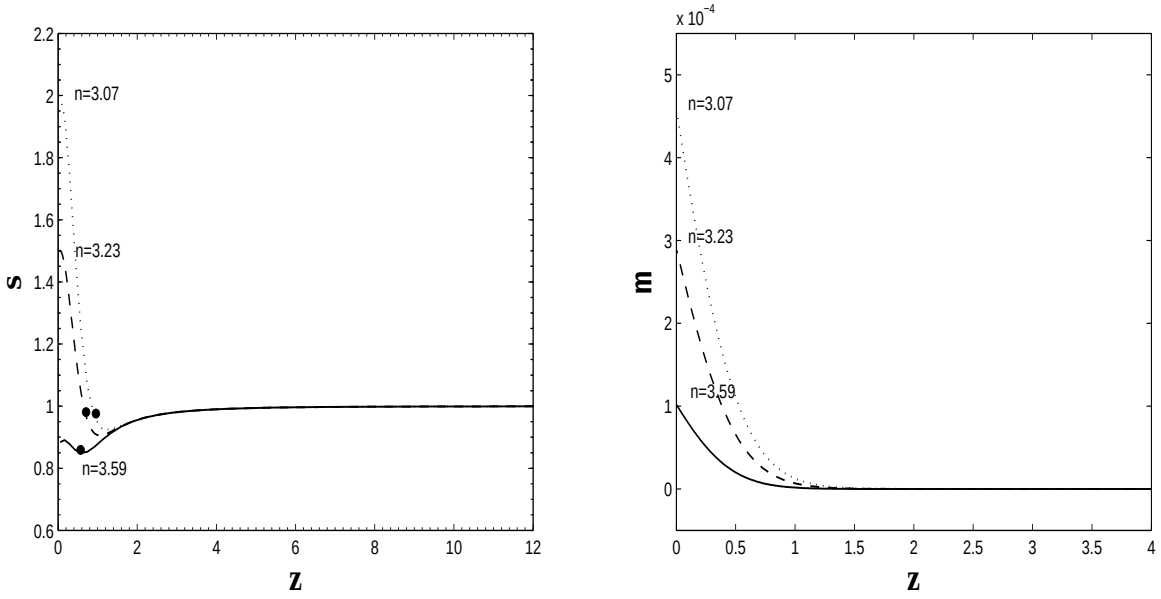

Figure 4.8: The evolution of perturbations for the model $f(R) = R - \lambda R_c[1 - (1 + R^2/R_c^2)^{-n}]$ with $\lambda = 2.5$. The left-hand panel depicts $s = \delta_m'/\delta_m$ versus the redshift, z, for the mode $k/a_0 H_0 = 600$ with three different values of n. The right-hand panel shows the evolution of the quantity m with respect to z for $k/a_0 H_0 = 600$.

We also find that in contrast to the model $f(R) = R - \lambda R_c(R/R_c)^\beta$ the constraints on n for the Starobinsky model are sensitive to the values of the parameter λ. For larger values

of λ the constraints on n are weaker. For example, for $\lambda = 10$ and $\lambda = 50$ we find the corresponding constraints on n imposed by (1.2) to be $n > 1.74$ ($m(z = 0) \sim 1.4 \times 10^{-4}$) and $n > 1.09$ ($m(z = 0) \sim 1.1 \times 10^{-4}$), respectively. This can be understood in the following way. When λ is increased, we obtain a larger ratio R_1/R_c from Eq. (4.143), which also leads to a larger ratio R/R_c in the past. Consequently from Eq. (4.144) a smaller value of n is sufficient to realise the condition $|m| \ll 1$. It can also be seen from the form of the action that the values of R_c can also effect the constraints on n. We find that for small values of λ, R_c has a small effect on the constraint, whereas for large values of λ the effect of changing R_c is negligible.

From Eq. (4.144) we find that m can be negative for $-\frac{1}{2} < n < 0$ (and $\lambda > 0$) in the regime $R \gg R_c$. When n is close to zero, the models are close to the model $f(R) = R - \lambda R_c (R/R_c)^{\beta}$ discussed above. We find that $s(z = 0)$ is larger than -1 for $|n| < 9.3 \times 10^{-5}$, in which case we have $|m(z = 0)| < 4.5 \times 10^{-5}$. When n is close to $-\frac{1}{2}$, Eq. (4.144) seems to suggest that the models should be close to the constant m models. However, care needs to be taken in this case since m changes sign from negative to positive values at $(R/R_c)^2 = 1/(2n + 1)$ deep into the matter-dominated epoch. As a result, for n close to $-\frac{1}{2}$, we numerically find that the growth rate shows a rapid increase for $(R/R_c)^2 < 1/(2n + 1)$. Thus, in the limit $n \to -\frac{1}{2}$, the models do not behave as constant m models and they are excluded observationally.

Analysis of the Hu & Sawicki [117] model, $f(R) = R - \lambda R_c \frac{(R/R_c)^{2n}}{(R/R_c)^{2n}+1}$ ($n > 0$), leads to constraints on the parameters n and $m(z = 0)$ such that $n > 3.33$ and $m(z = 0) < 2.15 \times 10^{-4}$, respectively, when $\lambda = 2.5$ and $k/a_0 H_0 = 600$. These are similar to the constraints derived above.

In summary, the present values of m are constrained to be $m(z = 0) \lesssim 10^{-4}$ from the bound (1.2) in both the Starobinsky and Hu & Sawicki models.

4.5 Summary

We have made a detailed study of the evolution of density perturbations in $f(R)$ gravity theories in both the metric and Palatini formalisms and employed this to determine the viability of models in each case. To study the viability of concrete models, we considered three sets of constraints provided by the background cosmological evolution, local gravity experiments and the evolution of matter density perturbations, respectively.

We began by considering the cosmological and local gravity constraints. For models satisfying these constraints, we then proceeded to determine additional bounds arising from the evolution of density perturbations. This allowed us to further constrain the model parameters as well as their deviation from the ΛCDM model.

The $f(R)$ theories in the metric formalism are equivalent to generalised Brans-Dicke theories with a scalar-field potential $V(\phi)$ and Brans-Dicke parameter $\omega_{\rm BD} = 0$. The presence of the field potential allows for the construction of $f(R)$ models that satisfy the local gravity constraints under the use of a chameleon mechanism. We found that if typical models of the forms (4.35) and (4.36) are to satisfy the cosmological and local gravity constraints, the parameter m must be much smaller than unity during the radiation and matter eras. However, it can grow to values of the order of 0.1 in the accelerated epoch. Models in the metric formalism also suffer from an additional fine-tuning due to the presence of scalaron oscillating modes (which are absent in the Palatini case). Finally, to be stable these theories require $f_{,RR}$ to be positive.

On the other hand, the $f(R)$ theories in the Palatini formalism correspond to generalised Brans-Dicke theories with a scalar-field potential $V(\phi)$ and Brans-Dicke parameter $\omega_{\rm BD} = -\frac{3}{2}$. This makes these theories special in the sense that the oscillating scalar degree of freedom (scalaron) is absent in these theories and therefore the corresponding fine tuning is not required. Moreover, in contrast to the case of the metric formalism, there is no notion of field mass M that determines an interaction length mediated by a fifth-force. Thus the LGC for these theories need to be analysed separately in contrast to theories with $\omega_{\rm BD} \neq -\frac{3}{2}$. The main condition required in order to satisfy the LGC is that $|m|$ must be smaller than the order of unity. Moreover, the requirement for cosmological viability in the Palatini formalism is not severe compared to the metric case. Thus, in order to satisfy the cosmological and local gravity constraints, we do not require vanishingly small values of m during the radiation and matter dominated epochs and, furthermore, $f_{,RR}$ can be negative in this case. As a result, even models of the type $f(R) = R - \mu^{2(n+1)}/R^n$ with $n > 0$ are allowed at the background level, which is not so in the metric formalism.

We then studied the constraints provided by the evolution of density perturbations. In the case of the metric formalism we derived the equations for matter perturbations under sub-horizon approximations in several different gauges. In the regime $M^2 \gg k^2/a^2$ (i.e.,

$\xi \ll 1$), we found the approximate perturbation equations to be valid even without using sub-horizon approximations, provided that the scalaron mode is not dominant relative to the matter-induced mode. This is a consequence of the fact that, when $M^2 \gg k^2/a^2$, the evolution of perturbations mimics that in General Relativity. After the Universe enters the regime $M^2 \ll k^2/a^2$, the modes are inside the Hubble radius due to the fact that the condition $M^2 \gg R$ is required for compatibility with LGC. Thus, for the models that satisfy LGC, as long as the scalarons do not dominate over the matter-induced mode, approximate perturbation equations are valid even for those modes that initially lie outside the Hubble radius. In the Palatini case the approximate equations are even more reliable because of the absence of scalarons.

In the metric formalism, most viable $f(R)$ models take the form $m(r) = C(-r-1)^p$ ($p > 1$) in the regimes where the Ricci scalar is larger than its present cosmological value. In these models, the modes relevant to the observed matter power spectrum correspond to the regime $M^2 \gg k^2/a^2$ with the growth rate $s = \delta_m'/\delta_m = 1$ at the beginning of the matter era. These models typically enter the regime $M^2 \ll k^2/a^2$ during the matter era in which the growth rate of matter perturbations is given by $s = 1.186$. If we use the present observational bound $s \lesssim 1.5$, we do not obtain strong constraints on these models. However, since the transition time at $k/a = M$ depends upon the mode k, there is a difference in the spectral indices between the matter power spectrum and the CMB spectrum [see Eq. (4.106)]. If we take the bound $\Delta n < 0.05$, the models with $p \geq 5$ are allowed. The present value of the parameter m is constrained to be $m(z=0) \lesssim 10^{-1}$. Thus, while m needs to be negligibly small during the radiation and matter eras, one can have an appreciable deviation from the ΛCDM model around the present epoch.

In the Palatini formalism, the approximate matter perturbation equations are valid even for super-Hubble modes for models satisfying LGC ($|m| \ll 1$). If m is positive, there is a strong amplification of δ_m in the regime $\xi \gg 1$, whereas if $m < 0$ the matter perturbation exhibits a damped oscillation for $|\xi| \gg 1$. When the quantity m evolves as $m \propto t^{2p}$ during the matter era, we have analytically estimated the growth rate s for both positive and negative values of m [see Eqs. (4.132) and (4.135), respectively]. From the requirement that the Universe does not enter the regimes $|\xi| > 1$ during the matter era, we obtain the constraint $|m(z)| \lesssim (a_0 H_0/k)^2$ for $z > \mathcal{O}(1)$. While this is a good criterion to avoid non-standard evolution of matter perturbations, one needs to carry out a more detailed analysis to place constraints on the quantity m for each $f(R)$ model. When m is positive, we have obtained the constraint $m \lesssim 10^{-5}$ by considering the modes k relevant to the matter power spectrum. We also studied the evolution of perturbations for the models $f(R) = R - \lambda R_c (R/R_c)^\beta$ and $f(R) = R - \lambda R_c [1 - (1 + R^2/R_c^2)^{-n}]$. For these models we found the constraints $m(z=0) \lesssim 10^{-5}$ and $m(z=0) \lesssim 10^{-4}$, respectively, from the requirement $s \lesssim 1.5$. Thus, unlike the metric case, the deviation from the ΛCDM model at the present epoch is small

even when m grows from the matter era to the accelerated epoch. This situation does not change for negative values of m.

To summarise, therefore, for viable models in the metric formalism, the quantity m is constrained from LGC to be very much smaller than unity during the matter era, but it can grow to order 0.1 around the present epoch. In the Palatini formalism, LGC and background cosmological constraints do not place strong bounds on m (only requiring $|m| \lesssim 10^{-1}$), but the density perturbations can provide stringent constraints: $|m| \lesssim 10^{-5}$-10^{-4}. Thus, in the Palatini case the $f(R)$ theories are hardly distinguishable from the ΛCDM model even at the present epoch. This follows due to a peculiar evolution of the matter perturbations in the regime $|\xi| > 1$ that exhibits rapid growth (when $m > 0$) or damped oscillations (when $m < 0$).

While the constraints obtained here are sufficient to derive order of magnitude constraints on the allowed parameter values, it will be of interest to obtain more precise bounds by using recent and upcoming observational data, including large scale structure, CMB, Supernova Ia, gamma-ray bursts and weak lensing.

Chapter 5

Observational constraints on scalar-tensor models of dark energy

In the previous chapter we demonstrated that $f(R)$ gravity in the Einstein frame corresponds to a constant coupling, $Q = -1/\sqrt{6}$, between dark energy and the non-relativistic fluid. Basically, this is equivalent to the coupled quintessence scenario [133] with a specific coupling. Our aim in this chapter is to generalise the analyses of Chapter 4 to scalar-tensor theories with the action (5.9), in which case the coupling Q is an arbitrary constant. After the pioneering works of Refs. [81; 100; 134; 135; 136; 137; 138; 139] the dark energy dynamics in scalar-tensor theories has been investigated in many papers, including Refs. [140; 141; 142; 143; 144; 145; 146]. If the mass of the quintessence field, φ, is always of the order of H_0, the solar-system constraint $\omega_{\rm BD} > 4.0 \times 10^4$ [45; 46; 147] gives the bound $|Q| < 2.5 \times 10^{-3}$. Previous studies dealing with the compatibility of scalar-tensor DE models with LGC have restricted their analysis to this small coupling region [144; 145]. Here we extend the analysis to include cases in which the coupling $|Q|$ is larger than the above massless bound [148]. In fact, as we have already discussed, one can design the potential, $V(\varphi)$, in such a way that the mass of the field is sufficiently heavy in the high-density region so as to satisfy LGC through the chameleon mechanism. We shall construct such a viable field potential inspired by the case of $f(R)$ gravity and place experimental bounds on model parameters, which can be expressed as functions of Q [148].

We shall also study the variation of the equation of state for DE and the evolution of density perturbations in such scalar-tensor theories. Interestingly, we find that the divergent behaviour of $w_{\rm DE}$ is also present as in the case of both $f(R)$ gravity [148] and $f(\mathcal{G})$ gravity [149]. In all cases, this divergence is associated with the increase of F as we go back in time and occurs when $\Omega_m = F_0/F$, where F_0 is the present value of F. We also estimate the growth rate of matter perturbations and show that the non-standard evolution of perturbations manifests itself from a certain epoch (depending upon model parameters) during the matter

era [148]. This is useful to place constraints on model parameters using the data from large scale structure and the CMB.

5.1 Scalar-tensor theories

We start with a class of scalar-tensor theories, which includes the pure $f(R)$ theories as well as the quintessence models as special cases, of the form

$$S = \int \mathrm{d}^4x\sqrt{-g}\left[\frac{1}{2}f(\phi,R) - \frac{1}{2}\zeta(\phi)(\nabla\phi)^2\right] + S_m(g_{\mu\nu},\psi_m)\,. \tag{5.1}$$

Here, f is a general differentiable function of the scalar field ϕ and the Ricci scalar R, ζ is a differentiable function of ϕ, and S_m is a matter Lagrangian that depends on the metric $g_{\mu\nu}$ and matter fields ψ_m. The action (5.1) can be transformed to the Einstein frame under the conformal transformation (2.57):

$$\tilde{g}_{\mu\nu} = \Omega^2\, g_{\mu\nu}\,,$$

where

$$\Omega = \sqrt{F} \quad \text{and} \quad F = \frac{\partial f}{\partial R}\,.$$

In what follows we shall consider F to be positive in order to ensure that gravity is attractive.

We shall be considering theories of the type

$$f(\phi,R) = F(\phi)R - 2V(\phi)\,, \tag{5.2}$$

for which the conformal factor, Ω, depends upon ϕ only. Introducing a new scalar field φ (not be confused with the metric perturbation, φ, that appears in earlier chapters):

$$\varphi = \int\left[\sqrt{\frac{3}{2}\left(\frac{F_{,\phi}}{F}\right)^2 + \frac{\zeta}{F}}\right]\mathrm{d}\phi\,, \tag{5.3}$$

the action in the Einstein frame becomes

$$S_E = \int \mathrm{d}^4x\sqrt{-\tilde{g}}\left[\frac{1}{2}\tilde{R} - \frac{1}{2}(\tilde{\nabla}\varphi)^2 - U(\varphi)\right] + S_m(\tilde{g}_{\mu\nu}F^{-1},\psi_m)\,, \tag{5.4}$$

where a tilde represents quantities in the Einstein frame and

$$U = \frac{V}{F^2}\,. \tag{5.5}$$

We recall from Sec. 2.2.2 that in $f(R)$ gravity, the conformal factor, Ω, depends only

on R. Introducing the new scalar field (2.66), we found that the $f(R)$ action in the Einstein frame is given by (2.67) [or equivalently (5.4)] while the potential is defined in Eq. (2.68). Hence, the $f(R)$ gravity can be cast in the form of scalar-tensor theories of the type (5.1) with (5.2), by identifying the potential in the Jordan frame to be

$$V = \frac{RF - f}{2}. \tag{5.6}$$

In order to describe the strength of the coupling between dark energy and a non-relativistic matter, we introduce the following quantity

$$Q = -\frac{F_{,\varphi}}{2F}\,. \tag{5.7}$$

From Eq. (2.66) one has $F = e^{2\varphi/\sqrt{6}}$, which shows that the $f(R)$ gravity corresponds to

$$Q = -1/\sqrt{6}\,.$$

In what follows we shall study a class of scalar-tensor theories where Q is treated as an arbitrary constant. This class includes a wider family of models, including $f(R)$ gravity, induced gravity and quintessence models. Using Eqs. (5.3) and (5.7) we have the following relations

$$F = e^{-2Q\varphi}\,, \quad \zeta = (1 - 6Q^2)F\left(\frac{\mathrm{d}\varphi}{\mathrm{d}\phi}\right)^2\,. \tag{5.8}$$

Then action (5.1) in the Jordan frame together with (5.2) yields

$$S = \int \mathrm{d}^4x\sqrt{-g}\left[\frac{1}{2}FR - \frac{1}{2}(1 - 6Q^2)F(\nabla\varphi)^2 - V\right] + S_m(g_{\mu\nu}, \psi_m)\,. \tag{5.9}$$

Note that in the limit, $Q \to 0$, the action (5.9) reduces to the one for a minimally coupled scalar field, φ, with a potential $V(\varphi)$.

It is informative to compare (5.9) with the generalised Brans-Dicke theory (2.44):

$$S = \int \mathrm{d}^4x\sqrt{-g}\left[\frac{1}{2}\chi R - \frac{\omega_{\rm BD}}{2\chi}(\nabla\chi)^2 - V\right] + S_m(g_{\mu\nu}, \psi_m)\,. \tag{5.10}$$

Setting $\chi = F = e^{-2Q\varphi}$, one easily finds that the two actions are equivalent if the parameter $\omega_{\rm BD}$ is related to Q via the relation

$$3 + 2\omega_{\rm BD} = \frac{1}{2Q^2}\,. \tag{5.11}$$

Under this condition, the theories given by (5.9) are equivalent to the Brans-Dicke theories (2.44).

5.2 Background cosmological dynamics

In this section we shall discuss the cosmological dynamics for the action (5.9) in the flat FLRW spacetime (2.85). As a source of the matter action, S_m, we consider a non-relativistic fluid with energy density ρ_m and a radiation with energy density ρ_r. The evolution equations in the Jordan frame are then given by

$$3FH^2 = \frac{1}{2}(1-6Q^2)F\dot{\varphi}^2 + V - 3H\dot{F} + \rho_m + \rho_r \,, \tag{5.12}$$

$$2F\dot{H} = -(1-6Q^2)F\dot{\varphi}^2 - \ddot{F} + H\dot{F} - \rho_m - \frac{4}{3}\rho_r \,, \tag{5.13}$$

$$\dot{\rho}_m + 3H\rho_m = 0 \,, \tag{5.14}$$

$$\dot{\rho}_r + 4H\rho_r = 0 \,. \tag{5.15}$$

Taking the time-derivative of Eq. (5.12) and using Eq. (5.13), we obtain

$$(1-6Q^2)F\left(\ddot{\varphi} + 3H\dot{\varphi} + \frac{\dot{F}}{2F}\dot{\varphi}\right) + V_{,\varphi} + QFR = 0 \,, \tag{5.16}$$

where the Ricci scalar is given by Eq. (2.102).

In order to study the cosmological dynamics, it is convenient to introduce the following dimensionless phase space variables

$$x_1 = \frac{\dot{\varphi}}{\sqrt{6}H} \,, \quad x_2 = \frac{1}{H}\sqrt{\frac{V}{3F}} \,, \quad x_3 = \frac{1}{H}\sqrt{\frac{\rho_r}{3F}} \,. \tag{5.17}$$

Then the constraint equation (5.12) gives

$$\Omega_m \equiv \frac{\rho_m}{3FH^2} = 1 - (1-6Q^2)x_1^2 - x_2^2 - 2\sqrt{6}Qx_1 - x_3^2 \,. \tag{5.18}$$

We also define the following quantities

$$\Omega_r \equiv x_3^2 \,, \quad \Omega_{\rm DE} \equiv (1-6Q^2)x_1^2 + x_2^2 + 2\sqrt{6}Qx_1 \,. \tag{5.19}$$

Eq. (5.18) then yields the relation $\Omega_m + \Omega_r + \Omega_{\rm DE} = 1$.

From Eqs. (5.13) and (5.16) we obtain

$$\begin{aligned} \frac{\dot{H}}{H^2} &= -\frac{1-6Q^2}{2}\left[3 + 3x_1^2 - 3x_2^2 + x_3^2 - 6Q^2x_1^2 + 2\sqrt{6}Qx_1\right] \\ &\quad +3Q(\lambda x_2^2 - 4Q) \,, \end{aligned} \tag{5.20}$$

$$\frac{\ddot{\varphi}}{H^2} = 3(\lambda x_2^2 - \sqrt{6}x_1) + 3Q\left[(5-6Q^2)x_1^2 + 2\sqrt{6}Qx_1 - 3x_2^2 + x_3^2 - 1\right] \,. \tag{5.21}$$

Using these relations, we obtain the following autonomous equations:

$$\frac{\mathrm{d}x_1}{\mathrm{d}N} = \frac{\sqrt{6}}{2}(\lambda x_2^2 - \sqrt{6}x_1) + \frac{\sqrt{6}Q}{2}\Big[(5-6Q^2)x_1^2 + 2\sqrt{6}Qx_1 - 3x_2^2 + x_3^2 - 1\Big] - x_1\frac{\dot{H}}{H^2}\,, \tag{5.22}$$

$$\frac{\mathrm{d}x_2}{\mathrm{d}N} = \frac{\sqrt{6}}{2}(2Q-\lambda)x_1x_2 - x_2\frac{\dot{H}}{H^2}\,, \tag{5.23}$$

$$\frac{\mathrm{d}x_3}{\mathrm{d}N} = \sqrt{6}Qx_1x_3 - 2x_3 - x_3\frac{\dot{H}}{H^2}\,, \tag{5.24}$$

where λ is defined by

$$\lambda \equiv -\frac{V_{,\varphi}}{V}\,. \tag{5.25}$$

The exponential potential $V(\varphi) = V_0 e^{-\lambda\varphi}$ produces a constant value of λ. Generally, however, λ is dependent on φ, where the field φ is a function of x_1, x_2 and x_3 through the definition of x_2 and Eq. (5.20). Hence Eqs. (5.22)-(5.24) are closed. The effective equation of state[1] is given by

$$w_{\text{eff}} \equiv -1 - \frac{2}{3}\frac{\dot{H}}{H^2} = -1 + \frac{1-6Q^2}{3}(3 + 3x_1^2 - 3x_2^2 + x_3^2 - 6Q^2x_1^2 + 2\sqrt{6}Qx_1) - 2Q(\lambda x_2^2 - 4Q)\,. \tag{5.26}$$

In what follows we shall first discuss the case of constant λ and then proceed to consider the varying λ case.

5.2.1 Constant λ

If λ is a constant, one can derive the fixed points of the system by setting the right hand side of Eqs. (5.22)-(5.24) to zero. In the absence of radiation ($x_3 = 0$), we obtain the following fixed points:

[1]The effective pressure (p_{eff}) and energy density (ρ_{eff}) is obtained by expressing the right hand side of equations (5.12) and (5.13) as ρ_{eff} and $(p_{eff} + \rho_{eff})$, respectively. The effective equation of state can then be defined as $w_{eff} \equiv p_{eff}/\rho_{eff}$.

(a) φ matter-dominated era (φMDE [133])

$$\begin{aligned}(x_1, x_2) &= \left(\frac{\sqrt{6}Q}{3(2Q^2-1)}, 0\right), \quad \Omega_m = \frac{3-2Q^2}{3(1-2Q^2)^2}, \\ w_{\rm eff} &= \frac{4Q^2}{3(1-2Q^2)}.\end{aligned} \tag{5.27}$$

(b1) Kinetic point 1

$$(x_1, x_2) = \left(\frac{1}{\sqrt{6}Q+1}, 0\right), \quad \Omega_m = 0, \quad w_{\rm eff} = \frac{3-\sqrt{6}Q}{3(1+\sqrt{6}Q)}. \tag{5.28}$$

(b2) Kinetic point 2

$$(x_1, x_2) = \left(\frac{1}{\sqrt{6}Q-1}, 0\right), \quad \Omega_m = 0, \quad w_{\rm eff} = \frac{3+\sqrt{6}Q}{3(1-\sqrt{6}Q)}. \tag{5.29}$$

(c) Scalar-field dominated point

$$\begin{aligned}(x_1, x_2) &= \left(\frac{\sqrt{6}(4Q-\lambda)}{6(4Q^2-Q\lambda-1)}, \left[\frac{6-\lambda^2+8Q\lambda-16Q^2}{6(4Q^2-Q\lambda-1)^2}\right]^{1/2}\right), \\ \Omega_m &= 0, \quad w_{\rm eff} = -\frac{20Q^2-9Q\lambda-3+\lambda^2}{3(4Q^2-Q\lambda-1)}.\end{aligned} \tag{5.30}$$

(d) Scaling solution

$$\begin{aligned}(x_1, x_2) &= \left(\frac{\sqrt{6}}{2\lambda}, \left[\frac{3+2Q\lambda-6Q^2}{2\lambda^2}\right]^{1/2}\right), \\ \Omega_m &= 1-\frac{3-12Q^2+7Q\lambda}{\lambda^2}, \quad w_{\rm eff} = -\frac{2Q}{\lambda}.\end{aligned} \tag{5.31}$$

(e) de-Sitter point (present for $\lambda = 4Q$)

$$(x_1, x_2) = (0, 1), \quad \Omega_m = 0, \quad w_{\rm eff} = -1. \tag{5.32}$$

Note that, when $x_3 \neq 0$ we have a radiation fixed point $(x_1, x_2, x_3) = (0, 0, 1)$.

One can easily confirm that the de-Sitter point exists for $\lambda = 4Q$, by setting $\dot{\varphi} = 0$ in Eqs. (5.12), (5.13) and (5.16). This de-Sitter solution appears in the presence of the coupling Q. Note that this is a special case of the scalar-field dominated point (c).

When λ is a constant, one can analyse the stability of the critical points (x_1^c, x_2^c), i.e., Eqs. (5.27)-(5.32), by considering small perturbations δx_1 and δx_2 such that

$$x_1 = x_1^c + \delta x_1, \qquad x_2 = x_2^c + \delta x_1. \tag{5.33}$$

Then the autonomous equations (5.22)-(5.24) lead to first-order differential equations for the perturbations of the form:

$$\frac{\mathrm{d}}{\mathrm{d}N}\begin{pmatrix} \delta x_1 \\ \delta x_2 \end{pmatrix} = \mathcal{M}\begin{pmatrix} \delta x_1 \\ \delta x_2 \end{pmatrix}. \tag{5.34}$$

The eigenvalues μ_1 and μ_2 of the matrix $\mathcal{M}$ characterise the stability of the fixed points (x_1^c, x_2^c). The eigenvalues corresponding to the critical points (a)-(e) are given by

(a)

$$\mu_1 = -\frac{3-2Q^2}{2(1-2Q^2)}, \quad \mu_2 = \frac{3+2Q\lambda-6Q^2}{2(1-2Q^2)}. \tag{5.35}$$

(b1)

$$\mu_1 = \frac{3(\sqrt{6}+4Q-\lambda)}{\sqrt{6}+6Q}, \quad \mu_2 = \frac{3+\sqrt{6}Q}{1+\sqrt{6}Q}. \tag{5.36}$$

(b2)

$$\mu_1 = \frac{3(\sqrt{6}-4Q+\lambda)}{\sqrt{6}-6Q}, \quad \mu_2 = \frac{3-\sqrt{6}Q}{1-\sqrt{6}Q}. \tag{5.37}$$

(c)

$$\mu_1 = -\frac{6-\lambda^2+8Q\lambda-16Q^2}{2(1-4Q^2+Q\lambda)}, \quad \mu_2 = -\frac{3-\lambda^2+7Q\lambda-12Q^2}{1-4Q^2+Q\lambda}. \tag{5.38}$$

(d)

$$\mu_{1,2} = \frac{3(2Q-\lambda)}{4\lambda}\left[1 \pm \sqrt{1+\frac{8(6Q^2-2Q\lambda-3)(12Q^2+\lambda^2-7Q\lambda-3)}{3(2Q-\lambda)^2}}\right]. \tag{5.39}$$

(e)

$$\mu_1 = \mu_2 = -3\,. \tag{5.40}$$

Now given a value for λ, and using the stability conditions presented above, the cosmological dynamics can be specified. We shall briefly discuss the cases $Q = 0$ and $Q \neq 0$ in turn.

1. $Q = 0$

When $Q = 0$ (i.e., $F = 1$, which corresponds to a standard minimally coupled scalar field), the eigenvalues μ_1 and μ_2 of the Jacobian matrix for perturbations about the fixed points reduce to those derived in Ref. [22] (see Ref. [150; 151] for earlier works). In this case the matter-dominated era corresponds to either the point (a) or (d). The point (a) is a saddle node because $\mu_1 = -3/2$ and $\mu_2 = 3/2$. The point (d) is stable for $\lambda^2 > 3$, in which case $\Omega_m < 1$. The late-time accelerated expansion ($w_{\rm eff} < -1/3$) can be realised by using the point (c), under the condition $\lambda^2 < 2$. Under this condition the point (c) is a stable node. Hence, if $\lambda^2 < 2$, the saddle matter solution (a) is followed by the stable accelerated solution (c) [note that in this case $\Omega_m < 0$ for the point (d)]. The scaling solution, (d), can have a matter era for $\lambda^2 \gg 1$, but in this case the epoch following the matter era is not of an accelerated nature.

2. $Q \neq 0$

We next consider the case of non-zero values of Q. Here we do not consider the special case of $\lambda = 4Q$ which gives rise to the de-Sitter point. If the point (a) is responsible for the matter-dominated epoch, we require the condition $Q^2 \ll 1$. We then have $\Omega_m \simeq 1 + 10Q^2/3 > 1$ and $w_{\rm eff} \simeq 4Q^2/3$ for the φMDE. When $Q^2 \ll 1$ the scalar-field dominated point, (c), yields an accelerated expansion provided that $-\sqrt{2}+4Q < \lambda < \sqrt{2}+4Q^2$. Under these conditions the φMDE point is followed by a phase of late-time acceleration. It is worth recalling that in the case of $f(R)$ gravity ($Q = -1/\sqrt{6}$) the φMDE point corresponds to $\Omega_m = 2$ and

[2]Note that under the condition $Q^2 \ll 1$ and in the case where the dynamics is in the accelerated epoch, the condition $|Q\lambda| < 1$ is also satisfied.

$w_{\rm eff} = 1/3$. In this case the universe in the matter era prior to late-time acceleration evolves as $a \propto t^{1/2}$, which is different from the evolution in the standard matter dominated epoch.

We note that the scaling solution, (d), can give rise to the equation of state, $w_{\rm eff} \simeq 0$ for $|Q| \ll |\lambda|$. In this case, however, the condition $w_{\rm eff} < -1/3$ for the point (c) leads to $\lambda^2 \lesssim 2$. Consequently the energy fraction of the pressureless matter for the point (d) does not satisfy the condition $\Omega_m \simeq 1$. In summary, the viable cosmological sequence corresponds to a trajectory from the φMDE point to the scalar-field dominated point, (c), under the conditions $Q^2 \ll 1$ and $-\sqrt{2} + 4Q < \lambda < \sqrt{2} + 4Q$.

5.2.2 Varying λ

When the time-scale of the variation of λ is smaller than that of the cosmic expansion, the fixed points derived above, in the case of constant λ, can be regarded as "instantaneous" fixed points [152; 153]. We shall briefly consider the cases of $Q = 0$ and $Q \neq 0$ in turn.

1. $Q = 0$

We begin with a brief discussion of the $Q = 0$ case. If the condition $\lambda^2 < 2$ is satisfied throughout the cosmic evolution, the cosmological trajectory is similar to the constant λ case discussed above except for the fact that the fixed points are regarded as the "instantaneous" ones. In this case the saddle matter solution (a) is followed by the accelerated point (c).

When $\lambda^2 \gg 1$ the scaling solution, (d), is stable with $\Omega_m \simeq 1$. Hence the cosmological trajectory during the matter era chooses the scaling solution, (d), rather than the saddle point (a). If $|\lambda|$ decreases at late-times, such that it satisfies the acceleration condition $\lambda^2 < 2$, the trajectory stops following the solution represented by the matter point (d) to follow the scalar-field dominated point (c)[3]. A representative model of this type is provided by the double exponential potential, $V(\varphi) = V_0(e^{-\lambda_1\varphi} + e^{-\lambda_2\varphi})$, with $\lambda_1^2 \gg 1$ and $\lambda_2^2 < 2$ [154]. The assisted quintessence models in Ref. [155] also lead to a similar cosmological evolution.

2. $Q \neq 0$

We shall now proceed to consider the case of non-zero Q. If $|\lambda|$ is initially much larger than unity and decreases with time, it happens that the solutions finally approach the de-Sitter solution (e) with $\lambda = 4Q$. While the point, (e), is stable for constant λ, it is not obvious that this property also holds for a varying λ. In what follows we shall discuss the stability of the de-Sitter point.

It is convenient to consider the variable $\lambda(\varphi)$ as a function of $F(\varphi)$, i.e., $\lambda = \lambda(F)$. We

[3]Note that the de-Sitter solution (e), in this case, exists only for $\lambda = 0$, i.e., the cosmological constant.

define a variable, $x_4 \equiv F$, that satisfies the following equation

$$\frac{\mathrm{d}x_4}{\mathrm{d}N} = -2\sqrt{6}Qx_1x_4\,, \tag{5.41}$$

where the right hand side vanishes at the de-Sitter point (e). Considering the 3×3 matrix for perturbations δx_1, δx_2 and δx_4 around the point (e), we obtain the eigenvalues

$$\mu_1 = -3\,, \quad \mu_{2,3} = -\frac{3}{2}\left[1 \pm \sqrt{1 - \frac{8}{3}F_1 Q\frac{\mathrm{d}\lambda}{\mathrm{d}F}(F_1)}\right]\,, \tag{5.42}$$

where $F_1 \equiv F(\varphi_1)$ is the value of F at the de-Sitter point with the field value φ_1. Since $F_1 > 0$, we find that the de-Sitter point is stable for

$$Q\frac{\mathrm{d}\lambda}{\mathrm{d}F}(F_1) > 0\,, \quad \text{i.e.,} \quad \frac{\mathrm{d}\lambda}{\mathrm{d}\varphi}(\varphi_1) < 0\,. \tag{5.43}$$

We have checked that this agrees with the stability condition derived in Refs. [156; 157] by considering metric perturbations about the de-Sitter point.

In the context of $f(R)$ gravity this condition translates into $\mathrm{d}\lambda/\mathrm{d}F < 0$. Since in this case $F = e^{2\varphi/\sqrt{6}} = \mathrm{d}f/\mathrm{d}R$ and $V = (RF - f)/2$, we have $\lambda = -Rf_{,R}/\sqrt{6}V$. Then, together with the fact that $Rf_{,R} = 2f$ holds for the de-Sitter point, the condition $\mathrm{d}\lambda/\mathrm{d}F < 0$ is equivalent to $R < f_{,R}/f_{,RR}$. For positive R this gives

$$0 < \frac{Rf_{,RR}}{f_{,R}} < 1\,, \tag{5.44}$$

which agrees with the stability condition for the de-Sitter point derived in Ref. [43].

We recall that in the context of $f(R)$ gravity studied above, the model based on the lagrangian density (4.37):

$$f(R) = R - \mu R_c\left[1 - (R/R_c)^{-2n}\right] \quad (\mu > 0, R_c > 0, n > 0)\,,$$

was shown to be consistent with cosmological and local gravity constraints. For this model, φ is related to the Ricci scalar, R, via the relation $e^{2\varphi/\sqrt{6}} = 1 - 2n\mu(R/R_c)^{-(2n+1)}$. Hence the potential, $V = (FR - f)/2$, can be expressed in terms of the field, φ, as

$$V(\varphi) = \frac{\mu R_c}{2}\left[1 - \frac{2n+1}{(2n\mu)^{2n/(2n+1)}}\left(1 - e^{2\varphi/\sqrt{6}}\right)^{2n/(2n+1)}\right]\,. \tag{5.45}$$

The parameter λ is then given by

$$\lambda = - \frac{4n}{\sqrt{6}(2n\mu)^{2n/(2n+1)}}e^{2\varphi/\sqrt{6}}\left(1 - e^{2\varphi/\sqrt{6}}\right)^{-1/(2n+1)} \times \left[1 - \frac{2n+1}{(2n\mu)^{2n/(2n+1)}}\left(1 - e^{2\varphi/\sqrt{6}}\right)\right]^{-2n/(2n+1)}\,. \tag{5.46}$$

In the deep matter-dominated epoch in which the condition $R/R_c \gg 1$ is satisfied, the field φ is very close to zero. For n and μ of the order of unity, $|\lambda|$ is much larger than unity during this stage. Hence the matter era is realised by the instantaneous fixed point (d). As the ratio R/R_c gets smaller, $|\lambda|$ decreases to the order of unity. If the solutions reach the point $\lambda = 4Q = -4/\sqrt{6}$ and satisfy the stability condition, $\mathrm{d}\lambda/\mathrm{d}F < 0$, the final attractor corresponds to the de-Sitter fixed point (e).

For the theories with general couplings Q, let us consider the following scalar-field potential

$$V(\varphi) = V_0 \left[1 - C(1 - e^{-2Q\varphi})^p\right] \qquad (V_0 > 0,\ C > 0,\ 0 < p < 1)\,, \tag{5.47}$$

as a natural generalisation of Eq. (5.45). The slope of the potential is given by

$$\lambda = \frac{2C\,p\,Qe^{-2Q\varphi}(1 - e^{-2Q\varphi})^{p-1}}{1 - C(1 - e^{-2Q\varphi})^p}\,. \tag{5.48}$$

When $Q > 0$, the potential energy decreases from V_0 as φ increases from 0. On the other hand, if $Q < 0$, the potential energy decreases from V_0 as φ decreases from 0. In both cases we have $V(\varphi) \to V_0(1 - C)$ in the limits $\varphi \to \infty$ (for $Q > 0$) and $\varphi \to -\infty$ (for $Q < 0$).

In the model (5.47) the field is stuck around the value $\varphi = 0$ during the deep radiation and matter epochs. In these epochs one has $R \simeq \rho_m/F$ from Eqs. (5.12), (5.13) and (2.102) by noting that V_0 is negligibly small compared to ρ_m or ρ_r. Using Eq. (5.16), we obtain the relation $V_{,\varphi} + Q\rho_m \simeq 0$. Hence, in the high-curvature region the field, φ, evolves along the instantaneous minimum given by

$$\varphi_m \simeq \frac{1}{2Q}\left(\frac{2V_0pC}{\rho_m}\right)^{\frac{1}{1-p}}\,. \tag{5.49}$$

We stress here that a range of minima appears depending upon the magnitude of the energy density ρ_m of the non-relativistic matter. As long as the condition $\rho_m \gg V_0pC$ is satisfied, we have $|\varphi_m| \ll 1$ from Eq. (5.49).

Since Eq. (5.48) suggests that $|\lambda| \gg 1$ for field values around $\varphi = 0$, the instantaneous fixed point (d) can represent the matter-dominated epoch provided that $|Q| \ll |\lambda|$. The deviation from Einstein gravity manifests itself when the field begins to evolve towards the end of the matter era. The variable $F = e^{-2Q\varphi}$ decreases in time irrespective of the sign of the coupling strength and therefore $0 < F < 1$. This decrease of F is crucial to the divergent behaviour of the equation of state of DE, as we will see in Sec. 5.4.

The de-Sitter solution corresponds to $\lambda = 4Q$, i.e.,

$$C = \frac{2}{(1 - F_1)^{p-1}\left[2 + (p-2)F_1\right]}\,, \tag{5.50}$$

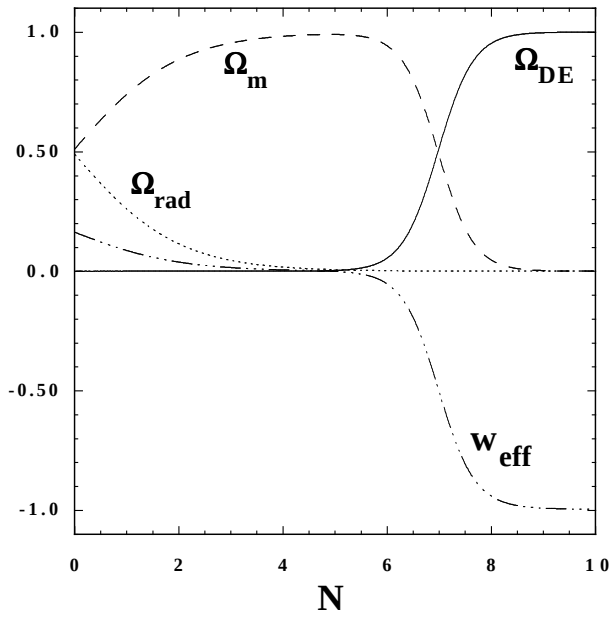

Figure 5.1: The evolution of $\Omega_{\rm DE}$, Ω_m, Ω_r and $w_{\rm eff}$ for the model (5.47) with parameters $Q = 0.01$, $p = 0.2$ and $C = 0.7$ and initial conditions $x_1 = 0$, $x_2 = 2.27 \times 10^{-7}$, $x_3 = 0.7$ and $x_4 - 1 = -5.0 \times 10^{-13}$.

where F_1 is the value of F at the point (e). Provided that the solution of this equation exists in the region $0 < F_1 < 1$, for given values of C and p, the de-Sitter point exists. From Eq. (5.48) we obtain

$$\frac{{\rm d}\lambda}{{\rm d}\varphi} = -\frac{4CpQ^2F(1-F)^{p-2}[1-pF-C(1-F)^p]}{[1-C(1-F)^p]^2}\,. \tag{5.51}$$

When $0 < C < 1$, one can easily show that the function $g(F) \equiv 1 - pF - C(1-F)^p$ is positive in the region $0 < F < 1$ giving ${\rm d}\lambda/{\rm d}\varphi < 0$. Hence, the conditions for a stable de-Sitter point are automatically satisfied. In this case the solutions approach the de-Sitter attractor after the end of the matter era.

When $C > 1$, the function $g(F)$ becomes negative for values of F that are smaller than the critical value F_c (< 1). The de-Sitter point (e) is stable under the condition $1 - pF_1 > C(1-F_1)^p$. Using Eq. (5.50) we find that this stability condition translates to

$$F_1 > \frac{1}{2-p}\,. \tag{5.52}$$

If this condition is violated, the solutions choose another stable fixed point as an attractor.

In summary, when $0 < C < 1$, the matter point (d) can be followed by the stable de-Sitter solution (e) for the model (5.47). In Fig. 5.1 we plot the evolution of $\Omega_{\rm DE}$, Ω_m, Ω_r and $w_{\rm eff}$ for $Q = 0.01$, $p = 0.2$ and $C = 0.7$. Beginning from the epoch of matter-radiation equality, the solutions first dwell around the matter point (d) with $w_{\rm eff} \simeq 0$ and finally approach the

de-Sitter attractor (e) with $w_{\rm eff} \simeq -1$. We have also numerically confirmed that λ is initially much larger than unity and eventually approaches the value $\lambda = 4Q$.

5.3 Local gravity constraints

In the absence of the potential, $V(\varphi)$, the Brans-Dicke parameter $\omega_{\rm BD}$ is constrained to be $\omega_{\rm BD} > 4.0 \times 10^4$ from solar-system experiments [45; 46]. Note that this bound also applies to the case of a nearly massless field with the potential $V(\varphi)$ in which the Yukawa correction, $e^{-M\ell}$, is close to unity (where M is the scalar field mass and ℓ is an interaction length). Using the bound $\omega_{\rm BD} > 4.0 \times 10^4$ in Eq. (5.11), we find

$$|Q| < 2.5 \times 10^{-3} \qquad (\text{for the massless case}). \tag{5.53}$$

This is a strong constraint under which the cosmological evolution for such theories is difficult to distinguish from the $Q = 0$ case. In this section we consider the case in which the mass, M, of the scalar field, φ, is sufficiently heavy so that the interaction range of the field ($\sim 1/M$) becomes short so as to satisfy LGC.

5.3.1 Solar system constraints

Here it is useful to recall our discussions from Sec. 4.1.2 on the chameleon mechanism in MG theories. There we essentially established that the models (4.37) can satisfy LGC because the mass, M, of the field potential (5.45) is sufficiently heavy in the high-density region where the Ricci scalar, R, is much larger than R_c. Since the field mass, m_φ, inside the body is much heavier than that outside the body, most of the volume element within the core does not contribute to the field profile at $\ell > \ell_\star$ except for a thin-shell around the surface of the body. (Note that this contribution is proportional to e^{-Mx}, where x is a distance from the volume element to a point outside the body). In the case of general couplings, Q, the models presented in Eq. (5.47) can be compatible with LGC. Under the condition $|Q\varphi| \ll 1$, one has $U_{,\varphi} \simeq -2V_0 QpC(2Q\varphi)^{p-1}$ for the potential $U = V/F^2$ in the Einstein frame (5.5). Then from Eq. (4.27) we obtain the field values at the potential minima inside/outside the body:

$$\varphi_A \simeq \frac{1}{2Q}\left(\frac{2V_0\, p\, C}{\rho_A}\right)^{\frac{1}{1-p}}, \quad \varphi_B \simeq \frac{1}{2Q}\left(\frac{2V_0\, p\, C}{\rho_B}\right)^{\frac{1}{1-p}}, \tag{5.54}$$

which satisfy $|\varphi_A| \ll |\varphi_B|$. Note that these are analogous to the field value, φ_m, derived in Eq. (5.49) in the cosmological setting. In order to realise the accelerated expansion at the present epoch, V_0 needs to be roughly the same order as the square of the present Hubble parameter H_0. Thus $V_0 \sim H_0^2 \sim \rho_0$, where $\rho_0 \simeq 10^{-29}$ g/cm^3 is the present cosmological density. Note that the baryonic/dark matter density in our galaxy corresponds to $\rho_B \simeq 10^{-24}$ g/cm^3 [158; 159; 160]. This then shows that the conditions $|Q\varphi_A| \ll 1$ and $|Q\varphi_B| \ll 1$ are in fact satisfied provided that C is not much larger than unity.

The field mass squared, $m_\varphi^2 \equiv {\rm d}^2U/{\rm d}\varphi^2$, at $\varphi = \varphi_A$ is approximately given by

$$m_\varphi^2(\varphi_A) \simeq \frac{1-p}{(2^p\, pC)^{1/(1-p)}} Q^2 \left(\frac{\rho_A}{V_0}\right)^{\frac{2-p}{1-p}} V_0\,. \tag{5.55}$$

This means that $m_\varphi(\varphi_A)$ can be much larger than H_0 due to the condition $\rho_A \gg V_0$. Therefore, while the mass m_φ is not different from the order of H_0 on cosmological scales, it increases in the regions with a higher energy density.

Let us place constraints on the model parameters by using the solar system bound (4.34). In so doing, we shall consider the case where the solutions finally approach the de-Sitter point (e). Since we have $\Delta\ell_\star/\ell_\star \simeq \varphi_B/(6Q\Phi_\star)$ with φ_B given in Eq. (5.54), the bound (4.34) translates into

$$(2V_0pC/\rho_B)^{1/(1-p)} < 1.2\times 10^{-10}|Q|\,, \tag{5.56}$$

where we have used the value $\Phi_\star = \Phi_\odot = 2.12\times 10^{-6}$ for the Sun [47; 124]. At the de-Sitter point, (e), one has $3F_1H_1^2 = V_0[1-C(1-F_1)^p]$ with C given in Eq. (5.50). Hence, we obtain the following relation

$$V_0 = 3H_1^2\frac{2+(p-2)F_1}{p}\,. \tag{5.57}$$

Substituting this into Eq. (5.56) we find

$$\left(\frac{R_1}{\rho_B}\right)^{1/(1-p)}(1-F_1) < 1.2\times 10^{-10}\,|Q|\,, \tag{5.58}$$

where $R_1 = 12H_1^2$ is the Ricci scalar at the de-Sitter point. Since the term $(1-F_1)$ is smaller than one half from the condition (5.52) we obtain the inequality $(R_1/\rho_B)^{1/(1-p)} < 2.4\times 10^{-10}|Q|$. We assume that R_1 is of the order of the present cosmological density $\rho_0 = 10^{-29}$ g/cm^3. Taking the baryonic/dark matter density to be $\rho_B = 10^{-24}$ g/cm^3 outside the Sun [158; 159; 160] we obtain the following bound

$$p > 1 - \frac{5}{9.6 - \log_{10}|Q|}\,. \tag{5.59}$$

For $|Q| = 10^{-2}$ and $|Q| = 10^{-1}$ this gives $p > 0.57$ and $p > 0.53$ respectively. The above bound corresponds to $p > 0.50$ for the case of $f(R)$ gravity, which translates into the condition $n > 0.5$ in Eq. (5.45). This agrees with the result found in Ref. [124].

5.3.2 Equivalence principle constraints

Let us proceed by considering the constraints resulting from a possible violation of the equivalence principle (EP). Under the condition that the neighbourhood of the Earth has a thin-shell, the tightest bound comes from solar system tests of the EP that make use of the free-fall accelerations of the Moon ($a_{\rm Moon}$) and the Earth ($a_\oplus$) toward the Sun [47; 124]. The bound on the differences between the two accelerations is [61]

$$2\frac{|a_{\rm Moon}-a_\oplus|}{a_{\rm Moon}+a_\oplus} < 10^{-13}\,. \tag{5.60}$$

Since the acceleration induced by a fifth-force with the field profile $\varphi(\ell)$ and the effective coupling is given by $a_{\rm fifth}=|Q_{\rm eff}\varphi(\ell)|$ we obtain [47]

$$\begin{aligned} a_\oplus &= \frac{G_N M_\odot}{r^2}\left[1+18Q^2\left(\frac{\Delta\ell_\oplus}{\ell_\oplus}\right)^2\frac{\Phi_\oplus}{\Phi_\odot}\right], \\ a_{\rm Moon} &= \frac{G_N M_\odot}{r^2}\left[1+18Q^2\left(\frac{\Delta\ell_\oplus}{\ell_\oplus}\right)^2\frac{\Phi_\oplus^2}{\Phi_\odot\Phi_{\rm Moon}}\right], \end{aligned} \tag{5.61}$$

where $\Phi_\odot \simeq 2.1\times10^{-6}$, $\Phi_\oplus \simeq 7.0\times10^{-10}$ and $\Phi_{\rm Moon}\simeq 3.1\times10^{-11}$, are the gravitational potentials of the Sun, the Earth and the Moon, respectively [47; 124]. Note that $\Delta\ell_\oplus/\ell_\oplus$ is the thin-shell parameter of the Earth. From the bound (5.60), this is constrained to be

$$\frac{\Delta\ell_\oplus}{\ell_\oplus} < \frac{8.8\times10^{-7}}{|Q|}\,. \tag{5.62}$$

Note also that the thin-shell condition for the neighbourhood outside the Earth provides the same order of the upper bound for $\Delta\ell_\oplus/\ell_\oplus$ [124].

Taking a similar procedure as in the case of the solar system constraints discussed above (using the value $R_1=10^{-29}$ g/cm^3 and $\rho_B=10^{-24}$ g/cm^3), we obtain the following bound:

$$p > 1-\frac{5}{13.8-\log_{10}|Q|}\,. \tag{5.63}$$

This is tighter than the bound (5.59). When $|Q|=10^{-2}$ and $|Q|=10^{-1}$ we have $p>0.68$ and $p>0.66$, respectively. In the case of $f(R)$ gravity the above bound corresponds to $p>0.65$ which translates to $n>0.9$ for the potential (5.45).

In summary, the LGC can be satisfied under the condition (5.63) for the potential (5.47).

5.3.3 General properties for models consistent with LGC

In this subsection we shall consider the general properties of scalar-tensor theories consistent with LGC, without specifying the form of the field potential. In order to satisfy the LGC

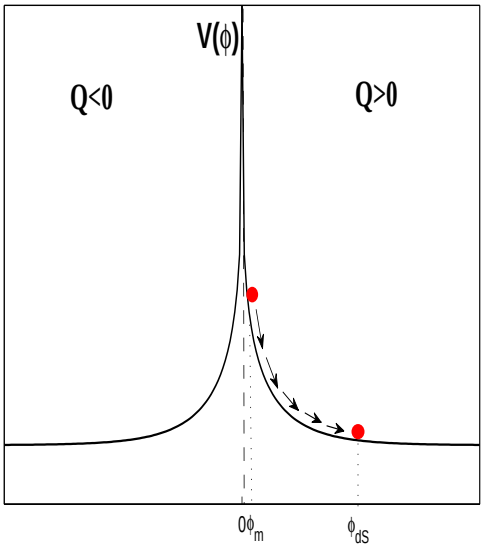

Figure 5.2: This illustration describes a field potential $V(\varphi)$ that is consistent with LGC. For a coupling Q that is positive (negative) the potential evolves in the region $\varphi \geq 0$ ($\varphi \leq 0$). In the figure φ_m represents the field value during the radiation/matter eras, which instantaneously changes in time. The field value $\varphi_{\rm dS}$ corresponds to the one at the de-Sitter point. Note that both φ_m and $\varphi_{\rm dS}$ are sustained by the presence of the coupling Q having potential minima characterised by the condition (5.64). In the early stages of the cosmological evolution, the mass M of the field φ is heavy for consistency with LGC. This mass gradually gets smaller as the system approaches the de-Sitter point.

we require that $|\varphi_B - \varphi_A|$ is much smaller than $|Q\Phi_\star|$ from Eq. (4.29). Since there is a gap between the energy densities inside and outside of the spherically symmetric body, we have $|\varphi_B - \varphi_A| \simeq |\varphi_B|$, which implies $|\varphi_B| \ll |Q\Phi_\star|$. The gravitational potential $\Phi_\star$ is very much smaller than unity in settings where local gravity experiments are carried out, hence this yields the constraint $|\varphi_B| \ll 1$. Cosmologically this means that $|\varphi|$ is much smaller than unity during matter/radiation epochs. When $|Q| \gg 1$ the condition $|\varphi_B| \ll 1$ is not necessarily ensured, but those cases are excluded by the constraints from density perturbations unless the model is very close to the ΛCDM model (as we shall see later). In the following we shall consider the theories with $|Q| \lesssim 1$.

In the region $|\varphi| \ll 1$ (i.e., $F \simeq 1$), the derivative terms are negligible in Eq. (5.16) and the field stays at the instantaneous minima given by

$$V_{,\varphi} + QFR = 0\,, \tag{5.64}$$

in the late radiation-dominated and matter-dominated eras. The condition (5.64) translates into $\lambda/Q = \rho_m/V$ which means that $\lambda/Q \gg 1$ in the radiation and matter epochs. This is in fact consistent with the condition $|w_{\rm eff}| = |2Q/\lambda| \ll 1$ for the existence of a viable matter

point (d). If the de-Sitter point (e) is stable, the solutions finally approach the minimum given by (5.64), i.e., $\lambda/Q = 4$.

The sign of λ needs to be the same as that of Q in order to realise the above cosmological trajectory. When $Q > 0$, we require $\lambda = -V_{,\varphi}/V > 0$, i.e., $V_{,\varphi} < 0$, which means that the field, φ, evolves along the potential toward larger positive values from $\varphi \simeq 0$. When $Q < 0$ the field evolves towards smaller negative values from $\varphi \simeq 0$.

Such potentials are illustrated in Fig. 5.2. Since the ratio λ/Q decreases from the radiation/matter epochs to the de-Sitter epoch, the derivative $\mathrm{d}\lambda/\mathrm{d}\varphi$ is negative irrespective of the sign of Q. We recall that in this case the stability of the de-Sitter point (e) is also ensured. Since $\mathrm{d}\lambda/\mathrm{d}\varphi = \lambda^2 - V_{,\varphi\varphi}/V$, the mass squared

$$M^2 \equiv V_{,\varphi\varphi}\,, \tag{5.65}$$

is required to be positive to satisfy the condition $\mathrm{d}\lambda/\mathrm{d}\varphi < 0$. Moreover, the mass, M, needs to be sufficiently heavy in order to satisfy the condition $M^2 > \lambda^2 V$ in the radiation/matter epochs. The model (5.47) provides a representative example which satisfies all the requirements discussed above.

It is worth mentioning that for the models that satisfy LGC, the quantity $F = e^{-2Q\varphi}$ in the matter/radiation eras is larger than its value at the de-Sitter point. It is this property which leads to an interesting observational signature for the DE equation of state, as we shall see in the next section.

5.4 The equation of state of dark energy

In scalar-tensor DE models, a meaningful definition of energy density and pressure of DE requires some care. In this section, following Ref. [140; 141], we shall discuss the evolution of the equation of state of DE, which could provide comparisons with observations. In the absence of radiation, Eqs. (5.12) and (5.13) can be written as

$$3F_0H^2 = \rho_{\rm DE} + \rho_m \,, \tag{5.66}$$

$$-2F_0\dot{H} = \rho_{\rm DE} + p_{\rm DE} + \rho_m \,, \tag{5.67}$$

where the subscript "0" represents present values and

$$\rho_{\rm DE} \equiv \frac{1}{2}(1-6Q^2)F\dot{\varphi}^2 + V - 3H\dot{F} - 3(F-F_0)H^2 \,, \tag{5.68}$$

$$p_{\rm DE} \equiv \frac{1}{2}(1-6Q^2)F\dot{\varphi}^2 - V + \ddot{F} + 2H\dot{F} + (F-F_0)(3H^2+2\dot{H}) \,, \tag{5.69}$$

which satisfy the usual conservation equation

$$\dot{\rho}_{\rm DE} + 3H(\rho_{\rm DE} + p_{\rm DE}) = 0 \,. \tag{5.70}$$

We define the equation of state of DE to be

$$w_{\rm DE} \equiv \frac{p_{\rm DE}}{\rho_{\rm DE}} = \frac{w_{\rm eff}}{1-(F/F_0)\Omega_m} \,, \tag{5.71}$$

where Ω_m and $w_{\rm eff}$ are defined in Eqs. (5.18) and (5.26), respectively. Integrating Eq. (5.14), we obtain

$$\rho_m = 3F_0\Omega_m^{(0)}H_0^2(1+z)^3 \,, \tag{5.72}$$

where $\Omega_m^{(0)}$ is the present energy fraction of the non-relativistic matter. On using Eqs. (5.66) and (5.67), we find

$$w_{\rm DE} = -\frac{3r-(1+z)(\mathrm{d}r/\mathrm{d}z)}{3r-3\Omega_m^{(0)}(1+z)^3} \,, \tag{5.73}$$

where $r = H^2(z)/H_0^2$. Note that this is the same equation as the one used in Einstein gravity [9]. By defining the energy density $\rho_{\rm DE}$ and the pressure $p_{\rm DE}$ as given in Eqs. (5.68) and (5.69), the resulting DE equation of state, $w_{\rm DE}$, agrees with the usual expression which can be used to confront the models with SNIa observations.

From Eq. (5.71) we find that $w_{\rm DE}$ becomes singular at the point $\Omega_m = F_0/F$. This happens for models in which F increases from its present value F_0 as we go back in time. From Eq. (5.8) it is clear that F decreases in time for $Q\dot{\varphi} > 0$. We note that even when

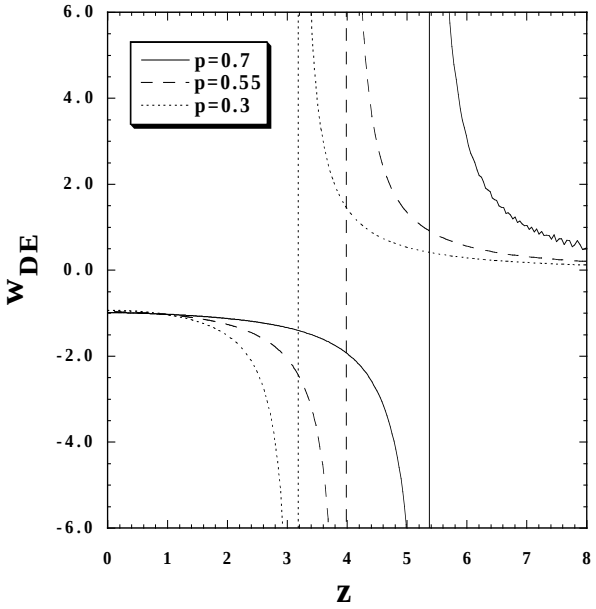

Figure 5.3: Figure depicting the evolution of $w_{\rm DE}$ for $Q = 0.1$ and $C = 0.95$ with three different values of p $(0.3, 0.55, 0.7)$. The redshift z_c at which the divergence of $w_{\rm DE}$ occurs decreases for smaller p.

the system crosses the point $\Omega_m = F_0/F$ physical quantities such as the Hubble parameter remain continuous.

The models (5.47) satisfy this condition regardless of the sign of Q, which means that the divergent behaviour of $w_{\rm DE}$ indeed occurs. We recall that in the context of $f(R)$ gravity ($Q = -1/\sqrt{6}$) the models $f(R) = R - \mu^{2(n+1)}/R^n$ ($n > 0$) correspond to a scalar field potential that decreases toward larger φ, i.e., $\dot{\varphi} > 0$ [161; 126; 37]. Hence, the divergence of $w_{\rm DE}$ does not occur in such models because of the decrease of F toward the past.

For the models that satisfy $|\lambda| \gg 1$ initially such that $|\lambda|$ decreases with time, the solutions are in the regime around the instantaneous fixed point (d) during the matter era and finally approach either the scalar-field dominated point (c) or the de-Sitter point (e). In Fig. 5.3 we plot the evolution of $w_{\rm DE}$ for the case $Q = 0.1$ and $C = 0.95$, with three different values of p. In these cases the final attractor corresponds to the de-Sitter point (e) satisfying the relation $\lambda = 0.4$. During the deep matter era the solutions evolve along the "instantaneous" fixed point (d) with Ω_m close to 1 (because $\lambda \gg 1$). After λ decreases to the order of unity, the solutions approach the de-Sitter solution (e) with $\Omega_m = 0$ and $w_{\rm DE} = w_{\rm eff} = -1$.

Figure 5.3 clearly shows that $w_{\rm DE}$ exhibits a divergence at a redshift z_c that depends on the values of p. When $p = 0.3$, for example, the divergence occurs around the redshift $z_c = 3$. For compatibility with LGC we require $p > 0.53$ from solar system constraints, and $p > 0.66$ from EP constraints, as was shown in the previous subsection. In those cases the critical redshift gets larger, which is out of the current SNIa observational range. Nevertheless, the DE equation of state shows a peculiar evolution that changes from $w_{\rm DE} < -1$ to $w_{\rm DE} >$

-1 at a redshift around $z_c = \mathcal{O}(1)$. This cosmological boundary crossing, similar to the divergence of $w_{\rm DE}$, is attributed to the fact that F increases as we go back in time. It is worth noting that this is a common feature among viable models that are consistent with LGC, as we have illustrated in the previous subsection. Moreover, this phenomenon seems to be present in other viable modifications of gravity, including $f(R)$ gravity [129] and $f(\mathcal{G})$ gravity [149], which we shall discuss in the next section.

Note that in the limit $Q \to 0$ the potential, $V(\varphi)$, approaches a constant value $V(\varphi) \to V_0(1-C)$. Hence, the models are hardly distinguishable from the ΛCDM model. In these cases the critical redshift, z_c, also goes to infinity. Thus, the effect of modified gravity is more apparent for larger $|Q|$ and smaller p. In $f(R)$ gravity, for example, the model given by Eq. (5.45) can give rise to the redshift z_c as close as a few [129] while satisfying the LGC ($p > 0.65$). These cases are particularly interesting to place tight bounds on model parameters from future high-precision observations.

5.5 Matter density perturbations

In this section we discuss the evolution of matter density perturbations and the resulting spectra for scalar-tensor theories. For this purpose we recall the results of Sec. 2.4. In the longitudinal gauge, under the redefinition $\alpha = \Phi$ and $\varphi = -\Psi$, the perturbed FLRW line element (2.118) is given by [97; 103; 104]

$$\mathrm{d}s^2 = -(1+2\Phi)\mathrm{d}t^2 + a^2(t)(1-2\Psi)\mathrm{d}x^i\mathrm{d}x^j\,. \tag{5.74}$$

Under this redefinition, it proves useful to restate some of the equations presented in Sec. 2.4. In Fourier space, matter perturbations satisfy the following equations of motion [Eqs. (2.122)-(2.123)]:

$$(\delta\rho_m/\rho_m)^{\cdot} = 3\dot{\Psi} - \frac{k^2}{a^2}v\,, \tag{5.75}$$

$$\Phi = \dot{v}\,, \tag{5.76}$$

where $v \equiv av_m$ is a covariant velocity perturbation. The evolution equation for the gauge-invariant density contrast, δ_m, derived in Eq. (2.131) becomes:

$$\ddot{\delta}_m + 2H\dot{\delta}_m + \frac{k^2}{a^2}\Phi = 3\ddot{B} + 6H\dot{B}\,, \tag{5.77}$$

where $B = Hv + \Psi$ and δ_m is defined in Eq. (2.137).

Moreover, the evolution equations for the scalar metric perturbations, Eqs. (2.140)-(2.143), become:

$$\frac{k^2}{a^2}\Psi + 3H(H\Phi + \dot{\Psi}) = -\frac{1}{2F}\Bigg[\omega\dot{\varphi}\delta\dot{\varphi} + \frac{1}{2}(\omega_{,\varphi}\dot{\varphi}^2 - F_{,\varphi}R + 2V_{,\varphi})\delta\varphi \tag{5.78}$$

$$-3H\delta\dot{F} + \left(3\dot{H} + 3H^2 - \frac{k^2}{a^2}\right)\delta F + (3H\dot{F} - \omega\dot{\varphi}^2)\Phi + 3\dot{F}(H\Phi + \dot{\Psi}) + \delta\rho_m\Bigg]\,,$$

$$H\Phi + \dot{\Psi} = \frac{1}{2F}\left(\omega\dot{\varphi}\delta\varphi + \delta\dot{F} - H\delta F - \dot{F}\Phi + \rho_m v\right)\,, \tag{5.79}$$

$$\Psi - \Phi = \frac{\delta F}{F}\,, \tag{5.80}$$

$$\delta\ddot{\varphi} + \left(3H + \frac{\omega_{,\varphi}}{\omega}\dot{\varphi}\right)\delta\dot{\varphi} + \left[\frac{k^2}{a^2} + \left(\frac{\omega_{,\varphi}}{\omega}\right)_{,\varphi}\frac{\dot{\varphi}^2}{2} + \left(\frac{2V_{,\varphi} - F_{,\varphi}R}{2\omega}\right)_{,\varphi}\right]\delta\varphi$$

$$= \dot{\varphi}\dot{\Phi} + \left(2\ddot{\varphi} + 3H\dot{\varphi} + \frac{\omega_{,\varphi}}{\omega}\dot{\varphi}^2\right)\Phi + 3\dot{\varphi}(H\Phi + \dot{\Psi}) + \frac{1}{2\omega}F_{,\varphi}\delta R\,, \tag{5.81}$$

where $\delta\varphi$ pertains to the scalar field defined in Eq. (5.3), $\omega = (1-6Q^2)F$ and

$$\delta R = 2\left[-3(H\Phi + \dot{\Psi})^{\cdot} - 12H(H\Phi + \dot{\Psi}) + \left(\frac{k^2}{a^2} - 3\dot{H}\right)\Phi - 2\frac{k^2}{a^2}\Psi\right]\,. \tag{5.82}$$

As long as the mass, M, defined in Eq. (5.65) is sufficiently heavy, such that it satisfies the conditions $M^2 \gg R$ and $M^2 > \lambda^2 V$ (in order to ensure $\mathrm{d}\lambda/\mathrm{d}\varphi < 0$), one can approximate $((2V_{,\varphi} - F_{,\varphi}R)/2\omega)_{,\varphi} \simeq M^2/\omega$ in Eq. (5.81). While this quantity becomes negative for $Q^2 > 1/6$ this does not imply that the perturbation $\delta\varphi$ exhibits a negative instability. In fact we shall illustrate below, that due to the perturbation δR on the right hand side of Eq. (5.81), the effective mass produced is positive.

Generally, the solution of Eq. (5.81) consists of the sum of the matter-induced mode $\delta\varphi_{\rm ind}$ sourced by the matter perturbation and the oscillating mode $\delta\varphi_{\rm osc}$, i.e., $\delta\varphi = \delta\varphi_{\rm ind} + \delta\varphi_{\rm osc}$. The oscillating mode corresponds to the solution of Eq. (5.81) in the absence of the matter perturbation.

In order to derive the approximate perturbation equations on sub-horizon scales, we use the approximation according to which the terms containing k^2/a^2, $\delta\rho_m$, δR and M^2 dominate in Eqs. (5.78)-(5.81). This method was used in Refs. [9; 81; 100; 127] in the nearly massless case ($M^2 \lesssim H^2$). In the context of $f(R)$ gravity we saw in Sec. 4.3.4 that this approximation is extremely accurate even in the massive case ($M^2 \gg H^2$) as long as the oscillating degrees of freedom do not dominate over the matter-induced mode [69].

In order to extract the peculiar features of the matter perturbations in scalar-tensor gravity theories, let us first concentrate on the matter induced mode. Under the above-mentioned approximation, we have $\delta R_{\rm ind} \simeq -2(k^2/a^2)[\Psi + (F_{,\varphi}/F)\delta\varphi_{\rm ind}]$ from Eqs. (5.80) and (5.82), where the subscript "ind" represents a matter induced mode. Then from Eq. (5.81) we find

$$\delta\varphi_{\rm ind} \simeq \frac{2QF}{(k^2/a^2)(1-2Q^2)F + M^2}\frac{k^2}{a^2}\Psi\,. \tag{5.83}$$

Using Eq. (5.78) and (5.80) we obtain

$$\begin{aligned}\frac{k^2}{a^2}\Psi &\simeq -\frac{\delta\rho_m}{2F}\frac{(k^2/a^2)(1-2Q^2)F + M^2}{(k^2/a^2)F + M^2}\,,\\ \frac{k^2}{a^2}\Phi &\simeq -\frac{\delta\rho_m}{2F}\frac{(k^2/a^2)(1+2Q^2)F + M^2}{(k^2/a^2)F + M^2}\,.\end{aligned} \tag{5.84}$$

In the limit $M^2/F \gg k^2/a^2$ one has $(k^2/a^2)\Phi \simeq -\delta\rho_m/2F \simeq -4\pi G_N\delta\rho_m$, which recovers the standard Poisson equation. In the limit $M^2/F \ll k^2/a^2$ one has $(k^2/a^2)\Phi \simeq -(\delta\rho_m/2F)(1+2Q^2)$, where the effect of the coupling Q becomes important.

From Eq. (5.79) we find that v is of the order of $FH\Phi/\rho_m$. Using the fact that $(k^2/a^2)\Phi$ is of the order of $-(1/F)\delta\rho_m$ we can estimate that $|3Hv/(\delta\rho_m/\rho_m)| \sim (aH)^2/k^2 \ll 1$. Hence we have $\delta_m \simeq \delta\rho_m/\rho_m$ in Eq. (2.137). Similarly the terms on the right hand side of Eq. (5.77) can be neglected relative to those on the left hand side, which leads to the following equation for matter perturbations:

$$\ddot{\delta}_m + 2H\dot{\delta}_m - 4\pi G_{\rm eff}\rho_m\delta_m \simeq 0\,, \tag{5.85}$$

where the effective "cosmological" gravitational coupling is given by

$$G_{\rm eff} = \frac{1}{8\pi F}\frac{(k^2/a^2)(1+2Q^2)F + M^2}{(k^2/a^2)F + M^2}\,. \tag{5.86}$$

We can rewrite Eq. (5.85) by using derivatives with respect to N:

$$\frac{{\rm d}^2\delta_m}{{\rm d}N^2} + \left(\frac{1}{2} - \frac{3}{2}w_{\rm eff}\right)\frac{{\rm d}\delta_m}{{\rm d}N} - \frac{3}{2}\Omega_m\frac{(k^2/a^2)(1+2Q^2)F + M^2}{(k^2/a^2)F + M^2}\delta_m \simeq 0\,. \tag{5.87}$$

From Eq. (5.84) the effective gravitational potential as defined in Eq. (4.79) is given by

$$\Phi_{\rm eff} \simeq -\frac{a^2}{2k^2}\frac{\rho_m}{F}\delta_m\,. \tag{5.88}$$

This coincides with the analogous result in the $f(R)$ theory (4.80). The absence of the coupling in Eq. (5.88) indicates that the weak lensing in distant galaxies and the ISW effect in the CMB, both of which depend on $\Phi_{\rm eff}$, are not affected by Q.

Furthermore, in order to confront models with weak lensing observations, it is convenient to know the form of the anisotropic parameter η defined in Eq. (4.81). From Eq. (5.84) we obtain

$$\eta \simeq \frac{4Q^2(k^2/a^2)F}{(k^2/a^2)(1-2Q^2)F + M^2}\,, \tag{5.89}$$

which vanishes in the limit $M^2/F \gg k^2/a^2$, but approaches a value $\eta \to 4Q^2/(1-2Q^2)$ in the limit $M^2/F \ll k^2/a^2$. We also introduced the parameter Σ defined in Eq. (4.82). It follows that $\Sigma \simeq 1/F$, which shows that the effective potential can be written as $\Phi_{\rm eff} \simeq -(a^2/2k^2)\rho_m\delta_m\Sigma$. Hence, unlike the case of Einstein gravity the weak lensing potential in these scalar-tensor models of gravity is affected by the changes in Σ as well as δ_m.

During the matter era the field, φ, sits at the instantaneous minima characterised by the condition (5.64). This is analogous to the situation considered in Sec. 5.3.1, where for the models (5.47) the field value at the potential minimum and the mass squared m_φ^2 are given by Eqs. (5.54) and (5.55), respectively. Hence, we have the relations $\varphi \propto \rho_m^{\frac{1}{p-1}}$ and $M^2 \propto m_\varphi^2 \propto \rho_m^{\frac{2-p}{1-p}}$ during the matter-dominated epoch. The field, φ, can initially be heavy so as to satisfy the condition $M^2/F \gg k^2/a^2$ for the modes relevant to the galaxy power spectrum ($0.01h\,{\rm Mpc}^{-1} \lesssim k \lesssim 0.2h\,{\rm Mpc}^{-1}$). Depending upon the model parameters and the mode, k, the mass squared, M^2, can be smaller than k^2/a^2 during the matter era.

Let us now consider the behaviour of the oscillating mode. Using Eqs. (5.78) and (5.80) under the condition $k^2/a^2 \gg H^2$, the gravitational potentials for $\delta\rho_m = 0$ are expressed by $\delta\varphi_{\rm osc}$. Consequently, from Eq. (5.82), the perturbation δR corresponding to the oscillating

mode is given by

$$\delta R_{\rm osc} \simeq 6Q\left(\delta\ddot{\varphi}_{\rm osc} + 3H\delta\dot{\varphi}_{\rm osc} + \frac{k^2}{a^2}\delta\varphi_{\rm osc}\right) . \tag{5.90}$$

Substituting this into Eq. (5.81), we find

$$\delta\ddot{\varphi}_{\rm osc} + 3H\delta\dot{\varphi}_{\rm osc} + \left(\frac{k^2}{a^2} + \frac{M^2}{F}\right)\delta\varphi_{\rm osc} \simeq 0\,, \tag{5.91}$$

which is valid in the regimes $M^2 \gg \{R, \lambda^2 V\}$. Equation (5.91) clearly shows that the effective mass for the oscillating mode is positive even for $Q^2 > 1/6$.

In the following we shall confirm that as long as the oscillating mode does not initially dominate over the matter-induced mode, it remains subdominant throughout the cosmic history. As before, we shall discuss the two cases: (i) $M^2/F \gg k^2/a^2$ and (ii) $M^2/F \ll k^2/a^2$, separately.

5.5.1 The case $M^2/F \gg k^2/a^2$

In this regime the matter perturbation equation (5.87) reduces to the standard one in Einstein gravity. The evolutions of δ_m and $\Phi_{\rm eff}$ during the matter era, characterised by $w_{\rm eff} \simeq 0$ and $\Omega_m \simeq 1$, are described by Eq. (4.90).

For the model (5.47) the matter-induced mode of the field perturbation evolves as

$$\delta\varphi_{\rm ind} \propto \frac{\delta\rho_m}{M^2} \propto t^{\frac{2(4-p)}{3(1-p)}}.$$

When the frequency $\omega_\varphi = \sqrt{k^2/a^2 + M^2/F}$ changes adiabatically (i.e. $|\dot{\omega}_\varphi/\omega_\varphi^2| \ll 1$), the WKB solution to Eq. (5.91) is given by

$$\delta\varphi_{\rm osc} \propto a^{-3/2}\frac{1}{\sqrt{2\omega_\varphi}}\cos\left(\int\omega_\varphi {\rm d}t\right) . \tag{5.92}$$

For the model (5.47), in the regime $M^2/F \gg k^2/a^2$, this oscillating mode evolves as

$$\delta\varphi_{\rm osc} \propto t^{\frac{p}{2(1-p)}}\cos\left(ct^{-\frac{1}{1-p}}\right), \tag{5.93}$$

where c is a constant.

Now since the background field, φ, during the matter era evolves as $\varphi \propto t^{\frac{2}{1-p}}$, we find

$$\frac{\delta\varphi}{\varphi} \simeq c_1 t^{2/3} + c_2 t^{-\frac{4-p}{2(1-p)}}\cos\left(ct^{-\frac{1}{1-p}}\right) . \tag{5.94}$$

This indicates that the matter-induced mode dominates over the oscillating mode with time. While the solution of the oscillating mode in Eq. (5.94) is valid only in the WKB regime

($|\dot{\omega}_\varphi/\omega_\varphi^2| \ll 1$), we have checked that $\delta\varphi$ approaches a constant value with oscillations at the later stage in which the WKB approximation is violated. Hence, as long as the oscillating mode is not overproduced in the early universe, it remains sub-dominant relative to the matter-induced mode. Note that this property also holds during the radiation-dominated epoch.

5.5.2 The case $M^2/F \ll k^2/a^2$

In this regime the effective gravitational coupling (5.86) is given by $G_{\rm eff} = (1+2Q^2)/8\pi F$, which means that the effect of modified gravity becomes important. From Eqs. (5.87) and (5.88) we obtain

$$\delta_m \propto t^{\frac{\sqrt{25+48Q^2}-1}{6}} \quad \text{and} \quad \Phi_{\rm eff} \propto t^{\frac{\sqrt{25+48Q^2}-5}{6}}\,, \tag{5.95}$$

which grow faster than the solutions given in Eq. (4.90). This leads to changes in the matter power spectrum of the large scale structure as well as in the ISW effect in the CMB.

The field perturbation, $\delta\varphi$, is the sum of the matter-induced mode given in Eq. (5.83) and the oscillating mode $\delta\varphi_{\rm osc}$ given in Eq. (5.91). Using the WKB solution (5.92) for the latter mode, we have

$$\delta\varphi = c_1 t^{\frac{\sqrt{25+48Q^2}-5}{6}} + c_2 t^{-2/3}\cos(ct^{1/3})\,. \tag{5.96}$$

Since the frequency has a dependence $|\dot{\omega}_\varphi/\omega_\varphi^2| \simeq H \propto 1/t$, the WKB approximation tends to be accurate at late times. Equation (5.96) shows that the matter-induced mode dominates over the oscillating mode with time.

5.5.3 The matter power spectra

The models (5.47) have a heavy mass, M, which is much larger than H in the deep matter-dominated epoch, but which gradually decreases to become of the order of H around the present epoch. Depending on the modes, k, the system crosses the point $M^2/F = k^2/a^2$ at $t = t_k$ during the matter era. As shown above, in the context of $f(R)$ gravity this indeed occurs for the modes relevant to the galaxy power spectrum [69]. Since for the model (5.47) M evolves as $M \propto t^{-\frac{2-p}{1-p}}$ during the matter era, the time t_k has a scale-dependence given by $t_k \propto k^{-\frac{3(1-p)}{4-p}}$. When $t < t_k$, the evolution of δ_m is given by Eq. (4.90), but for $t > t_k$ its evolution changes to the form given by (5.95).

The growth rate of matter perturbations, defined in Eq. (4.105), is $s = 1$ in the regime $M^2/F \gg k^2/a^2$. After the system enters the regime $M^2/F \ll k^2/a^2$ during the matter-

dominated epoch, we have

$$s = \frac{\sqrt{25+48Q^2}-1}{4}\,. \tag{5.97}$$

During the matter era the mass squared is approximately given by

$$M^2 \simeq \frac{1-p}{(2^p\,p\,C)^{1/(1-p)}}Q^2\left(\frac{\rho_m}{V_0}\right)^{\frac{2-p}{1-p}}V_0\,. \tag{5.98}$$

Using the relation $\rho_m = 3F_0\Omega_m^{(0)}H_0^2(1+z)^3$, we find that the critical redshift, z_k, at time t_k can be estimated as

$$z_k \simeq \left[\left(\frac{k}{a_0H_0}\frac{1}{Q}\right)^{2(1-p)}\frac{2^p pC}{(1-p)^{1-p}}\frac{1}{(3F_0\Omega_m^{(0)})^{2-p}}\frac{V_0}{H_0^2}\right]^{\frac{1}{4-p}} - 1\,, \tag{5.99}$$

where a_0 is the present scale factor. The critical redshift increases for larger $k/(a_0H_0)$. The matter power spectrum, in the linear regime, has been observed for the scales $0.01h\,\mathrm{Mpc}^{-1} \lesssim k \lesssim 0.2h\ \mathrm{Mpc}^{-1}$, which corresponds to $30a_0H_0 \lesssim k \lesssim 600a_0H_0$. In Fig. 5.4 we plot the evolution of the growth rate, s, for the mode $k = 600a_0H_0$ and the coupling $Q = 1.08$ with three different values of p. We find that, in these cases, the critical redshift exists in the region $z_k \gtrsim 1$ and that z_k increases for smaller p. When $p = 0.7$ we estimate $z_k = 3.9$, from Eq. (5.99), which is consistent with the numerical result in Fig. 5.4. The growth rate reaches a maximum value $s_{\rm max}$ and then begins to decrease around the end of the matter era.

If we use the criterion $s < 2$ for the analytic estimation (5.97), we obtain the bound $Q < 1.08$. Figure 5.4 shows that $s_{\rm max}$ is smaller than the analytic value $s = 2$ (which corresponds to $Q = 1.08$). When $p = 0.7$, for example, we find that $s_{\rm max} = 1.74$. For the values of p that are very close to 1, $s_{\rm max}$ can be smaller than 1.5. However these cases are hardly distinguishable from the ΛCDM model. In any case the current observational data on the growth rate is not enough to place tight bounds on Q and p.

The growth of matter perturbations continues up to the time t_Λ characterised by the condition $\ddot{a} = 0$. At time t_Λ the matter power spectrum $P_{\delta_m} = (k^3/2\pi^2)|\delta_m|^2$ exhibits a difference compared to the ΛCDM model given by

$$\frac{P_{\delta_m}(t_\Lambda)}{P_{\delta_m}^{\Lambda\mathrm{CDM}}} = \left(\frac{t_\Lambda}{t_k}\right)^{2\left(\frac{\sqrt{25+48Q^2}-1}{6}-\frac{2}{3}\right)} \propto k^{\frac{(1-p)(\sqrt{25+48Q^2}-5)}{4-p}}\,. \tag{5.100}$$

The CMB power spectrum is also affected by the non-standard evolution of $\Phi_{\rm eff}$ given in Eq. (5.95). This mainly happens for low multipoles because of the ISW effect. Since the smaller scale modes in the CMB relevant to the galaxy power spectrum are hardly affected by this modification, there is a difference between the spectral indices of the matter power

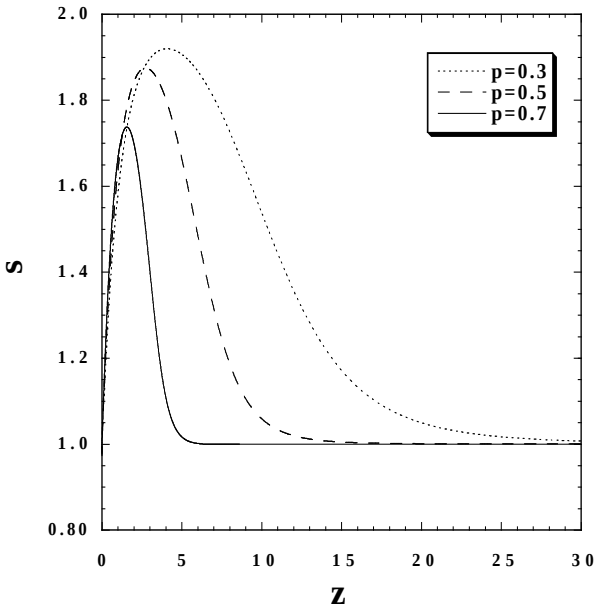

Figure 5.4: The evolution of the growth rate, s, of matter perturbations in terms of the redshift, z, for $Q = 1.08$ and $k = 600a_0H_0$ with three different values of p. For smaller p the critical redshift, z_k, gets larger. The growth rate, s, reaches a maximum value and begins to decrease after the system enters the accelerated epoch. For smaller p the maximum value of s tends to approach the analytic value given in Eq. (5.97).

spectrum and of the CMB spectrum on the scales $k > 0.01h\,\mathrm{Mpc}^{-1}$:

$$\Delta n(t_\Lambda) = \frac{(1-p)(\sqrt{25+48Q^2}-5)}{4-p}\,. \tag{5.101}$$

This reproduces the result of $f(R)$ gravity derived in Sec. 4.3.5. In Ref. [129] it was shown that this analytic estimation agrees well with numerical results except for large values of p close to unity. This reflects the fact that for larger p the redshift $z = z_k$ at time $t = t_k$ gets smaller (being of the order of $z_k = \mathcal{O}(1)$) so the approximations used in deriving the solutions (5.95), based on $w_{\rm eff} = 0$ and $\Omega_m = 1$, break down. In Ref. [129] it was further shown that the difference $\Delta n(t_0)$ integrated to the present epoch does not show a significant difference compared to (5.101).

Because we do not, at present, have any observationally significant evidence to suggest the presence of a difference between the spectral indices of the CMB and the matter power spectra [162], in Fig. 5.5 we plot the constraints coming from the criterion $\Delta n(t_\Lambda) < 0.05$. If $|Q|$ is smaller than 0.1, this condition is trivially satisfied. For larger $|Q|$ the constraints on the values of p tend to be stronger. In the case of $f(R)$ gravity we obtain the bound $p > 0.78$, which is stronger than the constraint coming from the violation of the equivalence principle. If we adopt the criterion $\Delta n(t_\Lambda) < 0.03$, the bound on p becomes tighter: $p > 0.87$. Meanwhile, if $|Q|$ is smaller than the order of 0.1, the EP constraint gives the tightest

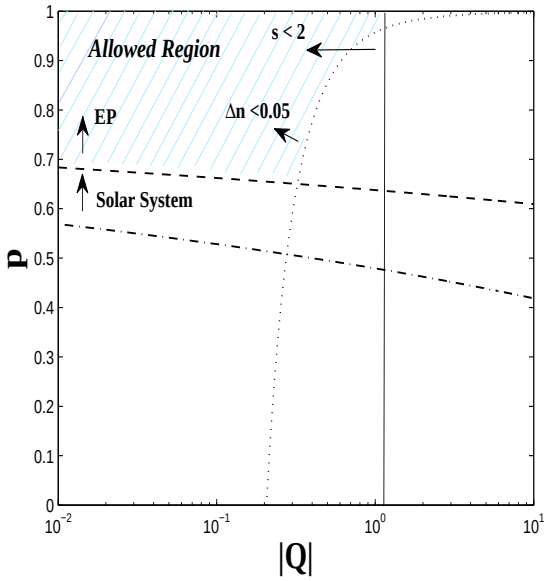

Figure 5.5: The allowed region of the parameter space in the (p, Q) plane. We show the bounds coming from the conditions $\Delta n(t_\Lambda) < 0.05$ and $s < 2$ as well as the solar-system constraint (5.59) and the EP constraint (5.63).

bound. If we use the criterion $s < 2$ for the analytic estimation (5.97), the coupling, $|Q|$, is bounded from above ($Q < 1.08$).

In Fig. 5.5 we show the allowed parameter space consistent with current observational and experimental constraints. The constraints coming from the ISW effect in the CMB due to the change in evolution of the gravitational potential do not provide tighter bounds compared to those shown in Fig. 5.5.

5.6 Summary

We have considered a class of dark energy models based on scalar-tensor theories given by the action (5.9). In these theories, expressed in the Einstein frame, the scalar field φ is coupled to the non-relativistic matter with a constant coupling Q. The action (5.9) is equivalent to the Brans-Dicke theory with a field potential V, where the Brans-Dicke parameter, $\omega_{\rm BD}$, is related to the coupling, Q, via the relation $3 + 2\omega_{\rm BD} = 1/(2Q^2)$. These theories include the $f(R)$ gravity theories and the quintessence models as special cases where the coupling is given by $Q = -1/\sqrt{6}$ (i.e., $\omega_{\rm BD} = 0$) and $Q = 0$ (i.e., $\omega_{\rm BD} \to \infty$), respectively.

We began by studying the background cosmological dynamics in a homogeneous and isotropic setting, without specifying the field potential, $V(\varphi)$, but under the assumption that the slope of the potential, $\lambda = -V_{,\varphi}/V$, is constant. The varying λ case can also be studied by treating the fixed points as instantaneous ones. We found that for a range of values of the coupling constant, $|Q|$, not much smaller than unity the matter era can be realised by the solution corresponding to the point (d) in Eq. (5.31) subject to the condition $\lambda/Q \gg 1$. Interestingly the presence of a non-zero coupling leads to a de-Sitter solution characterised by the condition $V_{,\varphi} + QFR = 0$ (i.e., $\lambda = 4Q$), which can lead to late-time acceleration. (The condition for the stability of this de-Sitter solution is given by $\mathrm{d}\lambda/\mathrm{d}\varphi < 0$ at the fixed point.)

In the absence of the scalar-field potential, solar-system tests constrain the coupling, Q, to have values in the range $|Q| < 2.5 \times 10^{-3}$. The presence of the potential, on the other hand, allows the LGC to be satisfied for larger values of $|Q|$, if the field is sufficiently heavy in the high-curvature region where gravity experiments are carried out. We found that even when $|Q|$ is of the order of 1, a thin-shell can form inside a spherically symmetric body such that the effective coupling, $|Q_{\rm eff}|$, defined in Eq. (4.28) becomes much smaller than 1.

We then considered a family of models given by the scalar-field potentials (5.47) which generalise the corresponding potential in the $f(R)$ theory, while at the same time satisfying the LGC for appropriate choices of the parameters. In particular we found that as p approaches unity, the mass of the field, φ, becomes larger, thus allowing the LGC to be satisfied more easily [see Eq. (5.55)]. Using the constraints coming from solar system tests as well as compatibility with the equivalence principle, we obtained the bounds $p > 1 - 5/(9.6 - \log_{10}|Q|)$ and $p > 1 - 5/(13.8 - \log_{10}|Q|)$, respectively. In $f(R)$ gravity, for example, these constraints correspond to $p > 0.50$ and $p > 0.65$ respectively.

During radiation/matter eras the field, φ, needs to be very close to 0 for the compatibility with LGC, which results in $F = e^{-2Q\varphi} \simeq 1$. Figure 5.5 summaries the regions of the parameter space in the (p, Q) plane where the corresponding potentials lead to models compatible with the LGC.

For these models we found that the quantity F tends to increase from its present value

as we go into the past, which results in the equation of state $w_{\rm DE}$ of dark energy becoming singular when $\Omega_m = F_0/F$. This behaviour is similar to that found for $f(R)$ and $f(\mathcal{G})$ theories.

We also studied the evolution of density perturbations for these models in order to place constraints on the coupling, Q, as well as on the parameters of the field potential. In the deep matter era the mass, M, of the scalar field is sufficiently heavy to make these models compatible with LGC, but it gradually gets smaller as the Universe enters the accelerated epoch. For those models compatible with the galaxy power spectrum, there exists a "General Relativistic" phase during the matter era characterised by the condition $M^2/F \gg k^2/a^2$. At this stage the matter perturbation δ_m and the effective gravitational potential $\Phi_{\rm eff}$ evolve as $\delta_m \propto t^{2/3}$ and $\Phi_{\rm eff} = {\rm constant}$, respectively, as in the case of Einstein gravity. Around the end of the matter-dominated epoch, the deviation from Einstein gravity can be seen once M^2/F becomes smaller than k^2/a^2. The evolution of perturbations during this "scalar-tensor" regime is given by Eqs. (5.95). Under the criterion $s = \dot{\delta}_m/H\delta_m < 2$ for the growth rate of matter perturbations, and with the use of the analytic estimation (5.97), we obtain the bound $Q < 1.08$. The difference Δn of the spectral indices of the CMB and the matter power spectra gives rise to another constraint on the model parameter p and the coupling Q.

Figure 5.5 illustrates the bounds derived from the conditions $\Delta n < 0.05$ and $s < 2$, as well as those from local gravity constraints. The models with p close to 1 satisfy all these requirements. It will certainly be of interest to place more stringent constraints on the values of p and Q by using the recent data of the matter power spectrum, CMB and Lyman alpha forest. Moreover, the future surveys of weak lensing may find some evidence of an anisotropic stress between the gravitational potentials Φ and Ψ, which can be a powerful tool to distinguish modified gravity models from the ΛCDM cosmology.

Chapter 6

Cosmological scaling solutions in generalised Gauss-Bonnet gravity

In this chapter we consider the cosmology of models based on a class of generalised theories with an action of the form (2.54):

$$S = \int d^4x\sqrt{-g}\left(\frac{R}{2} + f(\mathcal{G})\right) + S_m, \tag{6.1}$$

where the Gauss-Bonnet (GB) invariant, $\mathcal{G}$, is defined in Eq. (2.53). We recall that in four dimensions, the GB term is a topological invariant and introducing a term proportional to $\mathcal{G}$ into the Einstein-Hilbert action does not modify the dynamics. In this chapter we investigate the existence and stability of cosmological power-law scaling solutions derived from theories of the type (6.1) in the presence of a perfect fluid matter source [71]. Scaling (attractor) solutions play an important role in cosmology, since they enable the asymptotic behaviour and stability of a particular cosmological background to be determined. Moreover, they provide a framework for establishing the behaviour of more general cosmological solutions [22; 25; 163; 164; 165].

6.1 Cosmological Field Equations

As was discussed in Sec. 2.2.4, the action (6.1) may be expressed in an equivalent form [166]:

$$S = \int d^4x\sqrt{-g}\left(\frac{R}{2} - V(\phi) - h(\phi)\mathcal{G}\right) + S_m, \tag{6.2}$$

where the scalar field, ϕ, is defined implicitly by

$$h(\phi) \equiv -F(\mathcal{G}) \tag{6.3}$$

for some function $h(\phi)$ and has an effective self-interaction potential

$$V(\phi) \equiv \mathcal{G}F(\mathcal{G}) - f(\mathcal{G}), \tag{6.4}$$

where $F \equiv \partial f/\partial\mathcal{G}$. Eq. (6.2) may be interpreted as an effective 'scalar-tensor' theory, where the scalar field has a vanishing kinetic term.

To study cosmological models based on action (6.1), one may proceed directly by varying the action to derive the field equations or, indirectly, by varying the equivalent action (6.2). We employ the latter approach in the present work in view of its potential simplicity. The field equations in this case take the form given in Eq. (2.84). The equation of motion for the scalar field takes the form

$$V_{,\phi}(\phi) + h_{,\phi}(\phi)\mathcal{G} = 0. \tag{6.5}$$

(This is Eq. (2.81) which we restate here for convenience).

The aim here is to study the dynamics of the isotropic and spatially flat FLRW universe sourced by a perfect barotropic fluid with an equation of state parameter, $w_m = p_m/\rho_m$. For this spacetime, the GB invariant is given by $\mathcal{G} = 24H^2(\dot{H} + H^2)$. The Friedmann and Raychaudhuri equations derived from Eq. (2.84) for this background are then given by [167; 31]

$$3H^2 = V(\phi) + 24H^3\dot{h} + \rho_m, \tag{6.6}$$

$$\left(2\frac{\dot{H}}{H^2} + 3\right)H^2 = V(\phi) + 8H^2\ddot{h} + 16H^3\dot{h}\left(1 + \frac{\dot{H}}{H^2}\right) - p_m, \tag{6.7}$$

respectively, and the scalar field equation (6.5) reduces to

$$V_{,\phi} + 24h_{,\phi}H^2(\dot{H} + H^2) = 0. \tag{6.8}$$

It proves convenient to interpret the GB gravitational terms on the right-hand side of the Friedmann equation (6.6) as an effective energy density, such that $\rho_{\mathcal{G}} \equiv T_{\mathcal{G}} + V(\phi)$, where $T_{\mathcal{G}} \equiv 24\dot{h}H^3$ plays the role of a kinetic energy. It is then natural to introduce the dimensionless variables

$$y_1 \equiv \frac{V(\phi)}{3H^2}, \quad y_2 \equiv 8H\dot{h}, \tag{6.9}$$

and the fractional energy densities

$$\Omega_m \equiv \frac{\rho_m}{3H^2} = 1 - y_1 - y_2, \tag{6.10}$$

$$\Omega_{\mathcal{G}} \equiv y_1 + y_2. \tag{6.11}$$

The background field equations (6.6)-(6.8) can then be expressed in terms of these variables such that

$$\frac{dy_1}{dN} = 2\varepsilon y_1 - (1-\varepsilon)y_2, \tag{6.12}$$

$$\frac{dy_2}{dN} = -2\varepsilon + 3(1-y_1) - (2-\varepsilon)y_2 + 3w_m\Omega_m, \tag{6.13}$$

where $\varepsilon \equiv -\dot{H}/H^2$ and $N \equiv \ln a$.

6.2 Cosmological scaling solutions

We wish to identify the class of GB theories that admit scaling solutions such that each of the terms in the Friedmann equation (6.6) scales at the same rate, $H^2 \propto \rho_m \propto V(\phi) \propto T_{\mathcal{G}}$ [168]. These conditions result in a power-law solution to Eqs. (6.6)-(6.8) of the form $a \propto t^{1/\varepsilon}$, where $\varepsilon = \text{constant}$. For such a scaling solution, it follows from Eq. (6.8) that

$$V_{,\phi} = -\frac{1}{\alpha}V^2 h_{,\phi} \tag{6.14}$$

when $\varepsilon \neq 1$, where α is a finite constant. Integrating Eq. (6.14) then implies that

$$h = \frac{\alpha}{V} + \beta, \tag{6.15}$$

where β is an arbitrary integration constant.

Relating the functions $V(\phi)$ and $h(\phi)$ in this way is equivalent to specifying the form of the GB function, $f(\mathcal{G})$, via the definition given in Eq. (6.4). Indeed, substituting Eq. (6.15) into Eq. (6.4) results in the first-order, non-linear differential equation

$$\left(\mathcal{G}\frac{df}{d\mathcal{G}} - f\right)\left(\frac{df}{d\mathcal{G}} + \beta\right) = -\alpha. \tag{6.16}$$

Eq. (6.16) is an example of Clairaut's equation [169] and may be solved in full generality by differentiating with respect to $\mathcal{G}$:

$$\frac{d^2 f}{d\mathcal{G}^2}\left[\left(\frac{df}{d\mathcal{G}} + \beta\right)^2 - \frac{\alpha}{\mathcal{G}}\right] = 0. \tag{6.17}$$

Eq. (6.17) is trivially solved by $f(\mathcal{G}) = \alpha_0 + \alpha_1\mathcal{G}$, where α_i are constants. However, this simply corresponds to the introduction of a cosmological constant in the action (6.1) and is not physically interesting to the present discussion. (Recall that a contribution of the form $f \propto \mathcal{G}$ is also uninteresting since the GB term is a topological invariant). On the other hand, a singular solution to Eq. (6.16) with no arbitrary constants can be found by setting the square

bracketed term in Eq. (6.17) to zero and substituting the result into Eq. (6.16). We find that

$$f(\mathcal{G}) = \pm 2\sqrt{\alpha \mathcal{G}}, \tag{6.18}$$

where we have specified $\beta = 0$ without loss of generality. Moreover, requiring the action (6.1) to be real implies that $\alpha\mathcal{G} > 0$.

Eqs. (6.15) and (6.18) represent the necessary and sufficient conditions for the existence of power-law scaling solutions, where $\varepsilon = \text{constant}$. More general solutions to the field equations, where ε is time-dependent, exist for this model. If the cosmological behaviour of the model (6.18) is to be determined, the coupled differential equations (6.12)-(6.13) must close. This implies that the parameter ε must be expressible as a function of y_1 and y_2 only. When Eq. (6.15) is satisfied, we find that

$$\varepsilon = 1 - \frac{3}{8\alpha} y_1^2. \tag{6.19}$$

Hence, substituting Eq. (6.19) into Eqs. (6.12)-(6.13) yields the plane autonomous system:

$$\frac{dy_1}{dN} = 2y_1 - \frac{3}{4\alpha} y_1^3 - \frac{3}{8\alpha} y_1^2 y_2, \tag{6.20}$$

$$\frac{dy_2}{dN} = 2(y_2 - 1) - \frac{3}{8\alpha} y_1^2 y_2 + \frac{3}{4\alpha} y_1^2 + 3(1 + w_m)(1 - y_1 - y_2). \tag{6.21}$$

Before concluding this section, it should be remarked that the equivalence between actions (6.1) and (6.2) does not apply for the special case $\varepsilon = 1$ $(y_1 = 0)$, corresponding to the coasting solution, $a \propto t$. In this case, integration of Eq. (6.8) would yield $V(\phi) = V_0 = \text{constant}$ and the solution to Eq. (6.4) would then be given by $f(\mathcal{G}) = -V_0 + c_1\mathcal{G}$ for some constant c_1. This disparity can be traced to the singular nature of the coasting solution for the model (6.18). Specifically, the Friedmann equation derived directly from action (6.1) for this model is given by

$$3H^2 = \mp\sqrt{6\alpha}\frac{H^2(2H^3 - \ddot{H})}{(\dot{H} + H^2)^{3/2}} + \rho_m \tag{6.22}$$

and the term originating from the GB contribution is ill-defined when $\varepsilon = 1$ $(y_1 = 0)$. Consequently, we do not consider this solution in the phase plane analyses of the following sections.

6.3 Vacuum solutions

In this Section, we consider vacuum solutions where $\Omega_m = 0$ and $y_1 = 1 - y_2$. The pair of equations (6.20)-(6.21) then reduces to the one-dimensional system

$$\frac{dy_1}{dN} = y_1 \left(2 - \frac{3}{8\alpha} y_1 - \frac{3}{8\alpha} y_1^2 \right). \tag{6.23}$$

There exist two power-law solutions when $y_1 \neq 0$:

$$y_1 = -\frac{1}{2} \pm \frac{1}{6}\sqrt{9 + 192\alpha}, \tag{6.24}$$

which we denote as $\mathcal{V}^{\pm}$, respectively. The reality of the fixed points requires that $\alpha \geq -9/192$. The power of the expansion can be expressed in terms of the effective equation of state parameter

$$w_{eff} \equiv -1 + \frac{2}{3}\varepsilon \tag{6.25}$$

such that $a(t) \propto t^{2/[3(1+w_{eff})]}$. It is determined by the value of the GB coupling parameter, α, and substituting Eqs. (6.19) and (6.24) into Eq. (6.25) implies that

$$w_{eff} = \frac{1}{24\alpha}\left[-40\alpha - 3 \pm \sqrt{9 + 192\alpha} \right], \tag{6.26}$$

where the $+/-$ corresponds to the points $\mathcal{V}^{\pm}$, respectively. This dependency of the effective equation of state on the GB parameter is illustrated in Fig. 6.1. The solution $\mathcal{V}^{+}$ corresponds to an inflationary cosmology when $\alpha > 0$ and the exponential, de Sitter solution arises when $\alpha = 3/8$. The solution $\mathcal{V}^{-}$ is in a super-inflationary regime ($w_{eff} < -1$) for $\alpha > 0$. When $\alpha < 0$, the effective equation of state corresponds to that of an ultra-stiff fluid ($w_{eff} \geq 1$). Our results are in line with the recent conclusions of Ref. [170], where a study of the late-time cosmology based on the model $f(\mathcal{G}) \propto -\mathcal{G}^n$ was made with the field equations derived directly from action (6.1).

The eigenvalues associated with the equilibrium points $\mathcal{V}^{\pm}$ are given by

$$\mu^{\pm} = -4 - \frac{3}{16\alpha} \pm \frac{1}{16\alpha}\sqrt{9 + 192\alpha}. \tag{6.27}$$

The solution $\mathcal{V}^{+}$ is stable for $\alpha > -9/192$. The solution $\mathcal{V}^{-}$ is a stable point when $\alpha > 0$ and unstable for $-9/192 < \alpha < 0$.

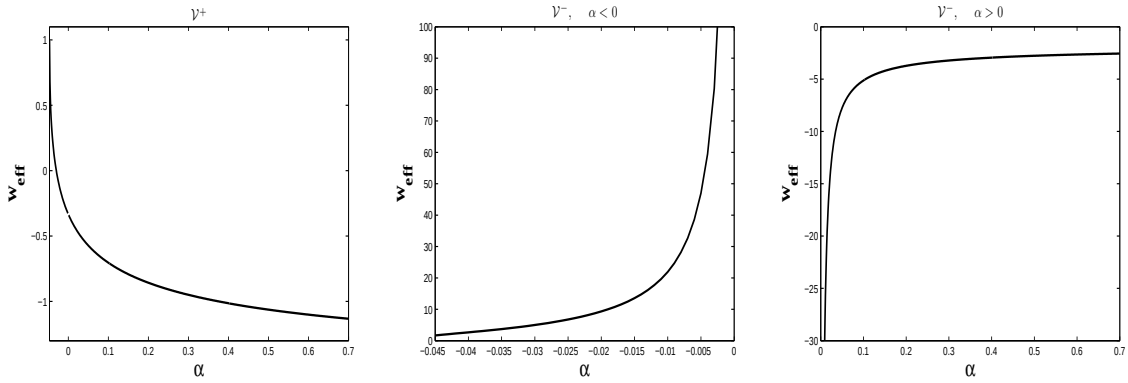

Figure 6.1: Illustrating the effective equation of state w_{eff} for the vacuum solutions $\mathcal{V}^+$ and $\mathcal{V}^-$. Requiring that the fixed points are real yields the condition $\alpha \geq -9/192$. The left-hand panel corresponds to $\mathcal{V}^+$, which shows that $\mathcal{V}^+$ is an accelerating solution for $\alpha > 0$ and corresponds to the de Sitter solution if $\alpha = 3/8$. The middle panel corresponds to $\mathcal{V}^-$ when $\alpha < 0$ and in this regime $w_{eff} \geq 1$. The right-hand panel corresponds to $\mathcal{V}^-$ when $\alpha > 0$ and in this regime $w_{eff} < -1$.

6.4 Non-vacuum solutions

In this Section, we study the background dynamics of models based on GB theories of the type (6.18) in the presence of a perfect fluid. The vacuum solutions $\mathcal{V}^{\pm}$ remain as equilibrium points of the autonomous system (6.20)-(6.21):

$$(y_1, y_2) = \left(-\frac{1}{2} \pm \frac{1}{6}\sqrt{9 + 192\alpha}, \quad \frac{3}{2} \mp \frac{1}{6}\sqrt{9 + 192\alpha} \right). \tag{6.28}$$

In addition, there exist two scaling solutions, where Ω_m and $\Omega_{\mathcal{G}}$ are constants:

$$(y_1, y_2) = \left(\pm\frac{2\sqrt{-3\alpha(1+3w_m)}}{3}, \quad \pm\frac{12\alpha(1+w_m)}{\sqrt{-3\alpha(1+3w_m)}} \right), \tag{6.29}$$

$$\Omega_m = 1 \mp \frac{2\sqrt{-3\alpha(1+3w_m)}}{3} \mp \frac{12\alpha(1+w_m)}{\sqrt{-3\alpha(1+3w_m)}}, \tag{6.30}$$

$$\Omega_{\mathcal{G}} = \pm\frac{2\sqrt{-3\alpha(1+3w_m)}}{3} \pm \frac{12\alpha(1+w_m)}{\sqrt{-3\alpha(1+3w_m)}} \tag{6.31}$$

and $w_{eff} = w_m$. We denote these solutions by $\mathcal{S}^{\pm}$.

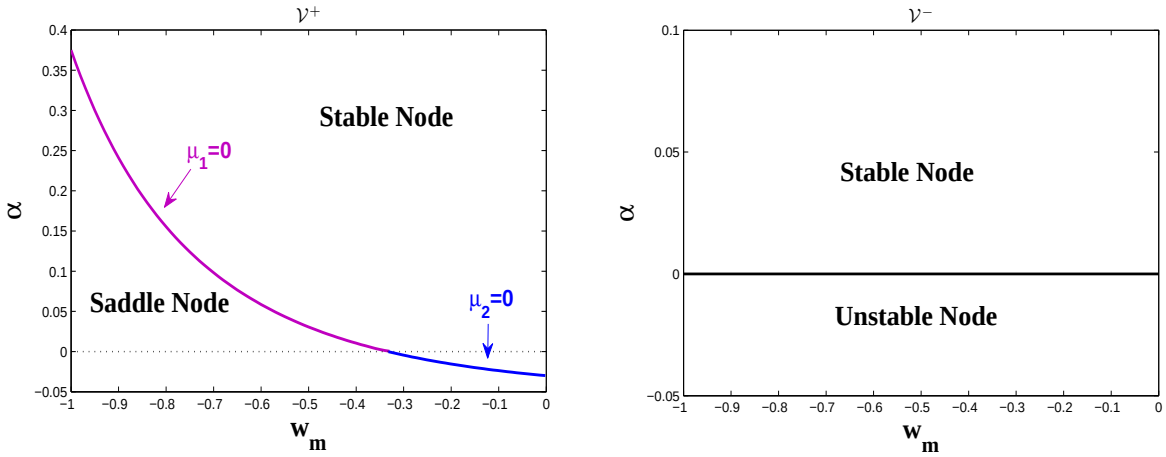

Figure 6.2: Illustrating the nature of the equilibrium points $\mathcal{V}^+$ (left-hand panel) and $\mathcal{V}^-$ (right-hand panel) in the parameter space spanned by (w_m, α). Both fixed points are real if $\alpha \geq -9/192$. On the boundary (denoted by the solid line) that distinguishes the stability of the fixed point $\mathcal{V}^+$, one of the eigenvalues $\mu^+_{1,2}$ vanishes. This is indicated in the figure by a change in colour. The dotted line in the left-hand panel represents the invariant sub-manifold $y_1 = 0$. In the case of the point $\mathcal{V}^-$, neither of the eigenvalues vanishes in any region of the (w_m, α) plane.

The eigenvalues associated with the equilibrium points $\mathcal{V}^\pm$ are given by

$$\mu_1^\pm = -\frac{1}{32\alpha}\left[48\alpha(3+w_m)+9\mp 3\sqrt{9+192\alpha}\right]+\lambda_1^\pm \tag{6.32}$$

$$\mu_2^\pm = -\frac{1}{32\alpha}\left[48\alpha(3+w_m)+9\mp 3\sqrt{9+192\alpha}\right]-\lambda_1^\pm \tag{6.33}$$

$$\lambda_1^\pm \equiv \frac{1}{32\alpha}\Bigg[256\alpha^2(1+3w_m)^2+288\alpha(1+w_m)+18 \mp 32\alpha(1+3w_m)\sqrt{9+192\alpha}\mp 6\sqrt{9+192\alpha}\Bigg]^{1/2}. \tag{6.34}$$

The stability of these vacuum solutions is altered when a matter source is introduced into the system and depends on both the GB parameter, α, and the perfect fluid equation of state, w_m. This dependency is illustrated in Fig. 6.2. The solid lines represent the regions where the nature of the equilibrium points changes as the parameter values are altered. The stability of $\mathcal{V}^-$ is determined by the sign of the GB parameter, α. On the boundary distinguishing the nature of the fixed point $\mathcal{V}^+$, one of the eigenvalues $\mu^+_{1,2}$ vanishes. To analyse the stability of the equilibrium point for these particular choices of parameter values would require a second-order analysis, which is beyond the scope of the present work.

The eigenvalues associated with the scaling equilibrium points $\mathcal{S}^{\pm}$ are given by

$$\mu_1^{\pm} = \frac{3}{4}(w_m - 1) + \tau_1^{\pm} \tag{6.35}$$

$$\mu_2^{\pm} = \frac{3}{4}(w_m - 1) - \tau_1^{\pm} \tag{6.36}$$

$$\tau_1^{\pm} \equiv \frac{1}{4\alpha}\Bigg[\pm 8\alpha(1+3w_m)\sqrt{-3\alpha(1+3w_m)} - \alpha^2(135w_m^2 + 306w_m + 71)\Bigg]^{1/2}. \tag{6.37}$$

The stability of these fixed points is illustrated in Fig. 6.3. The points are real in the region of parameter space, $\alpha(1+3w_m) \leq 0$. Furthermore, they are only physically meaningful if $\Omega_m = 1 - y_1 - y_2 \geq 0$. This results in a further restriction in the (w_m, α) plane after substitution of Eq. (6.30).

The top two panels of Fig. 6.3 correspond to the scaling solution $\mathcal{S}^+$ where $y_1 > 0$ and the bottom two panels correspond to $\mathcal{S}^-$ where $y_1 < 0$. The point $\mathcal{S}^+$ is either a stable node or a stable spiral. The point $\mathcal{S}^-$ is always a saddle. On the curve $\Omega_m = 0$, one of the eigenvalues of $\mathcal{S}^{\pm}$ vanishes.

To illustrate the scaling dynamics, let us consider the specific case where $(\alpha, w_m) = (0.05, -0.6)$. At this location in parameter space, there exist two equilibrium points[1]: the saddle point $\mathcal{V}^+$ and the stable node $\mathcal{S}^+$. The basin of attraction for $\mathcal{S}^+$ is shown in Fig. 6.4. As a second example, we consider the case $(\alpha, w_m) = (-0.005, -0.05)$, where there exist four equilibrium points: an unstable vacuum solution $\mathcal{V}^-$, a saddle point $\mathcal{S}^-$, a stable $\mathcal{V}^+$ and a stable spiral $\mathcal{S}^+$. The spiral nature of the point $\mathcal{S}^+$ is illustrated in the phase portrait of Fig. 6.5, where the initial conditions were specified to be $\Omega_m = \Omega_{\mathcal{G}} = 0.5$.

[1]Note that the point $\mathcal{V}^-$ also exists but this occurs in the region $y_1 < 0$. Stable scaling solutions arise only for $y_1 > 0$ and, since $y_1 = 0$ is a separatrix, a trajectory beginning in the region $y_1 < 0$ will not be able to reach $\mathcal{S}^+$. We therefore choose the initial conditions in Fig. 6.4 such that $y_1 > 0$. This is equivalent to choosing the negative sign in Eq. (6.15).

6.5 Summary

In this Chapter we have investigated the existence and stability of cosmological power-law scaling solutions sourced by a barotropic fluid when an appropriate function of the Gauss-Bonnet topological invariant is introduced into the Einstein-Hilbert action. It was found that the general class of such theories that admit power-law solutions is given by Eq. (6.18), i.e., $f(\mathcal{G}) = \pm 2\sqrt{\alpha \mathcal{G}}$ for some constant coefficient, α. By exploiting an equivalence between generalised Gauss-Bonnet gravitational theories and a corresponding higher-order, scalar-tensor theory, it was further shown that the Friedmann equations for this class of model can be written in the form of a two-dimensional dynamical system. The stability of the equilibrium points for both vacuum and non-vacuum models was established. In the former case, the GB parameter, α, determines the effective equation of state parameter. For non-vacuum solutions, the nature of the critical points depends on both α and the fluid equation of state parameter, w_m. The regions of parameter space (α, w_m) that admit stable non-vacuum scaling solutions were identified.

The models we have investigated do not admit a transition from a decelerating to an accelerating phase of cosmic expansion. However, our aim in this chapter has been to focus on power-law solutions rather than develop a phenomenological model of generalised Gauss-Bonnet gravity as a candidate for dark energy. Power-law solutions are of interest since they can be regarded as approximations to more realistic models. In particular, phenomenological models could be constructed where the parameter α is given by some function of $\mathcal{G}$ (or equivalently the scalar field ϕ), such that α is slowly varying for much of the history of the universe, but at some epoch undergoes a change in sign. In principle, this could cause the universe to enter a phase of accelerated expansion. It would be interesting to develop specific models of this type, along the lines outlined in Ref. [171].

For a number of explicit $f(\mathcal{G})$ models, it has recently been shown that a transition from decelerated to accelerated expansion is possible [171]. The viability of such an evolution is subject to the condition $\mathrm{d}^2 f/\mathrm{d}\mathcal{G}^2 > 0$, which ensures the stability of a late-time de-Sitter solution as well as the existence of standard radiation and matter dominated epochs. Through a phase space analysis, the conditions required for the existence of viable cosmological dynamics are generalised in Ref. [149]. In analogy with $f(R)$ gravity [43], the authors of Ref. [149] study the $m(r)$ curves [where $m \equiv \mathcal{G} f_{,\mathcal{G}\mathcal{G}}/f_{,\mathcal{G}}$ and $r = -\mathcal{G} f_{,\mathcal{G}}/f$] of $f(\mathcal{G})$ models and find that in order for a standard matter era to exist the conditions

$$m(-\frac{1}{2}) = -\frac{1}{2} \quad \text{and} \quad m'(-\frac{1}{2}) > -1,$$

need to be satisfied. The second condition ensures that the matter dominated epoch is a transient phase. It was found that models of the type $f(\mathcal{G}) = \alpha(\mathcal{G}^p - \beta)^q$, where α, β, p

and q are positive constants, can produce cosmologically viable trajectories with a de-Sitter epoch as the final attractor. In fact, the model $f(\mathcal{G}) = \alpha(\mathcal{G}^{\frac{3}{4}} - \beta)^{\frac{2}{3}}$ was studied explicitly [149]. We note that in the regime where $|\mathcal{G}|$ is much larger than the order of the present value $\mathcal{G}_0$, this model reduces to the model $f(\mathcal{G}) \propto \mathcal{G}^{\frac{1}{2}}$, considered here.

Given that models which admit viable background cosmological dynamics do indeed exist, the next step would be to place observational bounds on these models using LGC and matter density perturbations. Interestingly, as in the case of $f(R)$ gravity and scalar-tensor gravity, the oscillating mode and the deviation of w_{DE} is found to occur in viable $f(\mathcal{G})$ models (see Ref. [171] and Ref. [149], respectively). It would also be interesting to investigate whether or not these features are generic to viable MG theories.

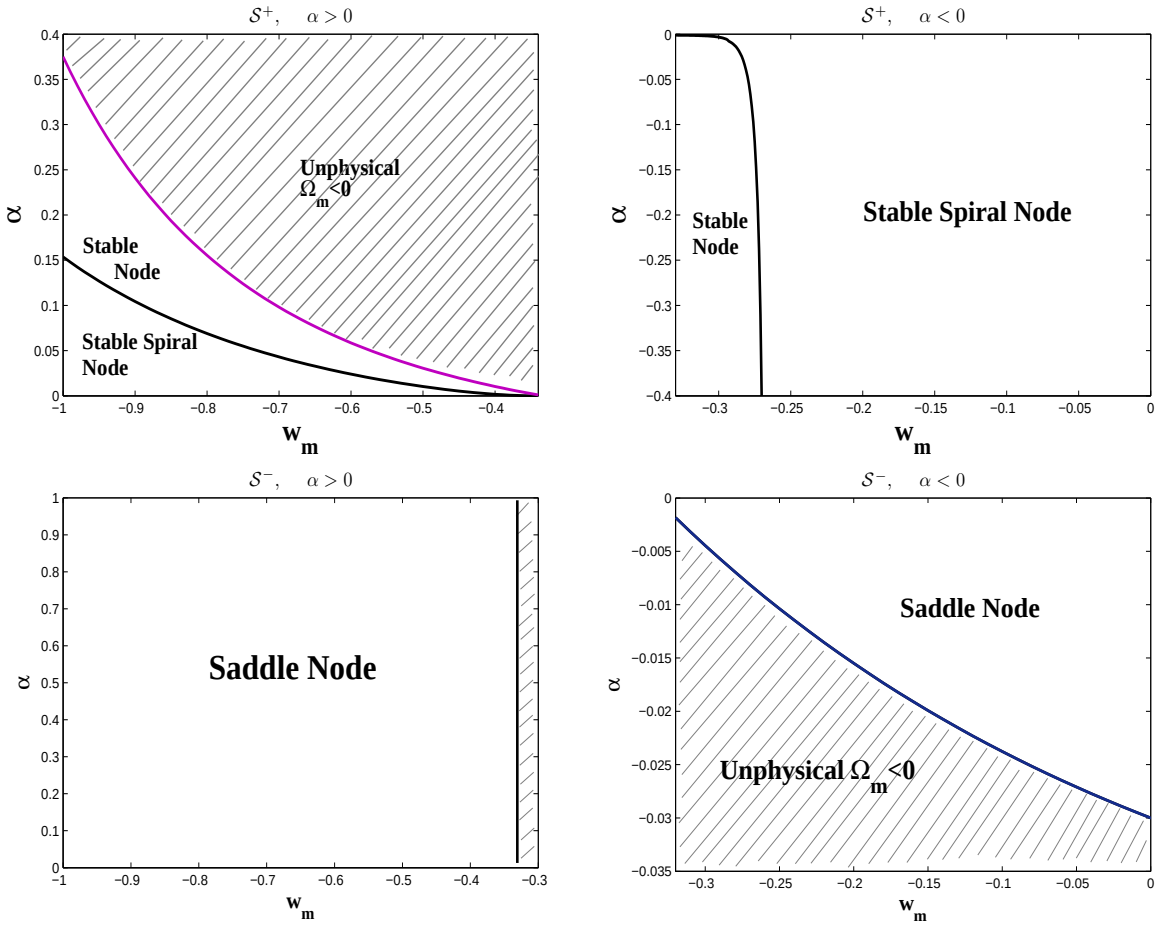

Figure 6.3: Illustrating the stability of the scaling equilibrium points $\mathcal{S}^{\pm}$ in the parameter space spanned by (w_m, α). The region of parameter space is restricted by the requirement that the equilibrium points are real, $\alpha(1+3w_m) \leq 0$, and also correspond to physically realistic solutions where $\Omega_m \geq 0$. The shaded areas depict the regions of parameter space where the solutions are unphysical. These restrictions imply that the analysis can be separated into regions where $\alpha > 0$ (left-hand panels) and $\alpha < 0$ (right-hand panels). The regions of parameter space where the fixed points correspond to either a saddle point or a stable/spiral node are identified. On the line $\Omega_m = 0$, the eigenvalue $\mu_1^+ = 0$ (for the scaling point $\mathcal{S}^+$) when $\alpha > 0$. Conversely, $\mu_2^- = 0$ (for the scaling point $\mathcal{S}^-$) when $\Omega_m = 0$ and $\alpha < 0$.

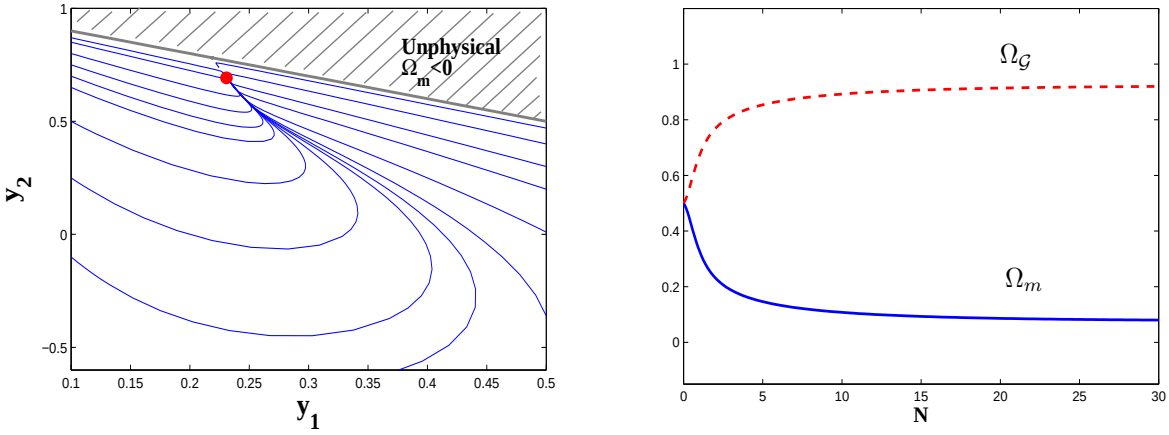

Figure 6.4: Illustrating the dynamics of the model (6.18) for the particular case where $(\alpha, w_m) = (0.05, -0.6)$. The left-hand panel depicts the phase space, where the straight line $y_1 = 1 - y_2$ corresponds to the vacuum solution $\Omega_m = 0$. The red dot represents the scaling fixed point $\mathcal{S}^+$. For the range of initial conditions chosen, all non-vacuum, physically acceptable solutions are attracted to $\mathcal{S}^+$. The right-hand panel depicts the evolution of the fractional energy densities of the perfect fluid, Ω_m, and the GB contribution, $\Omega_{\mathcal{G}}$, for the initial conditions $\Omega_m = \Omega_{\mathcal{G}} = 0.5$. It is seen that the fractional densities asymptote to constant values at late times, thus indicating that the solution is scaling.

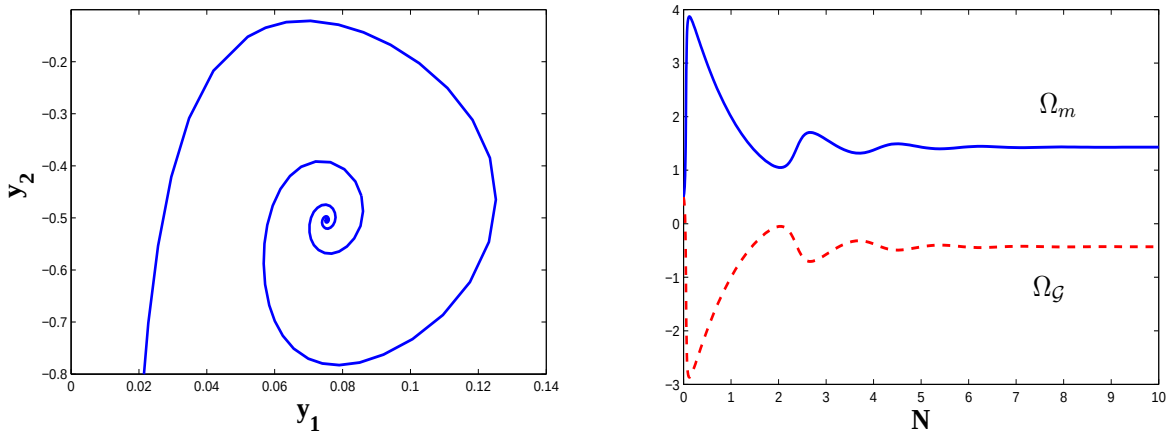

Figure 6.5: Illustrating the dynamics of the model (6.18) for the particular case where $(\alpha, w_m) = (-0.005, -0.05)$. The left-hand panel depicts the phase space for this scenario, whereas the right-hand panel depicts the evolution of the fractional energy densities Ω_m and $\Omega_{\mathcal{G}}$. The initial conditions were chosen such that $\Omega_m = \Omega_{\mathcal{G}} = 0.5$. At late times, the fractional energy densities of the fluid and GB contribution tend to constant values.

Chapter 7

Summary

The main focus of this thesis has been to investigate the cosmological viability of a number of classes of modified gravity theories which include: $f(R)$ gravity in both the metric and Palatini formalisms, scalar-tensor gravity and generalised Gauss-Bonnet gravity. In order to study the viability of concrete models we considered four sets of observational constraints provided respectively by the requirement of stability, consistent background cosmological dynamics, local gravity experiments and evolution of density perturbations. We found that these constraints impose stringent restrictions on the viable range of models.

In the case of $f(R)$ gravity in the metric formalism, the conditions (4.14)-(4.15) required for viable background dynamics, together with the stability conditions (4.43), greatly reduce the range of allowed models. For the special classes of models that satisfy these conditions [for instance those given by Eq. (4.37)], the most stringent constraints are imposed by solar system tests. The compatibility of models with such tests requires the formation of a thin-shell, which is developed under the condition $m \equiv Rf_{,RR}/f_{,R} \ll 1$ (in an environment where local gravity tests are carried out). Cosmologically this condition [i.e., (4.39)] implies that viable models need to be very close to the ΛCDM model during the radiation and matter dominated epochs. The study of density perturbations, on the other hand, provides bounds on the present value of the deviation parameter, m, which is constrained to be $m(z=0) \lesssim 0.1$. Hence, although m is constrained to be very small during the matter era, a notable deviation from the ΛCDM model can occur around the present epoch.

Unlike the metric formalism, the stability conditions (4.43) do not apply to $f(R)$ theories in the Palatini approach. In addition, compared with the metric formalism, the background dynamics and LGC only provide weak bounds on the parameter m. The density perturbations, however, provide stringent constraints: $|m| \lesssim 10^{-5}$-10^{-4}. Consequently, $f(R)$ models in the Palatini formalism that are consistent with observations are practically indistinguishable from the ΛCDM cosmology even at the present epoch. This follows due to the peculiar evolution of the matter perturbations in the regime $|\xi| > 1$.

Comparing these results with those obtained using the LuSS approach for studying den-

sity perturbations (outlined in Chapter 3), we find that the unconventional evolution of δ_m (i.e., a rapid growth when $m > 0$) does not occur. This discrepancy, therefore, suggests that one should be cautious in employing the LuSS approach when studying density perturbations in the Palatini formalism, especially in regimes where $|\xi| > 1$. As k/a decreases, however, the discrepancy between the LuSS and linearisation (KKS) approaches becomes less pronounced. We find that in the long-wavelength limit ($k^2/a^2 \ll H^2$), the LuSS and KKS approaches are compatible for the $f(R)$ models summarised in equations (3.23) and (3.24). A particular case of this class of models arises when $f(R)$ is a power law of the Ricci scalar. When the deviation from ΛCDM cosmology is small (i.e., m is small), we find that the LuSS and KKS approaches are always compatible.

We also considered a class of scalar-tensor theories (5.9) which admit a strong coupling of the scalar field to the non-relativistic matter in the Einstein frame. Inspired by $f(R)$ gravity we considered the class of models given by the potential (5.47), which satisfy the stability requirement $\mathrm{d}\lambda/\mathrm{d}\varphi < 0$ as well as producing viable background dynamics. The strong coupling of the scalar-tensor theories (5.9) violates all LGC. The existence of a matter dependent mass and a thin-shell effect, however, allows for such theories to be compatible with local gravity experiments. Using solar-system and equivalence principle constraints, we obtained the bounds (5.59) and (5.63), respectively. These constraints, along with the bounds derived from the conditions $\Delta n < 0.05$ and $s < 2$ for matter density perturbations, are illustrated in Figure 5.5. Although the observations seem to prefer smaller values of $|Q|$, it is found that models with p close to unity satisfy all the experimental constraints considered. The allowed parameter space illustrated in Fig. 5.5 may be further restricted by considering future observational data.

Finally, we considered modified Gauss-Bonnet, $f(\mathcal{G})$, gravity. We established the conditions required for the existence and stability of cosmological power-law scaling solutions. The general form of the action that leads to such solutions was found to be $f(\mathcal{G}) = \pm 2\sqrt{\alpha \mathcal{G}}$. By employing the equivalence between $f(\mathcal{G})$ gravity and a corresponding scalar-tensor theory (2.76), the cosmological equations were written as a dynamical system and the stability of the equilibrium points for both vacuum and non-vacuum solutions was determined. In the case of the vacuum solutions, the stability was found to depend on the parameter α, while in the non-vacuum case the stability was found to depend on both α and the fluid equation of state.

In conclusion, the analyses carried out in this thesis suggest that confronting modified gravity theories with observational constraints restricts the viable range of models to be very close to (and in some cases indistinguishable from) the ΛCDM model.

Appendix A

Appendix

A.1 The $f(R)$ field equations for scalar perturbations in the Palatini formalism

This appendix summarises the derivations of the perturbed field equations presented in section 2.4.3 are provided[1] [69; 79]. We begin with the Einstein equation

$$G^a_{\ b} \equiv R^a_{\ b} - \frac{1}{2}\delta^a_{\ b}R = \tag{B.1}$$
$$\frac{1}{F}T^a_{\ b} + \frac{f - F\hat{R}}{2F}\delta^a_{\ b} + \frac{1}{F}(F_{;b}^{\ \ a} - \Box F\delta^a_{\ b}) - \frac{3}{4F^2}(2F^{;a}F_{;b} - 2F^{;c}F_{;c}\delta^a_{\ b}),$$

which we derive using Eqs. (2.19), (2.36) and (2.37). Looking back at sections 2.1.1 and 2.1.2, we notice that the problem of evaluating the perturbed Einstein tensor, $G^a_{\ b}$, reduces to computing the perturbations to the Christoffel symbols. At this point it is convenient to work in conformal time τ, in which case the perturbed metric (2.118) can be re-written as

$$ds^2 = a^2(\tau)\{-(1+2\alpha)d\tau^2 - 2b_{,i}d\tau dx^i + [(1+2\varphi)\delta_{ij} + 2E_{|ij}]dx^i dx^j\}. \tag{B.2}$$

For the metric (B.2), the components of the connection $\Gamma^a_{bc} = \bar{\Gamma}^a_{bc} + \delta\Gamma^a_{bc}$ are:

$$\begin{aligned}
\Gamma^0_{00} &= \mathcal{H} + \alpha_{,\tau}\,, \\
\Gamma^0_{0i} &= (\alpha - \mathcal{H}b)_{,i}\,, \\
\Gamma^i_{00} &= (\alpha - \mathcal{H}b - b_{,\tau})^{,i}\,, \\
\Gamma^i_{0j} &= (\mathcal{H} + \varphi_{,\tau})\delta^i_{\ j} - E_{,\tau|}^{\ \ \ i}{}_{j}\,, \\
\Gamma^0_{ij} &= (\mathcal{H}(1 - 2\alpha + 2\varphi) + \varphi_{,\tau})\delta^i_{\ j} + (b + 2\mathcal{H}E + E_{,\tau})_{|ij}\,, \\
\Gamma^i_{jk} &= \delta_{jk}(\mathcal{H}b - \varphi)^{;i} + \delta^i_{\ k}\varphi_{,j} + \delta^i_{\ j}\varphi_{,k} + (E_{|j}^{\ \ \ i}{}_{k} + E_{|k}^{\ \ \ i}{}_{j} - E_{|jk}^{\ \ \ i})\,,
\end{aligned} \tag{B.3}$$

[1] This summary is partially based on private communications with Nikolay A. Koshelev.

where $\mathcal{H} \equiv aH = \dot{a}$ and the indicies i, j, k run over the spatial coordinates.

We recall that the covariant derivatives of a scalar field $\psi(t, x^i)$ is just the partial derivative: $\psi_{,a}$. This means, for example, that $\psi_{;ab} = \psi_{,ab} - \Gamma^c_{ab}\psi_{,c}$. Hence, to linear order in perturbations, the covariant derivatives of a scalar field $\psi(t, x^i) = \bar{\psi}(t) + \delta\psi(t, x^i)$ are [96]:

$$
\begin{aligned}
\nabla^0\nabla_0\psi &= \frac{1}{a^2}\left[-\bar{\psi}_{,\tau\tau} - \delta\psi_{,\tau\tau} + \mathcal{H}\bar{\psi}_{,\tau} + \mathcal{H}\delta\psi_{,\tau} + \alpha_{,\tau}\bar{\psi}_{,\tau} + 2\alpha(\bar{\psi}_{,\tau\tau} - \mathcal{H}\bar{\psi}_{,\tau})\right] , \\
\nabla^i\nabla_0\psi &= \frac{1}{a^2}\left[\delta\psi_{,\tau} - \mathcal{H}\delta\psi - b\bar{\psi}_{,\tau\tau} - (\alpha - 2\mathcal{H}b)\bar{\psi}_{,\tau}\right]^{,i} , \\
\nabla^i\nabla_j\psi &= \frac{1}{a^2}\left[-(\bar{\psi} + \delta\psi_{,\tau})\mathcal{H}\delta^i{}_j + \delta\psi_{|}{}^i{}_j + [(2\mathcal{H}\alpha - \varphi_{,\tau})\delta^i{}_j - (b + E_{,\tau})_{|}{}^i{}_j]\bar{\psi}_{,\tau}\right] , \\
\nabla^k\nabla_k\psi &= \frac{1}{a^2}\left[-3\mathcal{H}(\bar{\psi} + \delta\psi_{,\tau}) + \delta\psi_{|}{}^k{}_k + [3(2\mathcal{H}\alpha - \varphi_{,\tau}) - (b + E_{,\tau})_{|}{}^k{}_k]\bar{\psi}_{,\tau}\right] , \\
\nabla^a\nabla_a\psi &= \frac{1}{a^2}\Bigg[-\bar{\psi}_{,\tau\tau} - \delta\psi_{,\tau\tau} - 2\mathcal{H}(\bar{\psi}_{,\tau} + \delta\psi_{,\tau}) + \delta\psi_{|}{}^k{}_k + \alpha(2\bar{\psi}_{,\tau\tau} + \mathcal{H}\bar{\psi}_{,\tau}) \\
&\quad + \alpha_{,\tau} + 3(\mathcal{H}\alpha - \varphi_{,\tau}) - (b + E_{,\tau})_{|}{}^k{}_k\Bigg]\bar{\psi}_{,\tau} .
\end{aligned}
$$

Bearing in mind the two spatially gauge-invariant combinations (2.125)-(2.124),

$$
\begin{aligned}
\chi &= a(b + E_{,\tau}) , && \text{(B.4)} \\
\kappa &= \frac{3}{a}(\mathcal{H}\alpha - \varphi_{,\tau}) + \frac{k^2}{a^2}\chi , && \text{(B.5)}
\end{aligned}
$$

and their derivatives

$$
\begin{aligned}
\chi_{,\tau} &= a\mathcal{H}(b + E_{,\tau}) , && \text{(B.6)} \\
\kappa_{,\tau} &\equiv \frac{3}{a}(\mathcal{H}\alpha_{,\tau} + \mathcal{H}_{,\tau}\alpha - \varphi_{,\tau\tau}) - \frac{3\mathcal{H}}{a}(\mathcal{H}\alpha - \varphi_{,\tau}) - \frac{k^2\mathcal{H}}{a}(b + E_{,\tau}) && \text{(B.7)} \\
&\quad + \frac{k^2}{a}(b_{,\tau} + E_{,\tau\tau}) ,
\end{aligned}
$$

the components of the Ricci tensor are:

$$
\begin{aligned}
R^0{}_0(g) &= \frac{1}{a^2}\left[3\mathcal{H}_{,\tau} + 3\left(\mathcal{H}^2 - \mathcal{H}_{,\tau} + \frac{k^2}{3}\right)\alpha - a\kappa_{,\tau} - 2a\mathcal{H}\kappa\right] , && \text{(B.8)} \\
R^i{}_j(g) &= \frac{1}{a^2}\Bigg[\varphi_{,\tau\tau} - \mathcal{H}(\alpha_{,\tau} - 5\varphi_{,\tau}) - 2(\mathcal{H}_{,\tau} + 2\mathcal{H}^2)\alpha - k^2\left(\frac{\mathcal{H}}{a}\chi - \varphi\right) \\
&\quad + (\mathcal{H}_{,\tau} + 2\mathcal{H}^2)\Bigg]\delta^i{}_j + \frac{1}{a^2}\left[-\alpha - \varphi + 2\frac{\mathcal{H}}{a}\chi + (b_{,\tau} + E_{,\tau\tau})\right]_{|}{}^i{}_j , \\
R^i{}_0(g) &= \frac{2}{a^2}[\mathcal{H}\alpha - \varphi_{,\tau} + (\mathcal{H}_{,\tau} - \mathcal{H}^2)b]^{,i} , \\
R^0{}_i(g) &= \frac{2}{a^2}[-\mathcal{H}\alpha + \varphi_{,\tau}]_{,i} ,
\end{aligned}
$$

$$R(g) = -\frac{2}{a^2}\left[a\kappa_{,\tau} + 4a\mathcal{H}\kappa + 3(\mathcal{H}-\mathcal{H}^2)\alpha - 2k^2\varphi - k^2\alpha - 3(\mathcal{H}_{,\tau}+\mathcal{H}^2)\right] .$$

We are now ready to compute the components of the field equations (B.1). The energy constraint (G^0_0 component of the field equation) is [69; 79]

$$\begin{aligned} - \quad & 2k^2\varphi + \left(2\mathcal{H} + \frac{F_{,\tau}}{F}\right)a\kappa + \frac{1}{F}\left(\frac{3}{2}\frac{(F_{,\tau})^2}{F} + 3\mathcal{H}F_{,\tau}\right)\alpha = \frac{1}{F}\Bigg[\\ & -a^2\delta\rho_m + \left(3\mathcal{H}^2 - \frac{3}{4}\left(\frac{F_{,\tau}}{F}\right)^2 - \frac{a^2}{2}R + k^2\right)\delta F + \left(\frac{3}{2}\frac{F_{,\tau}}{F} + 3\mathcal{H}\right)\delta F_{,\tau}\Bigg] , \end{aligned} \tag{B.9}$$

and the momentum constraint (G^0_i component of the field equation) is

$$\mathcal{H}\alpha - \varphi_{,\tau} = \frac{1}{2F}\left[av\rho_m - F_{,\tau}\alpha - \left(\mathcal{H} + \frac{3}{2}\frac{F_{,\tau}}{F}\right)\delta F + \delta F_{,\tau}\right] . \tag{B.10}$$

The shear propagation equation ($G^i_j - \frac{1}{3}\delta^i_j G^0_0$ component) is

$$\frac{\chi_{,\tau}}{a} + \left(\mathcal{H} + \frac{F_{,\tau}}{F}\right)\frac{\chi}{a} - \alpha - \varphi = \frac{\delta F}{F} , \tag{B.11}$$

and the Raychaudhuri equation ($G^i_i - G^0_0$ component) is

$$\begin{aligned} & 2a\kappa_{,\tau} + \left(4\mathcal{H} + \frac{F_{,\tau}}{F}\right)a\kappa + 3\frac{F_{,\tau}}{F}\alpha_{,\tau} + \\ & \left[6(\mathcal{H}_{,\tau} - \mathcal{H}^2) + 6\left(\frac{F_{,\tau\tau}}{F} - \left(\frac{F_{,\tau}}{F}\right)^2\right) - 3\mathcal{H}\frac{F_{,\tau}}{F} - 2k^2\right]\alpha \\ & = \frac{1}{F}\left[a^2\delta\rho_m + \left(6\mathcal{H}_{,\tau} + 3\left(\frac{F_{,\tau}}{F}\right)^2 - a^2R + k^2\right)\delta F - 6\frac{F_{,\tau}}{F}\delta F_{,\tau} + 3\delta F_{,\tau\tau}\right] . \end{aligned} \tag{B.12}$$

A.2 The thin-shell boundary conditions

This appendix summarises the boundary conditions that are required for the formation of a thin-shell.

If the field value at the centre, $\varphi(\tilde{\ell}=0)$, is close enough to the equilibrium value φ_A with $|\varphi(\tilde{\ell}=0)-\varphi_A| \ll |\varphi_A|$, the thin-shell solution is realised [47]. Because φ_A is a local extremum of $U_{\rm eff}$, the driving term $\mathrm{d}U_{\rm eff}/\mathrm{d}\varphi$ is initially negligible. In this case the field does not move away from $\varphi(\tilde{\ell}=0)$ practically up to a radius $\tilde{\ell}_1$ which satisfies

$$\frac{\Delta\tilde{\ell}_\star}{\tilde{\ell}_\star} \equiv \frac{\tilde{\ell}_\star-\tilde{\ell}_1}{\tilde{\ell}_\star} \ll 1\,. \tag{C.1}$$

At $\tilde{\ell}=\tilde{\ell}_1$, the field starts to roll down the potential and we find $|U_{,\varphi}(\varphi)| \ll |Qe^{Q\varphi}\rho_A^*|$ for $\tilde{\ell}_1<\tilde{\ell}<\tilde{\ell}_\star$. Under the condition $|Q\varphi_A| \ll 1$, the right hand side of Eq. (4.24) is approximately given by $\mathrm{d}U_{\rm eff}/\mathrm{d}\varphi \simeq Q\rho_A^*$. Substituting this in Eq. (4.24) and using the boundary conditions $\varphi=\varphi_A$ and $\mathrm{d}\varphi/\mathrm{d}\tilde{\ell}=0$ at $\tilde{\ell}=\tilde{\ell}_1$, the solution in the region $\tilde{\ell}_1<\tilde{\ell}<\tilde{\ell}_\star$ is given by

$$\varphi = \frac{Q\rho_A}{3}\left(\frac{\tilde{\ell}^2}{2}+\frac{\tilde{\ell}_1^3}{\tilde{\ell}}\right) - \frac{Q\rho_A\tilde{\ell}_1^2}{2} + \varphi_A. \tag{C.2}$$

Outside the body ($\tilde{\ell}>\tilde{\ell}_\star$) the gradient energies on the left hand side of Eq. (4.24) become important because the energy density drops down from ρ_A^* to ρ_B^*. Taking into account the mass term m_B of the effective potential $U_{\rm eff}$, one has $\mathrm{d}U_{\rm eff}/\mathrm{d}\varphi = m_B^2(\varphi-\varphi_B)$ on the right hand side of Eq. (4.24). Using the boundary condition $\varphi=\varphi_B$ as $\tilde{\ell}\to\infty$, the solution in the region $\tilde{\ell}>\tilde{\ell}_\star$ is given by [47; 124]

$$\varphi = \frac{Ce^{-m_B(\tilde{\ell}-\tilde{\ell}_\star)}}{\tilde{\ell}} + \varphi_B. \tag{C.3}$$

Matching the solutions (C.2) and (C.3) at $\tilde{\ell}=\tilde{\ell}_\star$, we find

$$C = -\frac{QM_\star}{4}\left[1-\left(\frac{\tilde{\ell}_1}{\tilde{\ell}_\star}\right)^3\right] \tag{C.4}$$

and

$$\left(\frac{\tilde{\ell}_1}{\tilde{\ell}_\star}\right)^2 \simeq 1-\frac{\varphi_B-\varphi_A}{3Q\Phi_\star}\,, \tag{C.5}$$

where

$$\Phi_\star \equiv \frac{M_\star}{8\pi\tilde{\ell}_\star} = \frac{G_N M_\star}{\tilde{\ell}_\star}\,. \tag{C.6}$$

In deriving Eqs. (C.4) and (C.5), we assumed the condition $m_B\tilde{\ell}_\star \ll 1$. The solution (C.3) now becomes

$$\varphi(\tilde{\ell}) \simeq -\frac{QM_\star}{4\pi}\left[1-\left(\frac{\tilde{\ell}_1}{\tilde{\ell}_\star}\right)^3\right]\frac{e^{-m_B(\tilde{\ell}-\tilde{\ell}_\star)}}{\tilde{\ell}} + \varphi_B\,. \tag{C.7}$$

Since we are in the thin-shell regime, the following relation is obtained from Eq. (C.5):

$$\frac{\Delta\tilde{\ell}_\star}{\tilde{\ell}_\star} \simeq \frac{\varphi_B-\varphi_A}{6Q\Phi_\star}\,. \tag{C.8}$$

The solution outside the body ($\tilde{\ell} > \tilde{\ell}_\star$) is then given by Eq. (4.28) with Eq. (4.29).

If the field value at $\tilde{\ell} = 0$ is not close to φ_A (i.e., $|\varphi(\tilde{\ell}=0)-\varphi_A| \gtrsim |\varphi_A|$), the field rapidly rolls down the potential at $\tilde{\ell}_1 \simeq 0$. Setting $\tilde{\ell}_1 = 0$ in Eq. (C.7), we obtain the solution (4.28) with $Q_{\rm eff}$ replaced by Q. This is the thick-shell regime in which the effective coupling is not small so as to satisfy the LGC.

A.3 Equations convenient for numerical simulations in the Palatini formalism

In this appendix we present the equations that are convenient for numerical simulations. From Eqs. (2.105), (2.107) and (2.108) we obtain

$$H^2 = \frac{2\rho_m + FR - f}{6F\zeta}\,, \quad \text{where} \quad \zeta = \left[1 - \frac{3}{2}\frac{F_{,R}(FR-2f)}{F(F_{,R}R-F)}\right]^2 . \tag{D.1}$$

Introducing a dimensionless quantity

$$y = \frac{FR - f}{6F\zeta H^2}\,, \tag{D.2}$$

we obtain the differential equation for y [10]:

$$y' = y(1-y)\left[3 + C(R)\right]\,, \tag{D.3}$$

where $C(R)$ is defined in Eq. (4.44).

The following relations also hold

$$\frac{FR - f}{FR - 2f} = -\frac{2y}{1-y}\,, \tag{D.4}$$

$$\Omega_m \equiv \frac{\rho_m}{3F\zeta H^2} = 1 - y\,. \tag{D.5}$$

Specifying the value of y, the initial Ricci scalar R is determined by Eq. (D.4). Solving Eq. (D.3), we obtain y, R, H and Ω_m from Eqs. (D.4), (D.2) and (D.5). The effective equation of state of dark energy is given by

$$w_{\rm eff} = -y + \frac{\dot{F}}{3HF} + \frac{\dot{\zeta}}{3H\zeta} - \frac{\dot{F}R}{18F\zeta H^3}\,. \tag{D.6}$$

As long as the deviation from the ΛCDM model is small ($|m| \ll 1$), we have $w_{\rm eff} \simeq -y_1$.

The perturbation equations (4.117) and (4.118) are given by

$$\delta_m'' + \frac{1}{2}(1 - 3w_{\rm eff})\delta_m' - \frac{3}{2}\zeta(1-y)\left(1 + \frac{\xi}{1-m}\right)\delta_m \simeq 0\,, \tag{D.7}$$

$$\Phi_{\rm eff} \simeq -\frac{3}{2}\left(\frac{aH}{k}\right)^2 \zeta(1-y)\delta_m\,. \tag{D.8}$$

Although we solve exact perturbation equations, the above approximate perturbation equations are found to be very accurate.

References

[1] E. KOMATSU et al. *Five-Year Wilkinson Microwave Anisotropy Probe (WMAP) Observations: Cosmological Interpretation*. Astrophys. J. Suppl. **180**:330 (2009). 0803.0547 [astro-ph].

[2] S. PERLMUTTER et al. *Measurements of Omega and Lambda from 42 High-Redshift Supernovae*. Astrophys. J. **517**:565 (1999). astro-ph/9812133.

[3] A. G. RIESS et al. *Observational Evidence from Supernovae for an Accelerating Universe and a Cosmological Constant*. Astron. J. **116**:1009 (1998). astro-ph/9805201.

[4] A. G. RIESS et al. *Type Ia Supernova Discoveries at $z > 1$ From the Hubble Space Telescope: Evidence for Past Deceleration and Constraints on Dark Energy Evolution*. Astrophys. J. **607**:665 (2004). astro-ph/0402512.

[5] P. ASTIER et al. *The Supernova Legacy Survey: Measurement of Ω_M, Ω_Λ and w from the First Year Data Set*. Astron. Astrophys. **447**:31 (2006). astro-ph/0510447.

[6] D. CLOWE et al. *A direct empirical proof of the existence of dark matter*. Astrophys. J. **648**:L109 (2006). astro-ph/0608407.

[7] U. SELJAK et al. *Cosmological parameter analysis including SDSS Ly-alpha forest and galaxy bias: Constraints on the primordial spectrum of fluctuations, neutrino mass, and dark energy*. Phys. Rev. **D71**:103515 (2005). astro-ph/0407372.

[8] D. J. EISENSTEIN et al. *Detection of the Baryon Acoustic Peak in the Large-Scale Correlation Function of SDSS Luminous Red Galaxies*. Astrophys. J. **633**:560 (2005). astro-ph/0501171.

[9] E. J. COPELAND, M. SAMI and S. TSUJIKAWA. *Dynamics of dark energy*. Int. J. Mod. Phys. **D15**:1753 (2006). hep-th/0603057.

[10] S. FAY, R. TAVAKOL and S. TSUJIKAWA. *f(R) gravity theories in Palatini formalism: cosmological dynamics and observational constraints*. Phys. Rev. **D75**:063509 (2007). astro-ph/0701479.

[11] S. M. CARROLL. *The cosmological constant*. Living Rev. Rel. **4**:1 (2001). astro-ph/0004075.

[12] V. F. MUKHANOV, L. R. W. ABRAMO and R. H. BRANDENBERGER. *On the back reaction problem for gravitational perturbations*. Phys. Rev. Lett. **78**:1624 (1997). gr-qc/9609026.

[13] R. MANSOURI. *Structured FRW universe leads to acceleration: A non- perturbative approach.* astro-ph/0512605.

[14] E. W. KOLB, S. MATARRESE and A. RIOTTO. *On cosmic acceleration without dark energy*. New J. Phys. **8**:322 (2006). astro-ph/0506534.

[15] A. ISHIBASHI and R. M. WALD. *Can the acceleration of our universe be explained by the effects of inhomogeneities?* Class. Quant. Grav. **23**:235 (2006). gr-qc/0509108.

[16] A. PARANJAPE and T. P. SINGH. *Cosmic Inhomogeneities and the Average Cosmological Dynamics*. Phys. Rev. Lett. **101**:181101 (2008). 0806.3497 [astro-ph].

[17] V. MARRA, E. W. KOLB and S. MATARRESE. *Light-cone averages in a swiss-cheese universe*. Phys. Rev. **D77**:023003 (2008). 0710.5505 [astro-ph].

[18] V. MARRA, E. W. KOLB, S. MATARRESE and A. RIOTTO. *On cosmological observables in a swiss-cheese universe*. Phys. Rev. **D76**:123004 (2007). 0708.3622 [astro-ph].

[19] R. A. VANDERVELD, E. E. FLANAGAN and I. WASSERMAN. *Luminosity distance in 'Swiss cheese' cosmology with randomized voids: I. Single void size*. Phys. Rev. **D78**:083511 (2008). 0808.1080 [astro-ph].

[20] B. RATRA and P. J. E. PEEBLES. *Cosmological Consequences of a Rolling Homogeneous Scalar Field*. Phys. Rev. **D37**:3406 (1988).

[21] I. P. C. HEARD and D. WANDS. *Cosmology with positive and negative exponential potentials*. Class. Quant. Grav. **19**:5435 (2002). gr-qc/0206085.

[22] E. J. COPELAND, A. R. LIDDLE and D. WANDS. *Exponential potentials and cosmological scaling solutions*. Phys. Rev. **D57**:4686 (1998). gr-qc/9711068.

[23] R. R. CALDWELL, R. DAVE and P. J. STEINHARDT. *Cosmological Imprint of an Energy Component with General Equation-of-State*. Phys. Rev. Lett. **80**:1582 (1998). astro-ph/9708069.

[24] R. J. VAN DEN HOOGEN, A. A. COLEY and D. WANDS. *Scaling Solutions in Robertson-Walker Spacetimes*. Class. Quant. Grav. **16**:1843 (1999). gr-qc/9901014.

[25] A. R. LIDDLE and R. J. SCHERRER. *A classification of scalar field potentials with cosmological scaling solutions*. Phys. Rev. **D59**:023509 (1999). astro-ph/9809272.

[26] P. J. E. PEEBLES and B. RATRA. *The cosmological constant and dark energy*. Rev. Mod. Phys. **75**:559 (2003). astro-ph/0207347.

[27] P. J. E. PEEBLES and A. VILENKIN. *Quintessential inflation*. Phys. Rev. **D59**:063505 (1999). astro-ph/9810509.

[28] N. BILIC, G. B. TUPPER and R. D. VIOLLIER. *Unification of dark matter and dark energy: The inhomogeneous Chaplygin gas.* Phys. Lett. **B535**:17 (2002). astro-ph/0111325.

[29] R. J. SCHERRER. *Purely kinetic k-essence as unified dark matter*. Phys. Rev. Lett. **93**:011301 (2004). astro-ph/0402316.

[30] M. SAMI and A. TOPORENSKY. *Phantom Field and the Fate of Universe*. Mod. Phys. Lett. **A19**:1509 (2004). gr-qc/0312009.

[31] I. P. NEUPANE. *On compatibility of string effective action with an accelerating universe*. Class. Quant. Grav. **23**:7493 (2006). hep-th/0602097.

[32] T. PADMANABHAN. *Cosmological constant: The weight of the vacuum*. Phys. Rept. **380**:235 (2003). hep-th/0212290.

[33] V. SAHNI. *Dark matter and dark energy*. Lect. Notes Phys. **653**:141 (2004). astro-ph/0403324.

[34] U. ALAM, V. SAHNI, T. D. SAINI and A. A. STAROBINSKY. *Is there Supernova Evidence for Dark Energy Metamorphosis ?* Mon. Not. Roy. Astron. Soc. **354**:275 (2004). astro-ph/0311364.

[35] S. NOJIRI and S. D. ODINTSOV. *Where new gravitational physics comes from: M-theory*. Phys. Lett. **B576**:5 (2003). hep-th/0307071.

[36] A. A. STAROBINSKY. *A new type of isotropic cosmological models without singularity*. Phys. Lett. **B91**:99 (1980).

[37] S. M. CARROLL, V. DUVVURI, M. TRODDEN and M. S. TURNER. *Is cosmic speed-up due to new gravitational physics?* Phys. Rev. **D70**:043528 (2004). astro-ph/0306438.

[38] A. D. DOLGOV and M. KAWASAKI. *Can modified gravity explain accelerated cosmic expansion?* Phys. Lett. **B573**:1 (2003). astro-ph/0307285.

[39] Y.-S. SONG, W. HU and I. SAWICKI. *The large scale structure of f(R) gravity*. Phys. Rev. **D75**:044004 (2007). astro-ph/0610532.

[40] I. SAWICKI and W. HU. *Stability of Cosmological Solution in f(R) Models of Gravity*. Phys. Rev. **D75**:127502 (2007). astro-ph/0702278.

[41] X. MENG and P. WANG. *Modified Friedmann Equations in R^{-1}-Modified Gravity*. Class. Quant. Grav. **20**:4949 (2003). astro-ph/0307354.

[42] L. AMENDOLA, D. POLARSKI and S. TSUJIKAWA. *Are f(R) dark energy models cosmologically viable ?* Phys. Rev. Lett. **98**:131302 (2007). astro-ph/0603703.

[43] L. AMENDOLA, R. GANNOUJI, D. POLARSKI and S. TSUJIKAWA. *Conditions for the cosmological viability of f(R) dark energy models*. Phys. Rev. **D75**:083504 (2007). gr-qc/0612180.

[44] P. TEYSSANDIER and P. TOURRENC. *The Cauchy problem for the $R + R^2$ theories of gravity without torsion*. J. Math. Phys. **24**:2793 (1983).

[45] S. S. SHAPIRO, J. L. DAVIS, D. E. LEBACH and J. S. GREGORY. *Measurement of the Solar Gravitational Deflection of Radio Waves using Geodetic Very-Long-Baseline Interferometry Data, 1979-1999*. Phys. Rev. Lett. **92**:121101 (2004).

[46] B. BERTOTTI, L. IESS and P. TORTORA. *A test of general relativity using radio links with the Cassini spacecraft*. Nature **425**:374 (2003).

[47] J. KHOURY and A. WELTMAN. *Chameleon cosmology*. Phys. Rev. **D69**:044026 (2004). astro-ph/0309411.

[48] D. F. MOTA and D. J. SHAW. *Evading equivalence principle violations, astrophysical and cosmological constraints in scalar field theories with a strong coupling to matter*. Phys. Rev. **D75**:063501 (2007). hep-ph/0608078.

[49] E. BARAUSSE, T. P. SOTIRIOU and J. C. MILLER. *A no-go theorem for polytropic spheres in Palatini f(R) gravity*. Class. Quant. Grav. **25**:062001 (2008). gr-qc/0703132.

[50] K. KAINULAINEN, J. PIILONEN, V. REIJONEN and D. SUNHEDE. *Spherically symmetric spacetimes in f(R) gravity theories*. Phys. Rev. **D76**:024020 (2007). 0704.2729 [gr-qc].

[51] N. LANAHAN-TREMBLAY and V. FARAONI. *The Cauchy problem of f(R) gravity*. Class. Quant. Grav. **24**:5667 (2007). 0709.4414 [gr-qc].

[52] P. SOLIN. *Partial Differential Equations and the Finite Element Method*. Wiley (2006).

[53] S. CAPOZZIELLO and S. VIGNOLO. *The Initial Value Formulation of f(R)-gravity in the metric-affine formalism*. 0901.3136 [gr-qc].

[54] S. CAPOZZIELLO, R. CIANCI, C. STORNAIOLO and S. VIGNOLO. *$f(R)$ gravity with torsion: the metric-affine approach*. Class. Quant. Grav. **24**:6417 (2007). 0708.3038 [gr-qc].

[55] R. P. WOODARD. *Avoiding dark energy with 1/R modifications of gravity*. Lect. Notes Phys. **720**:403 (2007). astro-ph/0601672.

[56] A. DE FELICE, M. HINDMARSH and M. TRODDEN. *Ghosts, instabilities, and superluminal propagation in modified gravity models*. JCAP **0608**:005 (2006). astro-ph/0604154.

[57] I. I. SHAPIRO. *Fourth Test of General Relativity*. Phys. Rev. Lett. **13**:789 (1964).

[58] C. M. WILL. *The confrontation between general relativity and experiment*. Living Rev. Rel. **4**:4 (2001). gr-qc/0103036.

[59] M. BARTELMANN and P. SCHNEIDER. *Weak Gravitational Lensing*. Phys. Rept. **340**:291 (2001). astro-ph/9912508.

[60] C. M. WILL. *Theory and experiment in gravitational physics*. Cambridge University Press (1993).

[61] C. M. WILL. *The Confrontation between General Relativity and Experiment*. Living Rev. Relativity **9**:3 (2006).

[62] M. COLLESS et al. *The 2dF Galaxy Redshift Survey: Final Data Release*. astro-ph/0306581.

[63] G. F. SMOOT et al. *Structure in the COBE differential microwave radiometer first year maps*. Astrophys. J. **396**:L1 (1992).

[64] P. MCDONALD et al. *The Linear Theory Power Spectrum from the Lyman-alpha Forest in the Sloan Digital Sky Survey*. Astrophys. J. **635**:761 (2005). astro-ph/0407377.

[65] M. VIEL and M. G. HAEHNELT. *Cosmological and astrophysical parameters from the SDSS flux power spectrum and hydrodynamical simulations of the Lyman-alpha forest*. Mon. Not. Roy. Astron. Soc. **365**:231 (2006). astro-ph/0508177.

[66] C. DI PORTO and L. AMENDOLA. *Observational constraints on the linear fluctuation growth rate*. Phys. Rev. **D77**:083508 (2008). 0707.2686 [astro-ph].

[67] K. A. MALIK and D. WANDS. *Cosmological perturbations*. Phys. Rept. **475**:1 (2009). 0809.4944 [astro-ph].

[68] K. UDDIN, J. E. LIDSEY and R. TAVAKOL. *Cosmological perturbations in Palatini modified gravity*. Class. Quant. Grav. **24**:3951 (2007). 0705.0232 [gr-qc].

[69] S. TSUJIKAWA, K. UDDIN and R. TAVAKOL. *Density perturbations in f(R) gravity theories in metric and Palatini formalisms*. Phys. Rev. **D77**:043007 (2008). 0712.0082 [astro-ph].

[70] D. BLASCHKE and M. P. DABROWSKI. *Conformal relativity versus Brans-Dicke and superstring theories*. hep-th/0407078.

[71] K. UDDIN, J. E. LIDSEY and R. TAVAKOL. *Cosmological scaling solutions in generalised Gauss-Bonnet gravity theories*. 0903.0270 [gr-qc].

[72] H. A. BUCHDAHL. *Non-linear Lagrangians and cosmological theory*. Mon. Not. Roy. Astron. Soc. **150**:1 (1970).

[73] M. S. MADSEN and J. D. BARROW. *De-Sitter ground states and boundary terms in generalzed gravity*. Nucl. Phys. **B323**:242 (1989).

[74] T. P. SOTIRIOU. *Modified Actions for Gravity: Theory and Phenomenology*. 0710.4438 [gr-qc].

[75] G. MAGNANO and L. M. SOKOLOWSKI. *On physical equivalence between nonlinear gravity theories and a general relativistic selfgravitating scalar field*. Phys. Rev. **D50**:5039 (1994). gr-qc/9312008.

[76] C. W. MISNER, K. S. THORNE and J. A. WHEELER. *Gravitation*. Freeman Press (1973).

[77] T. P. SOTIRIOU and V. FARAONI. *f(R) Theories Of Gravity*. 0805.1726 [gr-qc].

[78] V. FARAONI. *Palatini f(R) gravity as a fixed point*. Phys. Lett. **B665**:135 (2008). 0806.0766 [gr-qc].

[79] T. KOIVISTO and H. KURKI-SUONIO. *Cosmological perturbations in the Palatini formulation of modified gravity*. Class. Quant. Grav. **23**:2355 (2006). astro-ph/0509422.

[80] M. MORTONSON. *Modified gravity theories in the Palatini approach and observational constraints.* Notes.

[81] B. BOISSEAU, G. ESPOSITO-FARESE, D. POLARSKI and A. A. STAROBINSKY. *Reconstruction of a scalar-tensor theory of gravity in an accelerating universe*. Phys. Rev. Lett. **85**:2236 (2000). gr-qc/0001066.

[82] M. SALGADO, D. M.-D. RIO, M. ALCUBIERRE and D. NUNEZ. *Hyperbolicity of scalar-tensor theories of gravity*. Phys. Rev. **D77**:104010 (2008). 0801.2372 [gr-qc].

[83] C. BRANS and R. H. DICKE. *Mach's principle and a relativistic theory of gravitation*. Phys. Rev. **124**:925 (1961).

[84] T. CLIFTON and J. D. BARROW. *The existence of Goedel, Einstein and de Sitter universes*. Phys. Rev. **D72**:123003 (2005). gr-qc/0511076.

[85] S. M. CARROLL et al. *The cosmology of generalized modified gravity models*. Phys. Rev. **D71**:063513 (2005). astro-ph/0410031.

[86] B. LI, J. D. BARROW and D. F. MOTA. *The Cosmology of Modified Gauss-Bonnet Gravity*. Phys. Rev. **D76**:044027 (2007). 0705.3795 [gr-qc].

[87] D. WANDS. *Extended gravity theories and the Einstein-Hilbert action*. Class. Quant. Grav. **11**:269 (1994). gr-qc/9307034.

[88] A. R. LIDDLE and D. H. LYTH. *Cosmological inflation and large-scale structure*. Cambridge University Press (2000).

[89] T. CLIFTON. *Alternative theories of gravity*. gr-qc/0610071.

[90] V. FARAONI, E. GUNZIG and P. NARDONE. *Conformal transformations in classical gravitational theories and in cosmology*. Fund. Cosmic Phys. **20**:121 (1999). gr-qc/9811047.

[91] E. E. FLANAGAN. *The conformal frame freedom in theories of gravitation*. Class. Quant. Grav. **21**:3817 (2004). gr-qc/0403063.

[92] T. CHIBA. *1/R gravity and scalar-tensor gravity*. Phys. Lett. **B575**:1 (2003). astro-ph/0307338.

[93] K.-I. MAEDA. *Towards the Einstein-Hilbert Action via Conformal Transformation*. Phys. Rev. **D39**:3159 (1989).

[94] T. P. SOTIRIOU and E. BARAUSSE. *Post-Newtonian expansion for Gauss-Bonnet Gravity*. Phys. Rev. **D75**:084007 (2007). gr-qc/0612065.

[95] S. NOJIRI, S. D. ODINTSOV and M. SASAKI. *Gauss-Bonnet dark energy*. Phys. Rev. **D71**:123509 (2005). hep-th/0504052.

[96] S. WEINBERG. *Cosmology*. Oxford University Press (2008).

[97] J. M. BARDEEN, P. J. STEINHARDT and M. S. TURNER. *Spontaneous Creation of Almost Scale - Free Density Perturbations in an Inflationary Universe*. Phys. Rev. **D28**:679 (1983).

[98] K. A. MALIK. *Cosmological perturbations in an inflationary universe*. astro-ph/0101563.

[99] J.-C. HWANG and H. NOH. *Classical evolution and quantum generation in generalized gravity theories including string corrections and tachyon: Unified analyses*. Phys. Rev. **D71**:063536 (2005). gr-qc/0412126.

[100] G. ESPOSITO-FARESE and D. POLARSKI. *Scalar-tensor gravity in an accelerating universe*. Phys. Rev. **D63**:063504 (2001). gr-qc/0009034.

[101] K. A. MALIK and D. WANDS. *Adiabatic and entropy perturbations with interacting fluids and fields*. JCAP **0502**:007 (2005). astro-ph/0411703.

[102] J.-C. HWANG. *Perturbations of the Robertson-Walker space - Multicomponent sources and generalized gravity*. Astrophys. J. **375**:443 (1991).

[103] H. KODAMA and M. SASAKI. *Cosmological Perturbation Theory*. Prog. Theor. Phys. Suppl. **78**:1 (1984).

[104] V. F. MUKHANOV, H. A. FELDMAN and R. H. BRANDENBERGER. *Theory of cosmological perturbations. Part 1. Classical perturbations. Part 2. Quantum theory of perturbations. Part 3. Extensions*. Phys. Rept. **215**:203 (1992).

[105] D. WANDS, K. A. MALIK, D. H. LYTH and A. R. LIDDLE. *A new approach to the evolution of cosmological perturbations on large scales*. Phys. Rev. **D62**:043527 (2000). astro-ph/0003278.

[106] K. A. MALIK and D. R. MATRAVERS. *A Concise Introduction to Perturbation Theory in Cosmology*. Class. Quant. Grav. **25**:193001 (2008). 0804.3276 [astro-ph].

[107] W. HU. *Covariant Linear Perturbation Formalism*. astro-ph/0402060.

[108] A. LUE, R. SCOCCIMARRO and G. STARKMAN. *Differentiating between Modified Gravity and Dark Energy*. Phys. Rev. **D69**:044005 (2004). astro-ph/0307034.

[109] T. MULTAMAKI, E. GAZTANAGA and M. MANERA. *Large scale structure in non-standard cosmologies*. Mon. Not. Roy. Astron. Soc. **344**:761 (2003). astro-ph/0303526.

[110] K. KOYAMA and R. MAARTENS. *Structure formation in the DGP cosmological model*. JCAP **0601**:016 (2006). astro-ph/0511634.

[111] M. AMARZGUIOUI, O. ELGAROY, D. F. MOTA and T. MULTAMAKI. *Cosmological constraints on f(R) gravity theories within the Palatini approach*. Astron. Astrophys. **454**:707 (2006). astro-ph/0510519.

[112] A. J. CHRISTOPHERSON and K. A. MALIK. *The non-adiabatic pressure in general scalar field systems*. Phys. Lett. **B675**:159–163 (2009). 0809.3518.

[113] D. ZWILLINGER. *Handbook of Differential Equations*. New York Academic (1988).

[114] S. CAPOZZIELLO, S. CARLONI and A. TROISI. *Quintessence without scalar fields*. Recent Res. Dev. Astron. Astrophys. **1**:625 (2003). astro-ph/0303041.

[115] G. ALLEMANDI, A. BOROWIEC and M. FRANCAVIGLIA. *Accelerated cosmological models in Ricci squared gravity*. Phys. Rev. **D70**:103503 (2004). hep-th/0407090.

[116] A. A. STAROBINSKY. *Disappearing cosmological constant in f(R) gravity*. JETP Lett. **86**:157 (2007). 0706.2041 [astro-ph].

[117] W. HU and I. SAWICKI. *Models of f(R) Cosmic Acceleration that Evade Solar-System Tests*. Phys. Rev. **D76**:064004 (2007). 0705.1158 [astro-ph].

[118] G. J. OLMO. *Post-Newtonian constraints on $f(R)$ cosmologies in metric and Palatini formalism*. Phys. Rev. **D72**:083505 (2005).

[119] I. NAVARRO and K. VAN ACOLEYEN. *f(R) actions, cosmic acceleration and local tests of gravity*. JCAP **0702**:022 (2007). gr-qc/0611127.

[120] T. CHIBA, T. L. SMITH and A. L. ERICKCEK. *Solar System constraints to general f(R) gravity*. Phys. Rev. **D75**:124014 (2007). astro-ph/0611867.

[121] B. LI and J. D. BARROW. *The Cosmology of f(R) Gravity in the Metric Variational Approach*. Phys. Rev. **D75**:084010 (2007). gr-qc/0701111.

[122] L. AMENDOLA and S. TSUJIKAWA. *Phantom crossing, equation-of-state singularities, and local gravity constraints in $f(R)$ models*. Phys. Lett. **B660**:125 (2008). 0705.0396 [astro-ph].

[123] T. FAULKNER, M. TEGMARK, E. F. BUNN and Y. MAO. *Constraining f(R) gravity as a scalar tensor theory*. Phys. Rev. **D76**:063505 (2007). astro-ph/0612569.

[124] S. CAPOZZIELLO and S. TSUJIKAWA. *Solar system and equivalence principle constraints on $f(R)$ gravity by chameleon approach*. Phys. Rev. **D77**:107501 (2008). 0712.2268 [gr-qc].

[125] P. BRAX, C. VAN DE BRUCK, A.-C. DAVIS and D. J. SHAW. *f(R) Gravity and Chameleon Theories*. Phys. Rev. **D78**:104021 (2008). 0806.3415 [astro-ph].

[126] S. CAPOZZIELLO, V. F. CARDONE, S. CARLONI and A. TROISI. *Curvature quintessence matched with observational data*. Int. J. Mod. Phys. **D12**:1969 (2003). astro-ph/0307018.

[127] S. TSUJIKAWA. *Matter density perturbations and effective gravitational constant in modified gravity models of dark energy*. Phys. Rev. **D76**:023514 (2007). 0705.1032 [astro-ph].

[128] L. AMENDOLA, M. KUNZ and D. SAPONE. *Measuring the dark side (with weak lensing)*. JCAP **0804**:013 (2008). 0704.2421 [astro-ph].

[129] S. TSUJIKAWA. *Observational signatures of f(R) dark energy models that satisfy cosmological and local gravity constraints*. Phys. Rev. **D77**:023507 (2008). 0709.1391 [astro-ph].

[130] W. J. PERCIVAL et al. *The shape of the SDSS DR5 galaxy power spectrum*. Astrophys. J. **657**:645–663 (2007). astro-ph/0608636.

[131] T. KOIVISTO. *The matter power spectrum in $f(R)$ gravity*. Phys. Rev. **D73**:083517 (2006). astro-ph/0602031.

[132] B. LI, K. C. CHAN and M. C. CHU. *Constraints on f(R) Cosmology in the Palatini Formalism*. Phys. Rev. **D76**:024002 (2007). astro-ph/0610794.

[133] L. AMENDOLA. *Coupled quintessence*. Phys. Rev. **D62**:043511 (2000). astro-ph/9908023.

[134] L. AMENDOLA. *Scaling solutions in general non-minimal coupling theories*. Phys. Rev. **D60**:043501 (1999). astro-ph/9904120.

[135] T. CHIBA. *Quintessence, the gravitational constant, and gravity*. Phys. Rev. **D60**:083508 (1999). gr-qc/9903094.

[136] J.-P. UZAN. *Cosmological scaling solutions of non-minimally coupled scalar fields*. Phys. Rev. **D59**:123510 (1999). gr-qc/9903004.

[137] N. BARTOLO and M. PIETRONI. *Scalar-Tensor Gravity and Quintessence*. Phys. Rev. **D61**:023518 (2000). hep-ph/9908521.

[138] F. PERROTTA, C. BACCIGALUPI and S. MATARRESE. *Extended quintessence*. Phys. Rev. **D61**:023507 (2000). astro-ph/9906066.

[139] C. BACCIGALUPI, S. MATARRESE and F. PERROTTA. *Tracking extended quintessence*. Phys. Rev. **D62**:123510 (2000). astro-ph/0005543.

[140] F. PERROTTA and C. BACCIGALUPI. *On the dark energy clustering properties*. Phys. Rev. **D65**:123505 (2002). astro-ph/0201335.

[141] D. F. TORRES. *Quintessence, super-quintessence and observable quantities in Brans-Dicke and non-minimally coupled theories*. Phys. Rev. **D66**:043522 (2002). astro-ph/0204504.

[142] A. RIAZUELO and J.-P. UZAN. *Cosmological observations in scalar-tensor quintessence*. Phys. Rev. **D66**:023525 (2002). astro-ph/0107386.

[143] S. CAPOZZIELLO, S. NESSERIS and L. PERIVOLAROPOULOS. *Reconstruction of the Scalar-Tensor Lagrangian from a LCDM Background and Noether Symmetry*. JCAP **0712**:009 (2007). 0705.3586 [astro-ph].

[144] J. MARTIN, C. SCHIMD and J.-P. UZAN. *Testing for $w < -1$ in the solar system*. Phys. Rev. Lett. **96**:061303 (2006). astro-ph/0510208.

[145] R. GANNOUJI, D. POLARSKI, A. RANQUET and A. A. STAROBINSKY. *Scalar-tensor models of normal and phantom dark energy*. JCAP **0609**:016 (2006). astro-ph/0606287.

[146] S. NESSERIS and L. PERIVOLAROPOULOS. *The Limits of Extended Quintessence*. Phys. Rev. **D75**:023517 (2007). astro-ph/0611238.

[147] C. D. HOYLE et al. *Sub-millimeter tests of the gravitational inverse-square law*. Phys. Rev. **D70**:042004 (2004). hep-ph/0405262.

[148] S. TSUJIKAWA, K. UDDIN, S. MIZUNO, R. TAVAKOL and J. YOKOYAMA. *Constraints on scalar-tensor models of dark energy from observational and local gravity tests*. Phys. Rev. **D77**:103009 (2008). 0803.1106 [astro-ph].

[149] S.-Y. ZHOU, E. J. COPELAND and P. M. SAFFIN. *Cosmological Constraints on $f(G)$ Dark Energy Models*. 0903.4610 [gr-qc].

[150] J. J. HALLIWELL. *Scalar Fields in Cosmology with an Exponential Potential*. Phys. Lett. **B185**:341 (1987).

[151] J. YOKOYAMA and K.-I. MAEDA. *On the Dynamics of the Power Law Inflation Due to an Exponential Potential*. Phys. Lett. **B207**:31 (1988).

[152] A. DE LA MACORRA and G. PICCINELLI. *General scalar fields as quintessence*. Phys. Rev. **D61**:123503 (2000). hep-ph/9909459.

[153] S. C. C. NG, N. J. NUNES and F. ROSATI. *Applications of scalar attractor solutions to cosmology*. Phys. Rev. **D64**:083510 (2001). astro-ph/0107321.

[154] T. BARREIRO, E. J. COPELAND and N. J. NUNES. *Quintessence arising from exponential potentials*. Phys. Rev. **D61**:127301 (2000). astro-ph/9910214.

[155] A. A. COLEY and R. J. VAN DEN HOOGEN. *The dynamics of multi-scalar field cosmological models and assisted inflation*. Phys. Rev. **D62**:023517 (2000). gr-qc/9911075.

[156] V. FARAONI. *de Sitter attractors in generalized gravity*. Phys. Rev. **D70**:044037 (2004). gr-qc/0407021.

[157] V. FARAONI. *Modified gravity and the stability of de Sitter space*. Phys. Rev. **D72**:061501 (2005). gr-qc/0509008.

[158] J. A. R. CALDWELL and J. P. OSTRIKER. *The Mass distribution within our Galaxy: A Three component model*. Astrophys. J. **251**:61–87 (1981).

[159] E. I. GATES, G. GYUK and M. S. TURNER. *The Local halo density*. Astrophys. J. **449**:L123–L126 (1995). astro-ph/9505039.

[160] J. BAHCALL, T. PIRAN and S. WEINBERG. *Dark Matter in the Universe*. Jerusalem Winter School for Theoretical Physics. World Scientific Publishing (2004).

[161] S. CAPOZZIELLO. *Curvature Quintessence*. Int. J. Mod. Phys. **D11**:483 (2002). gr-qc/0201033.

[162] M. TEGMARK et al. *Cosmological Constraints from the SDSS Luminous Red Galaxies*. Phys. Rev. **D74**:123507 (2006). astro-ph/0608632.

[163] C. RUBANO and J. D. BARROW. *Scaling solutions and reconstruction of scalar field potentials*. Phys. Rev. **D64**:127301 (2001). gr-qc/0105037.

[164] E. J. COPELAND, S.-J. LEE, J. E. LIDSEY and S. MIZUNO. *Generalised cosmological scaling solutions*. Phys. Rev. **D71**:023526 (2005). astro-ph/0410110.

[165] S. TSUJIKAWA and M. SAMI. *A unified approach to scaling solutions in a general cosmological background*. Phys. Lett. **B603**:113 (2004). hep-th/0409212.

[166] S. NOJIRI and S. D. ODINTSOV. *Modified Gauss-Bonnet theory as gravitational alternative for dark energy*. Phys. Lett. **B631**:1 (2005). hep-th/0508049.

[167] G. COGNOLA, E. ELIZALDE, S. NOJIRI, S. D. ODINTSOV and S. ZERBINI. *Dark energy in modified Gauss-Bonnet gravity: Late-time acceleration and the hierarchy problem*. Phys. Rev. **D73**:084007 (2006). hep-th/0601008.

[168] S. TSUJIKAWA and M. SAMI. *String-inspired cosmology: Late time transition from scaling matter era to dark energy universe caused by a Gauss-Bonnet coupling*. JCAP **0701**:006 (2007). hep-th/0608178.

[169] M. HAZEWINKEL. *Encylopedia of Mathematics*. Kluwer Academic Publishers (2003).

[170] M. ISHAK and J. MOLDENHAUER. *A minimal set of invariants as a systematic approach to higher order gravity models*. JCAP **0901**:024 (2009). 0808.0951 [astro-ph].

[171] A. DE FELICE and S. TSUJIKAWA. *Construction of cosmologically viable f(G) dark energy models*. Phys. Lett. **B675**:1 (2009). 0810.5712 [hep-th].